Studies on molecular Oxo and Imido complexes of the group 6 metals and supported chromium oxide polymerisation catalysts

Philip William Dyer

Studies on Molecular Oxo and Imido Complexes of the Group 6 Metals and Supported Chromium Oxide Polymerisation Catalysts

by

Philip William Dyer, B.Sc. (Dunelm), G.R.S.C.

University of Durham

A thesis submitted in part fulfilment of the requirements for the degree of Doctor of Philosophy at the University of Durham.

November 1993.

STATEMENT OF COPYRIGHT

DECLARATION

The work described in this thesis was carried out in the Department of Chemistry of the University of Durham between October 1990 and September 1993. All the work is my own, unless stated to the contrary, and it has not been submitted previously for a degree at this or any other University.

This thesis is for Mum, Dad, and Claire.

"That," I replied cordially, "is what it doesn't do anything else but."
- P.G. Wodehouse.

Acknowledgements

I would like to express my sincere thanks to my supervisors Prof. Vernon Gibson and Dr Jas Pal Badyal for all their help, encouragement, and enthusiasm over the past three years. They have both made it a great pleasure to work in their laboratories. I think there is only one thing to be said "It better be a benzyne Vern!!"

Dave, Oli, Ulrich, Jens, Kuymars, Eduardo, Tina, and Mike, have all made working in CG 19 great fun. Matt has kept us all amused for hours with his "stories." Brenda was a great "Geoff" even if she does hold me responsible for her doing an M.Sc. Ed and Jon must be thanked for all the good times, especially playing football in the kitchen in Hallgarth St. Andy, I can only say one thing: "Wibble!" Thanks must go to Leela for all her "deafening" encouragement during the final writing! And lastly, to Martyn and the cat for all the good times at No. 16.

All the occupants of lab 100 deserve a special mention, especially Ian (Lardy Lavender) and Lisa for making the Rectory so much more bearable, and to Christine for all her fashion tips!

Lab 98, past and present, Alex, Sue, Simon, Pete, Zé, Campbell, Martin, Oli, and Janet need thanking for all the times they've had to "trap" my mass spectrometer! Thanks Rachel for your friendship over the last six years.

The Durham Crystallographers, especially Susanna, Roy and Claire must be thanked for all their help, patience, and coffee while I was pestering them for data and pictures!

I am especially indebted to Prof W. Clegg (University of Newcastle) and Prof. J. Howard (University of Durham) for solving the crystal structures described in this thesis. Dr Alan Kenwright and Mrs Julia Say must get a special mention for their invaluable help and perseverance with all those "simple" NMR problems and experiments.

I am grateful to Dr Tony Royston for his help with the XPS and MS programs, Ray Hart and Gordon Haswell for glassblowing (usually in a hurry), and all the other technical staff here in Durham who have made this thesis possible.

Financial support from Crosfield Chemicals and the SERC are gratefully acknowledged.

Lastly, but by no means least, the people who count most, all my family, especially Mum, Dad, Claire, and my grandparents, thanks for all your understanding, encouragement and moral support throughout all the years I've been doing chemistry.

Abstract

Studies on Molecular Oxo and Imido Complexes of the Group 6 Metals and Supported Chromium Oxide Polymerisation Catalysts

This thesis describes studies directed towards the preparation of bis (imido) complexes of the Group 6 metals containing olefin, phosphine, acetylene, and alkyl ligands with particular emphasis on their relationship with Group 4 bent metallocenes. The polymerisation mechanism of the Phillips catalyst (CrO_3/SiO_2) is examined using XPS (X-Ray Photoelectron Spectroscopy) and *in situ* mass spectroscopy.

Chapter 1 highlights properties of some of the important ligand classes that are used throughout the remainder of this thesis.

Chapter 2 describes a high yield one-pot synthesis of molybdenum bis (imido) complexes of the type $Mo(NR')(NR'')Cl_2.DME$. In addition a number of attempts to extend this strategy to other metals are described, including a novel synthesis of the chromium complex $[Cr_2Cl_9]\ [NHEt_3]_3$.

Chapter 3 describes the synthesis, characterisation, and reactivity of the bis (imido) bis (phosphine) complexes $Mo(NAr)_2(PMe_3)_2$ and $[Mo(N^tBu)(\mu\text{-}N^tBu)(PMe_3)]_2$. Further studies on bis (imido) olefin complexes of the type $Mo(NAr)_2(PMe_3)_2(\eta^2\text{-}C_2H_4)$ and $Mo(N^tBu)_2(PMe_3)(\eta^2\text{-}C_2H_4)$ was undertaken and concentrated on their structural relationship to Group 4 metallocene species.

Chapter 4 describes the preparation, structure, and reactivity of some bis (imido) acetylene complexes $Mo(NR)_2(PMe_3)(PhC{\equiv}CR')$ (R= Ar, ^{t}Bu; R'= Ph, H). Preparation of bis (imido) alkyls was undertaken in attempts to generate benzyne and alkylidene derivatives.

Chapter 5 studies the Phillips polymerisation catalyst using XPS and mass spectroscopy. Model systems were used to probe reactive surface species their use reveals a number of features that are difficult to observe with the actual catalyst. Aspects of molecular chemistry have been examined which are believed to relate directly to the heterogeneous system allowing a possible polymerisation mechanism to be postulated.

Chapter 6 gives experimental details for Chapters 2-5.

Philip William Dyer (November 1993)

Abbreviations

Ac	Acetate group (C(=O)OMe)
Cp	Cyclopentadienyl (C_5H_5)
Cp*	Pentamethylcyclopentadienyl (C_5Me_5)
Cp'	Generalised (C_5R_5) ligand
dd	Doublet of doublets
ddd	Doublet of doublets of doublets
COSY	Correlated Spectroscopy
DEPT	Distortionless Enhancement by Polarisation Transfer
DME	1,2-Dimethoxyethane
E	General main Group element (e.g. S, Se, Te, and N)
FWHM	Full width at half-maximum height
GC	Gas Chromatography
HETCOR	Heteronuclear Correlation
IR	Infrared
L	General 2-electron donor ligand
LUMO	Lowest Unoccupied Molecular Orbital
HOMO	Highest Occupied Molecular Orbital
NAr	2,6-diisopropylphenylimido
NMR	Nuclear Magnetic Resonance
NOE	Nuclear Overhauser Effect
py	Pyridine
R	General alkyl ligand
THF	Tetrahydrofuran
td	Triplet of doublets
tq	Triplet of quartets
tqd	Triplet of quartets of doublets
XPS	X-ray Photoelectron Spectroscopy
$\nu_{1/2}$	Peak width at half height
X	General 1-electron donor ligand

Contents

Chapter Three:- The Preparation, Reactivity, and Structure of Molybdenum Bis (Imido) Bis (Phosphine) and Bis (Imido) Olefin Complexes

Chapter One- Introduction

1.0 Introduction

The work described in this thesis is directed towards the development of the chemistry of Group 6 oxo and imido compounds. These studies have concerned the following areas:

i) The synthesis of molybdenum bis (imido) complexes using a simple, "one-pot" reaction.

ii) Bis (imido) complexes have been synthesised containing *inter alia* phosphine, olefin, and acetylene ligands.

iii) A comparative study was undertaken to compare the structural relationship that exists between Group 4 bent metallocenes and their pseudo-isolobal Group 6 bis (imido) counterparts.

iv) The chemistry of well-defined complexes of the Group 6 metals was used in conjunction with XPS and *in situ* mass spectroscopic studies with a view to assessing the mechanism of the silica supported Phillips olefin polymerisation catalyst.

Much of the work described below has involved the use of a number of common ligand types. Hence, the remainder of this chapter briefly discusses the important properties and characteristics of the main ligand classes used throughout this thesis. In particular complexes containing oxo, imido, phosphine, olefin (acetylene) and alkylidene moieties are included. This review is not intended to be comprehensive, but to highlight particular areas that are of relevance to this work.

1.1 Transition Metal Oxo Complexes and Main Group Oxides

Transition metal oxo complexes play a central rôle in a variety of laboratory, industrial and biological oxidation processes.[1] They exhibit a wide range of bonding modes as shown in Figure 1.0. Only terminal oxo species (structures **1** to **3**) will be discussed in detail.

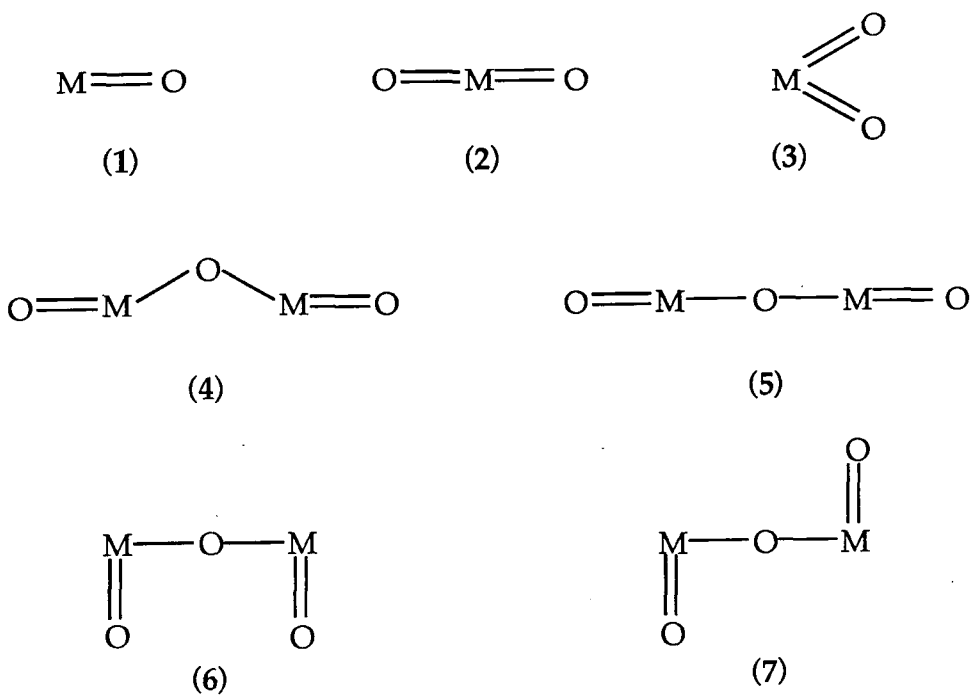

Figure 1.0 *Common structurally characterised oxo group geometries.*

Oxo ligands are frequently described as closed shell dianions[2] (O^{2-}). Metals in high oxidation states are required to maximise the degree of productive π bonding (i.e. π interactions that stabilise the metal oxygen bond). Thus, the vast majority of metal oxo compounds have either d^0, d^1 or d^2 electronic configurations. Only a few d^4 and d^5 complexes have been prepared.[3-8] d^4 $Re(O)X(RC{\equiv}CR)_2$ complexes tend to adopt an unusual tetrahedral geometry in order to accommodate the d-electrons in approximately non-bonding orbitals. This prevents occupation of Re-O π* orbitals.[9]

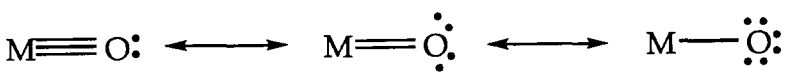

Scheme 1.0 *Contributions to metal-oxo bonding showing the variation in metal-oxo bond order.*

In general, metal-oxo complexes exhibit bond orders that range from one to three (Scheme 1.0), the high electronegativity of oxygen enables it to tolerate up to three lone pairs. Mono-oxo complexes usually contain metal-oxygen triple bonds[2] but, the bond order for di-oxo complexes is intermediate between that for double and triple bonds, a

result of competition for available metal-based π-symmetry orbitals. This latter situation is discussed in greater detail later.

Complexes containing the oxo moiety are known to play a part in both metal assisted hydrocarbon oxidation[10] and olefin metathesis.[11] The rôle of the oxo group in classical olefin metathesis using high valent Group 6 oxides has been the focus of a detailed *ab initio* study by Goddard and Rappé.[12] In $Mo(O)Cl_4$ the M-O bond has an order of three, whereas for the di-oxo complex $Mo(O)_2Cl_2$ the bond order is lower. The conclusion of Goddard and Rappé's study was that the increase in bond strength upon conversion of a metal oxygen double bond to a triple bond could provide a driving force for reactions occurring at a metal centre.

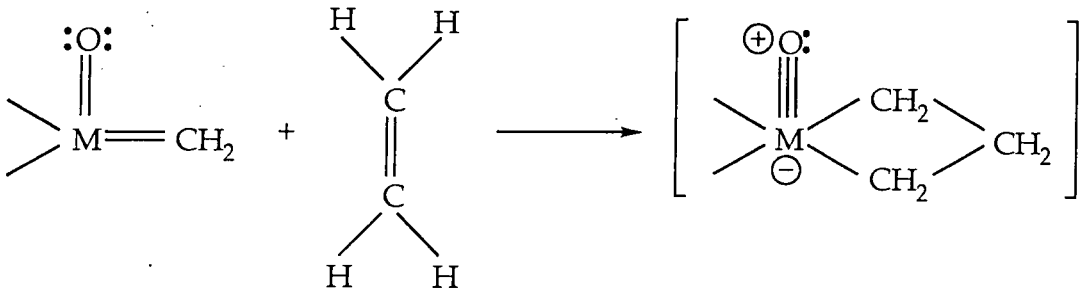

Scheme 1.1 *"Spectator Oxo" effect.*

Thus, the reaction of an olefin with an oxo group was calculated to be thermodynamically favourable only because the bond between the metal and second "spectator" oxo group becomes much stronger as the bond order increases from two to three, stabilising the metallacyclic intermediate (Scheme 1.1). Such an effect has been termed a *"Spectator-Oxo Effect"*.

Main Group oxides can be classed in general terms as being either normal oxides, suboxides, peroxides, or super oxides. Normal oxides are by far the most important class which contains species with simple E-O bonds (E= any element other than oxygen). They may be either covalent (e.g. O=C=O) or ionic (e.g. $Ca^{2+}O^{2-}$) in their nature. Further subdivision into subclasses depending on their behaviour with water, aqueous acids and alkalis can be made. This behaviour can be explained in terms of the relative differences in electronegativity between E and O. Thus most metal oxides are ionic and non-metal oxides polar covalent. However, transition metal oxides with oxidation states greater than +4, e.g. CrO_3, Mn_2O_7, are covalent and acidic as there is a large energy requirement for the formation of Cr^{6+} and Mn^{7+} which is not available in normal

chemical reactions. The acidic behaviour of amphoteric oxides (e.g. Al_2O_3, ZnO) is best explained in terms of removal of OH^- ions from solution rather than donation of protons.

The suboxide classification encompasses species that contain both E-E and E-O bonds but no O-O linkages. One example of this class is the gas C_3O_2 (i.e. O=C=C=C=O). Peroxides contain O-O as well as E-O bonds, but no E-E functionality, e.g. H_2O_2, Na_2O_2, K_2O_2. All peroxides afford H_2O_2 on treatment with water, or dilute acids. They are formed by all the metals of Groups 1 and 2 with the exception of beryllium. Superoxides are closely related to peroxides, but contain the $[O_2]^-$ ion. They are formed by all the metals of Group 1 with the exception of lithium (e.g. KO_2).

Later in this thesis metal species impregnated onto silica surfaces will be examined in detail. Thus, a brief summary of the nature and properties of silica will be given.

All the Group 14 elements form oxides of the type XO_2. Carbon dioxide is, however, the only molecular species, the other oxides being crystalline high melting point solids.

This disparity between carbon and the other elements of this group reflects the propensity of carbon to form stable, covalent, multiple bonds. This is readily explained in terms of the relative atomic radii of each of the elements. Carbon atoms are much smaller than those of silicon, and germanium etc. (C 0.77Å, Si 1.17Å, and Ge 1.22Å). Hence, the p orbitals required for multiple bond formation can readily overlap for carbon, yet for the heavier congeners the $p\pi$-$p\pi$ overlap is poor. Because the energy of the Si-O bond (452 kJ mol^{-1}) is much greater than that of a Si-Si bond (340 kJ mol^{-1}), the former are always preferred. Thus, when silicon is oxidised the basic unit ≡Si-O- can link up in three dimensions forming giant molecules.

The surface of silica (SiO_2) contains both hydrophobic siloxane bridges (Si-O-Si) and hydrophilic terminal hydroxide (silanol, Si-OH) groups. Under normal atmospheric conditions the surface will be covered by a multilayer of physisorbed water. Heating increases the concentration of siloxane bridges at the surface, but can never remove all the surface silanol groups. Thus, all silicas develop hydrophobicity upon thermal treatment. The silanol groups have been shown to have an associated pKa value in the range 4-7, dependent upon the method of preparation of the silica. This weakly acidic or near neutral behaviour means that silanols

can behave as reactive, coordinative, or inactive groups against metal carbonyls and other organometallic species.

1.2 Imido Complexes

Transition metal imido complexes, [M]=NR, constitute one of the richest classes of compounds, both in the variety of structural possibilities and the diversity of the chemistry associated with them.[2,13] Complexes containing this ligand have been proposed as intermediates in a variety of processes including selective oxidation,[14] ammoxidation,[15] and enzymatic transformations.[16]

Imido ligands have been observed to adopt five bonding modes, shown in Figure 1.1. Discussion will be limited to the most common arrangements, modes **1** to **3**, of relevance to the studies described in this Thesis.

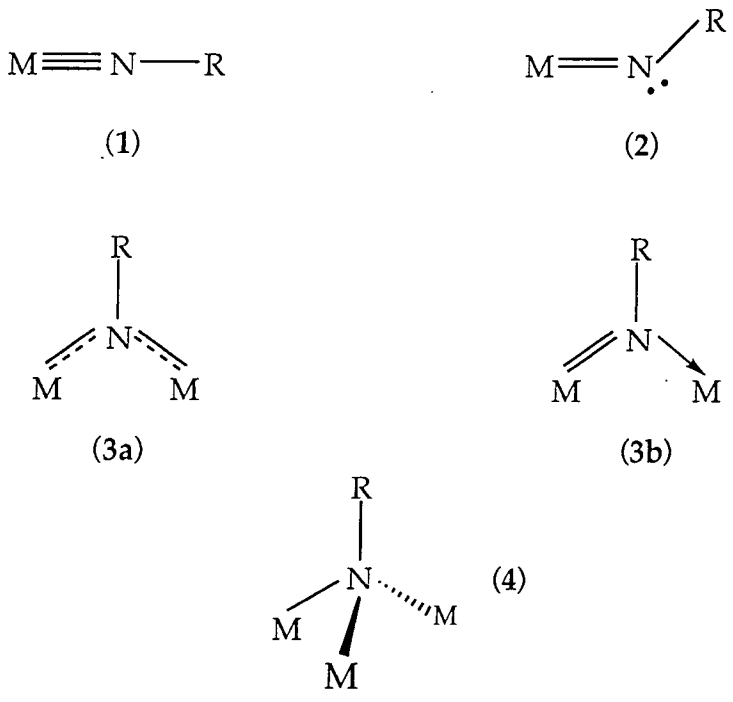

Figure 1.1 *Bonding modes of imido ligands.*

A linear M-N-C arrangement (structure 1) has generally been thought to imply a metal-nitrogen triple bond, formed by donation of the nitrogen lone pair of electrons to an empty metal d-orbital; nitrogen is thus sp-hybridised, forming one σ and two π bonds to the metal.

This relatively high bond order is a consequence of the electronegativity of the nitrogen atom, although a sufficient supply of vacant metal d orbitals is required to stabilise this bonding interaction. As a result, most fully characterised imido complexes are found with d^0, d^1, and d^2 configurations, although some d^6 and d^8 fluoro alkylimido complexes of iridium have been reported.[17]

Most structurally characterised imido complexes contain metals from Groups 5, 6, 7 and 8, although there are examples from most other groups, with recent reports of terminal imido complexes of all the Group 4 metals.[18] The most common metal-imido species are those from the second and third row metals; only more recently have first row imido complexes become more prevalent Horton having reported a number of vanadium mono- and bis (imido) species.[19]

Bonding mode **2** is thought to arise when bending of the imido unit occurs, leaving formally a lone pair of electrons on nitrogen, reducing the metal-nitrogen bond order. Bending is expected when the metal does not possess two vacant π-symmetry orbitals, i.e. when the donation of the nitrogen lone pair would force the metal to exceed the 18 electron count predicted by the effective atomic number rule,[2,20] or when occupation of destabilising antibonding orbitals would result.

Despite this argument, there is only one example of a structurally characterised "bent imido" ligand, namely $Mo(NPh)_2(S_2CNEt_2)_2$,[21] Figure 1.2. This complex has phenyl imido ligands in both geometries **1** (Mo-N-C bond angle 169.4(4)°) and **2** (Mo-N-C bond angle 139.9(4)°), and was thus described as having one nitrogen-metal triple bond (Mo-N = 1.754Å) and one double bond (Mo-N = 1.789Å), using the three d-orbitals of π-symmetry available at the metal centre.

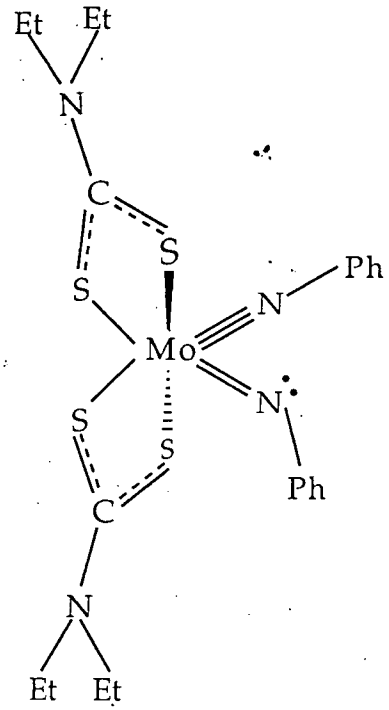

Figure 1.2
The molecular structure of $Mo(NPh)_2(S_2CNEt_2)_2$.

However, 20 electron complexes have recently been reported in which the M-N-C bond angle lay well within the limits usually assigned for *linear* imido ligands (161 to 180°)[2]. Schrock's trigonal planar Os(N-2,6-$^{i}Pr_2C_6H_3)_3$[22] complex possesses three imido ligands with Os-N-C bond angles of 178.0(5)° and 180° (by symmetry); furthermore, both $Cp^*_2Ta(NPh)(H)$,[23] and $Cp_2Zr(N^tBu)(THF)$[24] display near-linear M-N-C bond angles. All three complexes question the validity of the argument that linear (or near-linear) species are indicative of electron pair donation from nitrogen to the metal centre to form triple bonds. For the three complexes cited above, the electrons have been proposed to lie in nitrogen based non-bonding orbitals, thus alleviating the high metal electron count.

Recent work has focused upon the use of imido and oxo ligands to stabilise metal centres in high oxidation states,[2,25] a property due in part to their ability to participate in extensive ligand-to-metal π donation. The imido ligand has the advantage of being able to control stereoelectronic effects through choice of the organoimido substituent. For example, bulky substituents can reduce the tendency for imido-bridge formation, which often leads to oligomeric or cluster species for analogous oxo systems of the early transition metals.[26] The bulky 2,6-diisopropylphenyl substituent has proved particularly useful in stabilising low-coordinate and in some

cases highly reactive mononuclear metal fragments.[22] Other more spherically bulky substituents such as the tert-butyl group can also maintain a mono-nuclear geometry, the unusual "pogo-stick" complex Cp*Ir(N^{t}Bu) being an excellent example.[27] There are, however, a number of complexes that contain bridging tert-butyl imido and aryl imido ligands (structure 3, Figure 1.1).[28]

The imido moiety differs from its isoelectronic oxo counterpart in that:

a) Complexes containing the imido ligand are in general more soluble in hydrocarbon solvent.

b) The effects on a particular complex caused by changes in multiple bonding are more pronounced than for the oxo derivatives due to the lower electronegativity of nitrogen versus oxygen.[20]

c) The organic substituent provides a convenient probe of both bonding and electron distribution using ^{1}H, ^{13}C, ^{15}N NMR and crystallography.[21,29]

Just as a *spectator ligand effect* was observed for some di-oxo containing complexes, so imido groups have been postulated to exhibit a similar phenomenon. The reaction shown in Scheme 1.2 is more favoured than the analogous reaction involving Mo(X)Cl$_4$.[12]

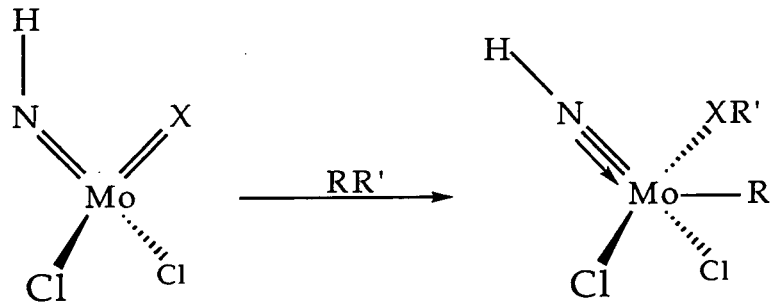

Scheme 1.2 *Imido ligand spectator effect.*

It was proposed that the smaller spectator effect of an imido may prove advantageous in Lewis acid-free metathesis catalysts, an effect borne out by well-defined olefin metathesis initiators reported by Schrock and co-workers;[30] this system possesses an ancillary 2,6-

diisopropylphenylimido unit cis to the important alkylidene ligand, Figure 1.3.

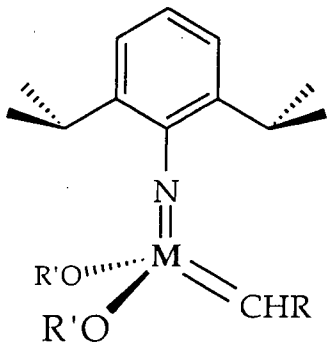

Figure 1.3
Schrock's well-defined ROMP initiator
(M= Mo, W; R= CMe_3, CMe_2Ph; R'= CMe_3, CMe_2CF_3, $CMe(CF_3)_2$, $CF_2CF_2CF_2CF(CF_3)_2$).

1.3 Tertiary Phosphine Complexes

Tertiary phosphines (PR_3) have found use in many areas of transition metal chemistry, for a variety of reasons:

a) They are one of the few classes of ligands in which electronic and steric factors can be varied in a systematic way over a very wide range, through variation in R; both these contributions have been quantified by Tolman.[31, 32]

b) They are known to bind elements throughout the transition series.

c) The ^{31}P nucleus has nuclear spin = $\frac{1}{2}$, 100% natural abundance and good receptivity, all of which facilitate study by NMR spectroscopy.

Coordination of tertiary phosphines to transition metals permits structural and electronic modifications to the metal environment, thus influencing the reactivity at the metal centre. The influence exerted by tertiary phosphines can be attributed to :

a) The coordinative stabilisation and solubilisation of low nuclearity, transition metal fragments.

b) The generation of a labile coordination sphere, either through association/dissociation of the phosphine ligands themselves, or through their influence on the coordinating ability of attendant ligands.

c) The stabilisation of an exceptionally wide variety of catalytically important ligands of interest both in the laboratory and industrially, as their phosphine complexes $(R_3P)_nM\text{-}L$, eg. H_2, CO, CO_2, olefins and acetylenes.

1.4 Complexes of π - Bound Olefins and Acetylenes

1.4.1 Metal Olefin Complexes

The first transition metal complex containing an unsaturated hydrocarbon ligand, the so-called Zeise's salt, $K[PtCl_3(C_2H_4)].H_2O$, was synthesised as early as 1837, although it wasn't until the 1950's that the actual structure was established.

The interaction of an olefin or an acetylene with a transition metal centre consists of both a σ and a π component, and bears similarity to carbon monoxide coordination. The best bonding picture is generally accepted as being the Dewar-Chatt-Duncanson model,[33] which involves donation of the C=C π electrons to an empty dσ orbital on the metal, accompanied by back donation from a filled metal dπ orbital into the C=C π* level, as shown in Figure 1.4. As is the case for CO, a σ bond is insufficient on its own to stabilise the complex.

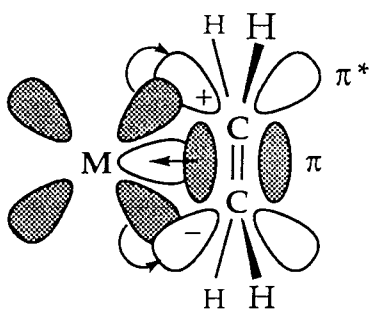

Figure 1.4 *Dewar-Chatt-Duncanson model of metal-olefin bonding.*

The electronic environment of the metal dictates the structure and reactivity of the resulting complexes. The more electron rich metal centre

[formally Pt(0)] shown in Figure 1.5b, reveals a correspondingly longer C=C bond than in Zeise's salt itself (Figure 1.5a), in which M-L σ bonding predominates. In strongly π basic complexes such as $Pt(PPh_3)_2(C_2H_4)$ the metal olefin system is usually considered as approaching the metallacyclopropane extreme.

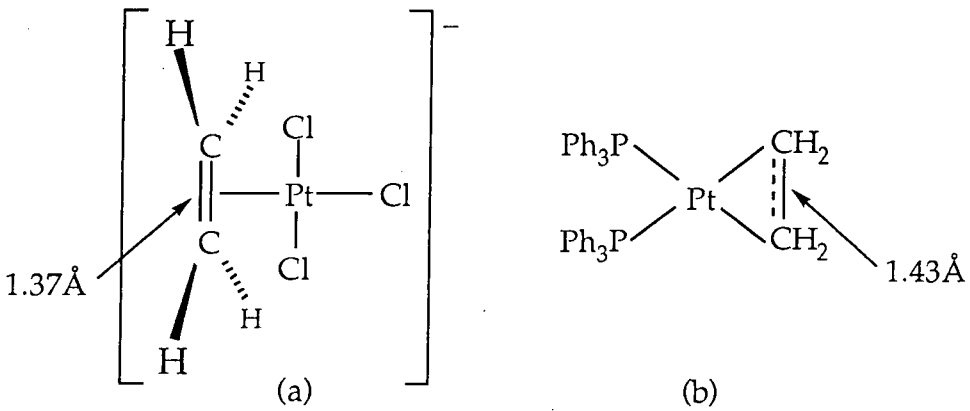

Figure 1.5

Π-backbonding also causes the hybridisation of the olefinic carbons to approach sp^3, forcing the substituents to bend away from the metal upon coordination. Metal complexes that contain unsymmetrical α-olefins exhibit metal-olefin carbon bonds lengths that differ significantly *via* "slip distortion". The metal-carbon bond length to the substituted olefinic carbon is usually longer than to the unsubstituted carbon.[33]

Coordination of an olefin by transition metals often renders the olefin inert towards cycloaddition and catalytic hydrogenation, provided the metal is coordinatively saturated. However, both nucleophilic and electrophilic reagents can attack coordinated olefins. Normally, free olefins are not susceptible to nucleophilic attack, but when complexed to metals in relatively high oxidation states (II to IV) in cationic systems, nucleophilic addition is possible. In contrast, complexes with the metal in a low formal oxidation state tend to react like metallacyclopropanes, and are attacked by electrophiles such as protons at electron-rich metal-carbon σ bonds.

1.4.2 Metal Acetylene Complexes

The coordination of acetylenes to transition metal centres is broadly similar to olefins, but being more electrophilic, they tend to encourage

back donation and bind more strongly. Upon coordination the acetylenic substituents tend to distort towards the geometry of a cis-olefin (typically bending by 30-40°), with M-C bond distances that are slightly shorter than in a corresponding olefin complex. Often the metallacyclopropene model is the most appropriate description of metal-acetylene bonding.

As for olefins, acetylenes can be treated by the Dewar-Chatt-Duncanson model, although they have two bonding and two antibonding π symmetry orbitals. Thus, acetylenes, formally neutral two electron σ donors can also behave as two electron π donors, using the perpendicular π orbital.

As a consequence, acetylenes can appear to form coordinatively unsaturated metal complexes, although it is likely that the acetylene is using its second C=C π bonding orbital making it a *four* electron donor.[34] A good example is $W(CO)(PhC{\equiv}CPh)_3$,[35] Figure 1.6a. Depending on whether the acetylene is classed as a two or four electron donor, this complex is either a 14 or 20 electron complex, respectively. But, one combination of π orbitals, Figure 1.6b, finds no symmetry match among the metal d orbitals, making the true electron count 18.

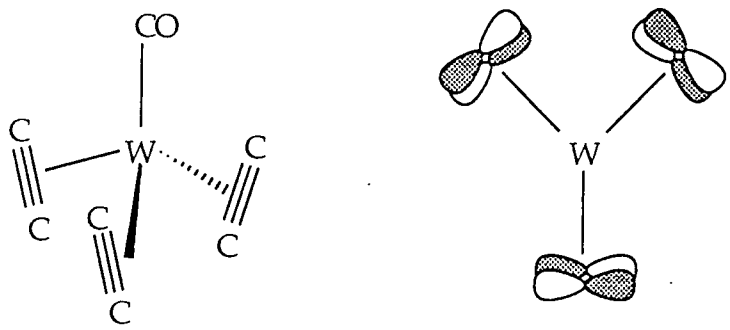

(a) (b)

Figure 1.6 *Acetylenic substituents omitted for clarity.*

Yet, complexes have been characterised in which the acetylene donates an intermediate number of electrons to the overall metal count; for example in the complex $[CpMo(CO)_2(MeC{\equiv}CMe)]^+$ the acetylene is acting as a three electron donor.[36] An extensive study of acetylene complexes has been performed using ^{13}C NMR spectroscopy to quantify the degree of electron donation from the ligand.[37] Furthermore, acetylenes can readily bridge two metal centres, acting as a two electron donor to each. The geometry of the resulting complex can be described as

two interconnected metallacyclopropanes, or a tetrahedrane. Figure 1.7 shows the two bonding extremes.[38]

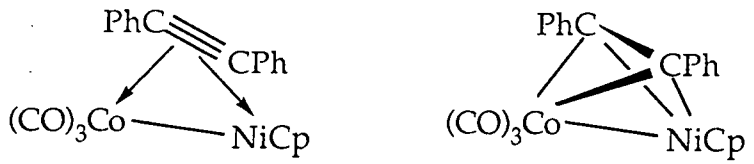

(a) (b)

Figure 1.7

Certain strained cycloalkynes that are unstable in the free state have been stabilised by complexation in tertiary phosphine containing metal compounds. For example, cyclohexyne and cycloheptyne have been "trapped" in the complexes (a)[39] and (b)[40] in Figure 1.7. In both cases the coordinated acetylene is best viewed as a metallacyclopropene complex.

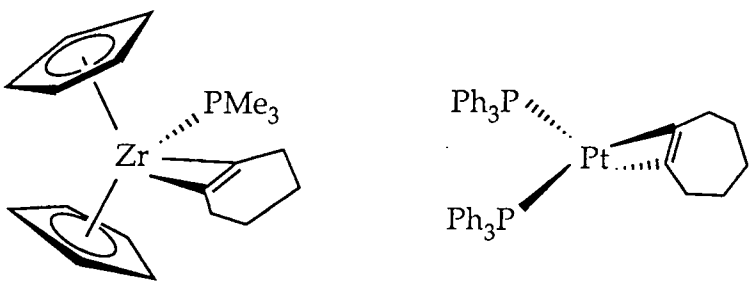

(a) (b)

Figure 1.8

1.5 Alkylidene Complexes

The terms carbene and alkylidene refer to complexes that contain a formal M=C double bond. The latter description is used to define carbenes which possess only alkyl substituents. Carbenes in general differ from both oxo and imido ligands being *single faced* π donors, and as such can only form one metal ligand π bond. This limits the metal carbon bond order to a maximum of two, i.e. a double bond.

Conventionally the two types of carbene ligand are distinguished as Fischer carbenes[41] and Schrock alkylidenes.[42] The former are electrophilic in nature and are viewed as singlet carbenes, Figure 1.9b, donating a pair of electrons *via* an sp^2 hybrid orbital, while receiving back-donation from the

electrons *via* an sp^2 hybrid orbital, while receiving back-donation from the metal into an empty p orbital. They generally occur in low valent complexes and possess π donor substituents such as -OMe on the carbene carbon, and are frequently produced by alkylation of acyl complexes on oxygen.

Figure 1.9a illustrates the nucleophilic Schrock type alkylidene which have triplet ground states as the free carbene. These complexes can be viewed as arising from spin coupling between the carbene triplet state and two electrons on the metal centre. They are frequently found on highly electropositive early transition metals in complexes which are formally electron deficient. The general preparation of such species is by the removal of an α hydrogen atom from an alkyl ligand.[30]

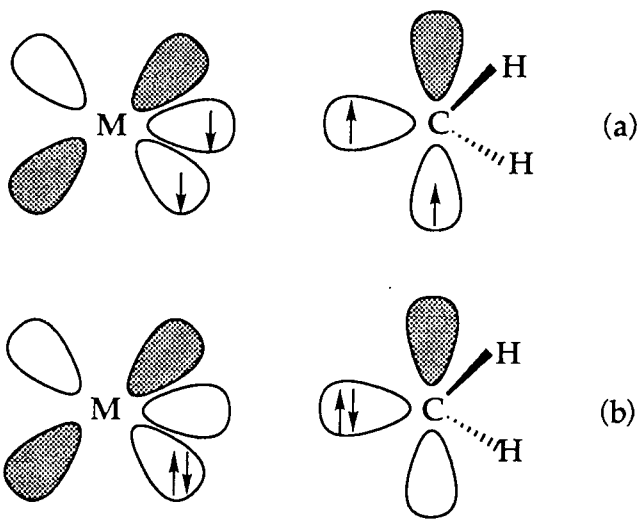

Figure 1.9 *(a) Nucleophilic Schrock alkylidene, (b) Electrophilic Fischer carbene.*

If one of the two substituents is hydrogen (-$[CRH]^{2-}$), then generally a highly distorted geometry is observed in the solid state. Typically the M-C-C framework is nearly linear, typically 160°; the M-C-H angle is quite small, 90° or less, and the C-H distance is significantly lengthened compared to that expected for sp^2 hybridised carbon. Spectroscopically this distorted geometry manifests itself by an unusually low ν(C-H), and an unusually low ^{13}C-^{1}H coupling constant of typically 100 Hz or less.[43] This distortion results from interaction of the C-H bond with the coordinatively unsaturated metal centre, in what is generally referred to as an "agostic" manner.[44]

1.6 References

1. W.A. Herrmann, *Angew. Chem., Int. Ed. Engl.*, 1986, **25**, 56; R.A. Sheldon and J.K. Kochi, *"Metal Catalysed Oxidations of Organic Compounds"*, Academic Press, New York, 1981.
2. W.A. Nugent and J.M. Mayer, *"Metal Ligand Multiple Bonds,"* Wiley, New York, 1988.
3. J.M. Mayer, T.H. Tulip, J.C. Calabrese, E. Valencia, *J. Am. Chem. Soc.*, 1987, **109**, 157.
4. J.M. Mayer, D.L. Thorn, T.H. Tulip, *J. Am. Chem. Soc.*, 1985, **107**, 7454.
5. L. Roeker, T.J. Meyer, *J. Am. Chem. Soc.*, 1986, **108**, 4066.
6. M.E. Marmion, K.J. Takeuchi, *J. Am. Chem. Soc.*, 1986, **108**, 510.
7. D.W. Pipes, T.J. Meyer, *Inorg. Chem.*, 1986, **25**, 3256.
8. E. Valencia, B.D. Santarsiero, S.J. Geib, A.L. Rheingold, J.M. Mayer, *J. Am. Chem. Soc.*, 1987, **109**, 6896.
9. J.M. Mayer, *Comments Inorg. Chem.*, 1988, **8**, 125.
10. K.B. Wiberg, *"Oxidation in Organic Chemistry,"* Part A, Academic Press, New York, 1965, pp69-184.
11. J.P. Collman, L.S. Hegedus, J.R. Norton, and R.G. Finke, *"Principles and Applications of Organotransition Metal Chemistry,"* University Science Books, California, 1987.
12. A.K. Rappé and W.A. Goddard, *J. Am. Chem. Soc.*, 1982, **104**, 448; A.K. Rappé and W.A. Goddard, *J. Am. Chem. Soc.*, 1982, **104**, 3287; J.A. Allison and W.A. Goddard, *A.C.S. Symposium Series* "Solid State Chemistry in Catalysis", 1985, **25**, 279.
13. See for example: W.A. Nugent and B.L. Haymore, *Coord. Chem. Rev.*, 1980, **31**, 123; R.R. Schrock, R.T. DePue, J. Feldman, K.B. Yap, D.C. Yang, W.M. Davis, L. Park, M. DiMare, M. Scofield, J.T. Anhaus, E. Walborsky, E. Evitt, C. Kruger and P. Betz, *Organometallics*, 1990, **9**, 2262 and references therein; R.R. Schrock, J.S. Murdzek, G.C. Bazan, J. Robbins, M. DiMare, and M. O'Regan, *J. Am. Chem. Soc.*, 1990, **112**, 3875; L.M. Atagi, D.E. Over, D.R. McAlister, and J.M. Mayer, *J. Am. Chem. Soc.*, 1991, **113**, 870; R.R. Schrock, S.A. Krouse, K. Knoll, J. Feldman, J.S. Murdzek, and D.C. Yang, *J. Mol. Catal.*, 1988, **46**, 243; G.R. Clark, A.J. Nielson, C.E.F. Richards and D.C. Ware, *J. Chem. Soc. Chem. Commun.*, 1989, 343; J.T. Anhaus, T.P. Kee, M.H. Schofield, and R.R. Schrock, *J. Am.*

Chem. Soc., 1990, **112**, 1642; D.N. Williams, J.P. Mitchell, A.D. Poole, U. Siemeling, W. Clegg, D.C.R. Hockless, P. A. O'Neil, and V.C. Gibson, *J. Chem. Soc. Dalton Trans.*, 1992, 739.

14. J.N. Allison and W.A. Goddard, *ACS Symposium Series*, 1985, **279**, 23; L. Kihlborg, *Arkiv Kemi*, 1963, **21**, 357; J. Belgacem, J. Kress, and J.A. Osborn, *J. Chem. Soc. Chem. Commun.*, 1993, 1125.
15. See for example: J.D. Burrington, C. Kartisek, and R.K. Grasselli, *J. Catal.*, 1984, **87**, 363; D.M.T. Chan and W.A. Nugent, *Inorg. Chem.*, 1985, **24**, 1422; D.M.T. Chan, W.C. Fultz, W.A. Nugent, D.C. Roe, and T.H. Tulip, *J. Am. Chem. Soc.*, 1985, **107**, 251.
16. J. Chatt, J.R. Dilworth, and R.L. Richards, *Chem. Rev.*, 1978, **78**, 589; D. Mansuy, P.Battioni and J.P. Mayer, *J. Am. Chem. Soc.*, 1982, **104**, 4487.
17. M.J. McGlinchey and F.G.A. Stone, *J. Chem. Soc. Chem. Commun.*, 1970, 1265; J. Ashley-Smith, M. Green, N. Mayre and F.G.A. Stone, *J. Chem. Soc. Chem. Commun.*, 1969, 409; J. Ashley-Smith, M. Green, and F.G.A. Stone, *J. Chem. Soc. Dalton Trans.*, 1972, 1805.
18. H.W. Roesky, H. Voelker, M. Witt, M. Noltemeyer, *Angew. Chem. Int. Ed. Engl.*, 1990, **29**, 669; C.C. Cummins, G.D. Van Duyne, C.P. Schaller, and P.T. Wolczanski, *Organometallics*, 1991, **10**, 164; R.D. Profilet, C.H. Zambrano, P.E. Fanwick, and I.P. Rothwell, *Abstracts of Papers*, 201st National Meeting of the American Chemical Society; Washington, DC, 1991; INOR 321.
19. A.D. Horton and J. deWith, *Angew. Chem., Int. Ed. Engl.*, 1993, **32**, 903; J. deWith, A.D. Horton and A.G. Orpen, *Abstracts of the American Chemical Society*, 1992, 204, Aug., p68.
20. W.A. Nugent and B.L. Haymore, *Coord. Chem. Rev.*, 1980, **31**, 123.
21. B.L. Haymore, E.A. Maata and R.A.D. Wentworth, *J. Am. Chem. Soc.*, 1979, **101**, 2063.
22. J.T. Anhaus, T.P. Kee, M.H. Schofield, and R.R. Schrock, *J. Am. Chem. Soc.*, 1990, **112**, 1642; M.H. Schofield, T.P. Kee, J.T. Anhaus, R.R. Schrock, K.H. Johnson, and W.M. Davis, *Inorg. Chem.*, 1991, **30**, 3595.
23. G. Parkin, A. van Asselt, D.J. Leahy, L. Whinney, W.G. Hua, R.W. Quan, L.M. Henling, W.P. Schaefer, B.D. Santarierso, and J.E. Bercaw, *Inorg. Chem.*, 1992, **31**, 82.
24. P.J. Walsh, F.J. Hollander, and R.G. Bergman, *J. Am. Chem. Soc.*, 1988, **110**, 8729; K.A. Jørgensen, *Inorg. Chem.*, 1993, **32**, 1521.

25. M.H. Schofield, T.P. Kee, J.T. Anhaus, R.R. Schrock, K.H. Johnson, and W.M. Davis, *Inorg. Chem.*, 1991, **30**, 3595; D.S. Williams, J. T. Anhaus, M.H. Schofield, R.R. Schrock, and W.M. Davis, *J. Am. Chem. Soc.*, 1991, **113**, 5480; C.C. Cummins, S.M. Baxter and P.T. Wolczanski, *J. Am. Chem. Soc.*, 1988, **110**, 8731; Y. W. Chao, P.M. Rodgers, D.E. Wigley, S.J. Alexander, and A.L. Rheingold, *J. Am. Chem. Soc.*, 1991, **113**, 6326; N. Bryson, M.T. Youinou and J.A. Osborn, *Organometallics*, 1991, **10**, 3389.

26. See for example: T.P. Kee and V.C. Gibson, *J. Chem. Soc. Chem. Commun.*, 1989, 656.

27. D.S. Glueck, F.J. Hollander, and R.G. Bergman, *J. Am. Chem. Soc.*,1989, **111**, 2719.

28. For examples see: D.J. Arney, M.A. Bruck, S.R. Huber, and D.E. Wigley, *Inorg. Chem.*, 1992, **31**, 3749; A. Gutierrez, B. Hussain-Bates, M.B. Hursthouse, and G. Wilkinson, *Polyhedron*, 1990, **9**, 2081; W. A. Nugent and R. L. Harlow, *Inorg. Chem.*,1979, **18**, 2030; D.C. Bradley and E.G. Torrible, *Can. J. Chem.*, 1963, **41**, 134.

29. D.C. Bradley, S.R. Hodge, J.D. Runnacles, M. Huges, J. Mason and R.L. Richards, *J. Chem. Soc. Dalton Trans.*, 1992, 1663.

30. R.R. Schrock, J.S. Murdzek, G.C. Bazan, J. Robbins, M. DiMare, and M.B. O'Regan, *J. Am. Chem. Soc.*, 1990, **112**, 3875; R.R..Schrock, R.T. DePue, J. Feldman, K.B. Yap, D.C. Yang, W.M. Davis, L.Y. Park, M. DiMare, M.H. Schofield, J.T.Anhaus, E. Walborsky, E. Evitt, C. Kruger, and P. Betz, *Organometallics*, 1990, **9**, 2262; J. Feldman and R.R. Schrock, *Progress in Inorganic Chemistry*, Vol. 39, 1; S.J. Lippard, Ed., Wiley and Son, New York, 1991.

31. C.A. Tolman, Chem. Rev., 1977, **77**, 313.

32. A. Pidcock, *"Transition Metal Complexes of Phosphorus, Arsenic, and Antimony Ligands,"* Edited by C.A. McAuliffe, MacMillan, London, 1973.

33. D.M.P. Mingos, *"Bonding of Unsaturated Organic Molecules to Transition Metals,"* in *"Comprehensive Organometallic Chemistry,"* G. Wilkinson, F.G.A. Stone, and E.W. Abel, Eds.; Pergaman, New York, 1982, **3**, 1.

34. K. Tatsumi, R. Hoffmann, and J.L. Templeton, *Inorg. Chem.*, 1982, **21**, 466.

35. R.M. Laine, R.E. Moriarty, and R. Bau, *J. Am. Chem. Soc.*, 1972, **94**, 1402.

36. K. A Mead, H. Morgan, and P. Woodward, *J. Chem. Soc. Dalton Trans.*, 1983, 271.
37. J.L. Templeton, and B.C. Ward, *J. Am. Chem. Soc.*,1980, **102**, 3288.
38. G. Palyi *et al.*, *"Stereochemistry in Organometallic and Inorganic Compounds,"* Vol. 1, I. Bernal, Ed., Elsevier, Amsterdam, 1986; B.H. Robinson, *Organometallics*, 1987, **6**, 1470.
39. S.L. Buchwald, R.T. Lum and J.C. Dewan, *J. Am. Chem. Soc.*,1986, **108**, 7441.
40. M.A. Bennett and T. Yoshida, *J. Am. Chem. Soc.*,1978, **100**, 1750.
41. E.O. Fischer and A. Maasbol, Angew. *Chem. Int. Ed. Engl.*, 1964, **3**, 580.
42. R.R. Schrock, *J. Am. Chem. Soc.*,1974, **96**, 6796.
43. J.P. Collman, L.S. Hegedus, J.R. Norton, and R.J. Finke, *"Principles and Applications of Organotransition Metal Chemistry,"* University Science Books, California, 1987, 130.
44. M. Brookhart and M.L.H. Green, *J. Organomet. Chem.*, 1983, **250**, 395.

Chapter Two- The Preparation and Characterisation of Molybdenum Bis (Imido) Complexes

2.0 Introduction

This chapter is concerned with the synthesis of a range of molybdenum bis (imido) complexes. A general high yield route for the synthesis of such species will be described. During the course of this study a high yield route for the synthesis of $[Cr_2Cl_9]$ $[NHEt_3]$ was developed.

The first imido complex, $Os(N^tBu)(O)_3$, was isolated by Clifford and Kobayashi in 1956.[1] Since then the synthesis of imido complexes has been the focus of a great research effort and a wide variety of methodologies have been employed. Some of the more important, general routes are outlined in the following Sections.[2]

2.1 General Syntheses of Imido Complexes

The simplest approach is to treat a metal oxo complex with a primary amine generating water and the desired imido compound, the reaction proceeding *via* H-atom transfer; an example is given in Scheme 2.0. Similar reactivity is exploited in the treatment of metal chlorides or metal bis-amides $[M(NR'_2)_2]$ with primary amines.

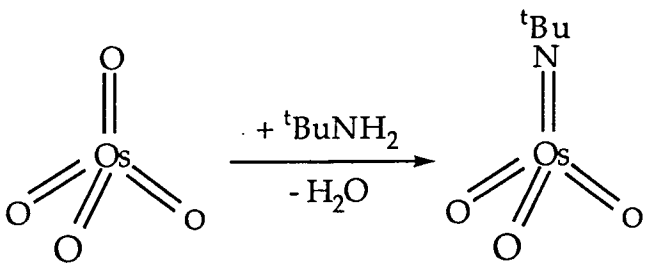

Scheme 2.0.

This general strategy has been exploited by Schrock who has developed a simple one-pot synthesis of molybdenum and rhenium bis (imido) complexes through reaction of a metal oxo salt with an amine a base being used to remove any acid generated *in situ*. Further discussion of this procedure is made in Sections 2.2 and 2.3.

One of the most convenient and widely applicable syntheses employs silylated amine derivatives $[NH(SiMe_3)R$ or $N(SiMe_3)_2R]$ which react cleanly and efficiently with both metal halides and metal oxo complexes (Scheme 2.1), a reaction that is facilitated by the strength of the resultant Si-O or Si-X bonds. This general approach has been utilised to

generate a variety of imido complexes, with examples including $(C_5R_5)M(NR')Cl_2$ (M= Nb, R= H, Me, R'= ^tBu, -2,6-$C_6H_3Pr^i_2$; M= Ta, R= Me, R'= -2-$C_6H_3Pr^i_2$, 6),[3,4] $Mo(N\text{-}2,6\text{-}C_6H_3Pr^i_2)Cl_2.DME$,[5] and $Cr(N^tBu)_2(OSiMe_3)_2$.[6]

$$M{-}O + RN(SiMe_3)_2 \longrightarrow M(NR) + (Me_3Si)_2O$$

$$Cl{-}M{-}O + 2\ RNH(SiMe_3) \longrightarrow Me_3SiO{-}M(NR) + Me_3SiN^+H_2RCl^-$$

Scheme 2.1 *Use of silylated amines for imido synthesis.*

A route that has proved particularly suitable for the formation of a wide variety of imido complexes is an oxo exchange reaction with isocyanates,[7] and to a lesser extent phosphinimines and sulfinylamines, according to Scheme 2.2. One example that is of particular relevance to this thesis is the synthesis of $Mo(N^tBu)_2Cl_2$, which is achieved by treating MoO_2Cl_2 with two equivalents of ^tBuNCO.[8] As for the reaction involving silylated amines, a powerful driving force for this reaction comes from the formation of the side-products which possess very strong bonds, eg. CO_2 or $R_3P{=}O$.

$$M{-}O + RNCO \longrightarrow M(NR) + CO_2$$

$$M{-}O + R'_3PNR \longrightarrow M(NR) + R'_3PO$$

$$M{-}O + RNSO \longrightarrow M(NR) + SO_2$$

Scheme 2.2 *Imido Synthesis via oxo group exchange.*

The mechanism of exchange is thought to proceed in a metathetical manner, ***via*** a four centre metallacyclic intermediate formed during a Wittig-like [2+2] cycloaddition across the isocyanate C=N bond; support for this pathway comes from the isolation of a cyclometallacarbamate, derived from treatment of $Cp_2Mo(O)$ with PhNCO; no loss of carbon dioxide was detected.[9]

The reaction of a halide complex with an alkali metal amide, such as LiNHR (R= alkyl) is a somewhat less widely used approach. Despite this a number of key imido complexes have been isolated from this type of reaction as illustrated in Scheme 2.3. Until recently single-metal

complexes that contained more than one bound imido ligand were restricted to the Group 6-8 metals.[10] However, bis (imido) complexes of Nb and Ta ($M(NAr)_2Cl(py)_2$) have been reported which were synthesised by treating $M(NEt_2)_2Cl_3(OEt_2)$ (M= Nb or Ta) with two equivalents of LiNHAr in the presence of pyridine.[11]

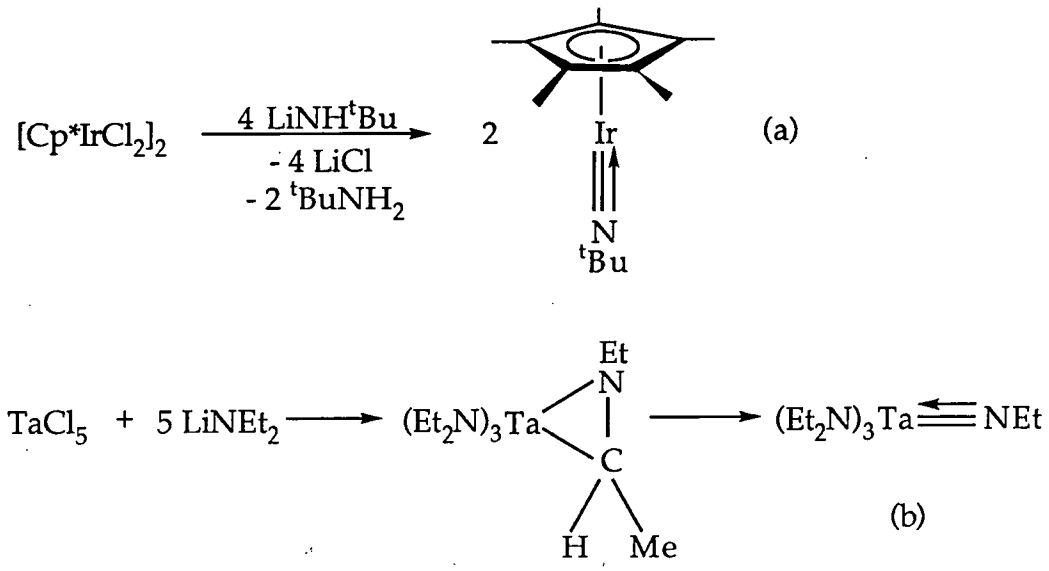

Scheme 2.3 *(a) Synthesis of a novel "Pogo-Stick" complex,*[12] *(b) synthesis of one of the first fully characterised imido complexes.*[13]

Organic azides are known to react with low valent coordinatively unsaturated mononuclear transition metal complexes generating imido species; the formation of the stable dinitrogen molecule supplying a large driving force. Many different azides have been employed; this includes $CF_3CFHCF_2N_3$,[14] Me_3SiN_3, $H_5C_6N_3$, *p*- $MeC_6H_4N_3$, and $H_5C_2N_3$. A useful reaction of this general type is illustrated in Scheme 2.4.

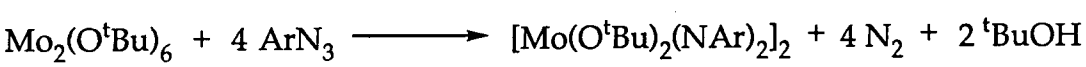

Scheme 2.4 *Synthesis of a binuclear complex bearing both bridging and terminal imido ligands.*[15]

2.1.1 General Syntheses of Group 6 Imido and Bis (Imido) Complexes

The syntheses of Group 6 imido complexes in general are not remarkable, the methods outlined in the previous Section are used with varying degrees of success, depending upon the particular system under investigation.

The synthesis of chromium imido complexes is very limited, there having been only two reports of this type of complex. Both involve the use of silicon reagents. The first reaction is encountered more in the literature; chromyl chloride (CrO_2Cl_2) is treated with two equivalents of $^tBuNH(SiMe_3)$ in refluxing heptane to afford $Cr(N^tBu)_2(OTMS)_2$ in high yield.[16] The second reaction allows for the isolation of an unusual dimeric species, which demonstrates a chromium-chromium interaction, Scheme 2.5.[17] To date no other chromium imido complexes have been prepared that contain different imido substituents, hence the chemistry of the lightest member of the Group 6 triad is limited to tert-butyl imido complexes.

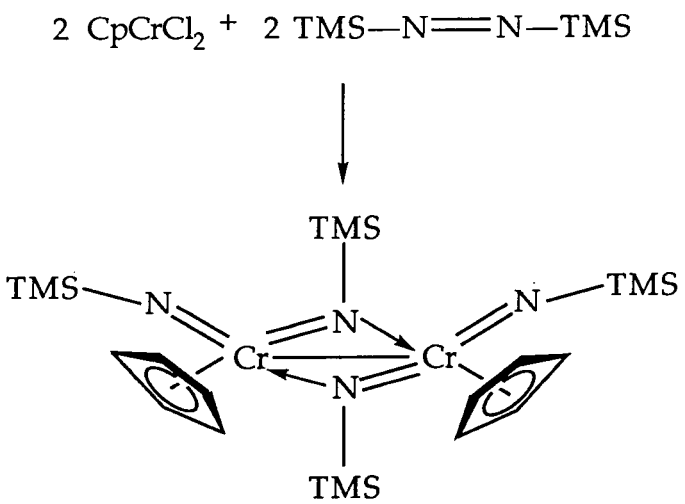

Scheme 2.5

Many syntheses involve either isocyanates, primary amines or silylated amines. The reactions tend to be sensitive to both metal and to organoimido substituent. This is illustrated in Table 2.0 which compares the reactivity of MO_2Cl_2 species with a variety of silylated amines.

MO_2Cl_2	RNH(SiMe$_3$)	Product	Ref.
Cr	^{t}Bu	$Cr(N^tBu)_2(OSiMe_3)_2$	16
Mo	^{t}Bu	$Mo(N^tBu)_2(OSiMe_3)_2$	16
W	^{t}Bu	Unidentified	16
Cr	Ar	Unidentified	16, 18
Mo	Ar	$Mo(NAr)_2Cl_2$.DME	19
W	Ar	$W(NAr)_2Cl_2$.DME	20, ‡
Cr	Adamantyl, Norbornyl	Unidentified	16
Mo	Adamantyl	Unidentified	16
"	Norbornyl	$Mo(NNorbornyl)_2(OSiMe_3)_2$	16
W	Adamantyl, Norbornyl	Unidentified	16

Table 2.0 *Differences observed in the reactivity of MO_2Cl_2 (M= Cr, Mo, W) for a variety of silylated primary amines. ‡ $W(N^tBu)_2Cl_2$.(bipy) has been isolated by another procedure.*[21]

Yet, the use of silylated amine reagents is still a viable route to many different imido containing complexes of molybdenum and tungsten. This strategy has also proved successful in the synthesis of more elaborate imido complexes, such as the novel dimeric mixed imido complex illustrated in Scheme 2.6.

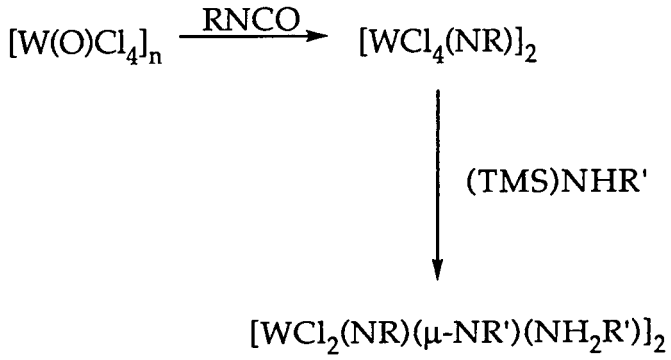

Scheme 2.6 *Synthesis of dimeric tungsten imido complexes containing both bridging and terminal imido ligands. (R= Ph, C_6H_4Me-p, ^{i}Pr, Me; R'= Ph, ^{t}Bu, ^{i}Pr, Et).*[21]

Similarly, the reactivity of Group 6 oxo complexes with isocyanates is dependent upon the organo-substituents of the isocyanate moiety. For example, MoO_2Cl_2 reacts smoothly with ArNCO in THF at 70°C over three days to afford $Mo(NAr)_2Cl_2.THF$,[22] yet the tert-butyl analogue is isolated from a similar reaction as the base-free complex, despite the reaction having been performed in acetonitrile.[8]

In contrast, the reaction of $MoO_2(mes)_2$ with PhNCO affords not the expected product, $Mo(NPh)_2(mes)_2$,[23] but eliminates PhNHCO(mes). The molybdenum containing product is thought to be a dimer species, formed from the insertion of isocyanate into one of the Mo-C σ bonds to the mesityl groups. Yet, other reactions involving PhNCO do react exactly as expected. For example $[CpMo(O)(\mu\text{-}O)]_2$ yields exclusively $[CpMo(NPh)(\mu\text{-}NPh)]_2$.[24]

As described previously (Section 2.1) a whole range of reactions has been exploited to synthesise imido complexes. A number of interesting molybdenum and tungsten examples are collected in Table 2.1, below.

2.2 Synthesis of Bis(imido) complexes of the type $Mo(NR)_2Cl_2.DME$

Preparative routes to bis (imido) complexes are in general less well developed than those for mono-organoimido complexes. The systematic study of the chemistry of molybdenum bis (imido) complexes has recently been facilitated by Schrock's report[31] of a simple, one-pot reaction that readily allows for the synthesis of a variety of organoimido compounds. In this chapter a modified synthetic approach is explored, based on cheaper and more readily available starting materials, and attempts are made to extend this approach to the synthesis of other Group 5 and 6 imido complexes.

2.2.1 Preparation of $Mo(NAr)_2Cl_2.DME$ (1)

Treatment of Na_2MoO_4 with two equivalents of $ArNH_2$ in the presence of both TMSCl and NEt_3 using DME as solvent allowed for the isolation of $Mo(NAr)_2Cl_2.DME$ (1) in excellent yield (typically 90%), Equation 2.1. (1) was found to be analytically pure on removal of solvent

Reactant	Reagent	Product	Ref.
$Mo(O)Cl_2(PMe_2Ph)_3$	$PhC(O)N(H)N(H)Ph$	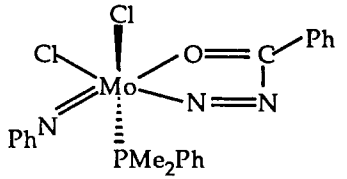	25
$MoCl_4.THF$	$All—N_3$ [All = $(CH_2=CH—CH_2)$-]	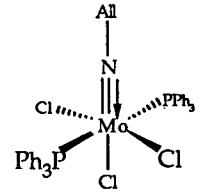	26
η^5-$CpMoCl_4$	RNH_2 (R= ^tBu, ^nPr, Ph)	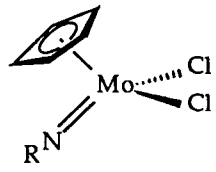	27
$W(O)Cl_4$	$^tBuNH_2$ $Q^+ Cl^-$ {Q = $[NBu^n_4]^+$}	$[W_4O_4Cl_{10}(N^tBu)_4]^{2-}$ $[Q]_2^+$	28
$Mo(NR)(O)(dtc)_2$ (R= tol; dtc= S_2CNEt_2)	0.5 Ph_3P (- Ph_3P=O)	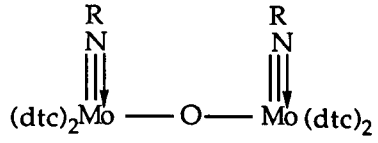	29
$W(NAr)_2Cl_2.(THF)_2$	2 LiNHAr	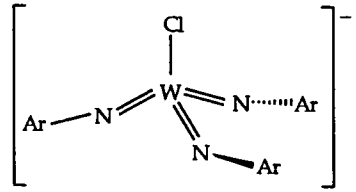	30

Table 2.1 *A summary of some unusual syntheses of Group 6 imido complexes.*

under reduced pressure, and hence required no further purification. The stoichiometry of the reaction is shown in Equation 2.1. The yield of the reaction is enhanced if an excess of TMSCl is employed.

$$Na_2MoO_4 + 2\,RNH_2 + 4\,NEt_3 + 11\,TMSCl \xrightarrow{DME\ /\ 70°C}$$

$$3TMSCl + 4HNEt_3Cl + 4(TMS)_2O + 2NaCl +$$

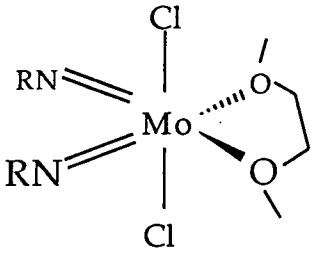

(2.1)

2.2.2 Mechanism of Formation of $Mo(NR)_2Cl_2.DME$

The precise mechanism of this reaction remains unclear. For the analogous rhenium bis (imido) synthesis,[32] equation 2.2, it is thought that the reaction proceeds by attack of the aniline at the metal followed by proton transfer (either directly or stepwise employing the external base) to an oxo ligand yielding the imido species and water. The water subsequently reacts with TMSCl forming TMS_2O and HCl, the latter being removed from the reaction through precipitation of pyridinium hydrochloride; this drives what may otherwise be an equilibrium to the right, as illustrated.

$$0.5\,Re_2O_7 + \begin{matrix}2\,ArNH_2\\7\,TMSCl\\xs.\ py\end{matrix} \xrightarrow[\begin{matrix}-3.5\,(TMS)_2O\\-4\,pyHCl\end{matrix}]{CH_2Cl_2}$$

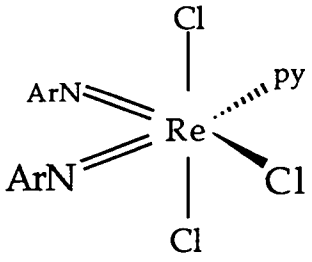

(2.2)

$$0.5\,Re_2O_7 + 9\,{}^tBuNH_2 + 6\,TMSCl \xrightarrow[\begin{matrix}-6\,{}^tBuNH_3Cl\\-2.5\,(TMS)_2O\end{matrix}]{CH_2Cl_2} Re(N^tBu)_3OTMS$$

(2.3)

The general applicability of this synthetic approach is illustrated by the synthesis of a Group 7 tris (imido) $Re(N^tBu)_3(OTMS)$, Equation 2.3. Schrock has demonstrated that initial precipitation of $^tBuNH_3Cl$ occurs with concomitant formation of $Re(N^tBu)_3(OTMS)$, the yield of the tris (imido) being greater than 90% after 20 minutes, but decreasing to only 65% after 2 days. $Re(N^tBu)_2Cl_3$ is thought not to form in this reaction as the HCl that is generated is very efficiently removed by the $^tBuNH_2$, and hence $Re(N^tBu)_3(OTMS)$ is not protonated. However, if the tris (imido) solution is subsequently treated with excess HCl at 0°C a further equivalent of $^tBuNH_3Cl$ is precipitated and $Re(N^tBu)_2Cl_3$ can be isolated.

It is not unreasonable to suppose that a similar mechanism operates for the synthesis of the bis (imido) molybdenum complexes. The TMSCl is thought to act as both chlorinating agent and to remove the water produced during the reaction. Thus, triethylamine must act as both a base, removing the HCl produced as the hydrochloride salt $NHEt_3^+Cl^-$, and as a proton transfer agent.

Despite this rationalisation of the reaction it is not possible to discount the *in situ* formation of a silylated amine species, RNH(TMS), which subsequently reacts with the metal oxo group, although it is thought that attack of the bulky silylated amine would be much slower than for the primary amine itself for steric reasons. The use of silylated amine reagents is well documented for the synthesis of molybdenum bis (imido) complexes of this type, and for many other metal imido complexes, (Section 2.1).

To investigate the possibility of silylated amine reagents being generated *in situ*, Na_2MoO_4 was treated with triethylamine, followed by two equivalents of $^tBuNH(TMS)$ in DME. The reaction was stirred efficiently at 70°C for 18 hours. On work-up no $Mo(N^tBu)_2Cl_2$.DME was recovered, which tends to discount the intermediacy of silylated amines.

Treatment of the hydrated sodium molybdate salt, $Na_2MoO_4.2H_2O$, with 2, 6-diisopropylphenyl amine in the presence of NEt_3 and a large excess of TMSCl, to remove the two waters of crystallisation, led to the formation of an impure oil.[33] ^1H NMR indicated the formation of what was thought to be the mono-siloxide species $Mo(NAr)_2(Cl)(OTMS)$, the only other species observed being unreacted starting materials. The formation of this complex was thought to have occurred through reaction of the proposed hydroxide intermediate with TMSCl; thus, the presence of

this mono-siloxide species supports the intermediacy of a protonated oxo group.

2.2.3 General Preparation of Complexes of the Type $Mo(NR)_2Cl_2.DME$

An analogous procedure to that described in Section 2.2.1 has been utilised to prepare a range of other complexes containing a variety of organoimido substituents; these complexes are shown in Table **2.2**.

Imido Substituent	Yield (%)
tert-Butyl	95
Adamantyl[34]	61
2, 6-Dichlorophenyl	50
2-*tert*-Butylphenyl[35]	98
Phenyl	98
Pentafluorophenyl[34]	60

Table 2.2 *Complexes of the type $Mo(NR)_2Cl_2.DME$ synthesised from the reaction of the corresponding primary amine RNH_2 with Na_2MoO_4.*

2.3 Preparation of Complexes of the Type $Mo(NR)(NR')Cl_2.DME$

Recent work within this group has shown that it is possible to synthesise a range of mixed bis (imido) complexes, of the type $Mo(NR)(NR')Cl_2.DME$, shown in Table 2.3, using a modification to the synthetic route described in Section 2.2.1, replacing the two equivalents of primary amine with one equivalent of both RNH_2 and $R'NH_2$.

R, R'	Yield (%)
Ar, ^tBu	50
Ar, Adamantyl[34]	66.7
C_6F_5, Adamantyl[34]	80
2,6-$C_6H_3Cl_2$, ^tBu[34]	60
C_6F_5, ^tBu[34]	95

Table 2.3 *Mixed imido complexes $Mo(NR)(NR')Cl_2.DME$ (C_6F_5 = Pentafluorophenyl, 2,6-$C_6H_3Cl_2$ = 2,6-dichlorophenyl).*

Previously only a limited number of unsymmetrical bis (imido) complexes of early transition metals have been reported. One such synthesis[21] is that reported for dimeric tungsten bis (imido) complexes of the type $[\{WCl_2(NR)(NR')(NHR')_2\}_2]$ (R=C_6H_5 or C_6H_4Me-4), which were synthesised *via* reaction of the tungsten mono (imido) tetrachloride dimers, $[\{WCl_4(NR)\}_2]$ as described previously (Section 2.1.2).

More recently, this group has reported that the bis (imido) bis (tert-butoxide) complex, **I**, reacts smoothly with 2 equivalents of amine, $R'NH_2$, to afford the mixed imido species **III** and the new bis (imido) species **II**, in a 2:1 ratio,[36] as indicated in Scheme 2.7. The mixed species could be isolated in small quantities.

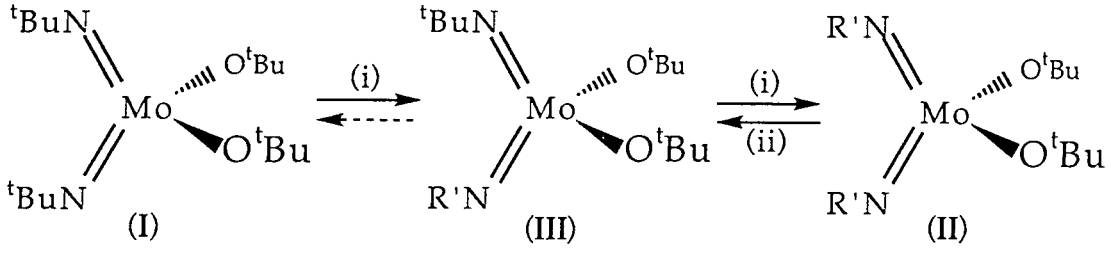

Scheme 2.7 *(i) 2 $R'NH_2$ (R'= Ar), (ii) 2 $NH_2{}^tBu$.*

This exchange reaction is likely to proceed *via* a trigonal-bipyramidal base adduct, Scheme 2.8, which must then undergo a proton transfer to give a bis (amide) intermediate, which to date has not been observed. Both the imido exchange reaction and the formation of the bis (imido) dichloride species described in Section 2.2.1, are believed to proceed *via* this type of protonation and proton transfer mechanism.

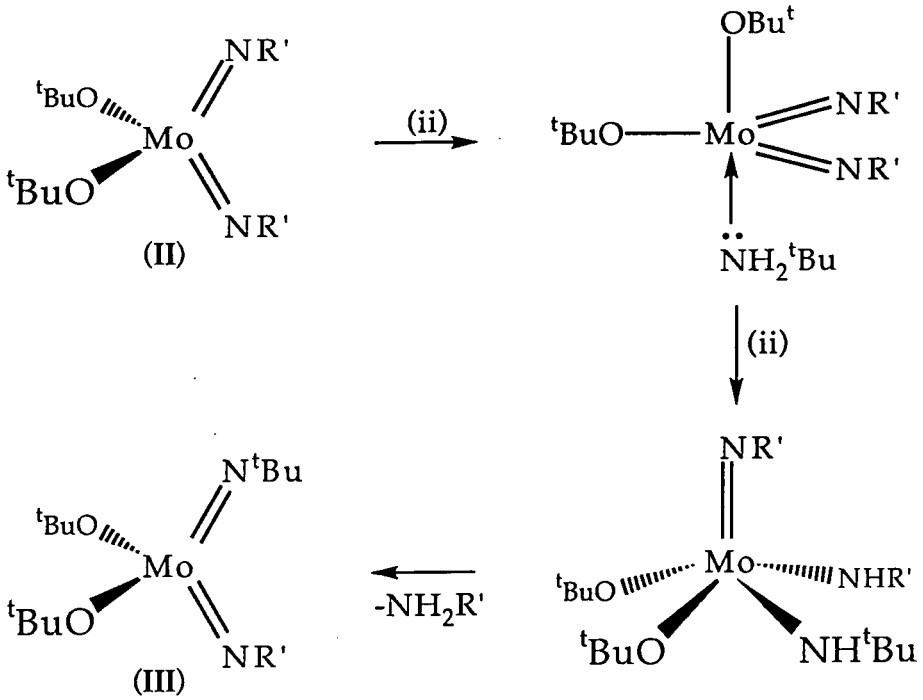

Scheme 2.8 *(i) 2 R'NH$_2$ (R'= Ar), (ii) 2 NH$_2$^{t}Bu.*

2.3.1 Preparation of Mo(NAr)(N^{t}Bu)Cl$_2$.DME (2)

The mixed imido dichloride (2) is readily synthesised from sodium molybdate and one equivalent of both tert-butyl and 2, 6-diisopropylaniline, according to the procedure described in Section 2.2.1.[37] After filtration and removal of solvent *in vacuo* a brick red solid was isolated. ^{1}H NMR of this crude product indicated that all three of the possible products had formed, Mo(NAr)$_2$Cl$_2$.DME, Mo(N^{t}Bu)$_2$Cl$_2$.DME and Mo(NAr)(N^{t}Bu)Cl$_2$.DME (2), in the ratio of 1:2:4 respectively. Subsequent recrystallisation from diethylether at -30°C afforded pure Mo(NAr)(N^{t}Bu)Cl$_2$.DME (2) as a microcrystalline dark orange solid. Further recrystallisation was performed which led to an overall yield of 50%. Repetition of this recrystallisation procedure eventually led to the isolation of an inseparable mixture of both Mo(NAr)(N^{t}Bu)Cl$_2$.DME and Mo(NAr)$_2$Cl$_2$.DME.

2.3.2 The Molecular Structure of $Mo(NAr)(N^tBu)Cl_2.DME$ (2)

Yellow plate-like crystals of (2) suitable for an X-ray structure determination were obtained by recrystallisation of a small (50 mg) sample of the microcrystalline product from a saturated diethylether solution. A crystal of dimensions 0.10 x 0.30 x 0.75 mm was sealed in a Lindemann capillary tube under an inert atmosphere. The structure was determined by Prof J.A.K. Howard, Mr. R.C.B. Copley, and Miss W. Wang within this department. The molecular structure of (2) is shown in Figures 2.0 and 2.1, with relevant bond distances and angles being tabulated in Table 2.4.

Complex (2) was found to adopt a highly distorted octahedral geometry, possessing two mutually cis imido ligands, two approximately trans chloride ligands and a chelating DME group. The Cl-Mo-Cl bond angle deviates markedly from linearity (158.85(2)°),[38] and the N-Mo-N angle of 105.91(9)° is much greater than expected for an octahedral geometry, although it is consistent with other d^0 complexes containing two cis multiply bonded ligands.[39] The relatively small "bite" angle of the chelating DME ligand, 69.29(5)°,[40] is likely to contribute at least partly to this observed distortion, an effect noted by Wentworth *et al.* with chelating dithiocarbamate ligands.[41] Similar asymmetry has been noted in other bis (imido) complexes of the Group 6 triad,[39] and was attributed to repulsion between the π electron density in the two bonds, leading to an opening of the N-Mo-N wedge. More recent theoretical work suggests that this distortion from the ideal 90° octahedral angle is the preferred geometry for the ME_2 fragment; simple repulsion of the two multiply bonded ligands being expected from only a VSEPR type argument.

Bond	Angle (°)
Cl(1)-Mo-Cl(2)	158.85(2)
O(1)-Mo-O(2)	69.29(5)
N(1)-Mo-N(2)	105.91(9)
Cl(1)-Mo-N(1)	95.49(6)
Cl(1)-Mo-O(1)	81.45(4)

Table 2.5 *Selected bond angles for $Mo(NAr)(N^tBu)Cl_2.DME$ (2) showing the distortion from octahedral geometry.*

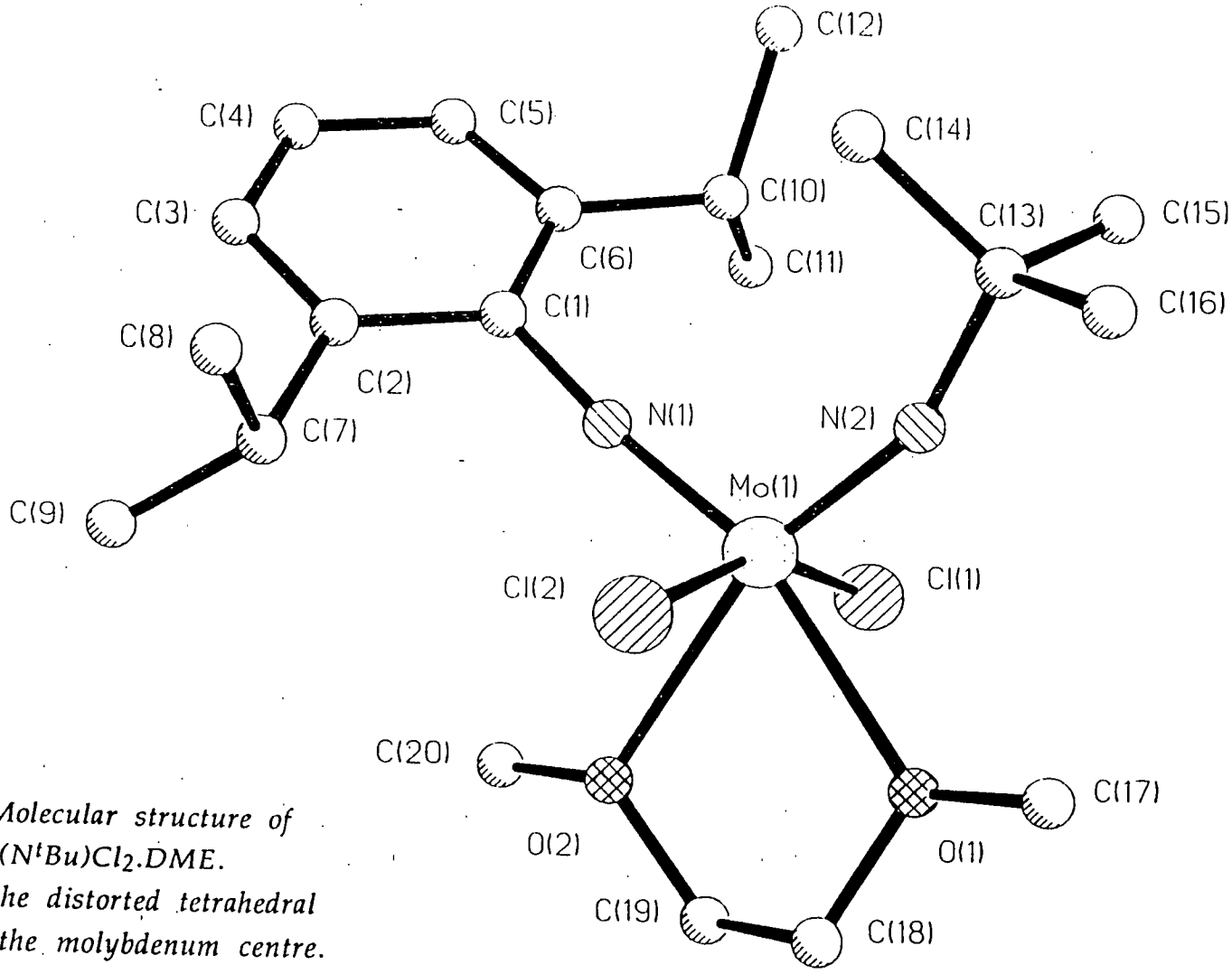

Figure 2.0a *Molecular structure of* $Mo(NAr)(N^tBu)Cl_2.DME$. *View showing the distorted tetrahedral geometry about the molybdenum centre.*

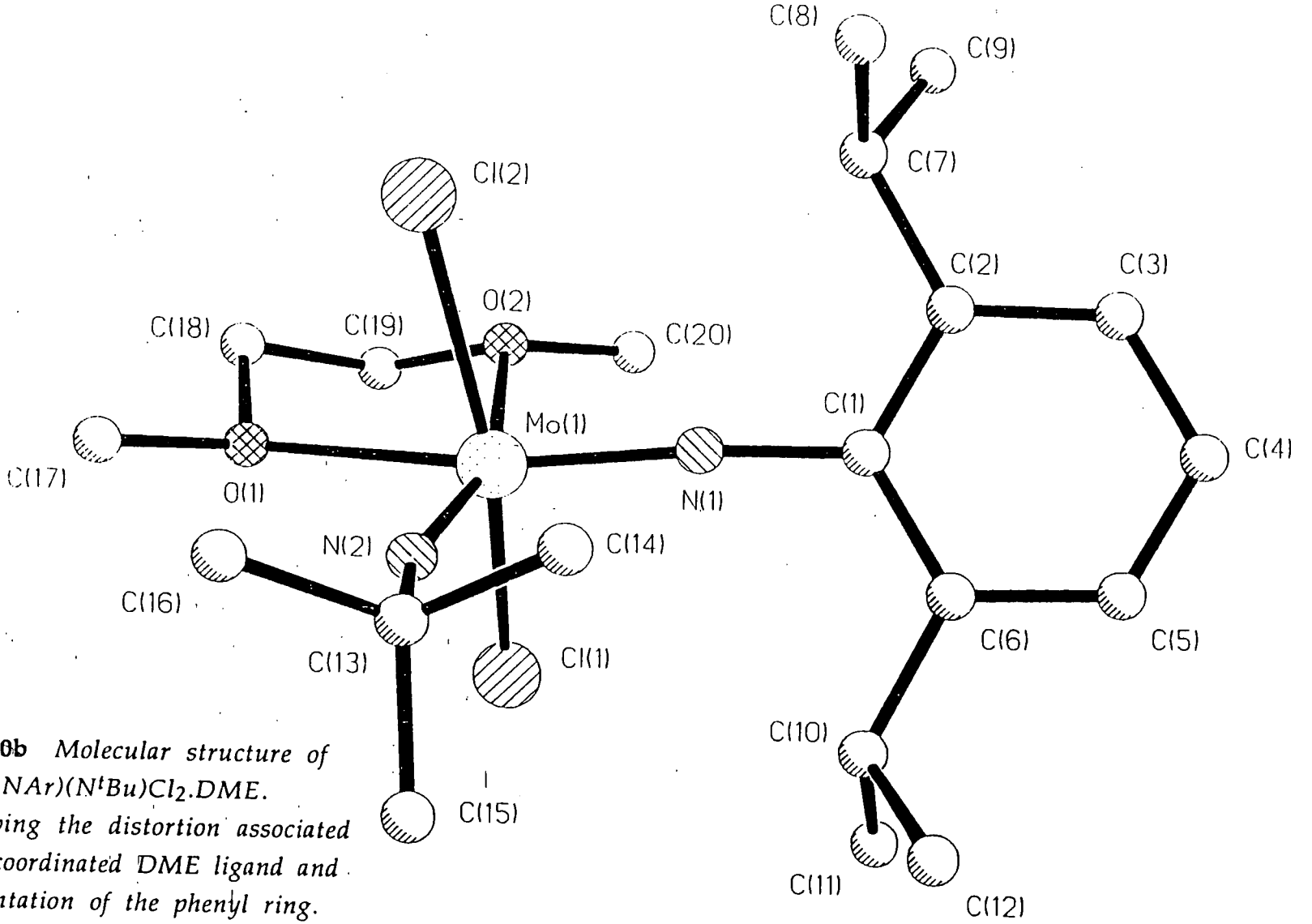

Figure 2.6b *Molecular structure of* $Mo(NAr)(N^tBu)Cl_2.DME$. *View showing the distortion associated with the coordinated DME ligand and the orientation of the phenyl ring.*

Table 2.4 *Selected bond lengths (Å) and angles (°) for $Mo(NAr)(N^tBu)Cl_2.DME$ (2) with estimated standard deviations in parentheses.*

Mo(1) - Cl(1)	2.4010(6)	C(2) - C(3)	1.393(3)
Mo(1) - Cl(2)	2.4085(6)	C(2) - C(7)	1.516(3)
Mo(1) - O(1)	2.330(2)	C(3) - C(4)	1.382(3)
Mo(1) - O(2)	2.392(1)	C(4) - C(5)	1.382(3)
Mo(1) - N(1)	1.753(2)	C(5) - C(6)	1.394(3)
Mo(1) - N(2)	1.728(2)	C(6) - C(10)	1.520(3)
O(1) - C(17)	1.430(3)	C(7) - C(8)	1.526(3)
O(1) - C(18)	1.445(3)	C(7) - C(9)	1.534(3)
O(2) - C(19)	1.442(3)	C(10) - C(11)	1.528(4)
O(2) - C(20)	1.422(3)	C(10) - C(12)	1.536(3)
N(1) - C(1)	1.387(3)	C(13) - C(14)	1.530(3)
N(2) - C(13)	1.452(3)	C(13) - C(15)	1.523(4)
C(1) - C(2)	1.422(3)	C(13) - C(16)	1.522(4)
C(1) - C(6)	1.416(3)	C(18) - C(19)	1.483(3)

Cl(1) - Mo(1) - Cl(2)	158.85(2)	C(2) - C(1) - C(6)	120.9(2)
Cl(1) - Mo(1) - O(1)	81.45(4)	C(1) - C(2) - C(3)	117.9(2)
Cl(1) - Mo(1) - O(2)	80.77(4)	C(1) - C(2) - C(7)	121.6(2)
Cl(1) - Mo(1) - N(1)	95.49(6)	C(3) - C(2) - C(7)	120.5(2)
Cl(1) - Mo(1) - N(2)	98.78(6)	C(2) - C(3) - C(4)	121.4(2)
Cl(2) - Mo(1) - O(1)	81.22(4)	C(3) - C(4) - C(5)	120.2(2)
Cl(2) - Mo(1) - O(2)	81.82(4)	C(4) - C(5) - C(6)	121.2(2)
Cl(2) - Mo(1) - N(1)	97.12(6)	C(1) - C(6) - C(5)	118.2(2)
Cl(2) - Mo(1) - N(2)	94.00(7)	C(1) - C(6) - C(10)	122.3(2)
O(1) - Mo(1) - O(2)	69.29(5)	C(5) - C(6) - C(10)	119.4(2)
O(1) - Mo(1) - N(1)	161.55(7)	C(2) - C(7) - C(8)	110.3(2)
O(1) - Mo(1) - N(2)	92.54(7)	C(2) - C(7) - C(9)	112.3(2)
O(2) - Mo(1) - N(1)	92.27(7)	C(8) - C(7) - C(9)	110.8(2)
O(2) - Mo(1) - N(2)	161.74(7)	C(6) - C(10) - C(11)	111.1(2)
N(1) - Mo(1) - N(2)	105.91(9)	C(6) - C(10) - C(12)	111.3(2)
Mo(1) - O(1) - C(17)	119.8(1)	C(11) - C(10) - C(12)	110.5(2)
Mo(1) - O(1) - C(18)	115.9(1)	N(2) - C(13) - C(14)	108.8(2)
C(17) - O(1) - C(18)	111.3(2)	N(2) - C(13) - C(15)	107.6(2)
Mo(1) - O(2) - C(19)	113.6(1)	N(2) - C(13) - C(16)	107.6(2)
Mo(1) - O(2) - C(20)	121.0(1)	C(14) - C(13) - C(15)	111.2(2)
C(19) - O(2) - C(20)	111.2(2)	C(14) - C(13) - C(16)	110.5(2)
Mo(1) - N(1) - C(1)	174.3(2)	C(15) - C(13) - C(16)	110.9(2)
Mo(1) - N(2) - C(13)	157.9(2)	O(1) - C(18) - C(19)	107.7(2)
N(1) - C(1) - C(2)	118.6(2)	O(2) - C(19) - C(18)	107.2(2)
N(1) - C(1) - C(6)	120.5(2)		

Furthermore, it is impossible to locate two formally *triple* bonds in a *cis*-orientation in an octahedral geometry, there being only 3 $d\pi$ symmetry orbitals available for bonding. Similarly, if both imido ligands are described as bonding to the metal centre through *triple* bonds, then the complex becomes a "formally" 20 electron species. The latter situation can be relieved by locating more of the nitrogen lone pair density on one of the nitrogen atoms. Both these factors must contribute to the distortion in the bond angles for the two imido ligands.

Both the metal-nitrogen bond lengths (Mo=NAr 1.753(2)Å and Mo=N^{t}Bu 1.728(2)Å) are consistent with the two imido ligands bonding to the metal centre *via* pseudo triple bonds; the corresponding bond angles being 174.3(2)° and 157.9(2)° for Mo-N-Ar and Mo-N-^{t}Bu respectively. Often, a low M-N bond order is associated with bending of the M-N-R bond angle, leaving the nitrogen with a lone pair of electrons and hence, sp^2 hybridised (this arises if the imido bond is described in valence bond terms[38]). One would expect that the more basic tert-butyl imido should exhibit the shorter, more linear metal-nitrogen bond, yet in (**2**) it is the shorter more bent of the two imido ligands. This is consistent with the more recently held notion that the angle at the imido nitrogen is not a particularly good indication of lone pair donation.

This apparent lengthening of the aryl imido M=N bond, relative to that for the tert-butyl imido M=N distance, can be rationalised in the following terms. The aryl imido can have some multiple bond character associated with the N-C bond, arising through conjugation with the π system of the aromatic ring (Figure 2.9a). If this is the case, then the Mo-N bond must show a related increase in length. In general terms, this effect is a manifestation of the desire of the nitrogen atom to maintain its valence state. Substituent effects of this type have been observed for Fischer carbyne complexes, in which bonding between a substituent lone pair and the carbyne carbon atom plays a major rôle (Figure 2.9b). Similar changes in metal-ligand and ligand-substituent bond order are well known for metal carbonyl complexes (e.g. M-C≡O vs. M=C=O).

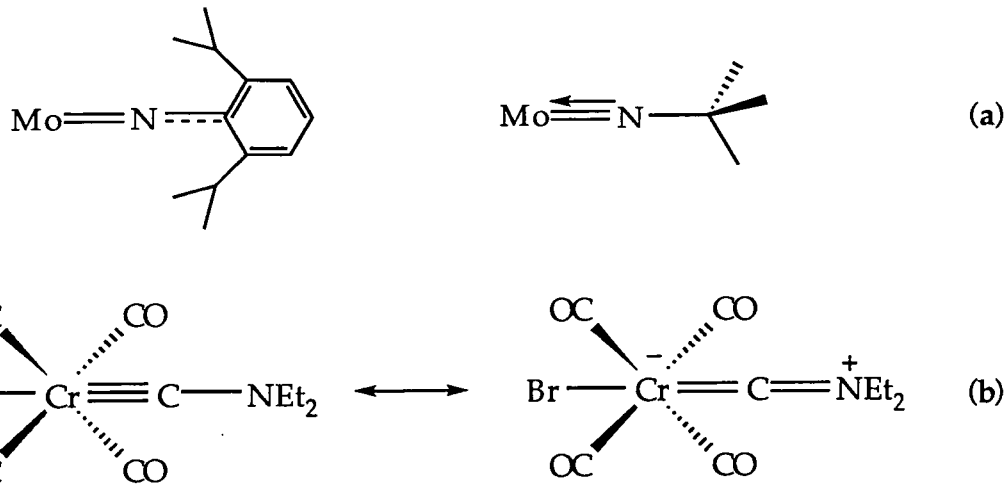

Scheme 2.9 *(a) Conjugation of the ring π system with the metal-ligand π orbitals causes an apparent lengthening of the M=N bond compared with the ^{t}BuN=M bond length. (b) Similar conjugation effects are important for complexes containing Fischer carbynes.*[42]

Examination of a number of other aryl and tert-butyl imido complexes indicates that this trend is quite general (Table 2.6). It is not confined only to molybdenum containing systems, but is readily apparent for other metal imido species (e.g. Nb and Os).

Complex	M=N Dist. (Å)	N-C Dist. (Å)	Refn.
$Mo(NAr)_2(PMe_3)_2$	1.802‡	1.390‡	43
$Mo(NAr)_2(Ph)_2(PMe_3)$	1.770‡	1.397‡	44
$Mo(N^tBu)_2(PMe_3)(C_3H_6)$	1.770‡	1.451‡	44
$Mo(N^tBu)(NAr)Cl_2.DME$	1.728(N^tBu)	1.452	45
	1.753(NAr)	1.387	
$Mo(NAd)(NC_6F_5)(CH_2CMe_2Ph)_2$	1.723(NAd)		46
	1.773(NAr^F)†	1.373	
$CpNb(NAr)(PMe_3)(CHPh)$	1.812	1.387	47
$CpNb(NAr)Cl_2$	1.761	1.408	48
$CpNb(N^tBu)Cl_2$	1.752	1.444	48
$Os(NAr)_3$	1.737‡	1.372‡	49
$[Os(N^tBu)_2(\mu\text{-}N^tBu)]_2$	1.589§	1.443§	50

Table 2.6 *Comparison of M=N and N-C bond distances for complexes containing the tert-butyl and aryl imido ligands. ‡ Average values are quoted; § These distances are for the terminal ligands. † Distortions in the aromatic ring C-C bond lengths were consistent with there being some multiple bond character between the C_{ipso} and N atoms.*

It is believed that the phenyl ring is orientated such that any steric interaction between the isopropyl groups and the adjacent bulky tert-butyl imido are minimised, Figure 2.0b. The strongest π donating imido ligand (shortest Mo-N distance), Mo=N^{t}Bu, is located trans to the longest metal-oxygen bond of the coordinated DME, as expected from consideration of the "trans influence".

Bercaw *et al.* have addressed the problem of whether the imido bond angle is a good indicator of bond order. Their study was based upon the molecular structure determination of $(Cp^*)_2Ta(H)(NPh)$.[51] The metal nitrogen bond was found to be nearly linear (177.8(9)°), with the phenyl group lying neatly in the equatorial plane. The hydride atom was also located and was found to lie in the same symmetry plane between the two Cp* ligands.

The immediate implication from the linear Ta-N-C*ipso* bond was that the nitrogen is *sp* (not sp^2) hybridised. Yet this linearity need *not* necessarily imply a formal triple bond as this would make this a formally 20 electron complex. However, if steric interactions force the phenyl ring into the equatorial plane, a linear Ta-N-C*ipso* bond (*sp*-hybridised N) with a double Ta=NPh bond and the lone pair residing in a nitrogen p-orbital could result (Figure 2.1 (I)). Yet, if the formal linear triple bond (N *sp*-hybridised) is invoked making this moiety a formally 20 electron species (II), then the electron pair on nitrogen would be forced into an orbital that is Ta-Cp* antibonding. Comparison of the Ta-Cp* distances with other *bona fide* 18 electron complexes indicated slight variations in Ta-Cp* distances implying that the Ta=N bond length was intermediate between being a double and a triple bond. Hence, no overall conclusion could be drawn, the actual structure being some intermediate between the two limiting structures, (I) and (II).

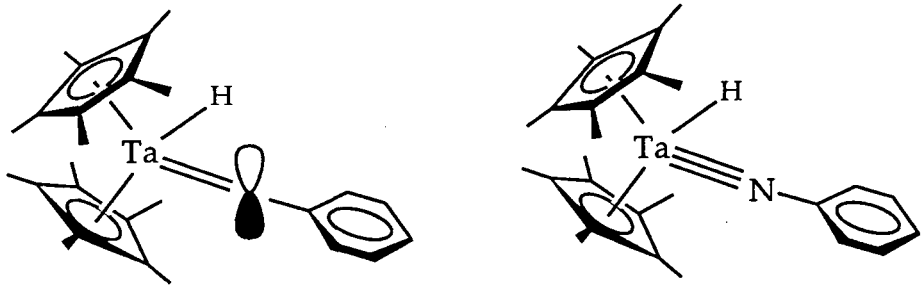

I $Ta{=}\ddot{N}{-}C_6H_5$ II $Ta{\equiv}\overset{+}{N}{-}C_6H_5$

Figure 2.1.

Schrock's novel planar tris-imido complex, $Os(NAr)_3$,[52] which has Os-N-C bond angles that are linear (two of the imidos exhibiting an angle of 178.5° and the third an angle of 180°), would also be a formally 20 electron complex if each imido bonds to the metal through a triple bond. Yet, under D_{3h} symmetry it is possible to construct molecular orbitals that would locate a pair of electrons in a nitrogen-centred non-bonding MO, leaving the metal electron count at 18, a situation that has been supported through SCF-Xα-SW calculations. Once again this description indicates that M-N-C bond angles do not necessarily reflect M-N bond order.

2.3.3 Reactions of Na_2MoO_4 with Primary Diamines

Recently, much research has focused on metallocene complexes in which the two cyclopentadienyl rings are linked through either an alkyl group or a heteroatom, Figure. 2.3; they are used as both model systems and catalysts for Ziegler-Natta type polymerisation and for catalytic and asymmetric induction.[53] These so called *ansa*-metallocene complexes exhibit remarkable iso- or syndiospecificities[54] in the polymerisation of α-olefins, and show novel reactivity, due in part to the control over steric congestion at the metal centre afforded by the variable Cp'-M-Cp' wedge angle[55].

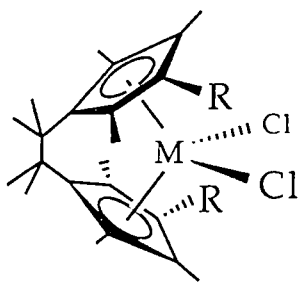

Figure 2.3 *Chiral ansa-metallocene used for the stereospecific polymerisation of α-olefins. (R= $C(Me)_3$, $Si(Me)_3$, $CH_2C_6H_5$; M= Ti, Zr).*[56]

Hence, attempts were made to synthesise the Group 6 bis (imido) analogues of these *ansa*-metallocenes, using the reaction of Na_2MoO_4 with one equivalent of a variety of primary diamines.

2.3.4 Reaction of Na_2MoO_4 with Ethylenediamine

In a reaction analogous to that used for the synthesis of the symmetrical bis (imido) complexes, $Mo(NR)_2Cl_2$.DME, Section 2.2.1, sodium molybdate was treated with one equivalent of ethylene diamine, as in Equation 2.4. On addition of the diamine solution to the stirred reaction mixture an immediate yellow colouration was observed which on heating turned dark brown/black.

$$Na_2MoO_4 + en + 4\,NEt_3 + 11\,TMSCl \xrightarrow{DME} \quad (2.4)$$

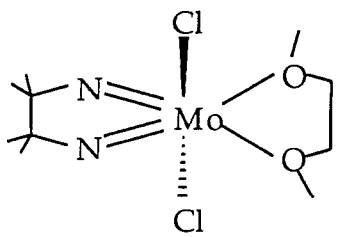

The reaction was left stirring for 12 hours at 70°C, with no further colour change. Upon work-up the reaction afforded an intractable brown solid, which was insoluble in all common NMR solvents. Both elemental analyses and Mass Spectroscopy proved inconclusive as to the nature of this product.

Another attempt to isolate a linked bis (imido) complex was made *via* imido exchange,[36] in which $Mo(N^tBu)_2(O^tBu)_2$ was treated with one equivalent of ethylene diamine in C_6D_6. Unfortunately this led to the formation of a black insoluble material, with both free tert-butylamine and tert-butanol being observed in the ^1H NMR spectrum. This indicated that protonation of both butoxide and imido ligands had occurred, presumably by the accessible acidic α-hydrogen atoms of the diamine itself. Both this intractable black product and the product from equation 2.4 are thought to be molybdenum containing polymeric materials; these were not investigated further .

2.3.5 Reaction of Na_2MoO_4 with 1,8 Diaminonaphthalene

Similar treatment of sodium molybdate with one equivalent of 1, 8 diaminonaphthalene in DME led to the immediate formation of a black

Figure 2.4 *400 MHz ^1H NMR ($CDCl_3$) spectrum showing the product obtained from the reaction of Na_2MoO_4 with 1,8-diaminonaphthalene and how it changes in solution over a period of time; * = Free DME, ◊ $CDCl_3$.*

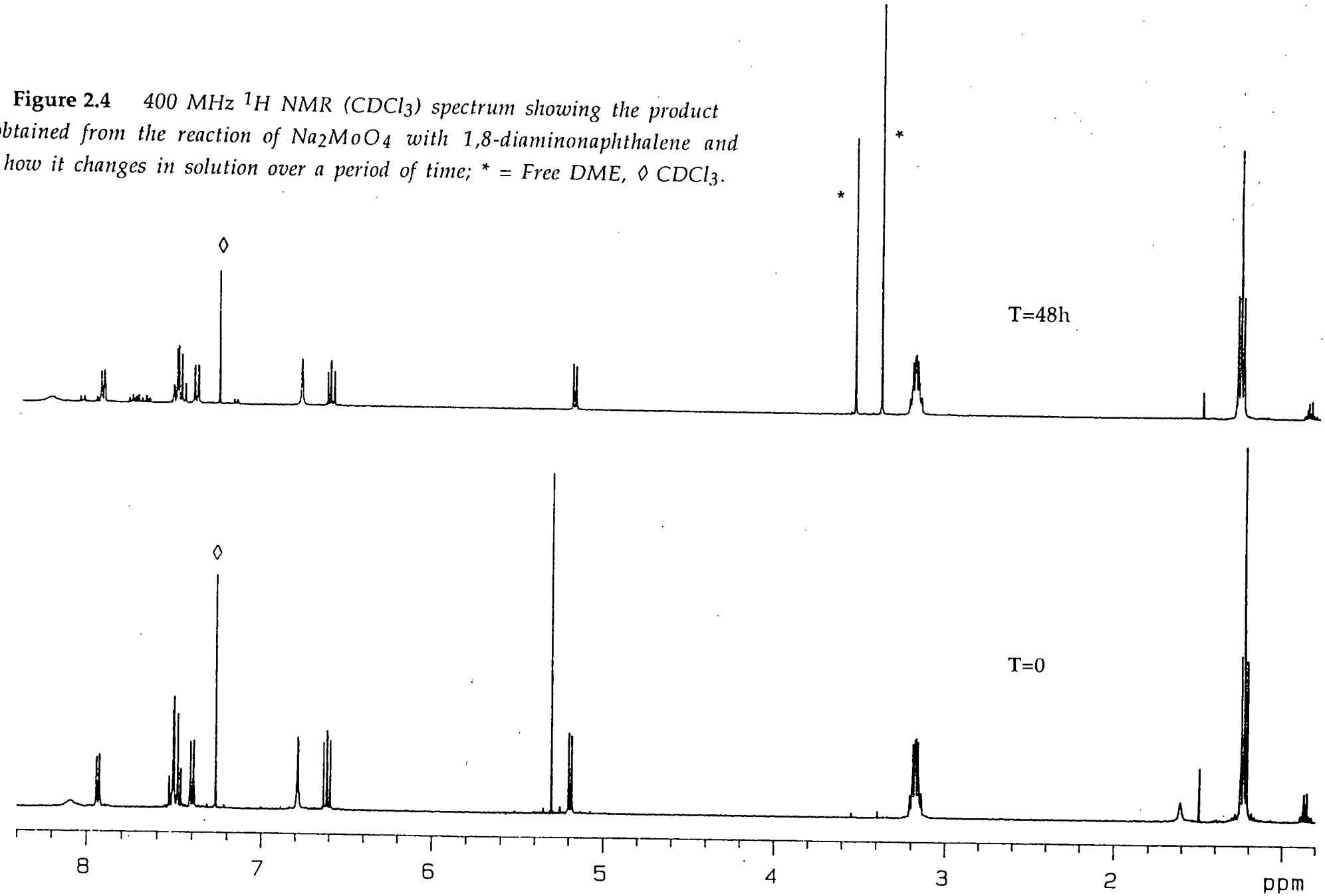

solution, which on work-up gave a clear yellow/orange solution. Recrystallisation from dichloromethane at -30°C afforded 1.8g of a red/brown microcrystalline material. Both NMR (^1H and ^{13}C) and elemental analyses were inconclusive as to the precise nature of the product, although it is likely that the naphthalene has adopted a metal-metal bridging position.

A room temperature C_6D_6 solution of the product evolved DME slowly over 2 days, as illustrated in Figure 2.4, with subsequent rearrangement of the complex. Facile exchange of DME has been observed on the NMR timescale for mononuclear species such as $Mo(NPh)_2Cl_2.DME$[31] and consistent elemental analyses for this complex were thwarted by the lability of the DME. Hence, it is not unreasonable to suppose that similar behaviour could occur here, giving rise to the observed inconsistencies in the elemental analyses. Unfortunately, the complex proved involatile and thus no mass spectrum could be obtained. The isolation of crystals suitable for a molecular structure determination proved elusive, hence the exact nature of the complex is still unknown

2.4 Oxo Anions: Routes to Bis (Imido) Complexes

It has been demonstrated that the reaction of a molybdate salt with a primary amine in the presence of triethylamine and TMSCl can be used as a general route to a large variety of molybdenum bis (imido) complexes. Analogously, Schrock[31] has demonstrated that it is possible to synthesise the analogous rhenium bis (imido) complexes through the reaction of either Re_2O_7 or $(NH_4)_2ReO_4$ with two equivalents of the desired primary amine. Further reactions of this type have been attempted to explore this synthetic strategy with the view to the synthesis of a variety of other bis (imido) complexes of the early transition metals.

2.4.1 Reaction of Na_2WO_4 with $ArNH_2$

Despite prolonged heating at 70°C, the reaction of Na_2WO_4 with NEt_3, TMSCl, and 2, 6-diisopropylaniline in DME did not yield any of the desired bis (imido) product. The analogous reaction was also attempted

using the potassium salt, which again afforded none of the desired product.

The reasons behind this lack of reactivity are unclear, although Schrock[31] has postulated that these reactions may fail due to the relatively slow reaction of tungsten compared to either molybdenum or rhenium, and that decomposition of the $W(NR)_2Cl_2$.DME complexes occur at temperatures where the rates of reaction are practical, as a consequence of the lower electrophilicity of molybdenum compared to tungsten.

2.4.2 Reaction of $(NH_4)_2Cr_2O_7$ with RNH_2 (R=Ar, ^tBu)

The synthesis of chromium bis (imido) species is limited to the bis (tert-butyl imido) complex, synthesised *via* the reaction of chromyl chloride with the corresponding monosilyl amine, according to Scheme 2.1[6] Other well established syntheses of imido complexes such as the reaction of a terminal metal oxo group with an isocyanate have proved useless for chromium; treatment of chromyl chloride with two equivalents of ArNCO in refluxing heptane does not afford a tractable product.[18]

Having exploited a simple reaction for the synthesis of molybdenum bis (imido) complexes (Sections 2.2-2.4) and having found that the strategy could not be extend to the heavier congener tungsten, we were intrigued to see whether this procedure could be applied to the synthesis of chromium bis (imido) complexes.

A suspension of $(NH_4)_2Cr_2O_7$ in DME was stirred at 70°C for 12 hours in the presence of 2 equivalents of 2,6-diisopropylphenyl amine, triethylamine, and TMSCl, according to equation 2.5. During this period the dichromate was slowly consumed with concomitant formation of an intense red/purple solution. On work-up (analogous to that used for molybdenum, Section 2.2.1), and subsequent removal of all volatiles *in vacuo* afforded a dark red/purple paramagnetic solid (**4**) in 72% yield. Subsequent analysis was consistent with (**4**) having a molecular formula of $3[NH(Et)_3]^+ [Cr_2Cl_9]^{3-}$.

$$(NH_4)_2Cr_2O_7 + 4\,NEt_3 + 17\,TMSCl + 4\,ArNH_2 \xrightarrow[70°C\,/\,12\,h]{dme} [Cr_2Cl_9][NHEt_3]_3 \quad \textbf{(4)} \qquad (2.5)$$

Extraction of a portion (50 mg) of (4) into dichloromethane followed by layering with an equal volume of toluene led to the isolation of dark blue/purple plate-like crystals at room temperature. A crystal of suitable dimensions was selected for an X-ray crystal structure determination and mounted in a Lindemann capillary under an inert atmosphere. The data were collected and the structure solved by Dr. J.C. Jeffery at the University of Bristol.

The X-ray analysis revealed that (4) had adopted a classical distorted confacial bioctahedral geometry typical of Group 6 enneahalodimetallates,[57] Figure 2.5, which was entirely consistent with the structure determined by Saillant and Wentworth for the analogous complex $[Cr_2Cl_9][(n\text{-}C_4H_9)_4]_3$ obtained from a different preparative procedure.[58] This type of geometry has been described in detail by Cotton and Ucko,[57] and consists of two chromium centred trigonal planar face sharing octahedra. Selected bond lengths and angles for (4) are collected in Table 2.7.

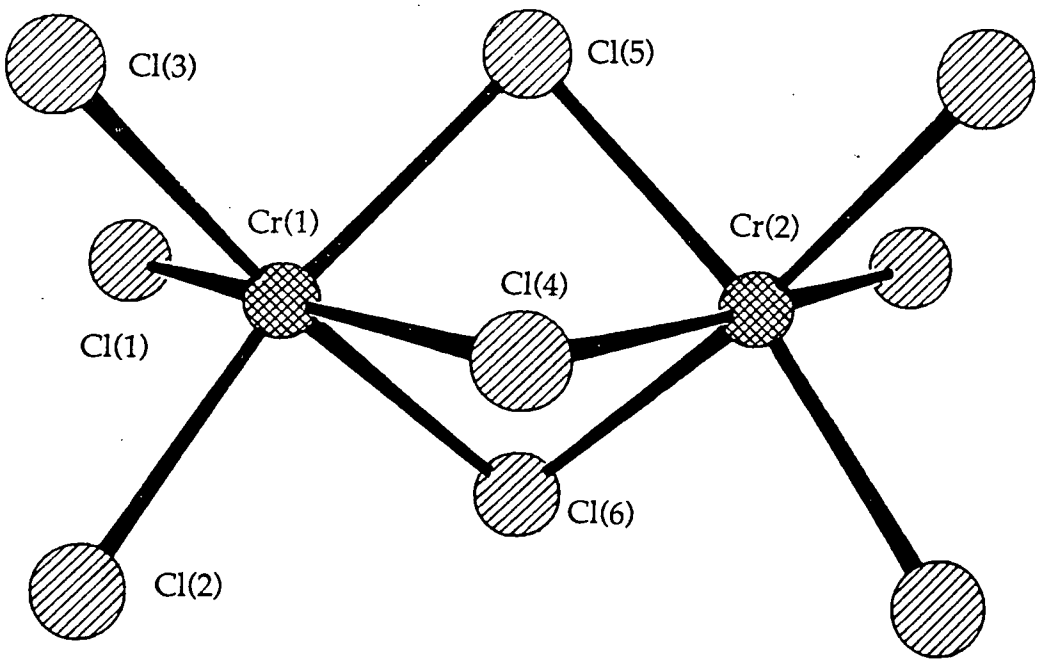

Figure 2.5 *Molecular structure of $[Cr_2Cl_9]$ $[NHEt_3]_3$ showing the anion only.*

Table 2.7 *Selected bond lengths (Å) and interbond angles (°) for $[Cr_2Cl_9][Et_3NH]_3$ (4) with estimated standard deviations in parentheses.*

Cr(1)-Cl(1)	2.305(2)	Cr(2)-Cl(4)	2.413(2)
Cr(1)-Cl(2)	2.310(2)	Cr(2)-Cl(5)	2.402(2)
Cr(1)-Cl(3)	2.286(2)	Cr(2)-Cl(6)	2.394(2)
Cr(1)-Cl(4)	2.404(2)	Cr(2)-Cl(7)	2.289(2)
Cr(1)-Cl(5)	2.415(2)	Cr(2)-Cl(8)	2.317(2)
Cr(1)-Cl(6)	2.418(2)	Cr(2)-Cl(9)	2.305(2)

Cl(1)-Cr(1)-Cl(2)	92.4(1)	Cl(5)-Cr(2)-Cl(6)	81.8(1)
Cl(1)-Cr(1)-Cl(3)	92.9(1)	Cl(4)-Cr(2)-Cl(7)	174.3(1)
Cl(2)-Cr(1)-Cl(3)	93.8(1)	Cl(5)-Cr(2)-Cl(7)	94.1(1)
Cl(1)-Cr(1)-Cl(4)	172.5(1)	Cl(6)-Cr(2)-Cl(7)	92.8(1)
Cl(2)-Cr(1)-Cl(4)	90.9(1)	Cl(4)-Cr(2)-Cl(8)	89.1(1)
Cl(3)-Cr(1)-Cl(4)	93.6(1)	Cl(5)-Cr(2)-Cl(8)	168.6(1)
Cl(1)-Cr(1)-Cl(5)	94.0(1)	Cl(6)-Cr(2)-Cl(8)	90.2(1)
Cl(2)-Cr(1)-Cl(5)	169.9(1)	Cl(7)-Cr(2)-Cl(8)	94.4(1)
Cl(3)-Cr(1)-Cl(5)	93.6(1)	Cl(4)-Cr(2)-Cl(9)	90.8(1)
Cl(4)-Cr(1)-Cl(5)	81.8(1)	Cl(5)-Cr(2)-Cl(9)	92.9(1)
Cl(1)-Cr(1)-Cl(6)	90.9(1)	Cl(6)-Cr(2)-Cl(9)	172.0(1)
Cl(2)-Cr(1)-Cl(6)	91.1(1)	Cl(7)-Cr(2)-Cl(9)	93.6(1)
Cl(3)-Cr(1)-Cl(6)	173.6(1)	Cl(8)-Cr(2)-Cl(9)	94.1(1)
Cl(4)-Cr(1)-Cl(6)	82.3(1)	Cr(1)-Cl(4)-Cr(2)	81.6(1)
Cl(5)-Cr(1)-Cl(6)	81.0(1)	Cr(1)-Cl(5)-Cr(2)	81.6(1)
Cl(4)-Cr(2)-Cl(5)	81.9(1)	Cr(1)-Cl(6)-Cr(2)	81.7(1)
Cl(4)-Cr(2)-Cl(6)	82.6(1)		

Since Olsson reported the synthesis of $K_3W_2Cl_9$ in 1914[59] many other complexes containing the $[M_2X_9]^{3-}$ (M=Cr, Mo, W; X=Cl, Br, I) anion have been reported. The interest in this class of complex has arisen from the unusual magnetic properties exhibited by the tungsten complex, which together with X-ray structural data indicated the presence of a W-W bond (W-W separation of 2.41Å).[60] Cotton[57] described this metal-metal interaction in terms of splitting of the metal t_{2g} level into degenerate σ and π orbitals imposed by the three-fold symmetry of the bioctahedra. These orbitals from each of the two metal centres can interact to form M-M bonding orbitals of σ and π types. Thus, the three metal d electrons can be accommodated to form a bonding $\sigma^2\pi^4$ configuration.

The molecular structure of (4) indicated a Cr-Cr separation of 3.15Å which is entirely consistent with the value of 3.12Å previously determined for $Cs_3Cr_2Cl_9$.[61] This value is indicative of repulsion between the two chromium atoms, thus no chromium-chromium bond can be inferred. The analogous molybdenum anion, $[Mo_2Cl_9]^{3-}$,[62] shows a Mo-Mo separation (2.66Å) and a magnetic moment intermediate between that of chromium and tungsten anions. The angles subtended by each of the three bridging chlorine atoms (81.6(1), 81.6(1) and 81.7(1)°) and the average Cr-μCl bond length of 2.407(2)Å are in good agreement with literature values for this anion,[52] and are characteristic of elongation of the bioctahedra along the C_3 axis. Furthermore, the structure of (4) indicated that the anion is symmetrical about a plane through the three bridging chlorine atoms.

Interestingly, the X-ray structure of (4) revealed the presence of hydrogen bonding interactions between the amine protons of the $[NHEt_3]^+$ cation and four of the terminal chloride atoms (Cl(1), Cl(2), Cl(8) and Cl(9)), Figure 2.6. These interactions ranged between 2.21 and 2.68Å which were consistent with normal N-H···Cl hydrogen bonding values, typically 2.40Å.[63] The corresponding Cr-Cl bond lengths showed an associated elongation exhibiting an average bond length of 2.309(2)Å compared to 2.288(2)Å for the remaining two non-hydrogen bonding terminal chlorines (Table 2.8).

The reaction shown in Equation 2.5 was repeated replacing the 2, 6-diisopropylphenyl amine ($ArNH_2$) with $^tBuNH_2$ (4 equiv.). Once again a dark red product was isolated which proved, on analysis, to have a molecular formula consistent with this product being identical to (4), indicating that the primary amine played only an indirect rôle in the

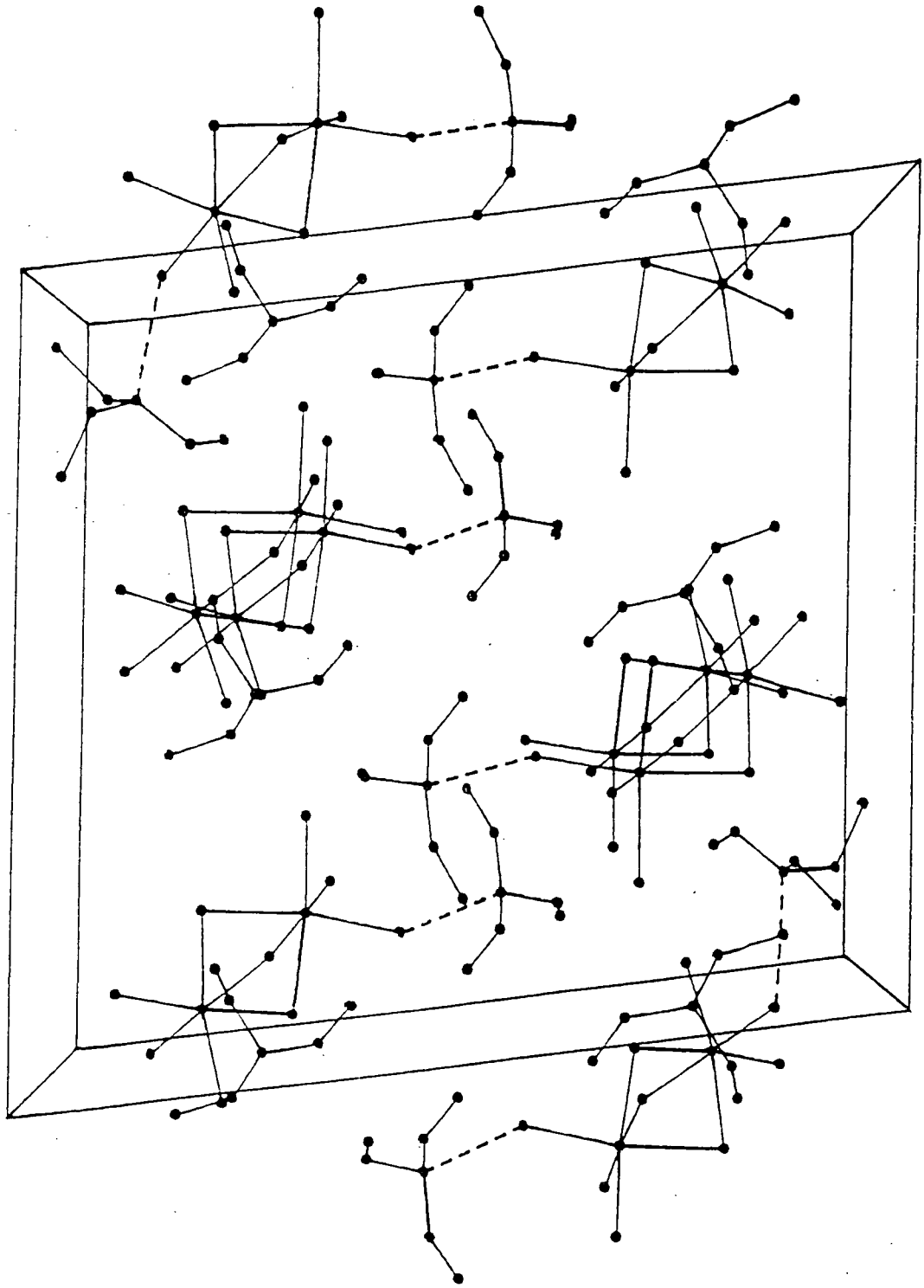

Figure 2.6 *Packing diagram for $[Cr_2Cl_9]$ $[NHEt_3]_3$ showing the N—H···Cl hydrogen bonding interactions.*

niobium (V) oxide (Nb_2O_5) or lithium niobate ($LiNbO_3$), the most readily available niobium oxo salt, with two equivalents of either of the primary amines $ArNH_2$ or $^tBuNH_2$ in the presence of NEt_3 and TMSCl in DME, according to Scheme 2.10, failed to afford any of the desired bis (imido) product. ^1H NMR of the crude reaction mixture revealed only unreacted starting materials. The niobate reaction was repeated using acetonitrile instead of DME as solvent, in the hope of breaking up the niobate oxide lattice, but once again, despite prolonged heating at 80°C, no reaction was observed.

$$LiNbO_3 + 2\,RNH_2 + 9\,TMSCl + 4\,NEt_3 \xrightarrow[\text{DME / 70 °C}]{} \not\rightarrow$$

Scheme 2.10 *Attempted synthesis of niobium bis (imido) complexes (R= Ar, or ^tBu).*

2.5 Summary

To date, only oxo salts of two metals have been shown to react with primary amines to afford their corresponding bis or tris (imido) derivatives. This reaction proceeds for molybdenum and rhenium according to equations 2.1-2.3. The lack of reactivity of tungsten has been explained by slow reaction at temperatures below that for decomposition of the bis (imido) product. When this reaction is attempted with chromium, a more energetically favourable pathway exists which allows the formation of anionic chromium (III) salts, $[Cr_2Cl_9]^{3-}$. The marked contrast between the reactivity of chromium and molybdenum is thought to be a consequence of the second and third row transition metals forming oxo anions in their highest oxidation states which are not readily reduced, whilst the analogous first row metal anions undergo facile reduction.

2.6 References

1 A.F. Clifford and C.S. Kobayashi, *Abstracts 130th National Meeting of the American Chemical Society*, Atlantic City, NJ, 1956, p50R; A.F. Clifford and C.S. Kobayashi, *Inorg. Synth.*, 1960, **6**, 207.

2 A general review of transition metal imido complexes is given by: W.A. Nugent and B.L. Haymore, *Coord. Chem. Rev.*, 1980, **31**, 123.

3 D.N. Williams, J.P. Mitchell, A.D. Poole, U. Siemeling, W. Clegg, D.C.R. Hockless, P.A. O'Niel, and V.C. Gibson, *J. Chem. Soc. Dalton Trans.*, 1992, 739.

4 V.C. Gibson, D.N. Williams, W. Clegg, and D.C.R. Hockless, *Polyhedron*, 1989, **8**, 1819.

5 R.R. Schrock, J.S. Murdzek, G.C. Bazan, J. Robbins, M. DiMare, and M. O'Regan, *J. Am. Chem. Soc.*, 1990, **112**, 3875.

6 W.A. Nugent, *Inorg. Chem.*, 1983, **22**, 965; W.A. Nugent and R.L. Harlow, *Inorg. Chem.*, 1980, **19**, 777.

7 I.S. Kolomnikov, Y.D. Koreshkov, T.S. Lobeeva, and M.E. Volpin, *J. Chem. Soc. Chem. Commun.*, 1970, 1432,

8 G. Schoettel, J. Kress, and J.A. Osborn, *J. Chem. Soc. Chem. Commun.*, 1989, 1062.

9 P. Jernakoff, G.L. Geoffroy, A.L. Rheingold, and S.J. Geib, *J. Chem. Soc. Chem. Commun.*, 1987, 1610.

10 W.A. Nugent and B.L. Haymore, *Coord. Chem. Rev.*, 1980, **31**, 123; W.A. Nugent and J.M. Mayer, *"Metal Ligand Multiple Bonds"*, John Wiley and Sons, New York, 1988.

11 Y.W. Chao, P.A. Wexler, and D.E. Wigley, *Inorg. Chem.*, 1990, **29**, 4592.

12 D.S. Glueck, J. Wu, F.J. Hollander, and R.G. Bergman, *J. Am. Chem. Soc.*, 1991, **113**, 2041.

13 D.C. Bradley and I.M. Thomas, *Can. J. Chem.*, 1962, **40**, 1355.

14 To date the only known examples of alkylimido derivatives of Ni triad: M.J. McGlinchey and F.G.A. Stone, *J. Chem. Soc. Chem. Commun.*, 1970, 1265.

15 M.H. Chisholm, K. Folting, J.C. Huffman, and A.L. Ratermann, *Inorg. Chem.*, 1981, **21**, 978.

16 W.A. Nugent, *Inorg. Chem.*, 1983, **22**, 965. Further discussion of this reaction is given: H. Lam, G. Wilkinson, B. Hussain-Bates, and M.B. Hursthouse, *J. Chem. Soc. Dalton Trans.*, 1993, 1477.

17 N. Wiberg, H.W. Häring and U. Schubert, Z. *Natuforsch. B*, 1978, **33**, 1365.

18 N. Meijboom and C.J. Schaverien, *Organometallics*, 1990, **9**, 774.

19 R.R. Schrock, J.S. Murdzek, G.C. Bazan, J.C. Robbins, M. DiMare, and M. O'Regan, *J. Am. Chem. Soc.*, 1990, **112**, 3875.

20 R.R. Schrock, R.T. DePue, J. Feldman, K.B. Yap, D.C. Yang, W.M. Davis, L. Park, M. DiMare, M. Schofield, J. Anhaus, E. Walborsky, E. Evitt, C. Kruger, and P. Betz, *Organometallics*, 1990, **9**, 2262.

21 B.R. Ashcroft, A.J. Nielson, D.C. Bradley, R.J. Errington, M.B. Hursthouse, and R.L. Short, *J. Chem. Soc. Dalton Trans.*, 1987, 2059; B.R. Ashcroft, A.J. Nielson, D.C. Bradley, R.J. Errington, G. R. Clark, and C.E.F. Richard, *J. Chem. Soc. Chem. Commun.*, 1987, 170.

22 N. Bryson, M.T. Youinou, and J.A. Osborn, *Organometallics*, 1991, **10**, 3389.

23 R. Lai, S. Mabille, A. Croux, and S. Le Bot, *Polyhedron*, 1991, **10**, 463; F. Bottomley and L. Sutton, *Adv. Organomet. Chem.*, 1988, **28**, 1988; S.F. Pederson, R.R. Schrock, *J. Am. Chem. Soc.*, 1982, **104**, 7483.

24 M.L.H. Green, and K.J. Moynihan, *Polyhedron*, 1986, **5**, 921.

25 J. Chatt and J.R. Dilworth, *J. Chem. Soc. Chem. Commun.*, 1972, 549.

26 E.A. Maata, Y. Du, and A.L. Rheingold, *J. Chem. Soc. Chem. Commun.*, 1990, 756.

27 M.L.H Green, P.C. Konidaris, P. Mountford, S.J. Simpson, *J. Chem. Soc. Chem. Commun.*, 1992, 256.

28 W. Clegg, R.J. Errington, D.C.R. Hockless, and C. Redshaw, *J. Chem. Soc. Dalton Trans.*,1993, 1965.

29 C.Y. Chou, D.D. Devore, S.C. Huckett, J.C. Huffman, F. Takusagawa, and E.A. Maatta, *Polyhedron*, 1986, **5**, 301.

30 Y.W. Chao, P.M. Rodgers, and D.E. Wigley, *J. Am. Chem. Soc.*, 1991, **113**, 6326.

31 H.H Fox, K.B. Yap, J. Robbins, S. Cai, and R.R. Schrock, *Inorg. Chem.*, 1992, **31**, 2287.

32 R. Toreki, R.R. Schrock, and W.M. Davis, *J. Am. Chem. Soc.*, 1992, **114**, 3367.

33 B. Whittle, P.W. Dyer, and V.C. Gibson, Unpublished results.

34 E.L. Marshall and V.C. Gibson, Unpublished results.

35 B. Whittle, M.Sc. Thesis, University of Durham, 1993.

36 M. Jolly, J.P. Mitchell, and V.C. Gibson, *J. Chem. Soc. Dalton Trans.*, 1992, 1329.

37 A number of other stoichiometries were attempted to try and maximise the overall yield of the mixed imido species, yet the 1 : 1 ratio proved the best; E.L. Marshall, and V.C. Gibson, Unpublished results.

38 Similar deviations in Cl-M-Cl bond angles have been noted: K. Dreisch, C. Andersson, and C. Stålhandske, *Polyhedron*, 1991, **10**, 2417; B.R. Ashcroft, D.C. Bradley, G.R. Clark, R.J. Errington, A.J. Nielson, and C.E.F. Rickard, *J. Chem. Soc. Chem. Commun.*, 1987, 170.

39 W.A. Nugent and J.M. Mayer, *"Metal Ligand Multiple Bonds"*, John Wiley and sons, New York, 1988.

40 Similar DME "bite angles" have been observed: K. Dreisch, C. Andersson, and C. Stålhandske, *Polyhedron*, 1991, **10**, 2417; B. Whittle, M.Sc. Thesis, University of Durham, 1993.

41 E.A. Maata and R.A.D. Wentworth, *J. Am. Chem. Soc.*, 1979, **101**, 2063.

42 E.O. Fischer, W. Kleine, G. Kreis, and F.R. Kreissl, *Chem. Ber.*, 1978, **111**, 3542; J.P. Collman, L.S. Hegedus, J.R. Norton, and R.G. Finke, *"Principles and Applications of Organotransition Metal Chemistry"*, University Science Books, California, 1987.

43 P.W. Dyer, V.C. Gibson, J.A.K. Howard, and C. Wilson, In press.

44 S. Bahar, P.W. Dyer, V.C. Gibson, J.A.K. Howard, and C. Wilson, In press.

45 See this thesis, Chapter 2.

46 E.L. Marshall, V.C. Gibson, and W. Clegg, Unpublished results.

47 J.K. Cockcroft, V.C. Gibson, J.A.K. Howard, A.D. Poole, and C. Wilson, *J. Chem. Soc. Chem. Commun.*, 1992, 1668.

48 D.N. Williams, J.P. Mitchell, A.D. Poole, U. Siemeling, W. Clegg, D.C. R. Hockless, P.A. O'Niel, and V.C. Gibson, *J. Chem. Soc. Dalton Trans.*, 1992, 739.

49 J.T. Anhaus, T.P. Kee, M.H. Schofield, and R.R. Schrock, *J. Am. Chem. Soc.*, 1990, **112**, 1642.

50 A.A. Danopoulos and G. Wilkinson, *Polyhedron*, 1990, **9**, 1009; A.A. Danopoulos, G. Wilkinson, B. Hussain-Bates, and M.B. Hursthouse, *J. Chem. Soc. Dalton Trans.*, 1991, 269.

51 G. Parkin, A. van Asselt, D.J. Leahy, L. Whinney, W.G. Hua, R.W. Quan, L.M. Henling, W.P. Schaefer, B.D. Santarierso, and J.E. Bercaw, *Inorg. Chem.*, 1992, **31**, 82; K.A. Jørgenson, *Inorg. Chem.*, 1993, **32**, 1521.

52 J.T. Anhaus, T.P. Kee, M.H. Schofield, and R.R. Schrock, *J. Am. Chem. Soc.*, 1990, **112**, 1642.

53 R.L. Halterman, *Chem. Rev.*, 1992, **92**, 965.

54 W.E. Piers, and J.E. Bercaw, *J. Am. Chem. Soc.*, 1990, **112**, 9406; W. Kaminsky, R. Engehausen, K. Zoumis, W. Spalek, and J. Rohrmann, *Makromol. Chem.*, 1992, **193**, 1643; J.A. Ewen, M.J. Elder, R.L. Jones, I. Haspeslagh, J.L. Atwood, S.G. Bott, and K. Robinson, *Makromol. Chem. Makromol. Symp.*, 1989, **48/49**, 253.

55 E. Bunel, B.J. Burger, and J.E. Bercaw, *J. Am. Chem. Soc.*, 1988, **110**, 976.

56 S. Gutmann, P. Burger, H. Hund, J. Hoffmann, and H. Brintzinger, J. *Organomet. Chem.*, 1989, **369**, 343.

57 F.A. Cotton and D.A. Ucko, *Inorg. Chim. Acta*, 1972, **6**, 161.

58 R. Saillant and R.A. Wentworth, *Inorg. Chem.*, 1974, **13**, 2552.

59 O. Olsson, *Z. Anorg. Allg. Chem.*, 1914, **88**, 49.

60 W.H. Watson and J. Wasser, *Acta. Cryst.*, 1958, **11**, 689.

61 G.J. Wessel and D.J. Ijdo, *Acta. Cryst.*, 1957, **10**, 466.

62 R. Saillant, R.B. Jackson, W.E. Strebb, K. Folting, and R.A. Wentworth, *Inorg. Chem.*, 1971, **10**, 1453.

63 W.C. Hamilton and J.C. Ibers, *"Hydrogen Bonding in Solids"*, W.A. Benjamin, New York, 1968.

Chapter Three- The Preparation, Reactivity, and Structure of Molybdenum Bis (Imido) Bis (Phosphine) and Bis (Imido) Olefin Complexes

3.0 Introduction

This chapter outlines attempts made to investigate the pseudo-isolobal relationship between Group 4 bent metallocenes and Group 6 bis (imido) complexes. The study has included the synthesis of reactive bis (phosphine) and olefin complexes and relates their reactivity and structure to that of their Group 4 analogues. As an introduction to this study the origins of this relationship are discussed.

The cyclopentadienyl group (Cp) is perhaps one of the most important groups in organometallic chemistry because it binds strongly to metals, is generally inert to both electrophiles and nucleophiles, and behaves as a stabilising ligand for many different types of complex. The Cp ligand is often regarded as a *spectator ligand.*

There are three main classes of η5-cyclopentadienyl (Cp) transition metal species, metallocenes, bent metallocenes and half-sandwich complexes. The former (Cp_2M) consist of two Cp ligands symmetrically disposed above and below the central metal atom. The latter ($CpML_x$, x= 1 to 4) have a single Cp ring and adopt a piano-stool geometry. Early transition metals attain the desired 18 electron configuration by incorporating additional ligands which forces the two Cp rings to fold back giving rise to the so-called bent metallocenes. The Group 4 derivatives display a rich chemistry and have found uses as reagents for a wide variety of processes that include hydrosilation,[1] hydrozirconation,[2] olefin metathesis,[3] and as soluble catalysts for Ziegler-Natta olefin polymerisations.[4]

Imido ligands have been proposed as reactive intermediates in a number of catalytic reactions, such as "ammoxidation". Yet, organoimido ligands are frequently becoming used as ancillary ligands, much like the Cp moiety. A number of homogeneous catalytic reactions are known that employ imido complexes. Perhaps the most well documented example is Schrock's well-defined four coordinate metathesis catalyst. In general, the imido ligand is "flexible" and can change the number of electrons that it donates to the metal centre, readily allowing other species to coordinate (cf. ring slippage associated with the Cp ligand).

3.1 The Pseudo-Isolobal Relationship between Cp_2M, $CpM'(NR)$, and $M''(NR)_2$

Simple MO treatments of the π-molecular orbitals of the cyclopentadienyl ligand $[Cp]^-$ reveal that it has an orbital of a_1 symmetry and a set of degenerate e_1 symmetry orbitals; the a_1 orbital is σ and the e_1 pair are π bonding with respect to the metal-ligand axis (Figure 3.1). The ring system also possesses an e_2 pair of δ symmetry unoccupied acceptor orbitals, although any interaction with these orbitals will be considerably weaker than with those of π symmetry. Early transition metals have no filled δ symmetry orbitals on the metal that can donate into these orbitals. It is unlikely, therefore, that a significant bonding rôle is played by these levels.

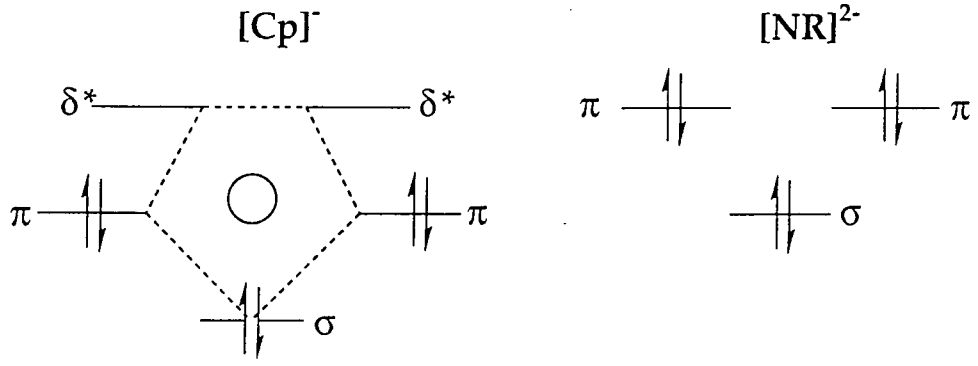

Figure 3.1 *Schematic representation of the frontier orbitals of the $[Cp]^-$ and $[NR]^{2-}$ fragments.*

Both this[5] and Schrock's group[6] have shown that the frontier orbitals of the imido ligand (NR^{2-}) in a terminal linear geometry (sp hybridised nitrogen) resemble those of the cyclopentadienyl unit, and thus also bond to the metal *via* one σ and 2 π interactions (Figure 3.1). This analogy has gained further support from PES studies of a range of osmium and iridium cyclopenatadienyl-imido complexes.[7]

Detailed calculations have been performed which examine the bonding and resultant geometry of the bent metallocenes. Lauher and Hoffmann[8] have studied the system using extended-Hückel molecular orbital (EHMO) calculations, whilst Zhu and Kostic[9] used the Fenske-Hall quantum method. Both reported similar frontier orbital characteristics for the $[M(\eta\text{-}C_5H_5)_2]^{2+}$ fragment. Hoffmann showed that as the angle between the normals to the rings in a metallocene decreases from 180° (i.e. a

ferrocene-like structure), towards that of a bent metallocene, three new highly directional metal based orbitals result, Figure 3.2. These new orbitals are used to bind further ligands to the metal centre and are essentially directed in the yz plane (Figure 3.2), the b_2 orbital being mainly of d_{yz} character, while the two a_1 orbitals are formed from the metal's s, p_z, d_{z^2}, and $d_{x^2-y^2}$ atomic orbitals. Thus, other ligands that bind to the metal centre should lie in the yz plane, bisecting the $Cp_{(centroid)}$-M-$Cp_{(centroid)}$ wedge angle. The two remaining metal d orbitals remain essentially non-bonding.[10]

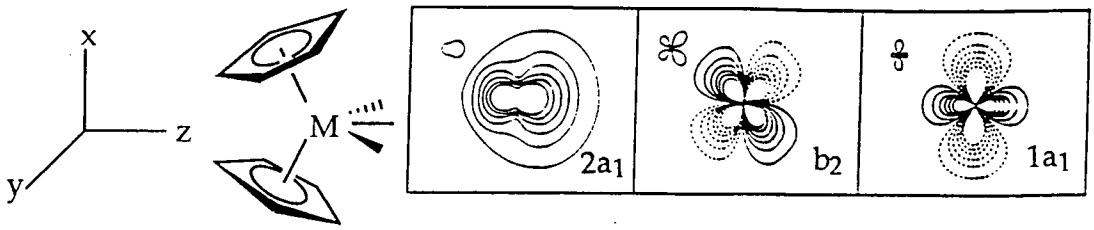

Figure 3.2 *Contour diagrams of the three bonding orbitals in the bent metallocene fragment [Cp_2M].*

Further Fenske-Hall quantum chemical calculations have been performed[5] which demonstrated that the frontier orbitals of Group 4 bent metallocene complexes are closely related to those of Group 5 half-sandwich imido complexes. The frontier orbitals of the two fragments $[CpNb(NR)]^{2+}$ and $[Cp_2Zr]^{2+}$ (Figure 3.3) are similar in their orientation. The only difference is in the composition of one of the low lying orbitals of $2a_1$ symmetry which, for $[CpNb(NMe)]^{2+}$, contains a significant contribution from the Nb d_{xz} orbital. This lies out of the normal metallocene "equatorial" ligand binding plane of the Cp_2M fragment and may account for the differences in the chemistry of the Cp_2M and CpM'(NR) fragments.

The cyclopentadienyl moiety formally donates five electrons to the valence electron count, whereas the linear imido ligand donates four electrons. Thus, in moving left to right across the series outlined in Figure 3.4, the Group 4 bent metallocene fragment is formally valence isoelectronic and pseudo-isolobal to the Group 5 half-sandwich complex. This analogy can be carried further[6] to include Group 6 bis (imido) species, which possess two, formally four electron donor ligands.

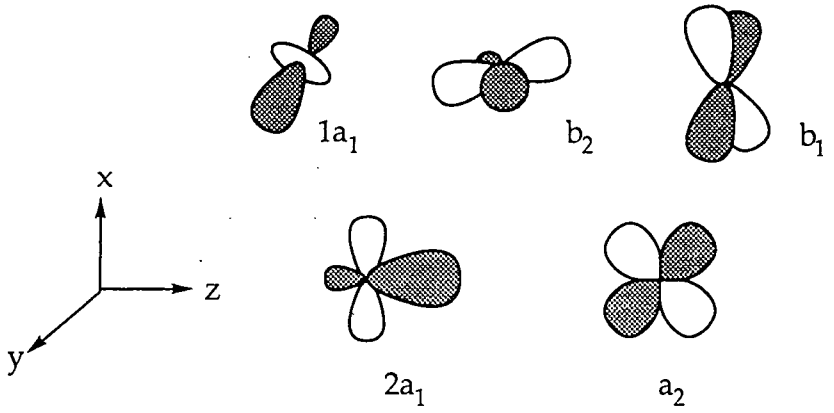

Figure 3.3 *Frontier MO's of the $[Cp_2Zr]^{2+}$ fragment (most important contributions only).*

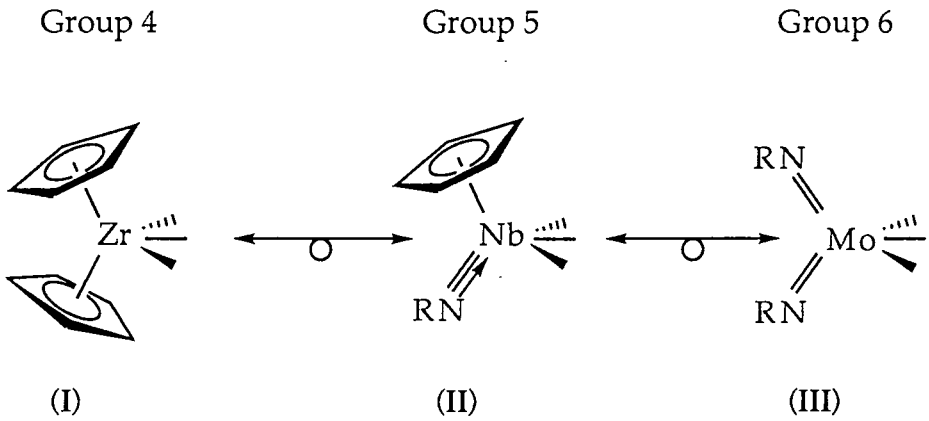

Figure 3.4.

A comparative study has been made of the chemistry of species (I) and (II) (Figure 3.4).[5,11] The following two chapters are thus devoted to an investigation of some chemistry of Group 6 bis (imido) complexes.

3.2 Reduction of $Mo(NR)_2Cl_2$.DME (R=Ar, ^tBu) in the Presence of PMe_3

Both of the versatile precursors $Cp_2Ti(PMe_3)_2$[12] and $Cp_2Zr(PR_3)_2$ (PR_3 = Me_3, Me_2Ph),[13] have been shown to react with alkynes. They afford synthetically useful metallacyclopentadienes *via* intermediate $Cp_2M(PMe_3)$(alkyne) complexes, which can often be observed spectroscopically.[14] More recently, Cp'Nb(NAr)$(PMe_3)_2$ (Cp' = Cp or Cp*)[15] and $W(NAr)_2(PMe_2Ph)_2$[16] have been isolated and have proven to be useful reagents for the synthesis of complexes containing unsaturated

hydrocarbon ligands. The niobium system also readily forms carbonyl and hydride derivatives. Hence, it was decided to synthesise the potentially useful molybdenum bis (imido) analogue.

3.2.1 Preparation of $Mo(NAr)_2(PMe_3)_2$ (5)

$Mo(NAr)_2(PMe_3)_2$ (5) may be isolated as an extremely air and moisture sensitive dark green solid *via* magnesium reduction of a THF solution of $Mo(NAr)_2Cl_2$.DME in the presence of excess PMe_3, Equation 3.1.[17]

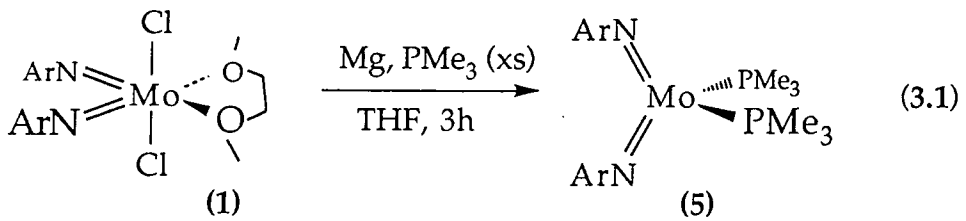

(1) (5) (3.1)

Room temperature NMR data are consistent with a highly symmetric structure in which the two imido ligands are equivalent. A single resonance at δ 1.03 ppm in the ^1H NMR spectrum attributed to bound PMe_3 is broadened ($\upsilon_{1/2}$ 36 Hz) due to rapid exchange with free phosphine. Consistently, addition of excess PMe_3 to a solution of (5) led to a marked broadening of the phosphine methyl resonance, with an associated shift of this resonance towards that of free PMe_3. Similarly, addition of excess $P(CD_3)_3$ to a solution of (5) led to a decrease in intensity of the bound phosphine resonance, which again showed a shift towards the position of free phosphine. ^{13}C NMR data were consistent with this structure showing, once again, a broadened resonance for the phosphine methyl carbons. Exchange of bound and free phosphine is observed when 2 equivalents of PMe_2Ph are added to a solution of (5) in C_6D_6.

Variable temperature ^1H NMR spectra of (5) in C_7D_8 (Figure 3.5) indicated that at low temperature the isopropyl groups became inequivalent. Two septets and two doublets were observed at low temperature which both exhibited a coalescence temperature (Tc) of 273 K. This inequivalence is believed to arise from slowing of the rotation of the imido ring substituent about the N-C_{ipso} axis. Schrock *et al* observed similar behaviour in the related tungsten system, $W(NAr)_2(PMe_3)_2$. The

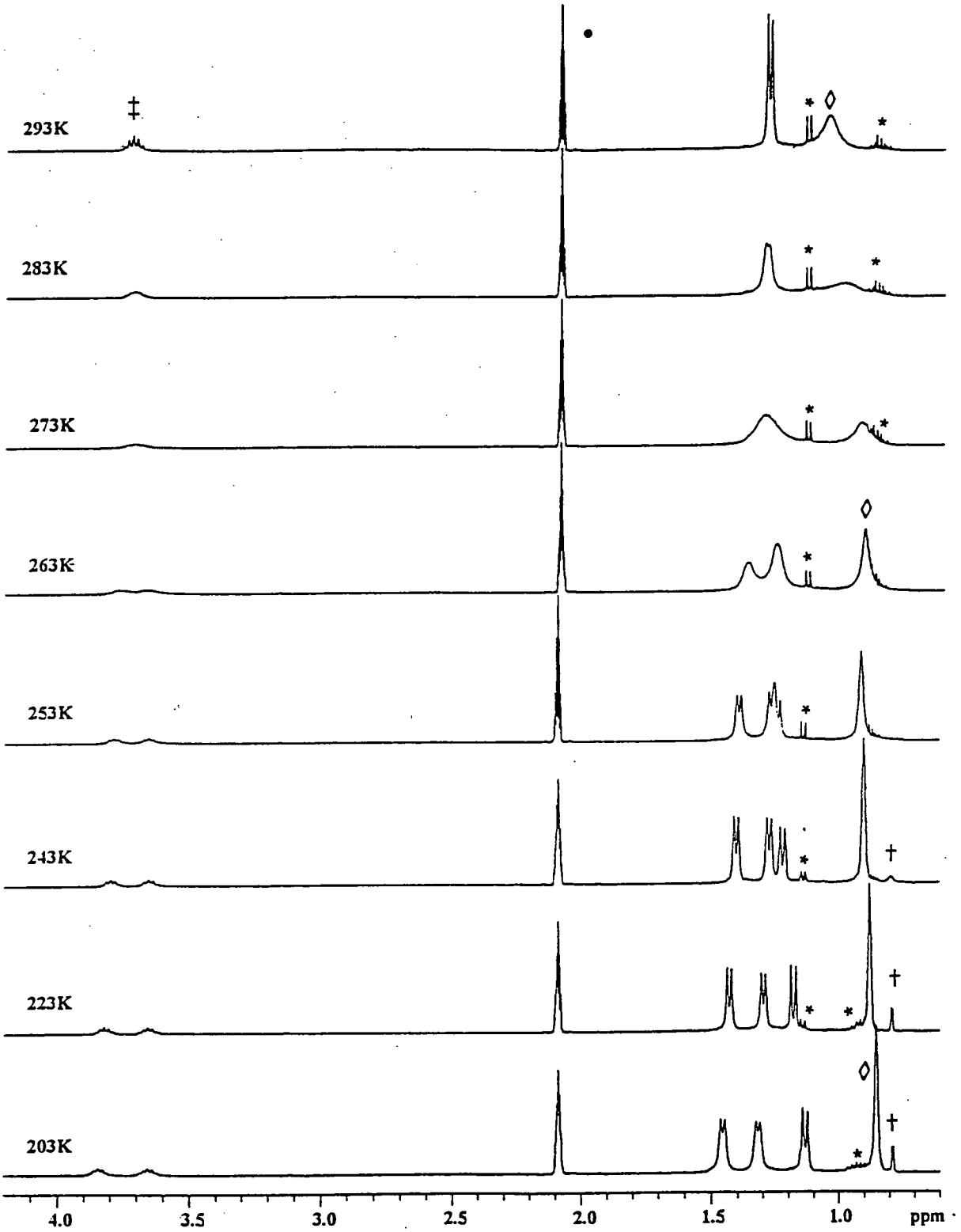

Figure 3.5 *Variable temperature 400 MHz ^1H NMR spectra for $Mo(NAr)_2(PMe_3)_2$. * denotes impurity, • solvent, † free PMe_3, and ◊ bound PMe_3, ‡ $C\underline{H}Me_2$.*

inequivalence of the isopropyl groups can be rationalised by the averaged signals for an 'inner' pair being distinct from the averaged signals of the two 'outer' isopropyl groups (Figure 3.6). Averaging occurs through residual slow rotation of the phenyl rings.

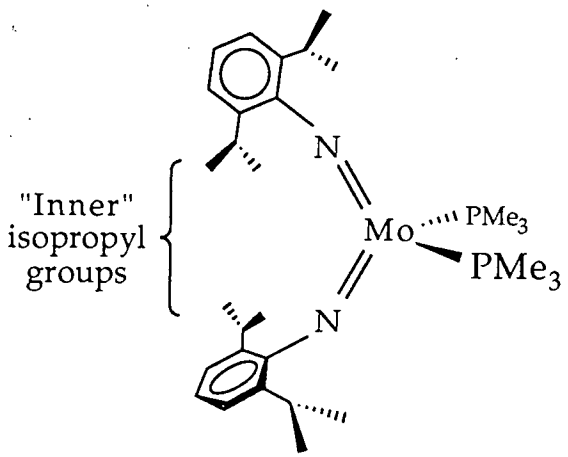

Figure 3.6
Schematic representation of the inequivalence observed for the isopropyl groups of $Mo(NAr)_2(PMe_3)_2$.

The rate constant of rotation, k, at the coalescence temperature (Tc) can be estimated from the ^1H NMR spectra using the relationship $k=\pi(\Delta\nu)(2)^{-1/2}$, where $\Delta\nu$ is the separation (in Hz) at the slow exchange limit, in this case 203 K.[18] Using this data it was also possible to obtain the free energy of rotation about the N-C_{ipso} bond using the relationship:

$$\Delta G^{\ddagger} = -RT[\ln (k/T) + \ln (h/K)]$$

R = molar gas constant, 8.314 $Jmol^{-1}K_{-1}$
K = Boltzmann's constant, 1.381 x 10^{-23} JK^{-1}
h = Planck's constant, 6.626 x 10^{-34} Js^{-1}
Tc = coalescence temperature, K.

The results of this analysis gave values for the rate constant of rotation (k) and for the free energy of rotation ($\Delta G^{\ddagger}$) of 167.1±18 s^{-1} and 55.0±1.0 $kJmol^{-1}$, respectively.

3.2.2 The Molecular Structure of $Mo(NAr)_2(PMe_3)_2$ (5)

Small prismatic dark green crystals of (5) were obtained from a cooled saturated diethylether solution maintained at -30°C. A crystal of dimensions 0.6 x 0.4 x 0.2 mm was selected for study and sealed in a glass Lindemann capillary under an inert atmosphere. The data were collected and the structure solved by Prof. J. A. K. Howard and Ms. C. Wilson within this department. The molecular structure of (5) is illustrated in Figure 3.7, and selected bond angles and distances are collected in Table 3.1.

The molecule is pseudo-tetrahedral with N–Mo–N and P–Mo–P bond angles of 137.1(5) and 97.0(2)° respectively. The Mo–N bond distances, at 1.789(10) and 1.794(12) Å, and their associated Mo–N–C angles (172.0(9) and 170.9(9)°) are consistent with linear imido units bound to molybdenum through pseudo triple bonds. These parameters are comparable with those of the tungsten analogue, $W(N\text{-}2,6\text{-}C_6H_3Pr^i_2)_2(PMePh_2)_2$, whose structure has recently been determined by Schrock and co-workers.[19] There is also a close correlation with the inter-ligand angles found in the isolobal d^2 complex $(\eta\text{-}C_5H_5)_2Ti(PMe_3)_2$[12], 92.9(1)° for P–Ti–P and 133.2(5)° for the ring centroid–Ti–ring centroid angle (c.f. 97.0(2)° for P–Mo–P and 137.1(5)° for N–Mo–N). This similarity between the bent metallocene and the bis (imido) complexes underlines the structural analogy that relates these Group 4 and Group 6 species.

Schrock *et al* have proposed that all four coordinate d^2 bis (imido) complexes will adopt a pseudo-tetrahedral geometry.[20] In a tetrahedron, two imido ligands (each a $1\sigma + 2\pi$ donor) can not form the maximum number of metal-nitrogen π bonds (four), there must be a "competition" for the fourth π-bond.[22] Only three π bonds can form in a *trans* square planar $M(NR)_2L_2$ species.[21]

The high reactivity of these d^2 bis (imido) complexes is thought to be a direct consequence of the fact that four, five, and six coordinate species can all readily form. This is believed to be due in part to the "flexible" nature of the imido moiety as a π bonding ligand. (cf. the cyclopentadienyl ligand in terms of π bonding.)[22] Also, there is increased space at the metal centre (an M=NR species has only one atom interacting with the metal centre while for the Cp-M fragment there are five).

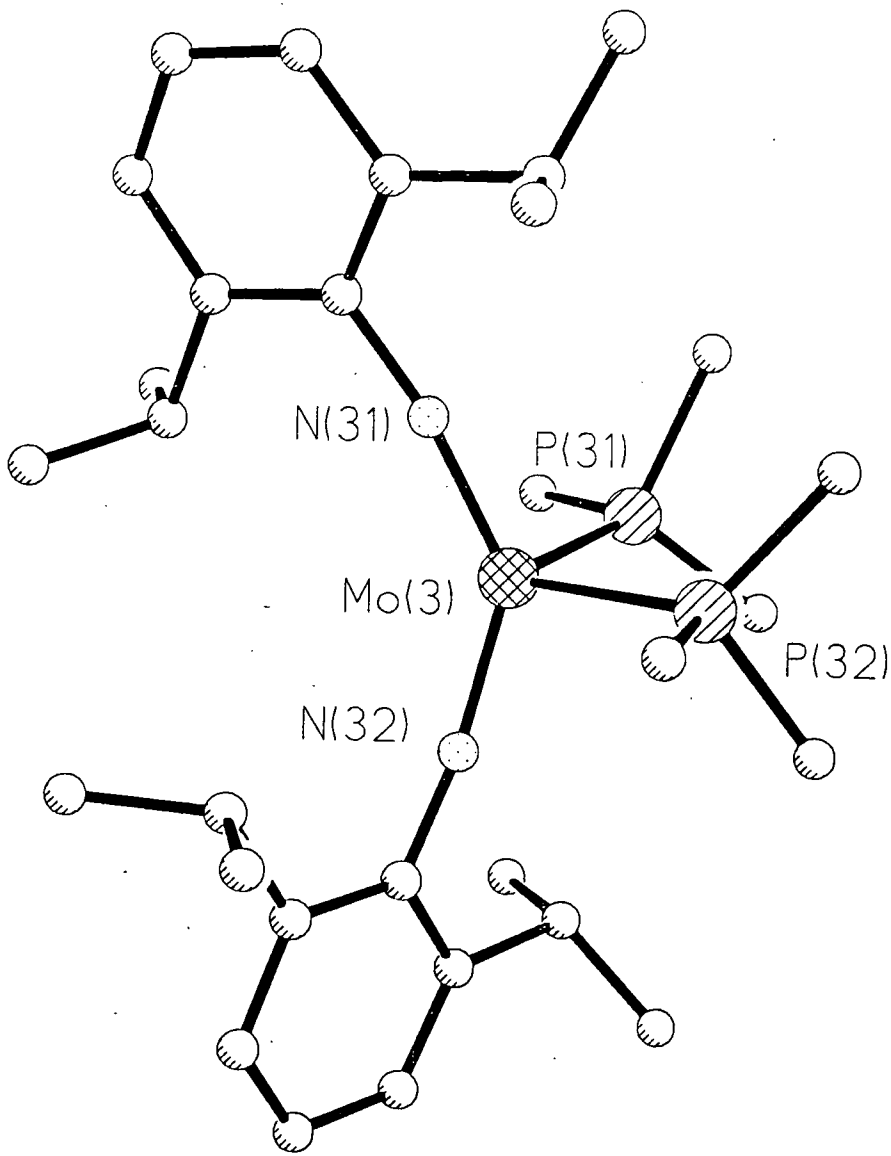

Figure 3.7 *Molecular structure of $Mo(NAr)_2(PMe_3)_2$.*

Table 3.1 *Selected bond distances (Å) and angles (°) for (5) with estimated standard deviations in parentheses.. This complex crystallised with one full and two half molecules in the asymmetric unit. The data presented are for the one full molecule.*

Mo(3)-P(31)	2.400(4)	Mo(3)-P(32)	2.405(5)
Mo(3)-N(31)	1.805(13)	Mo(3)-N(32)	1.797(10)
P(31)-C(31)	1.821(18)	P(31)-C(32)	1.813(14)
P(31)-C(33)	1.838(18)	P(32)-C(34)	1.823(15)
P(32)-C(35)	1.817(18)	P(32)-C(36)	1.825(15)
N(31)-C(311)	1.390(19)	C(311)-C(312)	1.422(17)
C(311)-C(316)	1.418(20)	C(312)-C(313)	1.412(22)
C(312)-C(330)	1.490(21)	C(313)-C(314)	1.385(22)
C(314)-C(315)	1.356(19)	C(315)-C(316)	1.378(22)
C(316)-C(317)	1.502(17)	C(317)-C(318)	1.504(20)
C(317)-C(319)	1.504(17)	C(330)-C(331)	1.504(19)
C(330)-C(332)	1.504(17)	N(32)-C(321)	1.414(15)
C(321)-C(322)	1.423(19)	C(321)-C(326)	1.421(17)
C(322)-C(323)	1.390(17)	C(322)-C(340)	1.501(18)
C(323)-C(324)	1.360(20)	C(324)-C(325)	1.376(22)
C(325)-C(326)	1.384(18)	C(326)-C(327)	1.504(19)
C(327)-C(328)	1.504(21)	C(327)-C(329)	1.504(24)
C(340)-C(341)	1.504(25)	C(340)-C(342)	1.504(21)

P(31)-Mo(3)-P(32)	96.9(2)	P(31)-Mo(3)-N(31)	98.9(3)
P(32)-Mo(3)-N(31)	109.0(4)	P(31)-Mo(3)-N(32)	110.1(3)
P(32)-Mo(3)-N(32)	98.5(4)	N(31)-Mo(3)-N(32)	137.1(5)
Mo(3)-P(31)-C(31)	112.8(5)	Mo(3)-P(31)-C(32)	114.3(5)
C(31)-P(31)-C(32)	101.3(7)	Mo(3)-P(31)-C(33)	121.8(5)
C(31)-P(31)-C(33)	101.4(8)	C(32)-P(31)-C(33)	102.5(7)
Mo(3)-P(32)-C(34)	113.1(6)	Mo(3)-P(32)-C(35)	114.4(6)
C(34)-P(32)-C(35)	101.1(8)	Mo(3)-P(32)-C(36)	121.8(6)
C(34)-P(32)-C(36)	102.3(7)	C(35)-P(32)-C(36)	101.5(8)
Mo(3)-N(31)-C(311)	169.8(9)	N(31)-C(311)-C(312)	119.4(12)
N(31)-C(311)-C(316)	121.1(10)	C(312)-C(311)-C(316)	119.5(13)
C(311)-C(312)-C(313)	118.9(13)	C(311)-C(312)-C(330)	120.5(13)
C(313)-C(312)-C(330)	120.6(11)	C(312)-C(313)-C(314)	119.5(13)
C(313)-C(314)-C(315)	121.1(15)	C(314)-C(315)-C(316)	122.0(15)

C(311)-C(316)-C(315)	118.8(12)	C(311)-C(316)-C(317)	120.6(13)
C(315)-C(316)-C(317)	120.6(13)	C(316)-C(317)-C(318)	112.1(11)
C(316)-C(317)-C(319)	112.8(11)	C(318)-C(317)-C(319)	109.0(12)
C(312)-C(330)-C(331)	111.1(11)	C(312)-C(330)-C(332)	115.5(12)
C(331)-C(330)-C(332)	109.1(11)	Mo(3)-N(32)-C(321)	172.3(9)
N(32)-C(321)-C(322)	120.5(10)	N(32)-C(321)-C(326)	119.4(11)
C(322)-C(321)-C(326)	120.1(11)	C(321)-C(322)-C(323)	119.7(12)
C(321)-C(322)-C(340)	118.5(10)	C(323)-C(322)-C(340)	121.7(12)
C(322)-C(323)-C(324)	118.5(13)	C(323)-C(324)-C(325)	123.2(13)
C(324)-C(325)-C(326)	120.4(13)	C(321)-C(326)-C(325)	117.8(13)
C(321)-C(326)-C(327)	121.2(10)	C(325)-C(326)-C(327)	121.0(12)
C(326)-C(327)-C(328)	109.3(13)	C(326)-C(327)-C(329)	113.0(12)
C(328)-C(327)-C(329)	109.1(12)	C(322)-C(340)-C(341)	112.2(12)
C(322)-C(340)-C(342)	113.4(14)	C(341)-C(340)-C(342)	109.1(12)

3.2.3 Reaction of $Mo(NAr)_2(PMe_3)_2$ (5) with excess CO

Rausch,[12] Siemeling,[15b] and Poole[23] have demonstrated that the three related complexes $Cp_2Ti(PMe_3)_2$, $Cp^*Nb(NAr)(PMe_3)_2$, and $CpNb(NAr)(PMe_3)_2$ respectively, all react cleanly with carbon monoxide to afford carbonyl derivatives *via* displacement of phosphine. Both the half-sandwich imido complexes react to form exclusively the mono-phosphine mono-carbonyl adducts, Equation 3.2 (Cp^* analogue), whereas the metallocene complex can react further to afford the dicarbonyl, $Cp_2Ti(CO)_2$.[12]

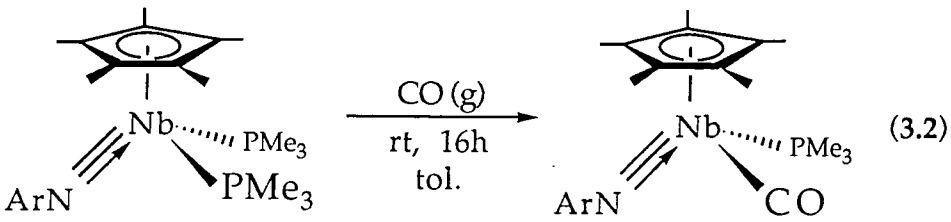

(3.2)

When a solution of the isolobal complex $Mo(NAr)_2(PMe_3)_2$ (5) was sealed in a thick-walled glass ampoule under 1 atm of CO, an intractable mixture of soluble and insoluble carbonyl containing products was obtained. This observation has been attributed to the greater reactivity of these bis (imido) complexes compared to that of either the related Cp'_2M' or $Cp'(NAr)M''$ (Cp' = Cp or Cp*; M'=Ti, Zr; M'' = Nb, Ta) species, and is believed to be a consequence of the greater steric protection imposed by the cyclopentadienyl ring compared to the imido ligand. Thus, the bis (imido) complex reacts readily with CO leading to a variety of carbonyl containing products. These have not yet been explored.

3.2.4 Reaction of $Mo(NAr)_2(PMe_3)_2$ (5) with H_2

$Cp_2Ti(PMe_3)_2$, $Cp^*Nb(NAr)(PMe_3)_2$, and $CpNb(NAr)(PMe_3)_2$ all react smoothly with hydrogen. $Cp^*Nb(NAr)(PMe_3)_2$ readily affords the stable dihydide complex $Cp^*Nb(NAr)(PMe_3)(H)_2$,[15b] which can be isolated as colourless crystals. However, by comparison, the less bulky niobium cyclopentadienyl (Cp) analogue has only been characterised spectroscopically,[24] as decomposition proceeds rapidly in solution at ambient temperature.

A similar study was undertaken with $Mo(NAr)_2(PMe_3)_2$ (5). A solution (C_6D_6) of (5) was sealed in an NMR tube under 1 atm of dihydrogen, and the reaction monitored by ^1H NMR. Surprisingly, even upon prolonged heating to 120°C no reaction was observed. This observation suggests that the pseudo-isolobal relationship that exists between Group 4 bent-metallocene and Group 6 bis (imido) complexes is largely a structural analogy that can not necessarily account for the reactivity of these species.

3.2.5 Reaction of $Mo(NAr)_2(PMe_3)_2$ (5) with Olefins

The reactive four coordinate 16 electron bis (phosphine) complexes all readily undergo reactions with olefins. Similar reactivity has been observed for both the Group 4 bent metallocene bis (phosphine) complexes,[12] and for their isolobal Group 5 half-sandwich imido analogues.[15,23] More recently, the Group 6 $W(NAr)_2(PMe_2Ph)_2$ complex[25] has been shown to react with a variety of olefins, affording a product dependent upon the size of the olefin.[19]

$Mo(NAr)_2(PMe_3)_2$ (5) reacts cleanly with both ethene and propene at room temperature to afford the unusual five coordinate complexes $Mo(NAr)_2(PMe_3)_2(\eta^2\text{-}CH_2{=}CHR)$ where R is either H (6), or CH_3 (7) (Equation 3.3).[26] The ethene complex (6) is easily isolated as a solid, its X-ray molecular structure having been determined (Section 3.3.2). However, in comparison, dissociation of olefin *in vacuo* is facile for the propene adduct, affording the bis (phosphine) complex (5); thus (7) could only be characterised spectroscopically (Section 3.3.3). The increased olefin lability in (7), has been attributed to the weaker interaction of this more sterically demanding olefin with the metal centre.

$$\underset{\textbf{(5)}}{Mo(NAr)_2(PMe_3)_2} \xrightarrow[R(H)C{=}CH_2]{} Mo(NAr)_2(PMe_3)_2(\eta^2\text{-}R(H)C{=}CH_2) \qquad \textbf{(3.3)}$$

The retention of phosphine for both the molybdenum and tungsten systems is of interest for comparison with the related bent-metallocene bis (phosphine) complex $Cp_2Ti(PMe_3)_2$.[27] This reacts with an excess of ethene in pentane at ambient temperature to afford the 16 electron ethene

complex $Cp_2Ti(C_2H_4)$,[27,28] with displacement of both the coordinated phosphine ligands. Surprisingly, the analogous reaction with acetylene yields the phosphine complex $Cp_2Ti(PMe_3)(C_2H_2)$.[29] The four coordinate $Cp_2M(PMe_3)(C_2H_4)$ (M= Ti, Zr) complexes have only been synthesised by reaction of the parent bis (phosphine) with ethene under a pressure of 50-60 bar.[30] Moreover, the titanium complex has only been identified spectroscopically as an intermediate in this type of reaction.

3.2.6 Reaction of $Mo(NAr)_2(PMe_3)_2$ (5) with Butadiene

$Mo(NAr)_2(PMe_3)_2$ (5) reacts with both ethene and propene to form five coordinate olefin adducts, without loss of phosphine. In an attempt to obtain the four coordinate mono-phosphine derivatives analogous to the metallocene examples,[12,13,30] the potentially chelating di-olefin butadiene was employed (Scheme 3.1).

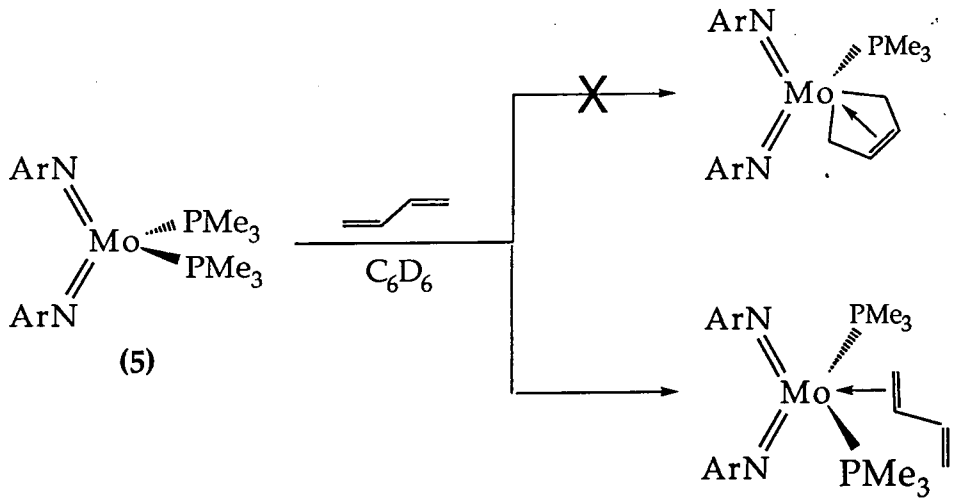

Scheme 3.1 *Reaction of $Mo(NAr)_2(PMe_3)_2$, (5), with 1, 3 butadiene.*

One equivalent of butadiene was condensed onto a solution of (5) (C_6D_6) in an NMR tube. On warming to room temperature the previously dark green solution turned an intense purple. ^1H NMR indicated that after 2 days at room temperature, smooth conversion of (5) to the five coordinate bis (phosphine) η^2-olefin adduct had occurred, Scheme 3.1. Despite prolonged warming to 70°C, no displacement of phosphine was observed, the butadiene remaining bound in an η^2 manner to the metal centre. Attempts to isolate the η^2 butadiene complex led only to the recovery of the bis (phosphine).

3.2.7 Attempted Reactions of $Mo(NAr)_2(PMe_3)_2$ (5) with $^tBuNH_2$ and $Ph_3P=C(H)(Ph)$

Work within this group has shown that bis (imido) complexes of the type $Mo(NR)_2(O^tBu)_2$ react with primary amines (notably $ArNH_2$) to afford other imido species. The exchange is thought to proceed *via* a trigonal-bipyramidal base adduct (Schemes 2.7 and 2.8).

$$\underset{\textbf{(5)}}{Mo(NAr)_2(PMe_3)_2} \xrightarrow[\text{xs } ^tBuNH_2]{C_6D_6} \not\rightarrow \quad Mo(NAr)(N^tBu)(PMe_3)_2 \qquad (3.4)$$

Two equivalents of tert-butyl amine were added to a solution of $Mo(NAr)_2(PMe_3)_2$ (5) in C_6D_6, in an attempt to isolate the tert-butyl imido containing species (Equation 3.4). On warming to room temperature there was no apparent colour change, the solution remained an intense dark green. Although the sample was kept at an elevated temperature (70°C) for two weeks no new species became apparent in the ^1H NMR spectrum. This is somewhat surprising as the bis (N^tBu) imido derivative (synthesised directly, Section 3.2.1) has proved relatively easy to isolate. The tert-butyl imido analogue differs in that it exists as the imido bridged dimer (Section 3.2.10). Imido complexes that contain the 2,6-diisopropylphenyl substituent are thought to favour mononuclear geometries on steric grounds.[31] It is often believed that tert-butyl substituents can allow a complex to adopt a bridging geometry, although the tert-butyl group is equally bulky. This implies that electronic effects are also likely to play a key rôle in controlling the resultant geometry of a complex. Thus, if the exchange of imido substituent is to proceed, a change of geometry is necessary, (terminal imido to bridging imido). The barrier to this interconversion could be a considerable.

The use of phosphoranes or phosphorus ylides such as $PR_3P=C(R')(R'')$ to generate metal carbon double bonds, or alkylidenes, is well documented.[32] An example of one such reaction is Schwartz's synthesis[33] of the unusual bent metallocene alkylidene complex, illustrated in Scheme 3.2. This reaction takes advantage of the fact that the valence orbitals of the metallocene can readily interact with the π system of the ylide. Dissociation of phosphine then occurs, which leads to the

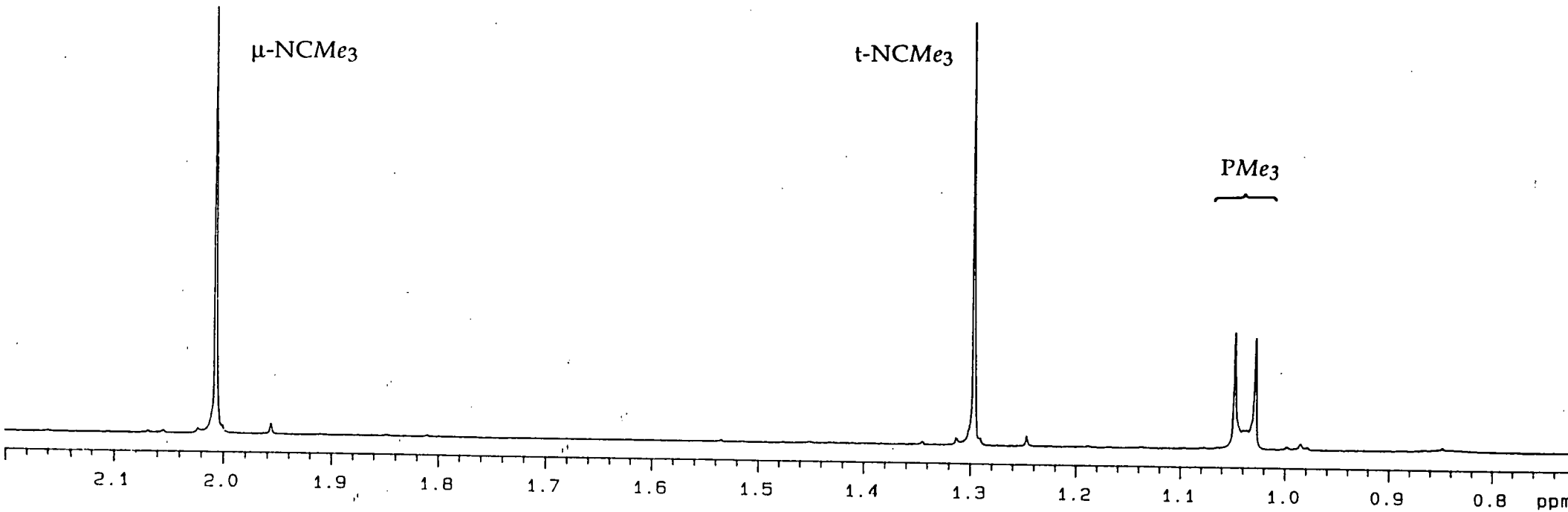

Figure 3.8 *^1H NMR spectrum of $[Mo(N^tBu)(\mu\text{-}N^tBu)(PMe_3)]_2$ (C_6D_6).*

generation of the alkylidene moiety. A similar approach was adopted by Schrock for the synthesis of $Cp_2Ta(CHR)(CH_3)$ (R= H, Me, Ph).[34]

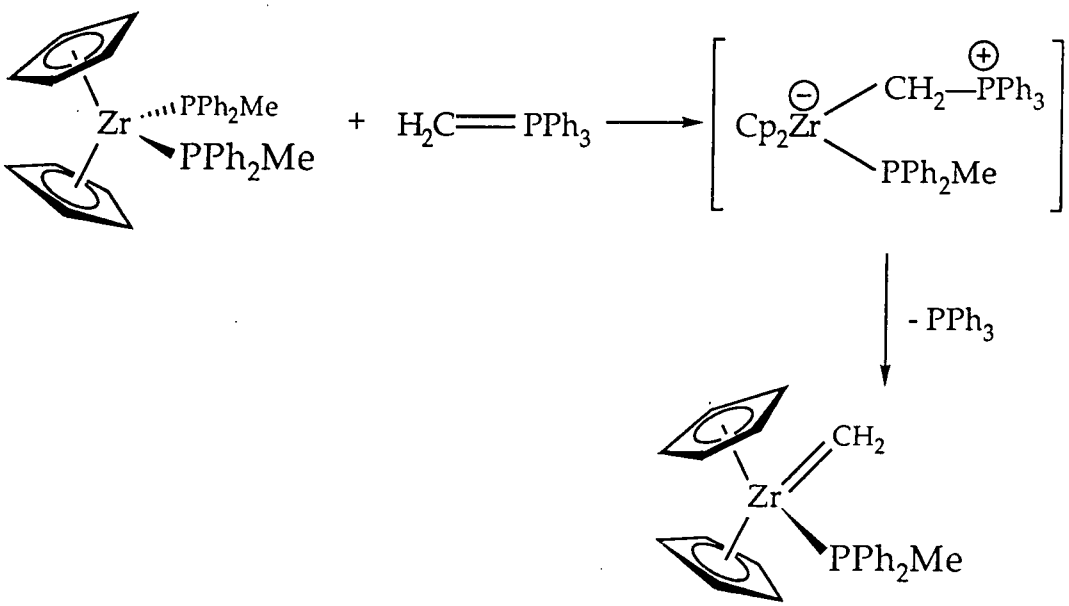

Scheme 3.2 *Preparation of a zirconocene methylidene species.*

In a comparable reaction, one equivalent of the ylide, $Ph_3P{=}C(H)(Ph)$, was added to a C_6D_6 solution of (**5**) in an NMR tube. Even after warming to 70°C there was no indication that any reaction had taken place.

The most likely explanation is that the ylide was too bulky to gain access to the metal centre to form a strong π type interaction. Despite this observation Sundermeyer *et al*,[35] have recently reported the synthesis of alkylidene complexes of Group 6 bis (imido) complexes, Equation 3.5. This latter reaction proceeds by a different mechanism to the reaction reported by Schwartz, i.e. by elimination of $[Ph_3PCH_3]Cl$.

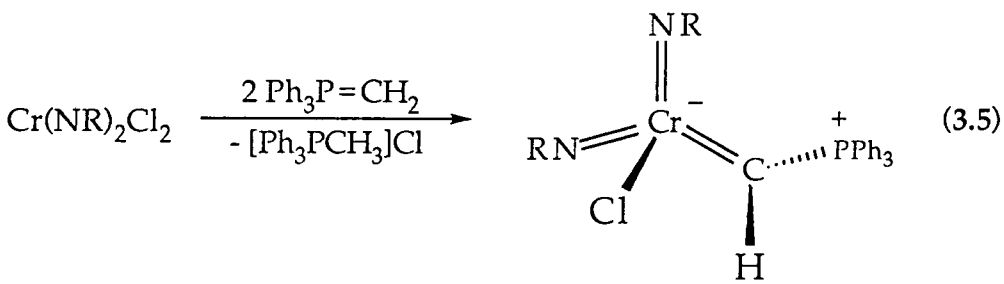

(3.5)

3.2.8 Reaction of $Mo(NAr)_2(PMe_3)_2$ (5) with Diphenylacetylene

In an attempt to generate the molybdenum bis (imido) derivative of the two isolobal species $Cp_2M(PR_3)(\eta^2\text{-PhC}\equiv\text{CPh})$ (M=Zr, PR_3= PMe_3 or PMe_2Ph;[13] M= Ti, PR_3= PMe_3[12]) and $Cp^*Nb(NAr)(PMe_3)(\eta^2\text{-PhC}\equiv\text{CPh})$,[36] (5) was treated with one equivalent of diphenylacetylene in an NMR tube in C_6D_6. Both ^1H and ^{31}P NMR indicated that PMe_3 was liberated [$\delta(^1H)$ 0.78 ppm and $\delta(^{31}P)$ -62.0 ppm], yet it was unclear as to the stoichiometry of the product. Thus, the reaction was repeated on a preparative scale.

Complex (5) reacted smoothly with 1 equivalent of diphenylacetylene, in toluene, over 12 hours at 60°C. On recrystallisation from n-pentane flocculent orange needles were isolated in low yield (30%) (8) (Equation 3.6). The resultant data are consistent with the formation of the four coordinate complex $Mo(NAr)_2(PMe_3)(\eta^2\text{-PhC}\equiv\text{CPh})$ (Equation 3.11, Section 3.4.1). Recently, Schrock[25] has shown that the four coordinate tungsten complex $W(NAr)_2(PMe_2Ph)(\eta^2\text{-HC}\equiv\text{CSiMe}_3)$ can be isolated, although a five coordinate species $W(NAr)_2(PMe_2Ph)_2(\eta^2\text{-HC}\equiv\text{CH})$ results if acetylene itself is used. Both the structures and syntheses of the molybdenum bis (imido) acetylene complexes are discussed in Section 4.1.

$$\underset{\textbf{(5)}}{Mo(NAr)_2(PMe_3)_2} \xrightarrow[-\,PMe_3]{PhC\equiv CPh} \underset{\textbf{(8)}}{Mo(NAr)_2(PMe_3)(\eta^2\text{-PhC}\equiv\text{CPh})} \qquad (3.6)$$

3.2.9 Preparation of $[Mo(N^tBu)(\mu\text{-}N^tBu)(PMe_3)]_2$ (9)

It has been noted that the chemistry of the two metal fragments $[Mo(NAr)_2]$ and $[Mo(N^tBu)_2]$ differ considerably.[37] The use of the tert-butyl substituent allows access to complexes that adopt a four coordinate manifold, which are therefore pseudo-isolobal to bent Group 4 metallocene complexes. However, the more "flexible" arylimido substituent favours the formation of a five coordinate geometry (i.e. the arylimido has the ability to rotate out of the way). In general the tert-butyl imido substituent can be regarded as being bulky in three dimensions whereas the arylimido is bulky in only two.

Complex (9) may be isolated as an air and moisture sensitive dark blue/green solid *via* magnesium reduction of a THF solution of $Mo(N^tBu)_2Cl_2.DME$ in the presence of excess PMe_3, Equation 3.7.

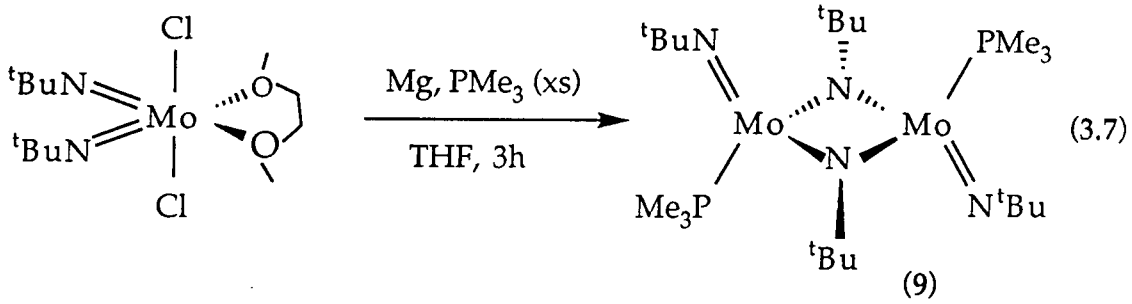

(3.7)

(9)

The 400 MHz ^1H NMR spectrum (C_6D_6) (Figure 3.8) revealed that this bis (phosphine) complex (9) had adopted an entirely different geometry to that found for (5), and was consistent with one terminal imido (δ 1.30 ppm) and one bridging imido (δ 2.01 ppm) per metal, Equation 3.7. The structure of (9), $[Mo(N^tBu)(\mu\text{-}N^tBu)(PMe_3)]_2$, was supported by both ^{13}C NMR data and elemental analyses. Attempts to grow crystals suitable for an X-ray structure determination were unsuccessful.

The arylimido bis (phosphine) (5) is thought unable to attain this type of dimeric structure as a consequence of the two bulky isopropyl groups on each of the imido phenyl rings, which tend to discourage such a bridging geometry. Initially, the orientational preference of (9) was attributed to the steric bulk of the phosphine in combination with the preference of the tert-butyl imido to adopt a bridging geometry. Yet, when the analogous synthesis was undertaken with both tri (cyclohexyl) and tri (tert-butyl) phosphines, a comparable bridging geometry was achieved. This implies that for complex (9), it is the imido substituent that directs the resultant geometry.

This type of binuclear structure is not uncommon. Nugent *et al*[38] isolated the dimeric complex $[Mo(N^tBu)(\mu\text{-}N^tBu)(Me)]_2$, Figure 3.9, which was the first example of an unsymmetrical bridging imido ligand. In this example each molybdenum exhibited a distorted trigonal-bipyramidal coordination. The asymmetry resulted from second order Jahn-Teller distortions, not unlike the localisation of bonding expected for antiaromatic cyclic hydrocarbons (eg. C_4H_4, C_8H_8).[39]

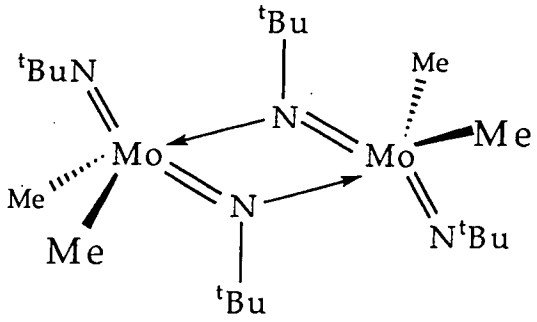

Figure 3.9
[Mo(N^{t}Bu)(μN^{t}Bu)(Me$_2$)]: an unsymmetrically bridged imido complex.

Unlike the reactive monomeric bis (phosphine) Mo(NAr)$_2$(PMe$_3$)$_2$, the imido-bridged dimer (**9**) has proved very stable and unreactive. No reaction was observed with either 2 equivalents of ArNH$_2$ or excess PMe$_3$, despite prolonged warming to 100°C. The reaction of (**9**) with excess ethene in an NMR tube (C_6D_6) indicated the slow formation of new species on prolonged heating, yet their identity could not be established. Both the complexity and extremely slow rate of reaction precluded further study of this latter reaction.

3.2.10 Reduction of Cr(N^{t}Bu)$_2$Cl$_2$ in the Presence of PMe$_3$

As previously demonstrated, it is possible to generate the reactive bis (imido) bis (phosphine) complexes of both molybdenum and tungsten. To extend this series to encompass the whole of the Group 6 triad, the synthesis of the chromium analogue was attempted.

Cr(N^{t}Bu)$_2$Cl$_2$ was synthesised according to a literature procedure,[40] and was treated with one equivalent of magnesium in THF solvent in the presence of excess PMe$_3$ (Equation 3.8). After 12 hours at room temperature, the solvent was removed *in vacuo* and the product extracted from the magnesium chloride residues with n-pentane. Subsequent recrystallisation from diethylether at -78°C afforded a small quantity of a dark brown/black amorphous solid.

$$Cr(N^tBu)_2Cl_2 \xrightarrow[\text{xs Mg / THF}]{PMe_3 / Et_2O} Cr(N^tBu)_2(PMe_3)_2 \qquad (3.8)$$

^{1}H NMR revealed a number of severely broadened resonances in the range δ 0 to 2 ppm. The broadening was attributed to the presence of a highly paramagnetic impurity. Elemental analyses were variable; the low

solubility of the material towards hydrocarbon solvents may be indicative of an aggregated or polymeric structure.

3.3 Preparation of 5 Coordinate Bis (Imido) Olefin Complexes

Transition metals are known to bind and activate a variety of unsaturated hydrocarbon ligands. Olefin complexes are involved in many reactions which are promoted or catalysed by these types of complex. Among the more common examples are olefin hydrogenation,[41] dimerisation, cyclisation, hydrocyanation,[42] hydroformylation,[43] and isomerisation.[44]

In recent years an increasing research effort has focused on metallocene complexes, especially with regard to their potential for olefin polymerisation catalyst precursors.[45] Equally, metal complexes containing multiply bound oxo or imido ligands and their reactions with neutral organic molecules such as olefins, have been scrutinised. These multiply bound ligands have been postulated as intermediates in a variety of catalytic processes such as ammoxidation,[46] and oxidation.[47]

For metals of the Group 6 triad there are few examples of such olefin containing bis (imido) species, to date the only direct examples are the tungsten complexes described recently by Schrock.[19,25]

3.3.1 Reaction of $Mo(NAr)_2Cl_2.DME$ with Ethyl Magnesium Chloride

Takahashi[48] has recently shown that Cp_2ZrCl_2 reacts smoothly with C_2H_5MgBr in the presence of a phosphine to yield the base stabilised metallocene olefin adduct, Figure 3.10. These types of species are of obvious importance with their relevance to metallocene based olefin polymerisation catalysts.

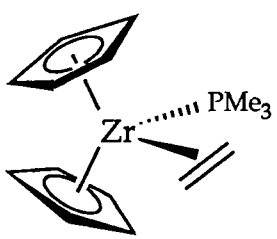

Figure 3.10 *Base stabilised zirconocene olefin complex.*

To further explore the pseudo-isolobal relationship that exists between Group 4 metallocenes, Group 5 half-sandwich imido, and Group 6 bis (imido) complexes, a study of the bis (imido) olefin adducts was undertaken.

Treatment of an ethereal solution of $Mo(NAr)_2Cl_2$.DME with two equivalents of ethylmagnesium chloride in the presence of excess trimethylphosphine resulted in the formation of an intense maroon coloured solution, Equation 3.9. On work-up dark red/purple needles were recovered from a concentrated n-pentane solution at -30°C.

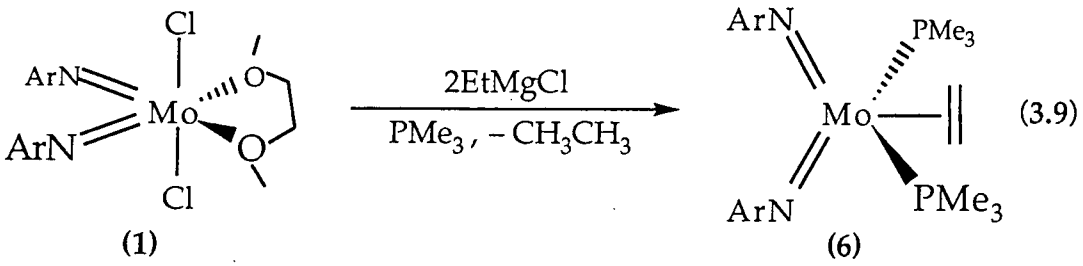

(1) (6) (3.9)

Both elemental analyses and NMR indicated that the reaction had indeed generated an olefin complex. The adduct had a stoichiometry consistent with the formation of $Mo(NAr)_2(PMe_3)_2(\eta^2\text{-}C_2H_4)$ (6). Rather than adopting a metallocene geometry analogous to either $Cp_2Zr(PMe_3)(\eta^2\text{-}PhC{=}CPh)$[49] or $CpNb(PMe_3)(\eta^2\text{-}C_3H_6)$,[50] (6) had coordinated a second phosphine. The reaction shown in Equation 3.9 was monitored by GC-MS, which revealed that ethane was generated consistent with the formation of (6) via β-elimination from an intermediate di-ethyl species. It has been shown that (6) can also be synthesised directly *via* the reaction of $Mo(NAr)_2(PMe_3)_2$ (5) with ethene, Section 3.2.5.

The room temperature 400 MHz ^1H NMR spectrum showed a single olefinic resonance at δ 1.70 ppm whose integration corresponded to all four of the ethene protons. A broad resonance at δ 3.42 ppm was assigned to the four methine protons from the isopropyl groups of the arylimido ligand. The poor resolution of this multiplet was attributed to either rotation of the olefin or rotation of the imido substituent about the *Cipso*-N bond. The room temperature 100 MHz ^{13}C NMR spectrum was consistent with the proposed structure of (6), indicating that the two ends of the bound olefin were equivalent, there being only a single olefinic

resonance at δ 32.77 ppm ($^1J_{CH}$ 156.1 Hz). The coordinated ethene did not exhibit any phosphorus coupling in either the ^1H or the ^{13}C NMR spectra. Displacement of ethene (δ 5.24 ppm) by d_4-ethene was observed to occur by ^1H NMR within 12 hours at 60°C. This led to a corresponding decrease in the intensity of the bound olefin resonance. NMR data alone were insufficient to determine whether the olefin was lying in the MoN_2 plane or perpendicular to it; however, this was resolved by a molecular structure determination, the results of which are discussed in Section 3.3.2.

Variable temperature ^1H NMR was performed on a sample of (6) in C_7D_8. The data were consistent with both ends of the olefin and the two phosphine ligands remaining equivalent on the NMR timescale at all temperatures over the range -80 to +50°C.

The magnetic equivalence of the olefin in both the ^1H and ^{13}C NMR spectra indicated that the broadening observed in the ^1H spectrum, for the imido isopropyl group CH's, could be attributed solely to the rotation of the imido substituent about the C-N bond. Elevated temperature ^1H NMR spectra revealed considerably sharpening of the isopropyl septet. When the same sample was cooled, two septets became apparent at -80°C which exhibited a coalescence temperature, Tc, of 283 K.

As described in Section 3.2.1, an estimation of both the rate constant and free energy of rotation for the imido substituent can be made from this variable temperature ^1H NMR data. Calculations based on the separation of the two isopropyl septets at the low temperature limit (641.6 Hz) gave values for k and $\Delta G^{\ddagger}$ of 1425±18 s^{-1} and 52.1±1.0 $kJmol^{-1}$, respectively. However, the same calculations using the separation of the two isopropyl doublets (100.8 Hz) gave slightly different values of 223±18 s^{-1} and 56.5±1.0$kJmol^{-1}$.

This discrepancy has been rationalised in the following terms. The coupling associated with the methyl protons and with the methine proton is inequivalent, as the angular distortion experienced by the methyl groups will be more significant than for the methine proton. Steric interactions associated with the isopropyl groups are believed to be the cause.

3.3.2. Molecular Structure of $Mo(NAr)_2(PMe_3)_2(\eta^2\text{-}C_2H_4)$ (6)

Crystals suitable for a molecular structure determination were obtained from a concentrated n-pentane solution of (6) at -30°C. A crystal of appropriate dimensions (0.08 x 0.18 x 0.46 mm) was mounted in a Lindemann capillary under an inert atmosphere. The X-ray structure was determined by Prof. W. Clegg at the University of Newcastle. Complex (6) is illustrated in Figure 3.12 with selected bond distances and angles presented in Table 3.2.

(6) was found to adopt a highly distorted trigonal-bipyramidal geometry, in which the two imido ligands are situated in the equatorial plane, whilst the two phosphines are located axially. The coordinated ethene ligand was found to occupy an equatorial site, with the carbon-carbon bond lying perpendicular to the trigonal plane, as shown in Figure 3.12. Schrock's related tungsten complex, $W(NAr)_2(PMe_3)_2(\eta^2\text{-}C_2H_4)$,[19] and the recently synthesised $Mo(N\text{-}2\text{-}C_6H_4{}^tBu)_2(PMe_3)_2(\eta^2\text{-}C_2H_4)$[51] are both thought to adopt a similar geometry, although solid state structures have not been obtained in these cases.

The Mo-N bond distances of 1.831(3)Å indicate that the imido ligands bind to the metal centre through pseudo-triple bonds although there is an apparent elongation of the Mo-N bond distances relative to those observed for $Mo(NAr)_2(PMe_3)_2$ (5), (1.789(10)° and 1.794(12)°); this may be indicative of weakened imido-metal interactions which will in effect reduce the overall electron count for the complex. The Mo-N-C bond angle of 172.4(2)° is well within the range for "linear" imido units.[22] The C(1)-C(1') separation within the ethene ligand, at 1.386(8)Å, is consistent with a relatively small degree of back donation from the metal centre when compared with the olefinic carbon-carbon bond distances observed in either of the four coordinate complexes $CpNb(N\text{-}2,6\text{-}C_6H_3Cl_2)(PMe_3)(\eta^2\text{-}C_2H_4)$ (1.431(5)Å)[52] and $Mo(N^tBu)_2(PMe_3)(\eta^2\text{-}C_3H_6)$ (1.418(6)Å).[53] Some difference is to be expected as these latter two complexes adopt a metallocene like geometry (see for example Figure 3.15). The idealised carbon-carbon bond distances for double and single bonds is 1.34Å and 1.54Å, respectively.[32a]

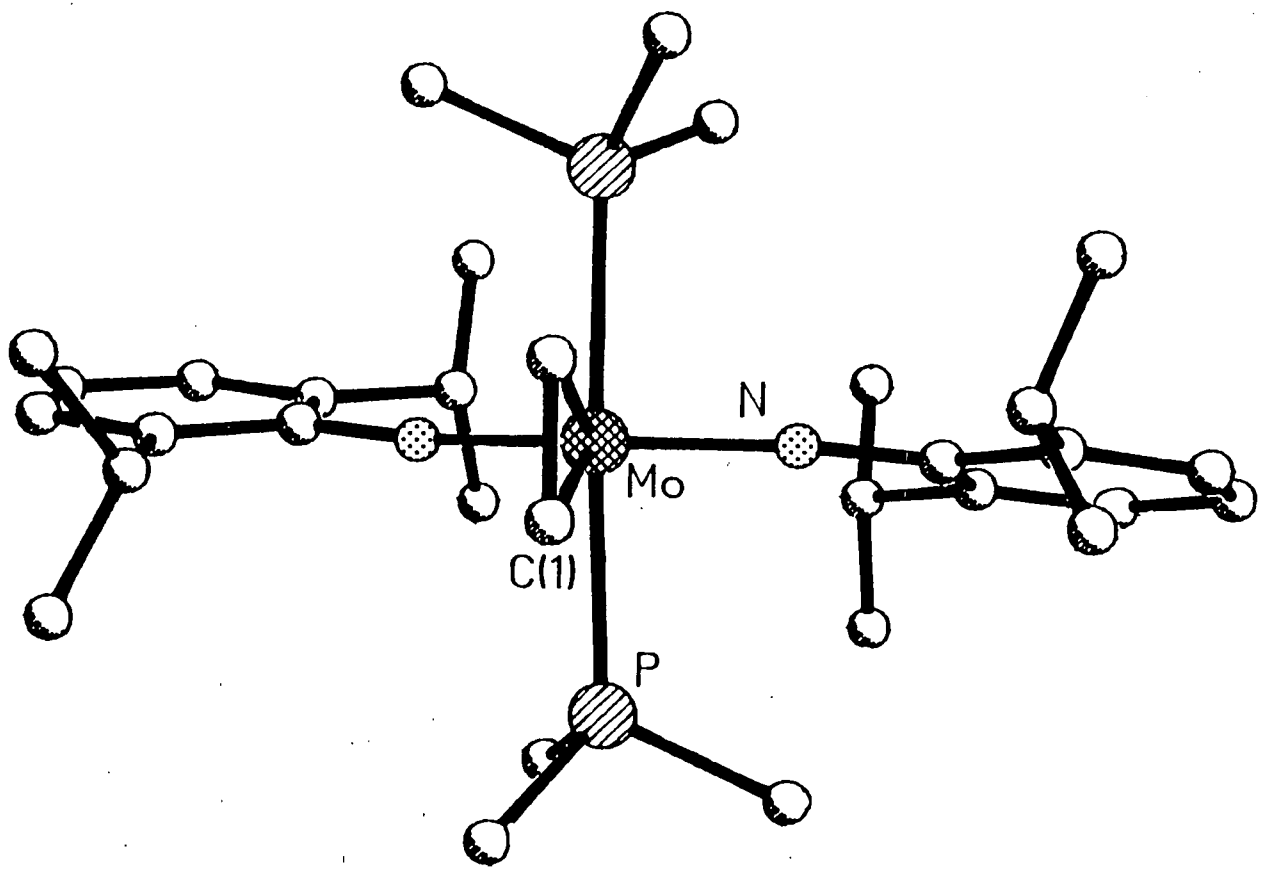

Figure 3.12 *Molecular structure of* $Mo(NAr)_2(PMe_3)_2(\eta^2\text{-}C_2H_4)$.

Table 3.2 *Bond lengths (Å) and angles(°) for $Mo(NAr)_2(PMe_3)_2(\eta^2\text{-}C_2H_4)$ (6) with estimated standard deviations in parentheses.*

Mo-C(1)	2.209(3)	Mo-P	2.538(1)
Mo-N	1.831(3)	C(1)-C(1′)	1.386(8)
P-C(2)	1.810(4)	P-C(3)	1.806(5)
P-C(4)	1.820(6)	N-C(5)	1.366(4)
C(5)-C(6)	1.428(4)	C(5)-C(10)	1.420(5)
C(6)-C(7)	1.394(5)	C(6)-C(11)	1.518(5)
C(7)-C(8)	1.379(6)	C(8)-C(9)	1.388(5)
C(9)-C(10)	1.392(5)	C(10)-C(14)	1.519(5)
C(11)-C(12)	1.525(5)	C(11)-C(13)	1.528(5)
C(14)-C(15)	1.458(7)	C(14)-C(16)	1.487(8)
C(1)-Mo-P	79.5(1)	C(1)-Mo-N	107.7(1)
P-Mo-N	87.2(1)	C(1)-Mo-C(1′)	36.6(2)
P-Mo-C(1′)	116.0(1)	N-Mo-C(1′)	107.3(1)
P-Mo-P′	164.6(1)	N-Mo-P′	87.9(1)
N-Mo-N′	143.1(2)	Mo-C(1)-C(1′)	71.7(1)
Mo-P-C(2)	115.2(2)	Mo-P-C(3)	114.3(1)
C(2)-P-C(3)	103.7(2)	Mo-P-C(4)	119.1(2)
C(2)-P-C(4)	100.7(3)	C(3)-P-C(4)	101.6(2)
Mo-N-C(5)	172.4(2)	N-C(5)-C(6)	122.3(3)
N-C(5)-C(10)	118.5(3)	C(6)-C(5)-C(10)	119.1(3)
C(5)-C(6)-C(7)	118.4(3)	C(5)-C(6)-C(11)	121.9(3)
C(7)-C(6)-C(11)	119.6(3)	C(6)-C(7)-C(8)	122.4(3)
C(7)-C(8)-C(9)	119.2(3)	C(8)-C(9)-C(10)	121.3(4)
C(5)-C(10)-C(9)	119.5(3)	C(5)-C(10)-C(14)	120.0(3)
C(9)-C(10)-C(14)	120.5(3)	C(6)-C(11)-C(12)	111.8(3)
C(6)-C(11)-C(13)	113.0(3)	C(12)-C(11)-C(13)	109.1(3)
C(10)-C(14)-C(15)	113.3(3)	C(10)-C(14)-C(16)	111.7(4)
C(15)-C(14)-C(16)	108.9(6)		

Complex (6) could formally be described as a 20 electron species which possesses an occupied π^* orbital. Hence, the N-Mo-N bond angle is large (143.1(2)°, cf. 137.1(5)° for $Mo(NAr)_2(PMe_3)_2$), in order to reduce the overall Mo-N bond order and minimise the destablising effect of the adopted configuration. Schrock *et al* attributed a similar effect to the distortion observed in the osmium bis (imido) complex $Os(NAr)_2(PMe_2Ph)I_2$, (151.2(3)°).[54] Should the N-M-N angle increase to 180°, forcing the complex to adopt a square pyramidal geometry, then only 16 electrons remain in metal-centred bonding orbitals, making the metal centre electron deficient. Further discussion of the geometrical preferences for these types of species is given in Sections 3.5 and 3.6.

3.3.3 Reaction of $Mo(NAr)_2Cl_2$.DME with n-Propyl Magnesium Chloride

An attempt to synthesise a higher homologue of the five coordinate olefin adduct was undertaken using an analogous route. The reaction appeared to proceed cleanly, with the formation of an intense purple/red solution on stirring at room temperature for 3 hours (Equation 3.10). However, on removal of solvent *in vacuo*, the solution began to change colour, leaving an intense green coloured solid. Subsequent extraction with n-pentane and recrystallisation at -30°C yielded $Mo(NAr)_2(PMe_3)_2$ (5), the olefin having been removed under reduced pressure. As described in Section 3.2.5 the lability of the olefin has been attributed to the steric hindrance of the two bulky trimethylphosphine ligands, which inhibit a strong metal olefin interaction.

$$\underset{\textbf{(1)}}{Mo(NAr)_2Cl_2.DME} + 2\ {}^{n}PrMgCl \xrightarrow[Et_2O]{\text{xs } PMe_3} \underset{\textbf{(7)}}{Mo(NAr)_2(PMe_3)_2(\eta^2\text{-}C_3H_6)} \xrightarrow{\text{Vacuum}} \underset{\textbf{(5)}}{Mo(NAr)_2(PMe_3)_2} \qquad \textbf{(3.10)}$$

The propene complex (7) can, however, be synthesised *in situ* through the reaction of the bis (phosphine) complex (5) with 1 equivalent

of propene. In the ^1H NMR spectrum (C_6D_6) of this reaction, two resonances attributable to the methyl group of propene were observed. The multiplet at δ 1.54 ppm was assigned to free propene, whilst the other resonance, a doublet at δ 1.98 ppm, was attributed to the methyl group of bound propene $Mo(NAr)_2(PMe_3)_2(\eta^2\text{-}C_3H_6)$ (7).

Homonuclear decoupling experiments were employed to confirm the assignment of the resonances due to the CH_2 and CH of the coordinated olefin. Irradiation of the methyl resonance at δ 1.98 ppm caused a dramatic loss of intensity in the corresponding resonance of free propene, δ 1.54 ppm (C_6D_6). This behaviour has been attributed to slow reversible dissociation of bound propene.

Such a dissociation process is equivalent to two species X and Y (bound and free propene, respectively) which are slowly interconverting with first order rate constants k_X and k_Y. Thus, an estimate of the rate of exchange of X and Y can be made using the Transfer of Saturation technique,[55] according to the Equation $Y_X = Y_0R_{1Y}/(R_{1Y} + k_X([X]/[Y]))$ (where Y_X and Y_0 are the intensities of the Y resonance in the absence and presence of saturation at X; R_{1Y} is the rate of spin-lattice relaxation of Y = $1/T_{1Y}$). So, the term $k_X([X]/[Y])$ represents the rate of saturation transfer from X to Y, and may be thought of as a pseudo-first-order rate constant. The results of this kinetic analysis for propene dissociation gave values for T_{1Y} = 1.21 s, R_{1Y} = 0.83 s^{-1}, Y_X = 25.96, Y_0 = 67.97, and $k_X([X]/[Y])$ = 1.34 Hz.

3.3.4 Attempted Isolation of $Mo(NAr)_2(\eta^2\text{-}C_2H_4)_2$

An attempt to isolate the diolefin derivative of (6) was undertaken *via* the reaction of $Mo(NAr)_2Cl_2$.DME in diethylether with two equivalents of C_2H_5MgCl under an ethene atmosphere. However, the reaction did not afford a tractable product. This may indicate that a diethene (or metallocyclopentane) species is too reactive or unstable to allow for its isolation. Similar observations have been made by Dr. A. Poole for the analogous reaction using $CpNb(NAr)Cl_2$.[24]

3.4 Other Attempted Reactions of $Mo(NAr)_2(PMe_3)_2(\eta^2\text{-}C_2H_4)$ (6)

The lability of the olefin in (6) has been explored through a variety of reactions. Simple dissociation of ethene, followed by coordination of other species was likely, by analogy with Schrock's tungsten complex. However, it was also envisaged that dissociation of phosphine could occur.

a) Reaction of $Mo(NAr)_2(PMe_3)_2(\eta^2\text{-}C_2H_4)$ (6) with Hydrogen

A C_6D_6 solution of (6) was sealed in an NMR tube under one atmosphere of hydrogen. Despite prolonged warming to 100°C, no reaction was observed. This lack of reactivity is not surprising since no reaction was observed with the bis (phosphine) complex, $Mo(NAr)_2(PMe_3)_2$.

b) Reaction of $Mo(NAr)_2(PMe_3)_2(\eta^2\text{-}C_2H_4)$ (6) with excess C_2H_4

It was envisaged that displacement of phosphine may occur, resulting in the generation of either bis (ethene) or more likely metallacyclopentane species. Yet, ^1H NMR analysis of a C_6D_6 solution of (6) with 20 equivalents of ethene showed no reaction, despite heating for an extended period. A similar lack of reactivity has been reported for both $CpNb(NAr)(PMe_3)(\eta^2\text{-}C_2H_4)$[24] and $Mo(N^tBu)_2(PMe_3)(\eta^2\text{-}C_2H_4)$.[56]

c) Reaction of $Mo(NAr)_2(PMe_3)_2(\eta^2\text{-}C_2H_4)$ (6) with excess Propene

In an attempt to generate the propene analogue, a solution of (6) was sealed in an NMR tube with an excess of the olefin. Heating to 70°C for two weeks gave no indication by ^1H NMR that any of the propene adduct had been generated. This lack of reaction was attributed to the much greater stability of the ethene analogue. The ethene derivative is readily isolated as a solid, yet the propene analogue proved unstable to vacuum. The overall stability of these five coordinate olefin complexes is dependent upon the size of the coordinated olefin.

d) Reaction of $Mo(NAr)_2(PMe_3)_2(\eta^2\text{-}C_2H_4)$ (6) with excess CO

Reaction of carbon monoxide with the metallocene and half-sandwich imido bis (phosphine) complexes readily yields the corresponding carbonyl derivatives, $Cp_2Ti(CO)(PMe_3)$,[12] and $CpNb(NAr)(PMe_3)(CO)$.[15a] A similar carbonylation reaction with the bis

(phosphine) complex $Mo(NAr)_2(PMe_3)_2$ gave a variety of carbonyl containing species, none of which could be identified. The complexity of this latter reaction prompted investigation of the interaction of (6) with CO. When an ethereal solution of the olefin adduct was stirred under an atmosphere of CO at ambient temperature for 3 hours, a comparable intractable mixture of carbonyl species was obtained.

3.4.1 Reaction of $Mo(NAr)_2(PMe_3)_2(\eta^2\text{-}C_2H_4)$ (6) with excess Diphenylacetylene

Analysis of the product obtained from the reaction of the bis (arylimido) bis (phosphine) complex (5) with diphenylacetylene, indicated that an adduct had been formed. However, purification and analysis of this product proved difficult, Section 3.2.9. Reactions with the olefin adduct (6) proved more satisfactory. A heptane solution of (6) was treated with one equivalent of diphenylacetylene and was heated to 60°C for one week (Equation 3.11) during which time the solution gradually turned from an intense red/purple to brown. On removal of the volatiles and subsequent recrystallisation at 5°C from a saturated THF solution, flocculent fine orange needles of the acetylene adduct of (8) were isolated in low yield.

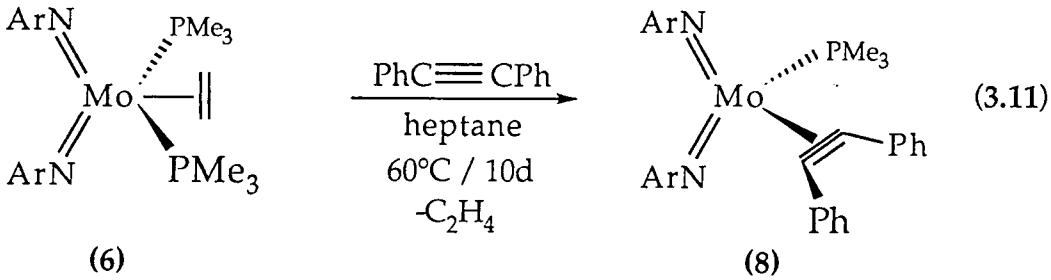

(6) (8) (3.11)

Gibson and Poole[50] observed that a similar displacement reaction performed with $CpNb(NAr)(PMe_3)(\eta^2\text{-}C_3H_6)$ did not lead to quantitative conversion to the acetylene complex. Instead, an equilibrium mixture was obtained which was rationalised according to the greater steric bulk of the acetylene destabilising its associated complex. This observation could explain the low yield of $Mo(NAr)_2(PMe_3)(\eta^2\text{-}PhC{\equiv}CPh)$, although no equilibrium was observed upon monitoring the reaction by ^1H NMR. A further discussion of acetylene complexes is given in Section 4.1.

3.4.2 Reaction of $Mo(NAr)_2(PMe_3)_2(\eta^2\text{-}C_3H_6)$ (7) with excess C_2H_4

To explore reactivity of the propene complex (7), a sample was generated in an NMR tube *via* reaction of the bis (phosphine) complex (5) with propene. Once the adduct had formed (monitored by ^1H NMR), the NMR tube was vented of excess propene. Subsequently, one equivalent of ethene was condensed into the tube. The reaction led to the generation of the more stable ethene complex slowly over 12 h at room temperature.

3.5 Preparation of 4 Coordinate Bis (Imido) Olefin Complexes

The previous study has shown that five coordinate olefin complexes are formed with the $[Mo(NAr)_2]$ fragment due to the ability of the arylimido unit to rotate out of the way. To generate olefin complexes that adopt a four coordinate metallocene-like geometry the tert-butyl imido ligand has been investigated.

3.5.1 Reaction of $Mo(N^tBu)_2Cl_2$.DME with Ethyl Magnesium Chloride

Treatment of $Mo(N^tBu)_2Cl_2$.DME with two equivalents of ethyl magnesium chloride in the presence of excess trimethylphosphine in diethylether, Equation 3.12 (R= H (**10**); R= Me (**11**)), afforded yellow crystals on work-up from a cooled (-30°C) n-pentane solution. Both NMR (^1H and ^{13}C) and elemental analyses were consistent with the formation of the mono-olefin mono-phosphine complex $Mo(N^tBu)_2(PMe_3)(\eta^2\text{-}C_2H_4)$ (**10**).[53] As for (**6**), GC-MS analysis of the volatiles generated during the reaction were consistent with (**10**) having formed *via* β-elimination from an intermediate diethyl species.

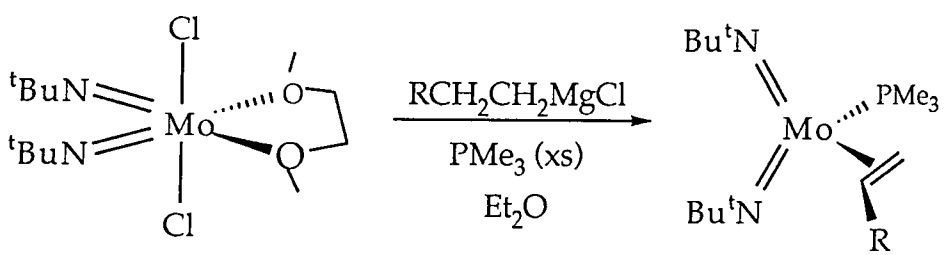

(3.12)

A room temperature 400 MHz ^1H NMR spectrum of (**10**) indicated that the two ends of the olefin were inequivalent. The ^1H NMR data are presented in Figure 3.13. The spectra were complicated by the coincidence of part of the olefinic resonances with the tert-butyl imido signals and the doublet from bound PMe_3. 500 MHz ^1H NMR spectra proved insufficient to resolve all three resonances.

The 100 MHz ^{13}C NMR spectrum of (**10**) indicated that the two olefinic carbons were inequivalent, δ 20.96 ppm ($^1J_{CH}$ 156.1 Hz) and δ 31.76 ppm ($^1J_{CH}$ 152.4 Hz). The two $^1J_{CH}$ coupling constants are within the range for sp^2 hybridised carbon atoms. The NMR data were supportive of (**10**), having adopted a bent metallocene-like geometry in which the olefinic carbons were occupying a plane with the Mo and P atoms perpendicular to the N=Mo=N plane. Conclusive proof of the orientation of the olefin could only be obtained from a solid state structure determination which proved unobtainable. It is thought that (**10**) would adopt a structure analogous to that determined by Rausch *et al* for $Cp_2Zr(PMe_3)(\eta^2\text{-}C_2H_4)$.[57]

Close inspection of the two olefinic carbon resonances revealed that the resonance at δ 31.76 ppm showed a small coupling to phosphorus, $^2J_{PC}$ 9.9 Hz, while the other carbon resonance at δ 20.96 ppm showed no indication of phosphorus coupling. Further discussion of this phenomenon is made in the following Section. Attempts to assign the hydrogens, and thus the carbons of the ethene ligand in (**10**), by NOE (nuclear Overhauser effect) and HETCOR (heteronuclear correlation spectroscopy) experiments proved unsuccessful.

3.5.2 Reaction of $Mo(N^tBu)_2Cl_2$.DME with ^{n}Propyl Magnesium Chloride

The reaction of $Mo(N^tBu)_2Cl_2$.DME using n-propyl magnesium chloride to generate the propene complex has also been studied (Equation 3.12). Upon work-up, yellow crystals were isolated from a saturated n-pentane solution at -30°C. NMR and elemental analyses were consistent with this complex having the molecular formula of $Mo(N^tBu)_2(PMe_3)(\eta^2\text{-}C_3H_6)$,[53] (**11**), analogous to the ethene adduct (**10**). GC-MS analysis supported the intermediacy of a dialkyl species in the generation of the olefin complex.

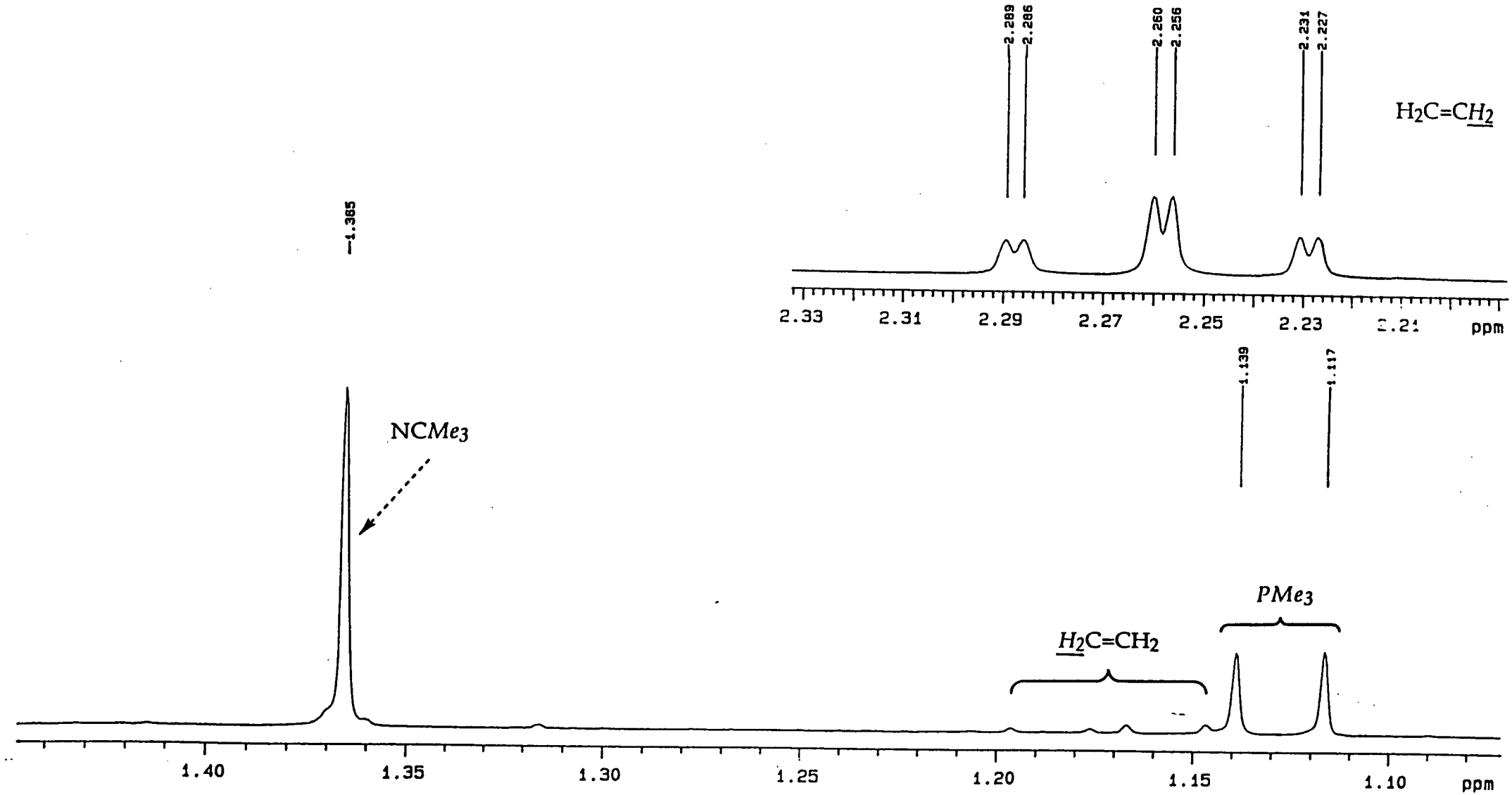

Figure 3.13a *400 MHz ^1H NMR spectrum of $Mo(N^tBu)_2(PMe_3)(\eta^2\text{-}C_2H_4)$.*

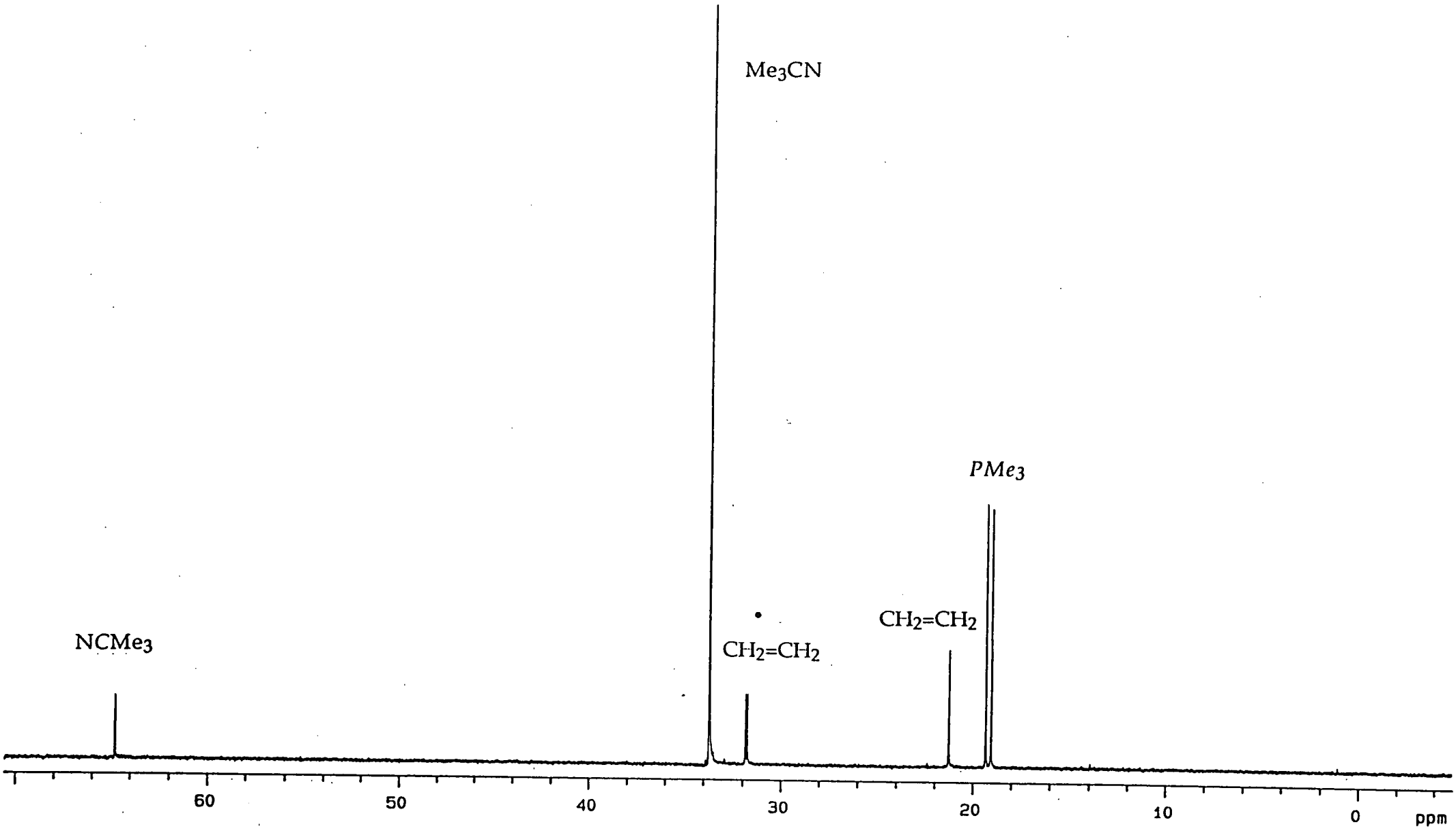

Figure 3.13b *100 MHz ^{13}C NMR spectrum of $Mo(N^tBu)_2(PMe_3)(\eta^2\text{-}C_2H_4)$.*

The ^1H NMR spectrum was complicated due to the unsymmetrical nature of the coordinated olefin and to the pro-chiral nature of the metal centre giving rise to an AA'MM' spin system for the coordinated olefin; ^1H NMR analysis (including $^1H\{^{31}P\}$) was undertaken to fully assign the spectra, the results being shown in Figure 3.14 and Table 3.3.

Assignment	^1H 500 MHz δ (ppm)	$^1H\{^{31}P\}$ multiplicities	Coupling Constants (Hz)
CH_2=C*H*(Me)	3.23 (tqd)	tq	$^3J_{HH}$ 10.8, $^3J_{HH}$ 6.3, $^3J_{PH}$ 1.4
CH_2=CH(*Me*)	2.24 (d)	d	$^3J_{HH}$ 6.3
$NCMe_3$	1.36 (s)	s	
$NCMe_3$	1.34 (td)	s	
C*H*$_2$=CH(Me)	1.22 (ddd)	dd	$^3J_{HH}$ 10.8, $^2J_{HH}$ 5.4, $^3J_{PH}$ 5.2
PMe_3	1.12 (d)	(s)	$^2J_{PH}$ 8.7
C*H*$_2$=CH(Me)	1.02 (ddd)	(dd)	$^3J_{HH}$ 10.8, $^2J_{HH}$ 5.4, $^3J_{PH}$ 5.2

Table 3.3 *Selected 500 MHz ^1H NMR data for $Mo(N^tBu)_2(PMe_3)(\eta^2$-$C_3H_6)$, (11).*

^{13}C NMR data (Figure 3.14c) were also consistent with the formulation of (**11**) and emphasised the inequivalence of the imido ligands. Resonances at δ 39.93 and 37.46 ppm were attributed to the carbons of the coordinated olefin (supported by a ^1H - ^{13}C HETCOR experiment), the latter exhibiting a coupling to phosphorus of 9.6 Hz. The intermediate values of the $^1J_{CH}$ coupling constants (148.6 and 148.8 Hz, respectively) are supportive of significant π back bonding from the olefin to molybdenum; thus, a metallacyclopropane bonding picture is appropriate. These data, in conjunction with both the proton coupled ^{13}C NMR spectrum and the solid state molecular structure (Section 3.4.9), enabled the absolute assignment of these two olefinic resonances. The carbon that is adjacent and effectively *cis* to the phosphine experiences a greater phosphorus coupling.

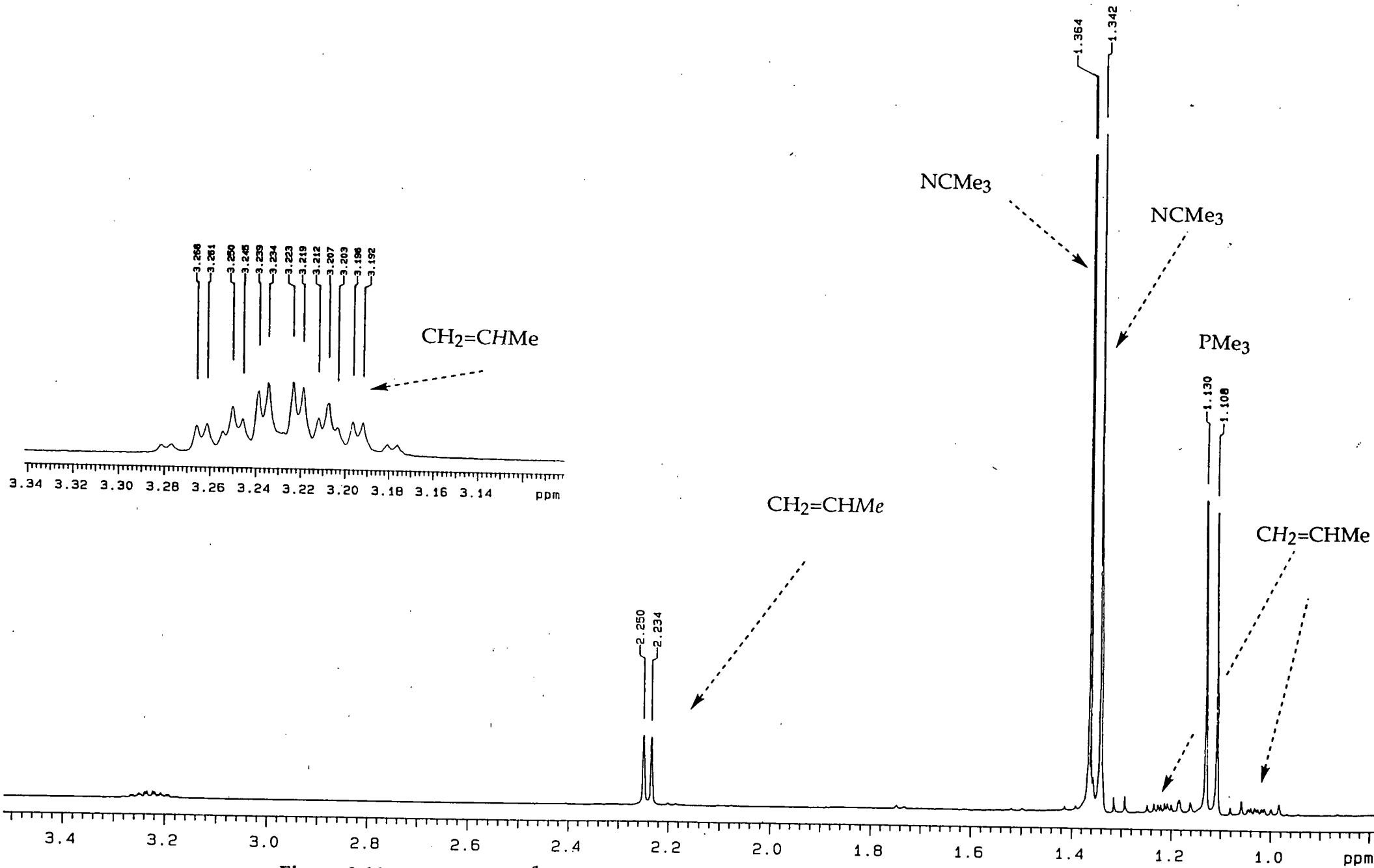

Figure 3.14a *400 MHz ^1H NMR spectrum of $Mo(N^tBu)_2(PMe_3)(\eta^2\text{-}C_3H_6)$.*

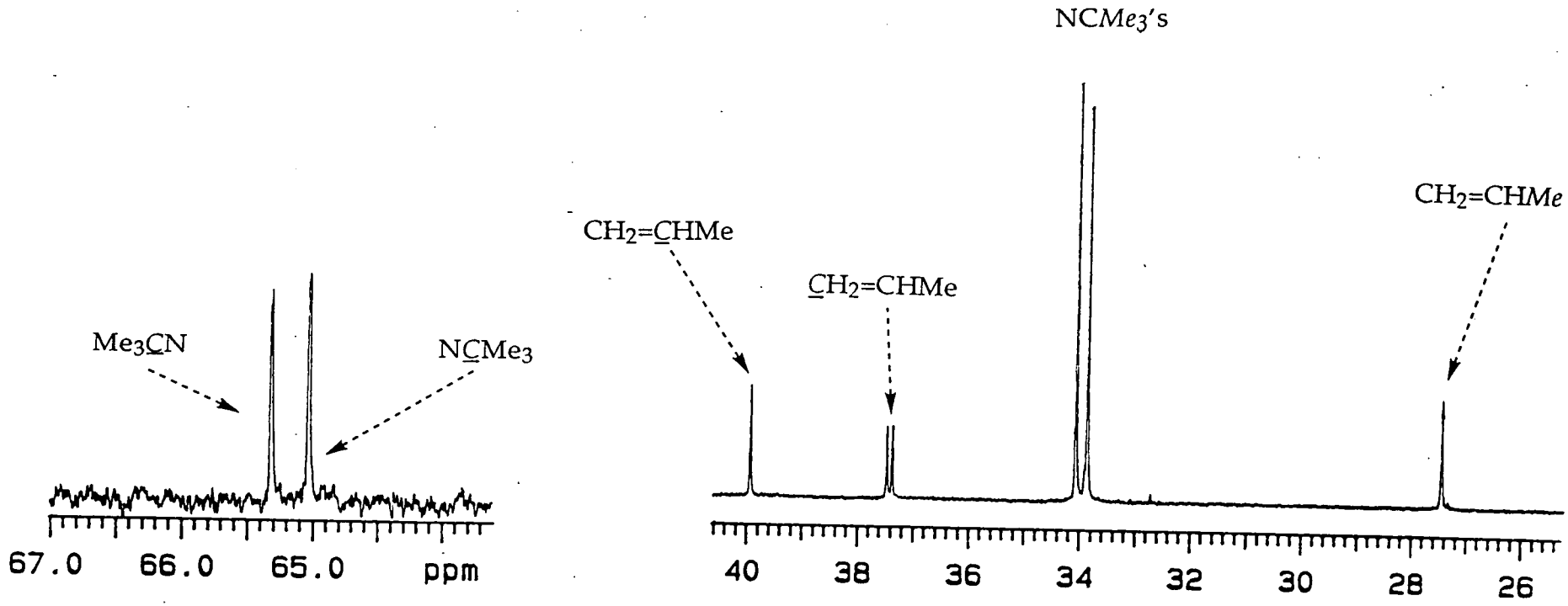

Figure 3.14c *100 MHz ^{13}C NMR spectrum of $Mo(N^tBu)_2(PMe_3)(\eta^2\text{-}C_3H_6)$.*

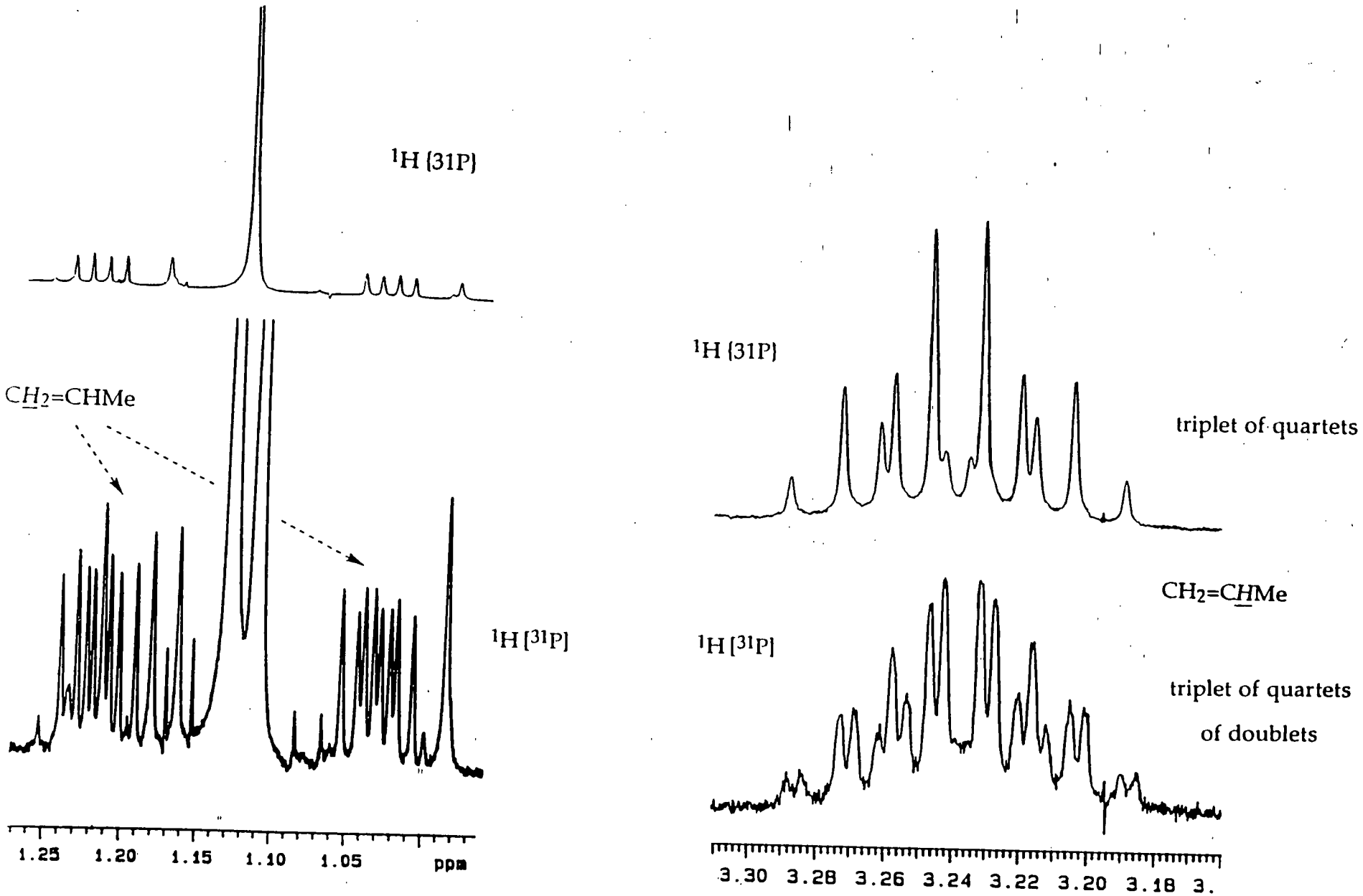

Figure 3.14 *Comparison of the ^{1}H [^{31}P] and ^{1}H {^{31}P} 500 MHz ^{1}H NMR spectra of Mo(N^{t}Bu)$_2$(PMe$_3$)(η^2-C$_3$H$_6$).*

Similar couplings to phosphorus have been detected for the acetylenic carbons of $Mo(N^tBu)_2(PMe_3)(PhC{\equiv}CH)$ (**16**) (Section 4.14). The asymmetric nature of the coordinated acetylene in conjunction with the results from a difference NOE experiment allowed the unambiguous assignment of the NMR spectra. As for (**10**) the unsaturated carbon atom that is adjacent to the phosphine exhibited the strongest ^{31}P coupling. Similar coupling to phosphorus was observed for $Cp_2Zr(PMe_3)(\eta^2\text{-}C_2H_4)$ (J_{PC}= 12.1 and 3.3 Hz).[57]

A similar geometric assignment was made by Bercaw *et al* for the complex $Cp^*_2Ta(H)(\eta^2\text{-}C_2H_4)$, which exhibited a small (2.7 Hz) coupling between the *endo* ethylenic hydrogens and the metal-bound hydride atom.[58]

Both (**10**) and (**11**) are readily soluble in hydrocarbon solvents and are stable for prolonged periods (months). Yet, both of these olefin complexes decompose rapidly in chlorocarbon solvents, a feature also observed for the five coordinate adduct, (**6**). In all cases free amine is liberated.

3.5.3 Molecular Structure of $Mo(N^tBu)_2(PMe_3)(\eta^2\text{-}C_3H_6)$ (11)

Yellow cubic crystals of suitable dimensions for a molecular structure determination were mounted in Lindemann capillaries under an inert atmosphere. The X-ray data were collected and the molecular structure solved by Prof. J.A.K. Howard and Ms. C. Wilson within this department. Selected bond angles and distances are given in Table 3.4 and the molecular structure is illustrated in Figure 3.15.[53]

(**11**) was found to adopt a pseudo-tetrahedral geometry with mean N-Mo-N and N-Mo-P angles of 123.0 and 100.7° respectively. The angles subtended at the molybdenum by the C(1)-C(2) centroid of the olefin and the N^tBu and PMe_3 ligands are 113.8 (mean) and 99.5(1)°. The Mo, P, C(1) and C(2) atoms lie in a pseudoplane (mean deviation 0.041Å), which bisects the N-Mo-N angle (deviation from orthogonality 0.4°). The Mo-N-C angles of 168.3(3) and 162.6(3)°, lie within the range of 'linear' imido units while the Mo=N distances, at 1.774(3) and 1.765(3)Å, are slightly elongated compared to those typically observed in mono-imido molybdenum complexes;[22] this is a reflection of the competition which exists between the two imido groups for the available π-symmetry metal

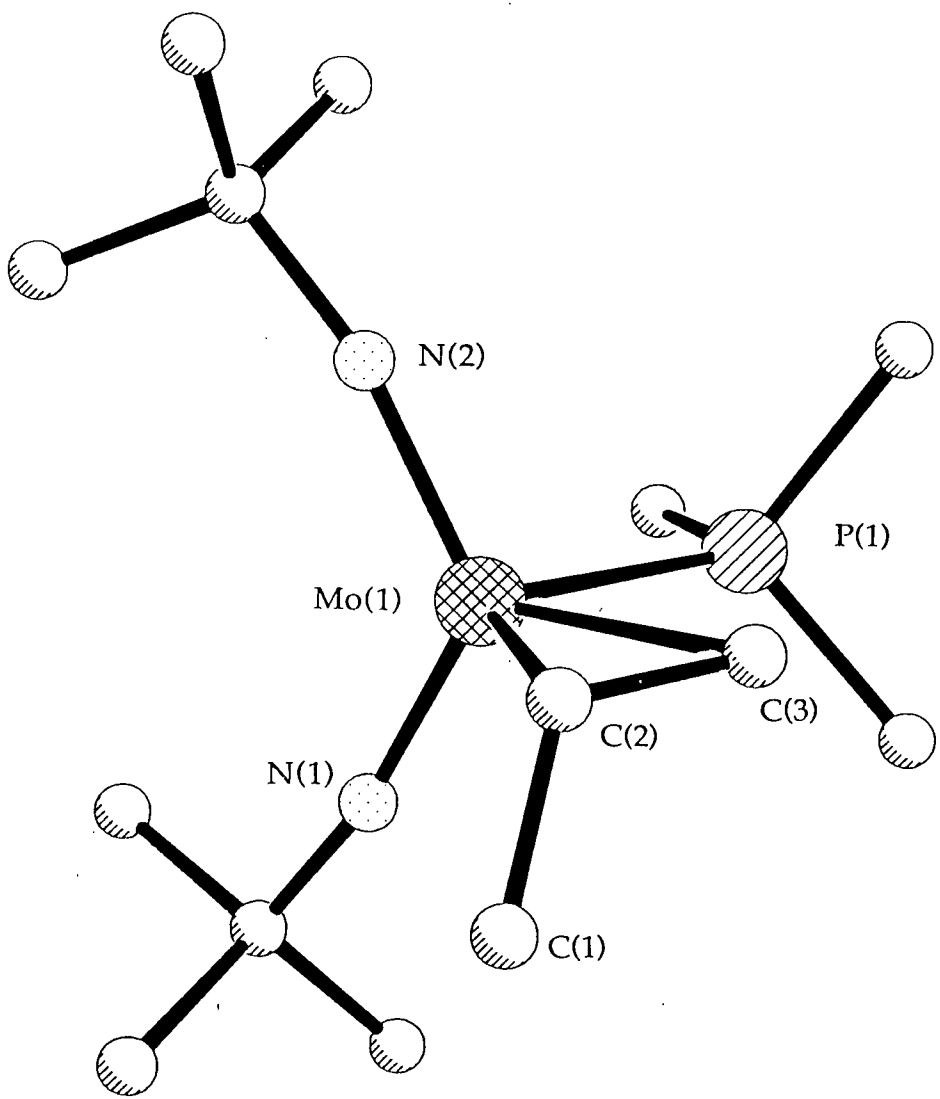

Figure 3.15 *Molecular structure of $Mo(N^tBu)_2(PMe_3)(\eta^2\text{-}C_3H_6)$.*

orbitals in a tetrahedral geometry.[22,25] The C(1)-C(2) separation within the propene ligand, 1.418(6)Å, is consistent with considerable back donation from the d^2 metal centre, and the alignment is supportive of bent-metallocene-like frontier orbitals for the $[Mo(N^tBu)_2]$ fragment.

Of the two possible isomers of (**11**), *exo* and *endo* , only one isomer is observed in solution by both ^1H and ^{13}C NMR spectroscopy. Difference NOE measurements were supportive of the *exo* geometry established in the solid state. Comparison of the molecular structure of (**11**) with that for $Cp_2Zr(PMe_3)(\eta^2\text{-}C_2H_4)$[57] indicated that a metallocene geometry had been adopted.

The propene adduct (**11**) was readily converted to the ethene analogue (**10**) upon treatment of (**11**) with one equivalent of ethene at 60°C for 10 hours. This reflects the greater steric congestion at the metal centre in the propene derivative. Similar steric arguments were used to explain the lack of stability of the five coordinate propene complex (**7**) compared to its ethene analogue, Section 3.3.3.

Table 3.4 *Selected bond lengths (Å) and angles (°) for $Mo(N^tBu)_2(PMe_3)(\eta^2\text{-}C_3H_6)$ (**11**) with estimated standard deviations in parentheses.*

Mo(1)-P(1)	2.445(1)	Mo(1)-N(1)	1.774(3)
Mo(1)-N(2)	1.765(3)	Mo(1)-C(1)	2.228(4)
Mo(1)-C(2)	2.182(3)	P(1)-C(12)	1.790(5)
P(1)-C(13)	1.813(5)	P(1)-C(14)	1.813(5)
N(1)-C(4)	1.447(4)	N(2)-C(8)	1.455(6)
C(1)-C(2)	1.418(6)	C(2)-C(3)	1.521(7)
C(4)-C(5)	1.529(6)	C(4)-C(6)	1.514(7)
C(4)-C(7)	1.528(6)	C(8)-C(9)	1.533(11)
C(8)-C(10)	1.592(14)	C(8)-C(11)	1.527(11)
C(8)-C(9A)	1.482(24)	C(8)-C(9B)	1.514(27)
C(8)-C(10A)	1.538(29)	C(8)-C(10B)	1.575(30)
C(8)-C(11A)	1.578(26)	C(8)-C(11B)	1.576(23)
C(9)-C(9A)	0.735(32)	C(9)-C(9B)	0.627(29)
C(10)-C(9A)	2.016(28)	C(10)-C(10A)	0.684(27)
C(10)-C(10B)	0.624(28)	C(11)-C(11A)	0.770(29)
C(11)-C(11B)	0.806(30)	C(9A)-C(9B)	1.297(40)
C(9A)-C(10B)	1.556(39)	C(9B)-C(11A)	1.723(34)
C(10A)-C(10B)	1.262(35)	C(10A)-C(11B)	1.450(38)
C(11A)-C(11B)	1.546(38)		

P(1)-Mo(1)-N(1)	101.7(1)	P(1)-Mo(1)-N(2)	99.7(1)
N(1)-Mo(1)-N(2)	123.0(1)	P(1)-Mo(1)-C(1)	81.1(1)
N(1)-Mo(1)-C(1)	116.0(2)	N(2)-Mo(1)-C(1)	119.1(2)
P(1)-Mo(1)-C(2)	118.4(1)	N(1)-Mo(1)-C(2)	108.2(1)
N(2)-Mo(1)-C(2)	106.5(2)	C(1)-Mo(1)-C(2)	37.5(2)
Mo(1)-P(1)-C(12)	116.3(2)	Mo(1)-P(1)-C(13)	114.1(2)
C(12)-P(1)-C(13)	102.2(3)	Mo(1)-P(1)-C(14)	116.0(2)
C(12)-P(1)-C(14)	103.6(2)	C(13)-P(1)-C(14)	102.8(3)
Mo(1)-N(1)-C(4)	162.6(3)	Mo(1)-N(2)-C(8)	168.3(3)
Mo(1)-C(1)-C(2)	69.5(2)	Mo(1)-C(2)-C(1)	73.0(2)
Mo(1)-C(2)-C(3)	116.3(3)	C(1)-C(2)-C(3)	119.6(4)
N(1)-C(4)-C(5)	110.4(3)	N(1)-C(4)-C(6)	108.5(3)
C(5)-C(4)-C(6)	109.9(4)	N(1)-C(4)-C(7)	109.1(3)
C(5)-C(4)-C(7)	110.2(4)	C(6)-C(4)-C(7)	108.7(4)
N(2)-C(8)-C(9)	109.0(5)	N(2)-C(8)-C(10)	106.4(5)
C(9)-C(8)-C(10)	108.9(7)	N(2)-C(8)-C(11)	108.3(5)
C(9)-C(8)-C(11)	116.1(7)	C(10)-C(8)-C(11)	107.7(7)
N(2)-C(8)-C(9A)	110.9(11)	C(9)-C(8)-C(9A)	28.1(12)
C(10)-C(8)-C(9A)	81.9(12)	C(11)-C(8)-C(9A)	134.8(12)
N(2)-C(8)-C(9B)	110.4(11)	C(9)-C(8)-C(9B)	23.7(11)
C(10)-C(8)-C(9B)	127.9(12)	C(11)-C(8)-C(9B)	94.3(11)
C(9A)-C(8)-C(9B)	51.3(15)	N(2)-C(8)-C(10A)	109.0(11)
C(9)-C(8)-C(10A)	127.8(11)	C(10)-C(8)-C(10A)	25.2(10)
C(11)-C(8)-C(10A)	83.5(11)	C(9A)-C(8)-C(10A)	103.8(15)

C(9B)-C(8)-C(10A)	139.1(16)	N(2)-C(8)-C(10B)	103.9(11)
C(9)-C(8)-C(10B)	89.1(11)	C(10)-C(8)-C(10B)	22.7(10)
C(11)-C(8)-C(10B)	128.3(11)	C(9A)-C(8)-C(10B)	61.1(15)
C(9B)-C(8)-C(10B)	111.0(14)	C(10A)-C(8)-C(10B)	47.8(14)
N(2)-C(8)-C(11A)	106.7(10)	C(9)-C(8)-C(11A)	91.0(10)
C(10)-C(8)-C(11A)	132.6(11)	C(11)-C(8)-C(11A)	28.7(10)
C(9A)-C(8)-C(11A)	115.8(14)	C(9B)-C(8)-C(11A)	67.7(13)
C(10A)-C(8)-C(11A)	110.5(14)	C(10B)-C(8)-C(11A)	147.6(15)
N(2)-C(8)-C(11B)	104.9(10)	C(9)-C(8)-C(11B)	139.9(11)
C(10)-C(8)-C(11B)	80.6(11)	C(11)-C(8)-C(11B)	30.0(11)
C(9A)-C(8)-C(11B)	143.3(15)	C(9B)-C(8)-C(11B)	122.0(14)
C(10A)-C(8)-C(11B)	55.5(14)	C(10B)-C(8)-C(11B)	103.0(14)
C(11A)-C(8)-C(11B)	58.7(14)	C(8)-C(9)-C(9A)	72.1(20)
C(8)-C(9)-C(9B)	76.4(26)	C(9A)-C(9)-C(9B)	144.5(35)
C(8)-C(10)-C(9A)	46.7(8)	C(8)-C(10)-C(10A)	73.0(26)
C(9A)-C(10)-C(10A)	114.0(27)	C(8)-C(10)-C(10B)	77.1(30)
C(9A)-C(10)-C(10B)	36.1(28)	C(10A)-C(10)-C(10B)	149.4(41)
C(8)-C(11)-C(11A)	79.3(20)	C(8)-C(11)-C(11B)	78.3(18)
C(11A)-C(11)-C(11B)	157.6(29)	C(8)-C(9A)-C(9)	79.8(21)
C(8)-C(9A)-C(10)	51.4(9)	C(9)-C(9A)-C(10)	129.0(24)
C(8)-C(9A)-C(9B)	65.6(16)	C(9)-C(9A)-C(9B)	16.3(16)
C(10)-C(9A)-C(9B)	113.0(18)	C(8)-C(9A)-C(10B)	62.4(14)
C(9)-C(9A)-C(10B)	141.7(28)	C(10)-C(9A)-C(10B)	13.7(10)
C(9B)-C(9A)-C(10B)	126.1(22)	C(8)-C(9B)-C(9)	79.9(28)
C(8)-C(9B)-C(9A)	63.1(16)	C(9)-C(9B)-C(9A)	19.2(21)
C(8)-C(9B)-C(11A)	57.9(12)	C(9)-C(9B)-C(11A)	136.4(35)
C(9A)-C(9B)-C(11A)	117.6(23)	C(8)-C(10A)-C(10)	81.8(26)
C(8)-C(10A)-C(10B)	67.6(18)	C(10)-C(10A)-C(10B)	14.6(20)
C(8)-C(10A)-C(11B)	63.6(16)	C(10)-C(10A)-C(11B)	145.2(37)
C(10B)-C(10A)-C(11B)	130.7(28)	C(8)-C(10B)-C(10)	80.2(29)
C(8)-C(10B)-C(9A)	56.5(14)	C(10)-C(10B)-C(9A)	130.2(35)
C(8)-C(10B)-C(10A)	64.6(18)	C(10)-C(10B)-C(10A)	16.0(22)
C(9A)-C(10B)-C(10A)	114.7(25)	C(8)-C(11A)-C(11)	72.0(21)
C(8)-C(11A)-C(9B)	54.4(12)	C(11)-C(11A)-C(9B)	122.0(28)
C(8)-C(11A)-C(11B)	60.6(14)	C(11)-C(11A)-C(11B)	11.4(16)
C(9B)-C(11A)-C(11B)	111.4(20)	C(8)-C(11B)-C(11)	71.6(18)
C(8)-C(11B)-C(10A)	61.0(14)	C(11)-C(11B)-C(10A)	127.2(26)
C(8)-C(11B)-C(11A)	60.7(13)	C(11)-C(11B)-C(11A)	10.9(14)
C(10A)-C(11B)-C(11A)	117.4(20)		

3.6 Calculations and Bonding in Complexes Containing the "$M(NR)_2$" Fragment

Schrock[59] has recently reported detailed SCF-Xα-SW calculations on the $M(NH)_2(PH_3)_2$ fragment and its interaction with olefins to form a five coordinate adduct. This study has shown that the symmetry properties and related energies of the frontier orbitals calculated for the "$W(NH)_2$" fragment are analogous to those obtained for the MCp_2 system.[8] This correlation strongly supports the proposed pseudo-isolobal relationship that exists between Group 6 bis (imido) complexes and bent Group 4 metallocenes.

From these calculations it was possible to rationalise the geometries adopted by both $W(NAr)_2(PMe_3)_2$ and $W(NAr)_2(PMe_3)_2(\eta^2\text{-}C_2H_4)$ (this later structure being predicted from the molecular structure determination of it's molybdenum analogue). The HOMO (level $4a_1$) consisted largely of a linear combination of $d_{x^2-y^2}$ and d_{z^2} character orientated in the y-direction. This is equivalent to the HOMO being of d_{y^2} character. The next highest levels were $2b_2$ and $5a_1$.

If the two phosphorus atoms are considered to be in a four coordinate geometry (cf. $W(NAr)_2(PMe_2Ph)_2$) then the linear combination of the P σ-orbitals transforms as A_1+B_2 symmetry. The B_2 component can then interact with the metal $2b_2$ level, the interaction being at a maximum when the P-W-P angle is 90°. The remaining A_1 combination can therefore interact with either the $4a_1$ or $5a_1$. Interaction with the $4a_1$ level was found to be disfavoured as this led to the occupation of a high lying σ* orbital, whereas the interaction with the $5a_1$ level was found to be stabilising. This latter interaction was found to increase as the P-W-P angle decreased. The experimentally determined value of this angle was 95° in the case of $W(NAr)_2(PMe_2Ph)_2$.

The results of these calculations were used to probe the bonding of the related five coordinate olefin adduct. The HOMO remained unchanged on coordination of the olefin, remaining the $4a_1$ level, the W-N-H σ and the W-N π levels changed only slightly. The orientation of the HOMO for $W(NH)_2(PH_3)_2$ forces the olefin to align in the yz plane perpendicular to the N=W=N wedge, such that π backbonding is possible. This predicted bonding preference is reinforced by the molecular structure determination of the molybdenum analogue, $Mo(NAr)_2(PMe_3)_2(\eta^2\text{-}C_2H_4)$,[60] which does indeed show the olefin orientated in this manner.

3.7 Fenske-Hall Calculations on the Model Compounds $Mo(NH)_2(PMe_3)_2(C_2H_4)$ and $Mo(NH)_2(PMe_3)(C_2H_4)$

Similar calculations using the Fenske-Hall quantum method have been undertaken by Dr. C. Housecroft (University of Cambridge)[61] to explore the bonding in both the four coordinate and five coordinate olefin complexes of molybdenum (Sections 3.3.2 and 3.5.3). These calculations were based upon the X-ray structural data obtained for the complexes $Mo(NAr)_2(PMe_3)_2(\eta^2\text{-}C_2H_4)$[60] and $Mo(N^tBu)_2(PMe_3)(\eta^2\text{-}C_2H_4)$,[53] although calculations were simplified by using the model complexes $Mo(NH)_2(PH_3)_2(\eta^2\text{-}C_2H_4)$ and $Mo(NH)_2(PH_3)(\eta^2\text{-}C_2H_4)$, whose geometry was based upon the experimentally determined structural data.

a) *$[Mo(NH)_2]$ fragment: Frontier MO's as a Function of N-Mo-N angle*

Calculations indicated that little variation of the molecular orbitals occurred as the N-Mo-N angle is varied between 120 and 150°. The composition of each of the MO's was found to be virtually independent of the actual angle which obviously includes both the HOMO and the LUMO.

b) Analysis of the $Mo(NH)_2(PH_3)(\eta^2\text{-}C_2H_4)$ Fragment

The interfragment interactions between MO's of the olefin and the bis (imido) fragment $[Mo(NH)_2(PH_3)]$ were classified according to the Dewar-Chatt-Duncanson model as being either σ donating or π back donating. The participation of the phosphorus atom, albeit weak, may be significant.

To address the question why should the olefin prefer to bond within the plane containing the Mo-P bond (i.e. in a bent metallocene-like geometry), point calculations were carried out on the $[Mo(NH)_2(PH_3)]$ fragment; the fragment was held constant whilst the olefin was rotated through 90° in 10° steps. The total MOP (Mulliken Overlap Population) between the fragments decreases from 0.341 to 0.258; the interaction which corresponds to the overlap between a molybdenum d_{xz} orbital and the olefin π^* MO has a major contribution when θ=0° (i.e. the olefin is orientated as observed in (**11**)), which falls to zero when θ=90°. Just as the SCF-Xα SW calculations showed the main driving force for a particular olefin orientation is maximisation of metal-olefin dπ-pπ back bonding.

c) *Analysis of the $Mo(NH)_2(PH_3)_2(\eta^2\text{-}C_2H_4)$ Fragment*

The frontier orbitals of the olefin in this fragment are identical to those observed for the olefin in the $Mo(NH)_2(PH_3)(\eta^2\text{-}C_2H_4)$ fragment. It is to be noted that these MO's are almost identical to those calculated by Schrock for the analogous $[W(NH)_2(PH_3)_2]$ fragment. As with $Mo(NH)_2(PH_3)(\eta^2\text{-}C_2H_4)$ the interactions of the bis (imido) fragment with the olefin in this five coordinate adduct may readily be classified in terms of σ donation and π back donation.

The same exercise was performed for this olefin fragment as for the previous complex. The olefin was rotated through 90° in 10° steps and point calculations were used to assess the changes in the interfragment interactions as a function of this angle θ. (θ=0° for the experimentally determined orientation). At θ=0°, the total Mulliken Overlap Population is 0.33 which drops to 0.250 for θ=90°. Two important metal-olefin interactions (d_{yz} and olefin π^* MO) were optimised at θ=0° and fell to zero at θ=90°. As in the four coordinate complex, the interfragment interactions that become allowed as the olefin rotates from θ=0° to 90 are not effective enough to compensate for the loss of the olefin-metal interaction, once again demonstrating that the orientation of the olefin is dominated by $d\pi$-$p\pi$ back bonding.

The calculated frontier molecular orbitals for the model fragment $Mo(NH_3)(PMe_3)(C_2H_4)$, shown in Figure 3.16, agree well with those calculated for the two fragments that have been postulated as being pseudo-isolobal to the former, namely $[Cp_2Zr]$ and [CpNb(NAr)].

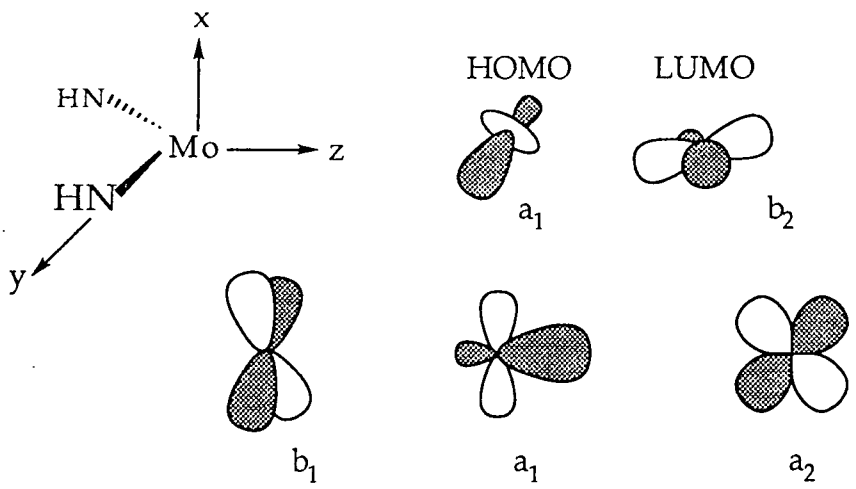

Scheme 3.16 *Most important calculated MO's for the [Mo(NR)] fragment.*

3.8 Displacement Reactions of $Mo(N^tBu)_2(PMe_3)(\eta^2\text{-}C_2H_3R)$, R= H, (10), R= Me (11)

The displacement reactions of the five coordinate olefin adduct $Mo(NAr)_2(PMe_3)_2(\eta^2\text{-}C_2H_4)$ and its tungsten analogue[19, 25] were limited to either exchange of olefin or acetylene. The olefin was smoothly displaced by CO, acetylenes, and a variety of multiply bonded ligands from the directly related half-sandwich niobium imido system, to afford tractable products. Thus, a similar study was undertaken for the metallocene-like molybdenum tert-butylimido complexes (10) and (11).

3.8.1 Reaction of $Mo(N^tBu)_2(PMe_3)(\eta^2\text{-}C_2H_3R)$, R= H, (10), R= Me (11) with H_2

A C_6D_6 solution of (10) was sealed in an NMR tube under 1 atm of hydrogen. Almost immediately a resonance attributable to $^tBuNH_2$ was observed by ^1H NMR. On prolonged warming at an elevated temperature (60°C) the originally yellow solution changed to light brown. After one week at this temperature no free dihydrogen could be observed in the ^1H spectrum. A variety of alkyl resonances was observed, including resonances attributable to ethane, $^tBuNH_2$ and free PMe_3; no new olefinic signals were observed; ^{31}P NMR showed 4 resonances at δ 11.66, 10.92, -3.11 and -62.0 ppm (free PMe_3). No proton resonances were observed that could be assigned unequivocally to metal hydride species over the range δ 20 to -20 ppm.

A similar reaction was attempted with the propene adduct (11), which again generated a number of alkyl species, $^tBuNH_2$ and free PMe_3. However, the complexity of this reaction precluded further study.

3.8.2 Reaction of $Mo(N^tBu)_2(PMe_3)(\eta^2\text{-}C_2H_3R)$, R= H, (10), R= Me (11) with CO

Previously it has been demonstrated that a solution of $CpNb(NAr)(PMe_3)(\eta^2\text{-}C_3H_6)$ reacts cleanly with carbon monoxide liberating propene. The carbonyl complex $CpNb(NAr)(CO)(PMe_3)$[50] is readily isolated and is analogous to the Group 4 complexes

$Cp_2M(PMe_3)(CO)$ (M=Ti, Zr)[12,13]. Similar reactivity has been reported for $Cp_2Ti(\eta^2\text{-}C_2H_4)$,[62] which cleanly affords the dicarbonyl, *via* dissociation of olefin.

However, treatment of either $Mo(N^tBu)_2(PMe_3)(\eta^2\text{-}C_2H_4)$ (**10**) or $Mo(N^tBu)_2(PMe_3)(\eta^2\text{-}C_3H_6)$ (**11**) with excess carbon monoxide in pentane resulted in the almost instantaneous formation of an insoluble yellow precipitate. Infra red spectroscopy indicated that carbonyl species in at least three environments had formed. The five coordinate ethene complex also reacted to give a variety of carbonyl containing products (Section 3.4).

Group 6 bis (imido) olefin complexes exhibit enhanced reactivity towards CO compared to their Group 5 half-sandwich imido and Group 4 metallocene analogues. Replacment of the sterically demanding Cp group with the much less bulky imido ligand is believed to be the cause.

3.8.3 Reaction of $Mo(N^tBu)_2(PMe_3)(\eta^2\text{-}C_3H_6)$ (11) with Acetylenes

A variety of Group 4 metallocene and Group 5 half-sandwich imido complexes exist that contain a coordinated acetylene ligand; the metallocene complexes are useful for a wide variety of organic transformations involving the acetylenic moiety.[63]

To generate the parallel Group 6 bis (imido) complexes the ready dissociation of the olefin moiety was exploited. The reaction of $Mo(N^tBu)_2(PMe_3)(\eta^2\text{-}C_3H_6)$ (**11**) with one equivalent of diphenylacetylene in heptane at 60 °C for 10 days readily afforded crystals of the acetylene adduct (**15**) in virtually quantitative yield, according to Equation 3.12 (R=H, Ph).

$$\underset{\textbf{(11)}}{Mo(N^tBu)_2(PMe_3)(\eta^2\text{-}C_3H_6)} + PhC{\equiv}CR \xrightarrow[60°C\ /\ 10d]{heptane} \underset{\textbf{(15)}}{Mo(N^tBu)_2(PMe_3)(\eta^2\text{-}PhC{\equiv}CR)} \quad (3.12)$$

$$-C_3H_6$$

Further discussion of this and other complexes containing multiply bonded units (eg. PhC≡CH, PhN=NPh, R^F-P=P-R^F) is to be found in Sections 4.2.

3.8.4 Reaction of $Mo(N^tBu)_2(PMe_3)(\eta^2\text{-}C_3H_6)$ (11) with Se

Although a vast number of mononuclear terminal oxo and sulfido complexes exist, comparatively few examples of the analogous selenido and tellurido compounds can be found. Group 5 half-sandwich imido compounds containing terminal selenide and telluride moieties have recently been synthesised by this group (Figure 3.17).[64] Therefore an attempt has been made to extend this series of complexes to include bis (imido) derivatives.

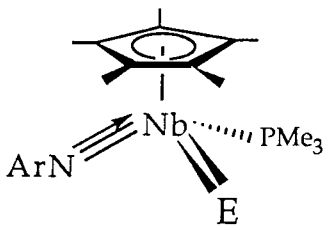

Figure 3.17
Half-Sandwich Chalcogenide Complex (E= S, Se, Te).

Once again the ready displacement of bound olefin from the four coordinate bis (imido) olefin complexes was utilised. A heptane solution of (**11**) was treated with one equivalent of selenium in the presence of a further equivalent of PMe_3 (used to deliver the chalcogenide to the metal centre) (Equation 3.13). On warming the mixture at 60 °C for 10 days, a dark red solid (**12**) was afforded after removal of solvent under reduced pressure. Subsequent recrystallisation from pentane yielded small intense dark red crystals.

$$\underset{\textbf{(11)}}{Mo(N^tBu)_2(PMe_3)(\eta^2\text{-}C_3H_6)} + Se + PMe_3 \xrightarrow[-C_3H_6]{\text{heptane}\ /\ 60°C\ /\ 10d} \textbf{(12)} \qquad \textbf{(3.13)}$$

Both ^1H and ^{13}C NMR revealed that the reaction had not followed a simple ligand displacement reaction (eg. Equation 3.13); six terminal imido environments were observed, with a resonance corresponding to only one bound phosphine (Figures 3.18 and 3.19). Careful examination of the ^{31}P NMR spectrum revealed the presence of selenium satellites symmetrically disposed about the single phosphine resonance (Figure 3.20).

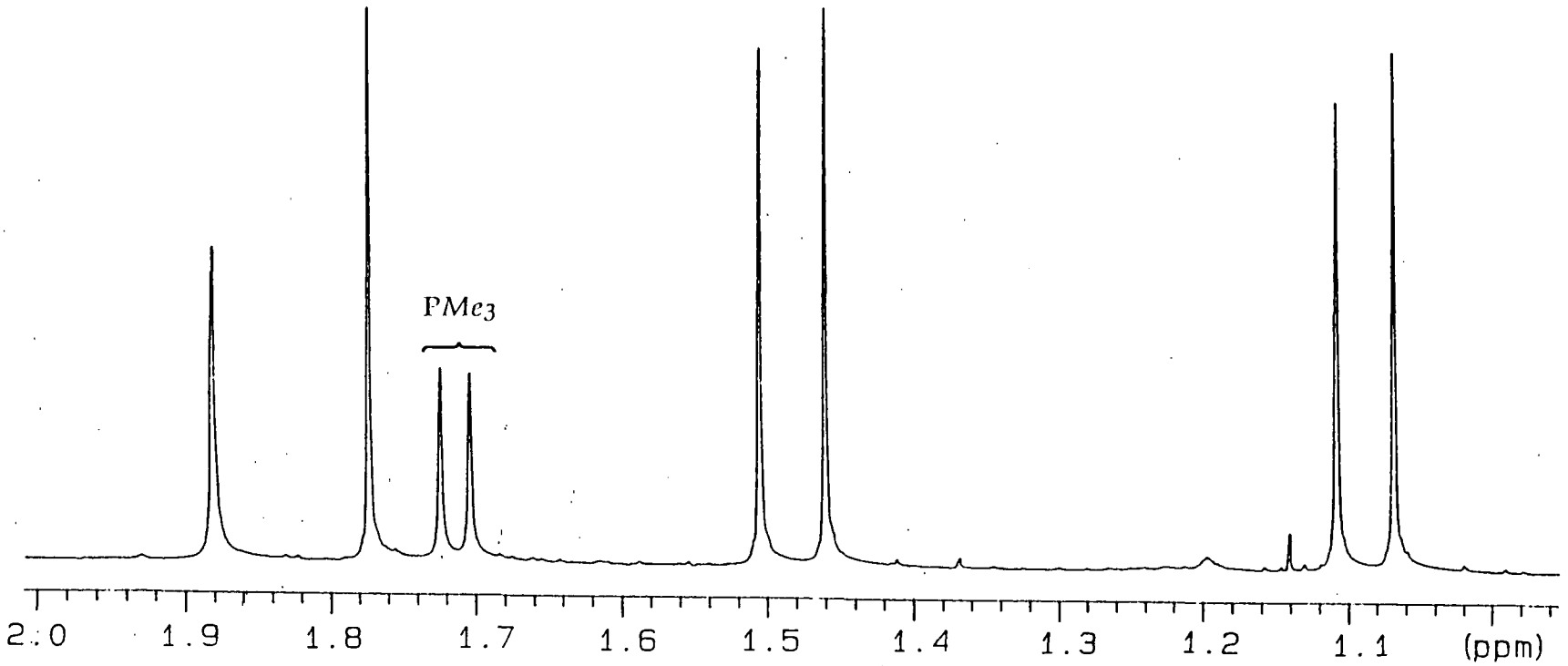

Figure 3.18 *400MHz ^1H NMR of the product obtained from the reaction of $Mo(N^tBu)_2(PMe_3)(C_3H_6)$ with Se.*

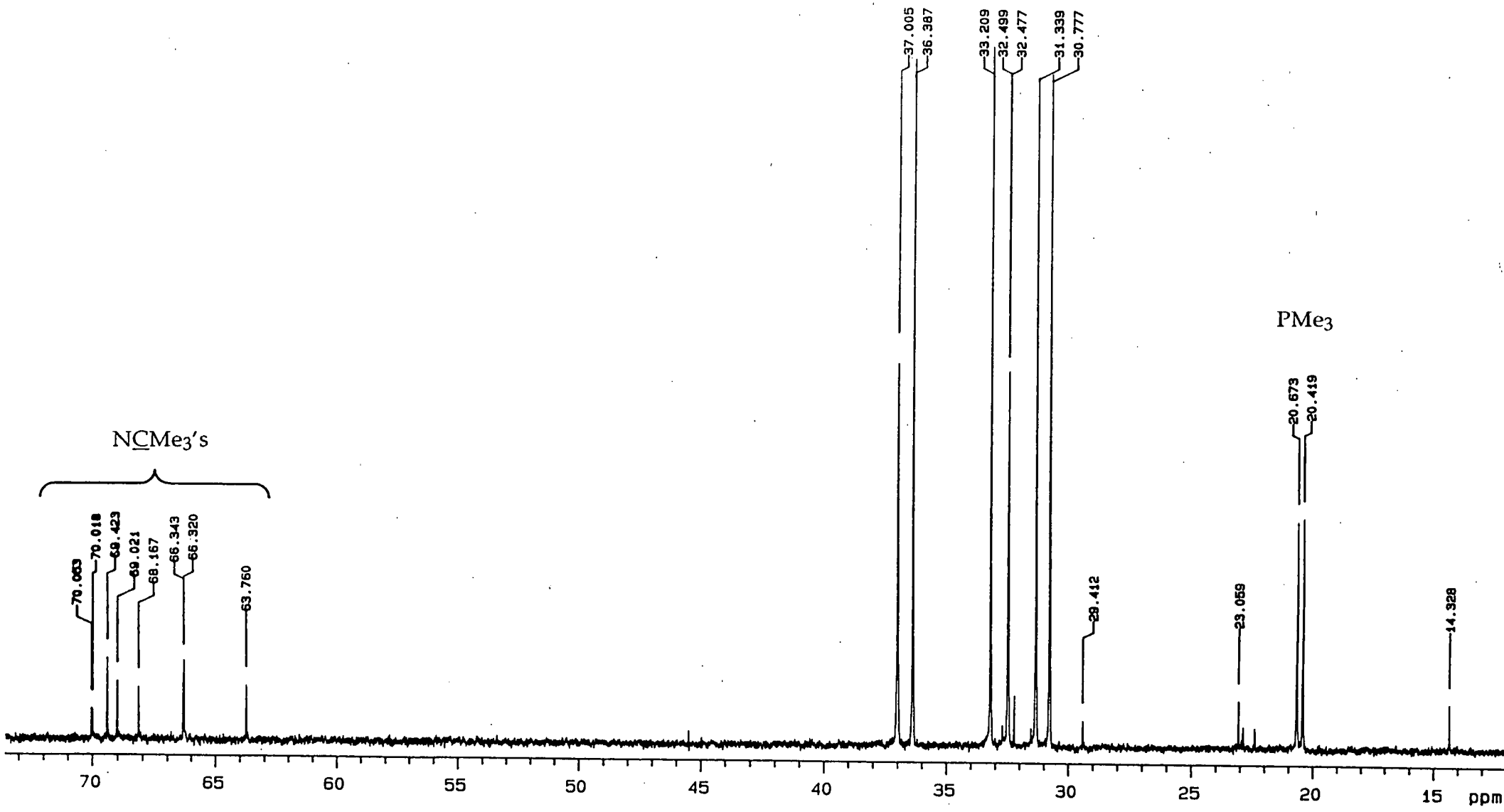

Figure 3.19 *100MHz ^{13}C NMR of the product obtained from the reaction of $Mo(N^tBu)_2(PMe_3)(C_3H_6)$ with Se.*

95.4 MHz ^{77}Se NMR spectra of (**12**) were subsequently obtained which showed a doublet resonance at δ 598.9 ppm ($\nu_{1/2}$= 10.5 Hz) with a J_{Se-P} coupling constant of 56.3 Hz, which correlated well with the value of 49.9 Hz obtained from the phosphorus spectra. The magnitude of this coupling is out side of the range associated with a $^{1}J_{SeP}$ coupling (200 to 1100 Hz).[65] Furthermore, the chemical shift of the selenium resonance was not indicative of a coordinated Me_3P=Se moiety.[66] No ^{13}C-^{77}Se coupling was observed in the ^{13}C NMR spectrum, suggesting that the Se has not coupled with hydrocarbon and thereby provides support for terminal or bridging Se atoms.

Comparison with the recently determined value of the ^{77}Se chemical shift for Cp*Nb(NAr)(PMe_3)(Se), a singlet resonance at δ 2532.2 ppm, ($\nu_{1/2}$= 28.4 Hz), proved of little use. In general, selenium chemical shifts are governed by the electron density at the selenium atom, so that Se(IV) and Se(VI) have chemical shifts in the high frequency part of the range.[65] Yet, there is an abundance of evidence indicating that in certain circumstances other effects can dominate.

The six differing imido environments precludes a simple geometry for (**12**), the formation of a metal cluster being most likely. There are many examples of the tert-butyl imido group adopting a bridging position, especially if there is competition for π bonding orbitals at the metal centre.[67] Furthermore, structurally characterised metal complexes containing chalcogenides in a wide variety of geometries especially cubane-like structures have been reported.[68]

Elemental analyses, infra red and mass spectroscopies were inconclusive as to the exact structure of (**12**). Crystals have been submitted for a molecular structure determination.

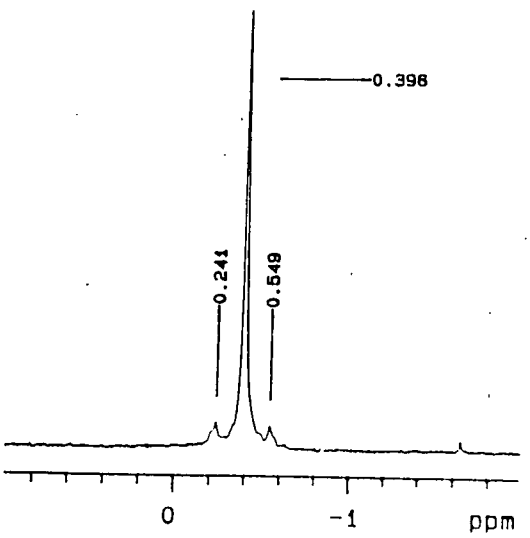

Figure 3.20 *162 MHz $^{31}P\{^{1}H\}$ Showing ^{77}Se satellites.*

3.9 Reaction of MoO_2Cl_2 with Ethylmagnesium Chloride

The Phillips catalyst used industrially for the large-scale production of polyethylene is based upon silica impregnated with CrO_3 which is activated under oxygen at 800°C.[69] In an attempt to mimic the first insertion with ethene we desired to isolate a dioxo analogue of either of the imido olefin complexes (**6**), (**10**), or (**11**).

To this end, MoO_2Cl_2[70] in DME was treated with two equivalents of ethylmagnesium chloride in the presence of excess PMe_3 at -196 °C (Equation 3.14). After 3h at room temperature an olive green solution was extracted by filtration from the magnesium chloride residues. Removal of solvent under reduced pressure afforded a blue/green solid (**13**) in low yield (≈20%).

$$2\,Mo(O)_2Cl_2 + 4\,EtMgCl \xrightarrow[xs\ PMe_3]{} \underset{(14)}{Mo(O)(PMe_3)_3Cl_2} + MoCl_3(PMe_3)_3 \qquad (3.14)$$

The 400 MHz ^1H NMR spectrum of (**13**) indicated a pseudo triplet at δ 1.38 ppm (arising through *virtual coupling* of two "mer" PMe_3 ligands[71]), and a doublet at δ 1.27 ppm. This spectrum was consistent with the unexpected formation of $Mo(O)(Cl)_2(PMe_3)_3$, as described by Wilkinson,[72] with further support being provided by its characteristic infra red spectrum.

Further investigation of the 400 MHz ^1H NMR spectrum revealed two broad upfield contact-shifted resonances at δ -16.25 and δ -32.90 ppm attributed to the presence of a small amount of the paramagnetic impurity $MoCl_3(PMe_3)_3$.[73]

3.10 Reaction of $Cr(N^tBu)_2Cl_2$ with RMgCl (R= Et, ^{n}Pr)

Examples of olefin containing bis (imido) complexes of both molybdenum and tungsten have been reported, yet little investigation has been made of such complexes for chromium, despite the well known rôle of chromium for the polymerisation of ethene in the Phillips process.[69] Hence, we have made an attempt to generate these lighter congeners using similar reactions to those used for molybdenum.

The only direct route into chromium bis (imido) chemistry is through $Cr(N^tBu)_2(OTMS)_2$,[39] which can readily be converted to the corresponding dichloride (**14**) in virtually quantitative yield, Scheme 3.5.[39,74] It was envisaged that treatment of (**14**) with two equivalents of an appropriate Grignard in the presence of phosphine would afford the desired olefin complex, yet realisation of this simple transformation has to date proved elusive.

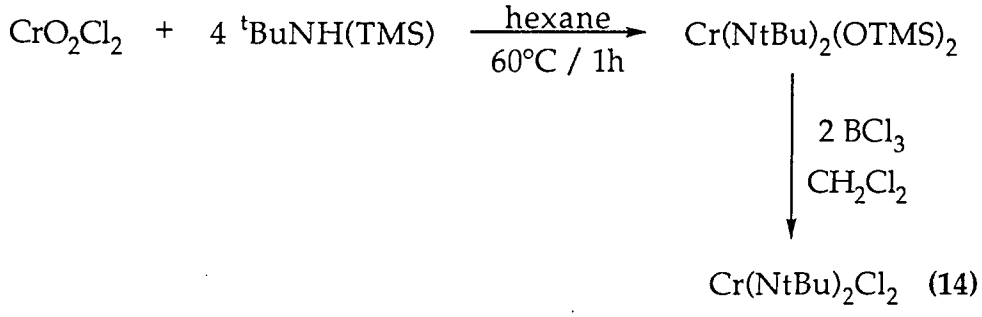

Scheme 3.5 *Synthesis of $Cr(N^tBu)_2Cl_2$ (14).*

Initial attempts involved direct treatment of the dichloride (**14**) with Ethyl Grignard in the presence of PMe_3, the reaction turning from dark red/purple to black within 12h. NMR of the black solid obtained was thwarted by the paramagnetic nature of the product. Elemental analyses also proved inconclusive due to facile decomposition of the product and to the "waxy" nature of the product obtained. Similar problems were encountered when the reaction was repeated using n-propyl Grignard reagent, again no tractable product being recovered.

In an attempt to overcome this apparent lack of crystallinity, the Grignard reaction was repeated in the presence of either PMe_2Ph or PPh_3, yet similar black or dark brown highly air and moisture sensitive paramagnetic materials were isolated. Disappointingly neither of these complexes could be conclusively identified. A C_6D_6 solution of a sample of the product obtained from the reaction with PPh_3 decomposed slowly to liberate ethene and $^tBuNH_2$ (by ^1H NMR). Despite prolonged monitoring no other diamagnetic species were observed. The observation of ethene implied that formation of the desired olefin complex had been achieved.

To monitor this reaction more carefully, the tertiary phosphine adduct $Cr(N^tBu)_2(PPh_3)Cl_2$ was first synthesised. $Cr(N^tBu)_2(PPh_3)Cl_2$ (**14a**) was isolated as an orange solid through treatment of $Cr(N^tBu)_2Cl_2$ with one equivalent of the phosphine in toluene (Equation 3.15). Subsequent

recrystallisation from warm THF afforded (**14a**) in 55% yield. Unlike the PMe_2Ph and PMe_3 adducts reported by Wilkinson[74] (**14a**) was only sparingly soluble in THF.

$$\underset{\textbf{(14)}}{Cr(NtBu)_2Cl_2} + PPh_3 \xrightarrow[C_7H_8]{} \underset{\textbf{(14a)}}{Cr(N^tBu)_2(PPh_3)Cl_2} \qquad (3.15)$$

An ethereal solution of (**14a**) was treated with ethylmagnesium chloride at -196 °C which, on warming to room temperature, afforded a dark red solution after 20 minutes. On work-up, a small quantity of a dark red/purple solid was isolated. Analyses indicated that the product was similar to that obtained from the "one-step" reaction.

Both the paramagnetic nature and instability of these chromium olefin complexes compared to their molybdenum and tungsten analogues is likely to be attributable to the enhanced propensity for reduction of the first row metals.

3.11 Summary

Our efforts to find a convenient entry into molybdenum bis (imido) chemistry *via* compounds of the general type $Mo(NR)(NR')Cl_2$ have been realised through the synthesis of a variety of six coordinate DME stabilised complexes. $Mo(NAr)Cl_2.DME$ (**1**) and $Mo(N^tBu)Cl_2.DME$ were obtained in excellent yields using a simple "one-pot" reaction involving the treatment of Na_2MoO_4 with the appropriate primary amine.

Use of these reagents allowed us to probe the pseudo-isolobal relationship that exists between Group 4 bent metallocenes, Group 5 half-sandwich imido and Group 6 bis (imido) species. This study has included the synthesis of a synthetically useful bis (phosphine) complex $Mo(NAr)_2(PMe_3)_2$ (**5**) (Scheme 3.6) and its tert-butyl counterpart $[Mo(N^tBu)(\mu\text{-}N^tBu)(PMe_3)]_2$ (**9**). Treatment of the six coordinate dichloride precursors with 2 equivalents of either ethylmagnesium chloride or n-propylmagnesium chloride in the presence of PMe_3 allowed an entry into the phosphine stabilised olefin complexes $Mo(NAr)_2(PMe_3)_2(\eta^2\text{-}C_2H_4)$ (**6**), and $Mo(N^tBu)_2(PMe_3)(\eta^2\text{-}C_2H_3R)$ (R = H (**10**); R = Me (**11**)). NMR and molecular structure studies revealed that (**6**)

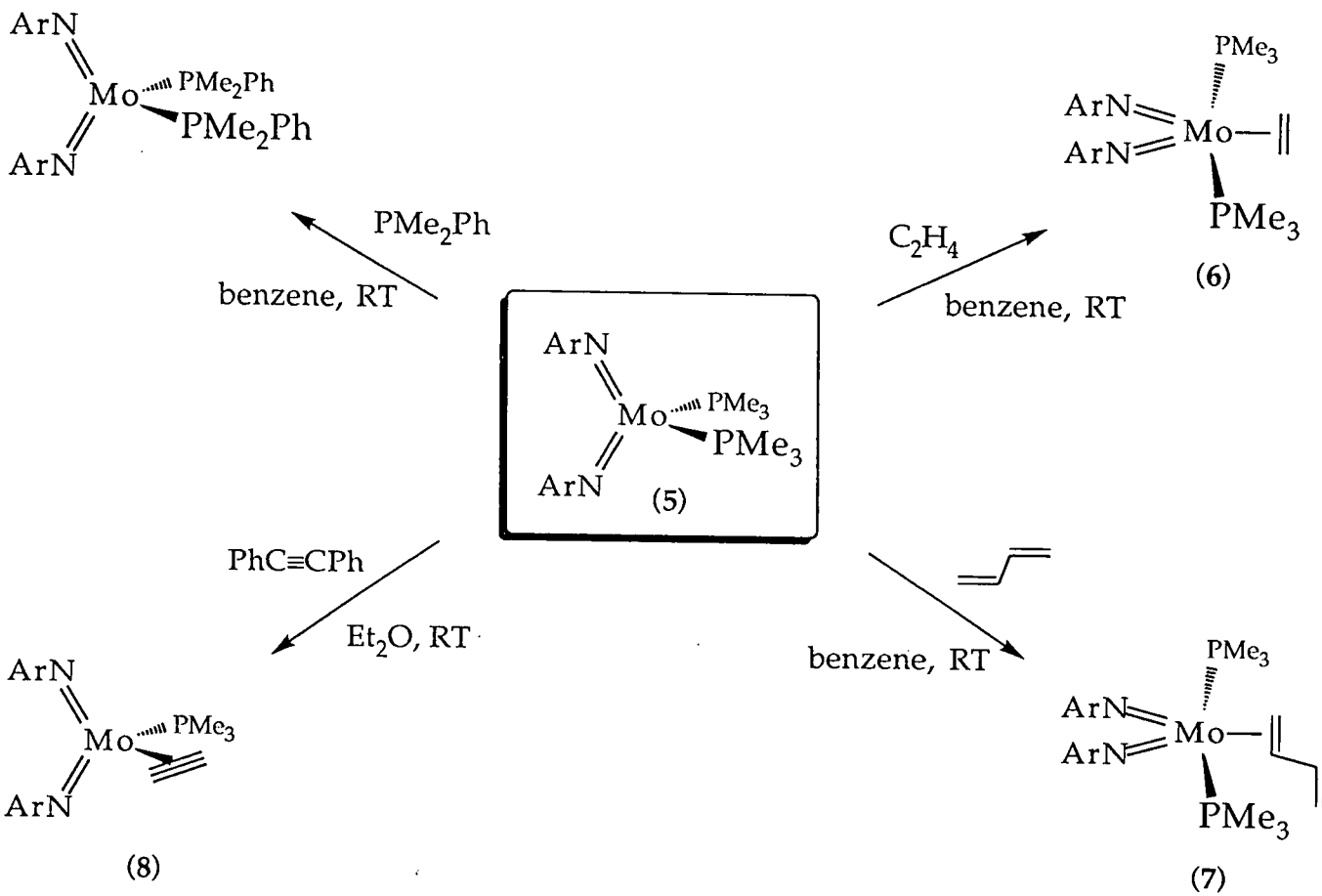

Scheme 3.6 *Summary of the reactivity of the four coordinate bis (phosphine) $Mo(NAr)_2(PMe_3)_2$. Phenyl rings have been omitted for clarity.*

adopted an unusual five coordinate geometry, whereas both (**10**) and (**11**) were isolated as four coordinate bent metallocene analogues.

This study has reinforced the idea of an isolobal relationship that links the three seemingly unrelated fragments, $[Cp_2M]$, [CpM'(NR)] and $[M''(NR)_2]$, yet has underlined the fact that this is a essentially structural analogy and can not be used to predict reaction pathways. The nature of the imido substituent for the Group 6 bis (imido) complexes has a profound influence upon the nature of the products obtained. These ideas are further investigated in Chapter 4.

3.12 References

1 T. Takahashi, M. Hasegawa, N. Suzuki, M. Saburi, C.J. Rousset, P.E. Fanwick, E. Negishi, *J. Am. Chem. Soc.*, 1991, **113**, 8564.

2 For a review see: J. Schwartz and J.A. Labinger, *Angew. Chem. Int. Ed. Engl.*, 1976, **15**, 333.

3 L.R. Gilliom and R.H. Grubbs, *J. Am. Chem. Soc.*, 1986, **108**, 733.

4 W.P. Long and D.S. Breslow, *J. Am. Chem. Soc.*, 1960, **81**, 1953; G. Henrici-Olive and S. Olive, *Angew. Chem. Int. Ed. Engl.*, 1967, **6**, 790; G. Fink and W. Zoller, *Makromol. Chem.*, 1981, **182**, 3265.

5 D.N. Williams, J.P. Mitchell, A.D. Poole, U. Siemeling, W. Clegg, D.C.R. Hockless, P.A. O'Neil, and V.C. Gibson, *J. Chem. Soc. Dalton Trans.*, 1992, 739.

6 D.S. Williams, J.T. Anhaus, M.H. Schofield, R.R. Schrock, and W.M. Davis, *J. Am. Chem. Soc.*, 1991, **113**, 5480.

7 D.S. Glueck, J.C. Green, R.I. Michelman, and I.N. Wright, *Organometallics*, 1992, **11**, 4221.

8 J.W. Lauher and R. Hoffmann, *J. Am. Chem. Soc.*, 1976, **98**, 1729.

9 L. Zhu and N.M. Kostic, *J. Organomet. Chem.*, 1987, **335**, 395.

10 It might be expected that the d_z^2 would also interact with the C_5H_5 a_1 orbital, but the π orbital lobes probe the region of the d_z^2 nodal surface, see ref. 9.

11 A.D. Poole, Ph.D. Thesis, University of Durham, 1992.

12 L.B. Kool, M.D. Rausch, H.G. Alt, M. Heberhold, U. Thewalt, and B. Wolf, *Angew. Chem. Int. Ed. Engl.*, 1985, **24**, 394.

13 L.B. Kool, M.D. Rausch, H.G. Alt, M. Heberhold, B. Honold, and U. Thewalt, *J. Organomet. Chem.*, 1987, **320**, 37; T. Takahashi, D.R. Swanson, and E. Negishi, *Chem. Letters*, 1987, 623.

14 G. Wilkinson, F.G.A. Stone, E.W. Abel, *"Comprehensive Organometallic Chemistry"*, Vol. 3, Pergamon, Oxford, 1982.

15 a) A.D. Poole, Ph.D. Thesis, University of Durham, 1992; b) U. Siemeling and V.C. Gibson, *J. Organomet. Chem.*, 1992, **426**, C25.

16 D.S. Williams, M.H. Schofield, J. T. Anhaus, and R.R. Schrock, *J. Am. Chem. Soc.*, 1990, **112**, 6728.

17 P.W. Dyer, V.C. Gibson, J.A.K. Howard, and C. Wilson, In press.

18 J. Sandström, *"Dynamic NMR Spectroscopy"*, Academic Press, London, 1984. Detailed examples using this technique are given by: M.L.H. Green, D.M. Michaelidou, P. Mountford, A.G. Suárez and

L.L. Wong, *J. Chem. Soc. Dalton Trans.*, 1993, 1593; M.L.H. Green, L.L. Wong, *Organometallics*, 1992, **11**, 2660.

19 D.S. Williams, M.H. Schofield, and R.R. Schrock, In press.

20 D.S.Williams, M.H. Schofield, J.T. Anhaus, and R.R. Schrock, *J. Am. Chem. Soc.*, 1990, **112**, 6728; M.H. Schofield, T.P. Kee, J.T. Anhaus, R.R. Schrock, K.H. Johnson, and W.M. Davis, *Inorg. Chem.*, 1991, **30**, 3595.

21 J.T. Anhaus, T.P. Kee, M.H. Schofield, and R.R. Schrock, *J. Am. Chem. Soc.*, 1990, **112**, 1642.

22 W.A. Nugent and J.M. Mayer, *"Metal Ligand Multiple Bonds"*, Wiley and Sons, New York, 1988.

23 A.D. Poole, V.C. Gibson, and W. Clegg, *J. Chem. Soc. Chem. Commun.*, 1992, 237.

24 A.D. Poole, Ph.D. Thesis, University of Durham, 1992.

25 D.S.Williams, M.H. Schofield, J.T. Anhaus, and R.R. Schrock, *J. Am. Chem. Soc.*, 1990, **112**, 6728.

26 P.W. Dyer, V.C. Gibson, J.A.K. Howard, and C. Wilson, In press.

27 H.G. Alt, M.D. Rausch, and U. Thewalt, *J. Organomet. Chem.*, 1988, **349**, No. 1-2.

28 S.A. Cohen, P.R. Auburn, and J. E. Bercaw, *J. Am. Chem. Soc.*, 1983, **105**, 1136.

29 H.G. Alt, H.E. Engelhardt, M.D. Rausch, and L.B. Kool, *J. Am. Chem. Soc.*, 1985, **107**, 3717; H.G. Alt, G.S. Herrmann and M.D. Rausch, *J. Organomet. Chem.*, 1988, **356**, 2; H.G. Alt, H.E. Engelhardt, M.D. Rausch, and L.B. Kool, *J. Organomet. Chem.*, 1987, **329**, 61.

30 L.B. Kool, M.D. Rausch, H.G. Alt, M. Heberhold, U. Thewalt, B. Wolf, *Angew. Chem., Int. Ed. Engl.*, 1985, **24**, 394; H.G. Alt, C.E. Denner, U. Thewalt, and M.D. Rausch, *J. Organomet. Chem.*, 1988, **356**, C83.

31 See Chapter One of this thesis for examples and discussion of the effects of imido substituents.

32 a) J.P. Collman, L.S. Hegedus, J.R. Norton, and R.G. Finke, *"Principles and Applications of Organotransition Metal Chemistry"*, University Science Books, California, 1987; b) T.J. Meyer, *J. Am. Chem. Soc.*, 1982, **104**, 5070.

33 J. Schwartz and K.I. Gell, *J. Organomet. Chem.*, 1980, **184**, C1; G. Erker, *Angew. Chem., Int. Ed. Engl.*, 1989, **28**, 397.

34 P.R. Sharp and R.R. Schrock, *J. Organomet. Chem.*, 1979, **171**, 43.

35 J. Sundermeyer, K. Weber, and H. Pritzkow, *Angew. Chem., Int. Ed. Engl.*, 1993, **32**, 731.

36 U. Siemeling and V.C. Gibson, *J. Organomet. Chem.*, 1992, **426**, C25.

37 See for example: P.W. Dyer, V.C. Gibson, J.A.K. Howard, C. Wilson, and B. Whittle, *J. Chem. Soc. Chem. Commun.*, 1992, 1666.

38 D.L. Thorn, W.A. Nugent and R.L. Harlow, *J. Am. Chem. Soc.*, 1981, **103**, 357.

39 W.T. Borden, *J. Am. Chem. Soc.*, 1975, **97**, 5968.

40 W.A Nugent, *Inorg. Chem.*, 1983, **22**, 965; W.A. Nugent and R.L. Harlow, *Inorg. Chem.*, 1980, **19**, 777; A.A. Danopoulos, WA-Hung Leung, G. Wilkinson, B. Hussain-Bates, and M.B. Hursthouse, *Polyhedron*, 1990, **9**, 2625.

41 B.R. James, *"Homogeneous Hydrogenation"*, Wiley-Interscience, New York, 1973; *Adv. Organomet. Chem.*, 1979, **17**, 319.

42 W.C. Siedel and C.A. Tolman, *Ann. NY Acad. Sci.*, 1983, **201**, 415.

43 L.H. Slaughand and R.D. Mullineaux, *J. Organomet Chem.*, 1968, *13*, 469.

44 D. Evans, J. Osborn, and G. Wilkinson, *J. Chem. Soc. A*, 1968, 3133; C.P. Casey and C.R. Cyr, *J. Am. Chem. Soc.*, 1973, **95**, 2248.

45 J.A. Ewen, R.L. Jones, A. Razavi, J.D. Ferrara, *J. Am. Chem. Soc.*, 1988, **110**, 6255, and references therein; W. Kaminsky, K. Kulper, H.H. Brintzinger, and F.R. Wild, *Angew. Chem., Int. Ed. Engl.*, 1985, **24**, 507; W. Kaminsky and N. Moller-Lindenhof, *Bull. Soc. Chem., Belg.*, 1990, **99**, 103 and references therein; P. Pino, P. Cioni, and J. Wei, *J. Am. Chem. Soc.*, 1987, **109**, 6198; W. Spalek, M. Antberg, V. Dolle, R. Klein, J. Rohrmann, and A. Winter, *New J. Chem.*, 1990, **14**, 499; R. Waymouth and P. Pino, *J. Am. Chem. Soc.*, 1990, **112**, 4911; L. Resconi and R.M. Waymouth, *J. Am. Chem. Soc.*, 1990, **112**, 4953.

46 J.N. Allison and W.A. Goddard, *ACS Symposium Series*, 1985, **279**, 23; L. Kihlborg, *Arkiv Kemi*, 1963, **21**, 357; J. Belgacem, J. Kress, and J.A. Osborn, *J. Chem. Soc. Chem. Commun.*, 1993, 1125; J.D. Burrington, C. Kartisek, and R.K. Grasselli, *J. Catal.*, 1984, **87**, 363;

D.M.T. Chan and W.A. Nugent, *Inorg. Chem.*, 1985, **24**, 1422; D.M.T. Chan, W.C. Fultz, W.A. Nugent, D.C. Roe, and T.H. Tulip, *J. Am. Chem. Soc.*, 1985, **107**, 251.

47 K.B. Wiberg, *"Oxidation in Organic Chemistry"*, Part A, Academic Press, New York, 1965, pp69-184.

48 T. Takahashi, T. Seki, Y. Nitto, M. Saburi, C.J. Rousset, and E. Negishi, *J. Am. Chem. Soc.*, 1991, **113**, 6266.

49 T. Takahashi, D.R. Swanson, and E. Negishi, *Chem. Letters*, 1987, 623.

50 A.D. Poole, V.C. Gibson, and W. Clegg, *J. Chem. Soc. Chem. Commun.*, 1992, 237.

51 B. Whittle, M.Sc. Thesis, University of Durham, 1993.

52 M.C. Chan and V.C. Gibson, Unpublished results.

53 P.W. Dyer, V.C. Gibson, J.A.K. Howard, B. Whittle, and C. Wilson, *J. Chem. Soc. Chem. Commun.*, 1992, 1666.

54 M.H. Schofield, T.P. Kee, J.T. Anhaus, R.R. Schrock, K.H. Johnson, and W.M. Davis, *Inorg. Chem.*, 1991, **30**, 3595.

55 J.K.M. Sanders and B.K. Hunter, *"Modern NMR Spectroscopy"*, OUP, Oxford, 1991.

56 See this thesis, Section 3.5.

57 H.G. Alt, C.E. Denner, U. Thewalt, and M.D. Rausch, *J. Organomet. Chem.*, 1988, **356**, C83.

58 W.J. Bruton, V.C. Gibson, R.D. Sanner and J.E. Bercaw, *Organometallics*, 1986, **5**, 976.

59 D.S. Williams, M.H. Schofield, and R.R. Schrock, In press.

60 See this thesis Section 3.3.2.

61 P.W. Dyer, V.C. Gibson, C.E. Housecroft, and L.C. Parlett, In press.

62 C. McDade, J.E. Bercaw, *J. Organomet. Chem.*, 1985, **279**, 281; S.A. Cohen and J.E. Bercaw, *Organometallics*, 1985, **4**, 1006; P.R. Auburn, S.A. Cohen, and J.E. Bercaw, *J. Am. Chem. Soc.*, 1982, **105**, 1136.

63 S.L. Buchwald, B.T. Watson, and J.C. Huffman, *J. Am. Chem. Soc.*, 1987, **109**, 2544.

64 U. Siemeling and V.C. Gibson, *J. Chem. Soc. Chem. Commun.*, 1992, 1670.

65 H.C.E. McFarlane and W. McFarlane, *"NMR of Newly Accessible Nuclei"*, Vol.2, Academic Press, London, 1983.

66 S.J. Anderson, P.L. Goggin, and R.J. Goodfellow, *J. Chem. Soc. Dalton Trans.*, 1976, 1959.

67 W. Clegg, R.J. Errington, D.C.R. Hockless and C. Redshaw, *J. Chem. Soc. Chem. Commun.*, 1993, 1965.

68 R.D. Adams, J.E. Babin, and K. Natarajan, *J. Am. Chem. Soc.*, 1986, **108**, 3518; W.A. Herrmann, J. Rohrmann, E. Herdtweck, H. Bock, and A. Veltmann, . *Am. Chem. Soc.*, 1986, **108**, 3134; L.Y, Goh and T.C.W. Mak, *J. Chem. Soc. Chem. Commun.*, 1986, 1474.

69 M.P. McDaniel, *Adv. Catal.*, 1985, **33**, 47.

70 MoO_2Cl_2 was prepared according to the prosedure described by: R.R. Schrock, J.S. Murdzek, G.C. Bazan, J. Robbins, M. DiMare, and M. O'Regan, *J. Am. Chem. Soc.*, 1990, **112**, 3875.

71 J.M. Jenkins and B.L. Shaw, *J. Chem. Soc. (A)*, 1966, 770.

72 E. Carmona, A. Galindo, L. Sanchez, A.J. Nielson, and G. Wilkinson, *Polyhedron*, 1984, **3**, 347.

73 P.J. Desrochers, K.W. Nebesny, M.J. LaBarre, S.E. Lincoln, T.M. Loehr, and J.E. Enemark, *J. Am. Chem. Soc.*, 1991, **113**, 9193.

74 A.A. Danopoulos, WA-Hung Leung, G. Wilkinson, B. Hussain-Bates, and M.B. Hursthouse, *Polyhedron*, 1990,.**9**, 2625; N. Meijboom and C.J. Schaverien, *Organometallics*, 1990, **9**, 774.

Chapter Four- Preparation and Reactivity of Bis (Imido) Phosphine Complexes Containing Acetylene and Alkyl Ligands

4.0 Introduction

This chapter will be concerned with the attempts to synthesise acetylene, benzyne, and alkylidene derivatives containing the "$Mo(NR)_2$" moiety. As a prelude to this study, relevant chemistry from the pseudo-isolobal bent metallocene system will be outlined.

Countless transition metal complexes containing the acetylene moiety have been structurally characterised, the ligand adopting a variety of orientations as described in Chapter 1. This diversity arises as acetylenes possess two perpendicular π systems that can both donate electrons to the metal centre.[1] Hence, it is capable of acting as either a 2 or 4 electron donor ligand.

An empirical relationship has been reported by Templeton *et al* that correlates the number of electrons formally donated by acetylene ligands (N) and the chemical shift of the bound acetylene nuclei in a series of mononuclear tungsten and molybdenum complexes.[2] The results of this study are given in Table 4.1 and Figure 4.1.

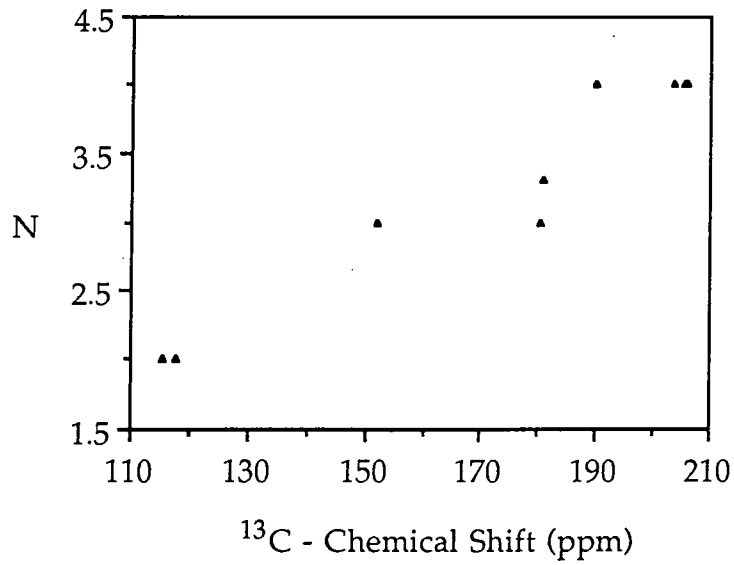

Figure 4.1
Acetylene ^{13}C chemical shifts vs. formal number of electrons donated per acetylene.

No other ligand that features in organometallic chemistry displays such a large ^{13}C chemical shift range upon coordination (≈ 100 ppm). The ability to vary its electron donation has important implications for catalytic reactions that involve interchange between 16 and 18 electron species.

Complex	$\delta(R^{13}C{\equiv}CR)$	δ_{av}	N	Ref.
$W(CO)(detc)_2(HC{\equiv}CH)$	206.1, 207.1	206.6	4	2
$W(CO)(detc)_2(HC{\equiv}CPh)$	205.7	205.7	4	2
$(\eta\text{-}Cp)W(CO)(CH_3)(HC{\equiv}CH)$	192.5, 187.4	190.0	4	3
$Mo(CO)(dmtc)_2(HC{\equiv}CH)$	203.7	203.7	4	2
$Mo(CO)(detc)_2(HC{\equiv}CPh)$	205.3	205.3	4	2
$W(CO)(EtC{\equiv}CEt)_3$	191.1, 170.8	181.0	$3\frac{1}{3}$	2
$[(\eta\text{-}Cp)W(CO)_2(MeC{\equiv}CC_4H_9)]^+$	162.2, 159.4, 144.8, 141.5	152.0	3	4
$Mo(detc)_2(HC{\equiv}CPh)_2$	183.2, 177.1	180.2	3	2
$(\eta\text{-}Cp)_2Mo(HC{\equiv}CH)$	117.7	117.2	2	5
$(\eta\text{-}Cp)_2Mo(MeC{\equiv}CMe)$	115.3	115.3	2	2

Table 4.1 *^{13}C Chemical shifts of acetylene complexes bound to Mo(II) and W(II). N= Formal number of electrons donated per acetylene ligand.*

Although there are many fully characterised simple acetylene complexes, the number is relatively small compared to that for the corresponding metal olefin species. This is because many acetylene complexes are quite reactive, often undergoing ligand coupling reactions to produce more elaborate species or organic products. In particular, metallocene complexes containing the acetylene moiety have received much attention in organic chemistry as reagents for a range of transformations. Hydrozirconation of terminal acetylenes using Schwartz's reagent ($Cp_2Zr(H)Cl$) proceeds with *cis* stereochemistry at the coordinated C=C bond, placing the metal at the terminal carbon atom. Unsymmetrically disubstituted acetylenes readily afford mixtures of alkenylzirconium derivatives in which the size of the substituents determine the preferred direction of insertion. Yet, if a slight excess of $Cp_2Zr(H)Cl$ is present then equilibration leads generally to mixtures greatly enriched in the less-hindered complex.

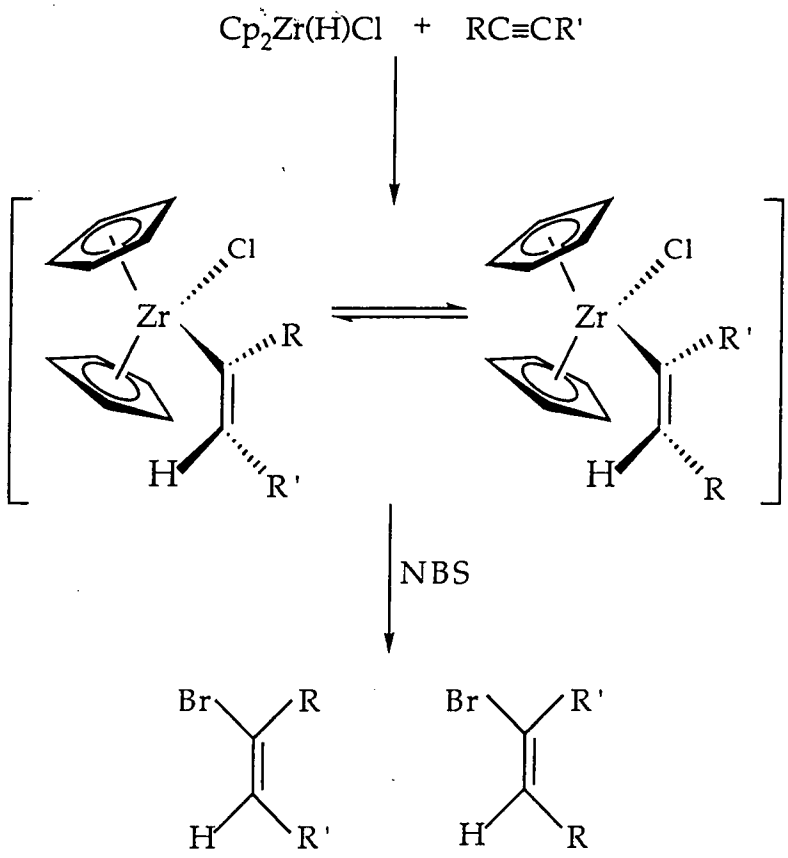

Scheme 4.1 *Hydrozirconation using Schwartz's reagent followed by cleavage with N-bromosuccinimide, illustrating the retention of a cis configuration.*

The reason that this chemistry is important is that a great deal of useful reactions can be performed at the Zr-C bond. For example, cleavage by N-bromosuccinimide produces the corresponding vinyl halide with retention of the *cis* geometry (Scheme 4.1).[6] Protonation readily affords the hydrocarbon, and bromination the alkyl bromide.[7] Oxidation leads to the alcohol, much like hydroboration/oxidation. This mechanism of electrophilic cleavage is unusual for transition metal alkyls as no *inversion* of configuration is observed. This *inversion* is normally associated with oxidation of the metal followed by S_N2 displacement. However, $Cp_2Zr(R)Cl$ is a d^0 complex and, as such, cannot readily undergo further oxidation.[8]

For some time it has been known that free metallocenes (i.e. Cp_2M, M= Ti, Zr, and Hf) can reductively couple two acetylenes resulting in the formation of symmetrically tetrasubstituted metallacyclopentadienes. This is generally assumed to proceed *via* a discrete metallocene acetylene complex (Scheme 4.2). There are many examples of these diene complexes

that involve diphenylacetylene. There are also a few examples where similar chemistry has allowed the isolation of metallacycles involving reactions with other internal acetylenes such as 2-butyne, 3-hexyne, and dimethyl acetylenedicarboxylate.[9]

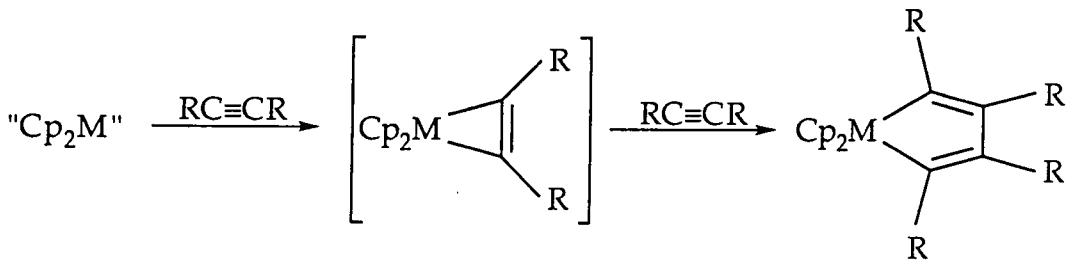

Scheme 4.2 *Reductive coupling of acetylenes to form a metallacyclopentadiene complex.*

Hydrolysis or iodinolysis-hydrolysis of metallacyclopentadienes afford the corresponding organic diene, again with the associated retention of configuration. The yield for this type of reaction is characteristically high.

After the initial formation of the metallacyclopentadiene other unsaturated reagents such as olefins, CO, nitriles, aldehydes, and even sulphur dihalides can be introduced. These species will subsequently undergo oxidative addition with concomitant ring expansion. Thus, this type of reactivity is particularly useful for the synthesis of a variety of functionalised ring systems (Scheme 4.3).

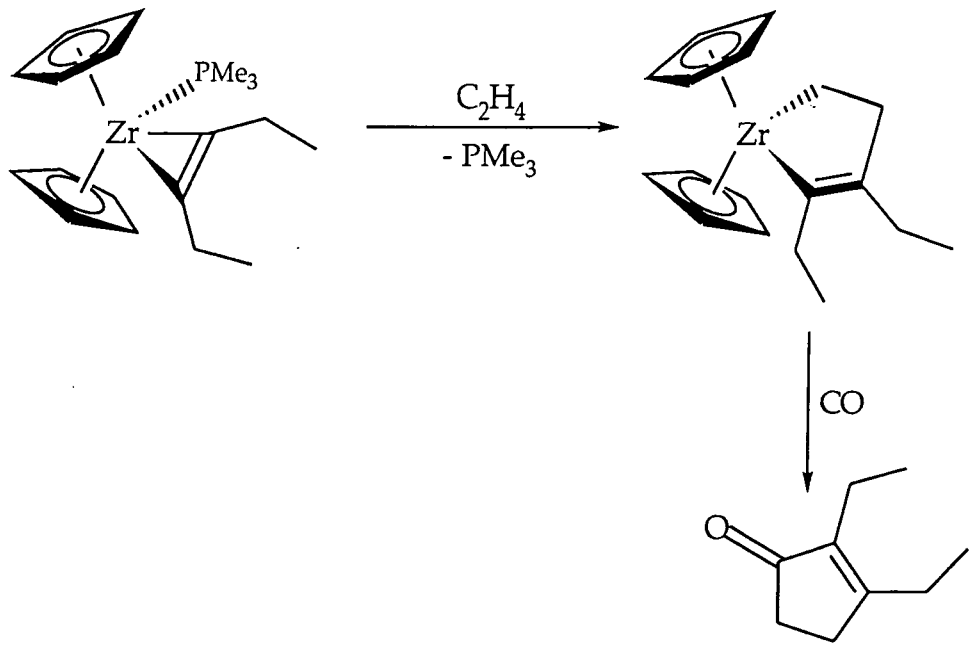

Scheme 4.3 *An example of organic ring synthesis using a zirconocene acetylene complex.*

The coordination of acetylenes in metal complexes is known to stabilise certain unstable species. For example, metal complexes containing cyclohexyne (a molecule that is unstable in its free state) have been synthesised and structurally characterised.[10] Even halogen-substituted acetylenes, which are in general explosive, are stabilised upon coordination to a metal (e.g. $[WCl_5(ClC{\equiv}CCl)]^-[PPh_4]^+$).[11] Perhaps the most remarkable examples of acetylene stabilisation are complexes which contain the highly reactive benzyne moiety, C_6H_4 (see Section 4.0).

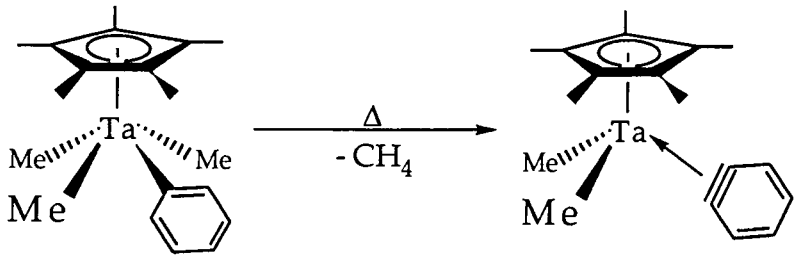

(4.1)

A number of such species have been synthesised. The first structurally characterised example was of a cyclopentadienyl tantalum derivative, synthesised by Schrock *et al* (Equation 4.1).[12] Examples of other η^2-benzyne complexes have been reported (Table 4.2).

Complex	N	Ref.
$CpTa(Me)_2(\eta^2\text{-}C_6H_4)$	4	12
$Ni(\eta^2\text{-}C_6H_4)((C_6H_{11})_2PCH_2CH_2P(C_6H_{11})_2)$	2	13
$[Nb(\eta^2\text{-}C_6H_4)_2Ph_3(LiPh.THF(Li.THF)_4]$ 0.5THF	2	14
$Ru(PMe_3)_4(\eta^2\text{-}C_6H_4)$	2	15
$Cp_2Zr(PMe_3)(\eta^2\text{-}C_6H_4)$	2	16
$[Re(\eta^2\text{-}2\text{-}C_6H_3Me)(2\text{-}C_6H_4Me)_2(PMe_3)_2][I_5]$	2	17

Table 4.2 *Representative examples of structurally characterised η^2-benzyne complexes. N denotes the number of electrons donated by the benzyne moiety.*

Several research groups have published synthetic routes for the generation of this type of benzyne complex. Perhaps the most general strategy has been through the synthesis of sigma bound diphenyl species. Thermolysis (often *in situ*) generates the desired fragment. However, many discrete benzyne complexes can not be isolated, but are trapped by other reagents such as acetylenes (as above). An example of just such an

approach is given in Scheme 4.3.[18] The reaction proceeds *via ortho*-hydrogen abstraction between the phenyl rings eliminating benzene.

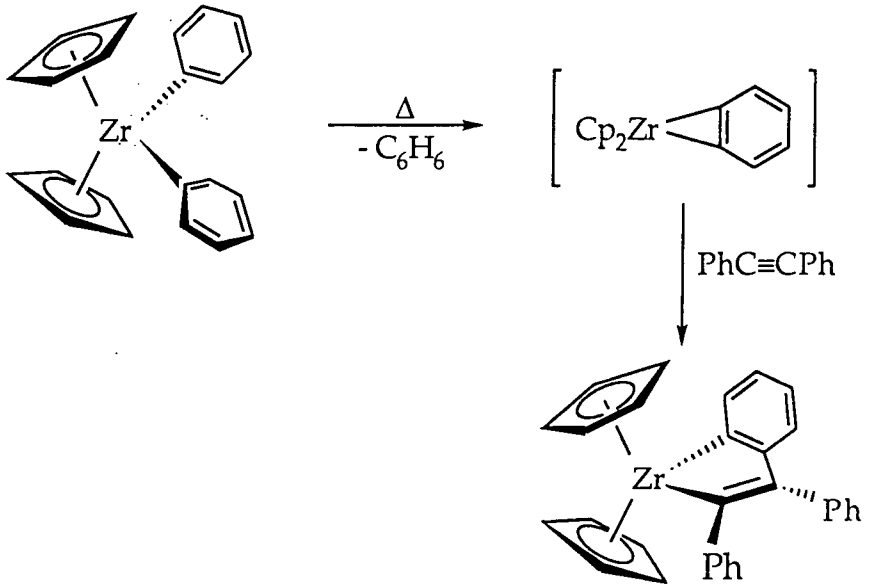

Scheme 4.3 *Thermolysis of $Cp_2Zr(Ph)_2$ in the presence of diphenylacetylene.*

Benzyne complexes have proved to be useful in a range of organic transformations. Coupling reactions with olefins and acetylenes have been demonstrated, the former generating the so-called metallaindan derivatives by reductive coupling,[19] while the latter form metallacyclic species containing the aromatic ring. Similarly, reaction with elemental selenium affords the diselenametallacycle, whilst nitriles lead to the formation of azazirconacyclopentenes (Scheme 4.4). Substituted benzynes have also been synthesised, which allow for the formation of substituted benzocyclobutenes, through reaction with ethylene.[20]

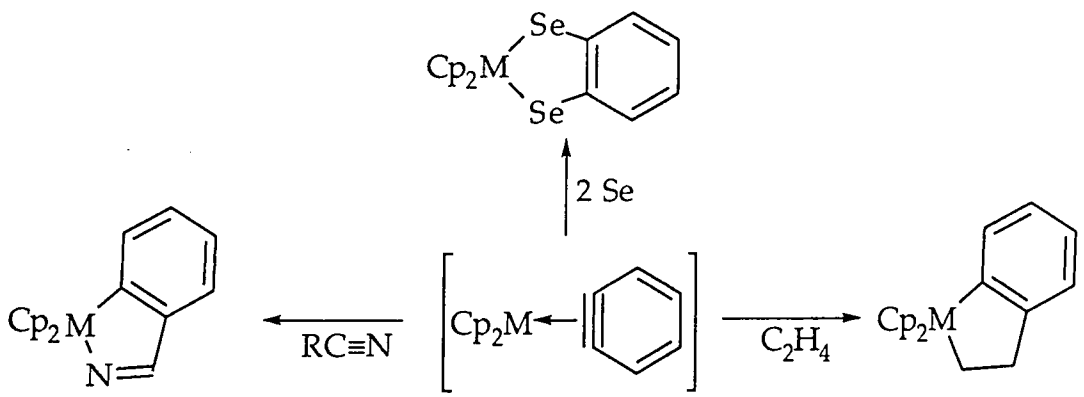

Scheme 4.4 *Some general reactions associated with benzyne complexes.*

In an elegant study, Hart and co-workers have detailed the use of benzdiyne equivalents in organic synthesis. Subsequently, Buchwald has outlined a synthesis of a benzdiyne complex stabilised by two zirconocene fragments (Equation 4.2),[21] which on treatment with olefin, iodine and excess n-BuLi yield benzbicyclobutanes. This provides further testimony to the use of metal complexes to stabilise useful reactive organic fragments.

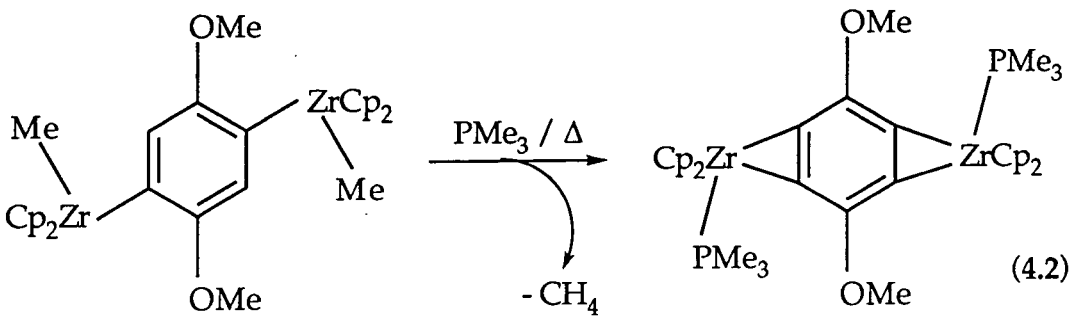

(4.2)

One research area of particular recent interest is that associated with alkylidene complexes which have long been associated with the useful olefin metathesis reaction. The mechanism for this process is given in Scheme 4.5.[22,23]

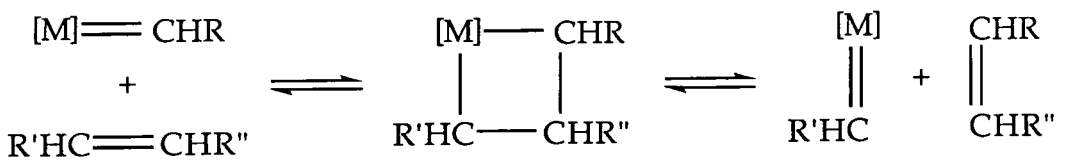

Scheme 4.5 *Chauvin and Hérisson olefin metathesis mechanism.*

An example of one such complex is Tebbe's reagent ($Cp_2Ti(\mu-CH_2)(\mu-Cl)AlMe_2$)[24] which, when combined with a nitrogen base is synthetically equivalent to the nucleophilic metallocene alkylidene $Cp_2Ti{=}CH_2$, although the reagent never dissociates into the alkylidene and Me_2AlCl themselves (Scheme 4.6). It reacts readily with olefins, forming stable metallacycles in the presence of base (used to help remove the aluminium fragment), which are generally more convenient precursors for "$Cp_2Ti{=}CH_2$" than the aluminium reagent itself. These metallacycles readily exchange with other olefins *via* metathesis processes.

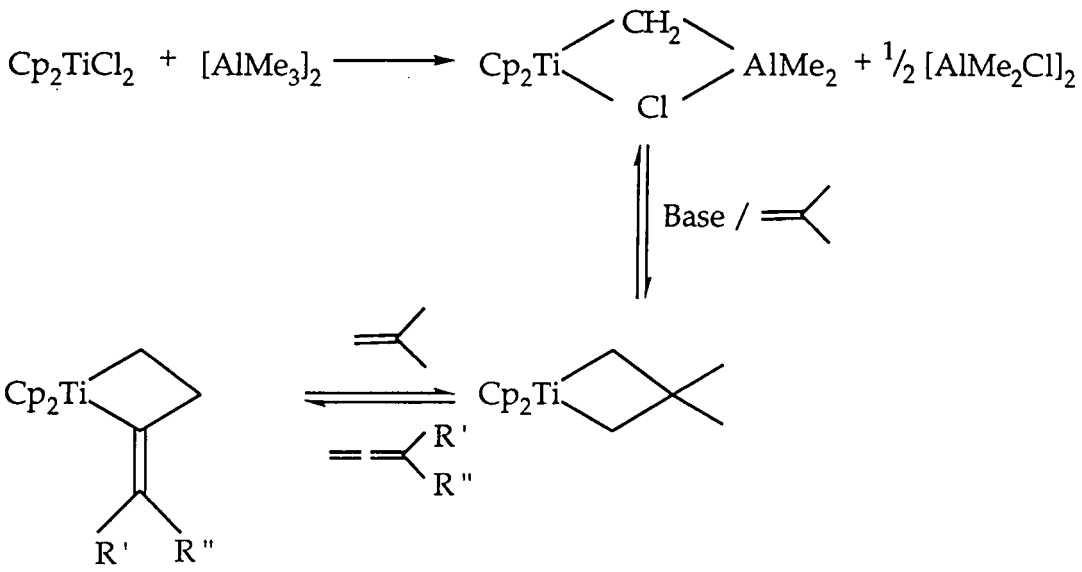

Scheme 4.6 *Synthesis and reaction of Tebbe's reagent.*

4.1 Synthesis and Reactivity of Acetylene Complexes of the type $Mo(NR)_2(PMe_3)(\eta^2\text{-}R'C{\equiv}CR'')$ [R=^{t}Bu, NAr]

4.1.1 Reaction of $Mo(NAr)_2(PMe_3)_2(\eta^2\text{-}C_2H_4)$ (6) with PhC≡CPh

Takahashi[25] has structurally characterised the Group 4 bent metallocene acetylene adduct $Cp_2Zr(\eta^2\text{-}PhC{\equiv}CPh)(PMe_3)$. This was synthesised by treating Cp_2ZrCl_2 with two equivalents of n-BuLi followed by the addition of diphenylacetylene in the presence of trimethylphosphine, according to Scheme 4.7. However, this strategy proved specific to the synthesis of this particular complex. Rausch[26] has shown that the bis (phosphine) complex $Cp_2Ti(PMe_3)_2$ dissociates one equivalent of phosphine when treated with a variety of acetylenes (including PhC≡CPh and C_2H_2) to generate the corresponding metallocene acetylene adduct.

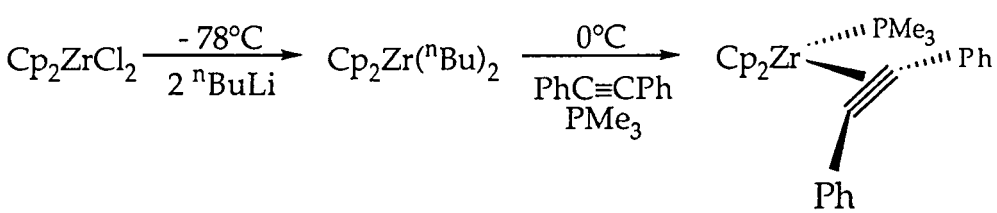

Scheme 4.7 *Synthesis of $Cp_2Zr(\eta^2\text{-}PhC{\equiv}CPh)(PMe_3)$.*

Analogously treatment of $Mo(NAr)_2(PMe_3)_2$, (5), with diphenylacetylene led to the isolation of the four coordinate acetylene complex $Mo(NAr)_2(PMe_3)(\eta^2\text{-}PhC{\equiv}CPh)$ (8) in low yield (Equation 4.3). However, this approach proved impractical as the reaction generated a number of uncharacterisable side products (as discussed in Chapter 2), although the related reaction for tungsten has proved to be more reliable.[27]

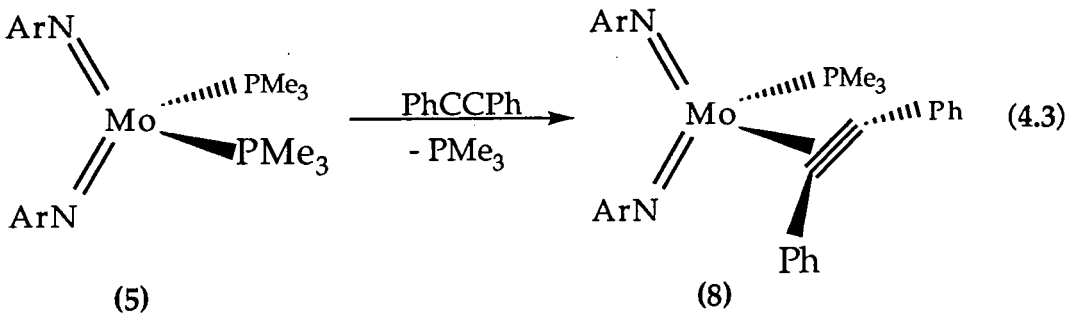

(5) (8) (4.3)

The synthetic strategy that proved most productive involved displacement of coordinated olefin from $Mo(NAr)_2(PMe_3)_2(\eta^2\text{-}C_2H_4)$ (6), according to Equation 4.4. Similar olefin displacement reactions have been reported for the related half-sandwich imido system, $CpNb(NAr)(PMe_3)_2(\eta^2\text{-}C_2H_4)$,[28] and for a hafnocene isobutene complex $Cp_2Hf(PMe_3)_2(\eta^2\text{-}C_4H_8)$.[29]

The molybdenum reaction proceeded smoothly in heptane at 60°C over 10 days; fine orange needles of the acetylene adduct (8) were isolated in 66% yield on cooling to room temperature. A sample was recrystallised from a concentrated THF solution at -10°C. Formation of the four coordinate adduct was confirmed by NMR spectroscopy and mass spectrometry (a parent ion at m/e 702 was observed). Elemental analyses were inconsistent due to residual THF solvent which could not be removed despite prolonged exposure to vacuum. Formation of the four coordinate complex is believed to be favoured over the five coordinate adduct on steric grounds.

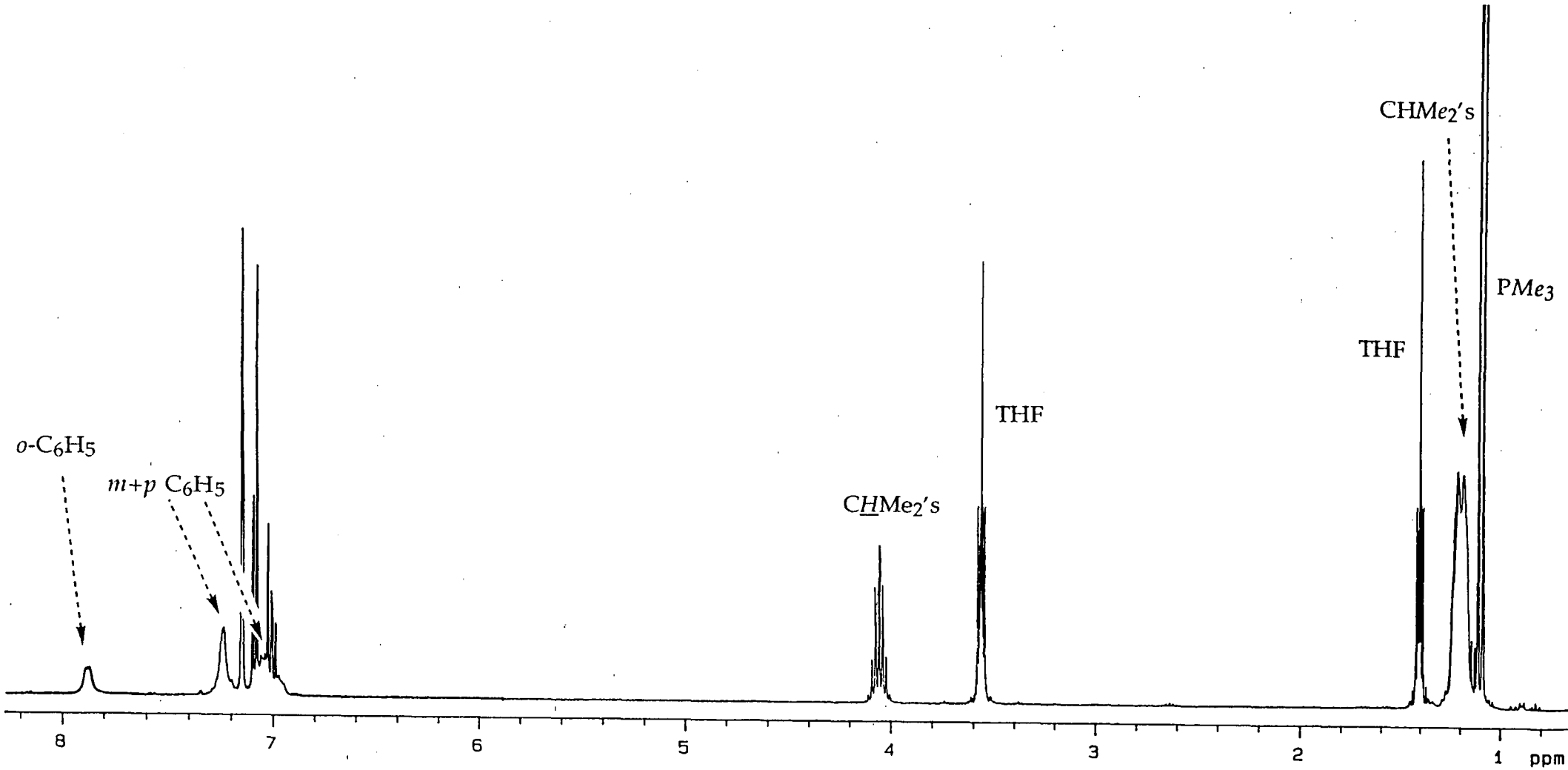

Figure 4.2 *400 MHz ^1H NMR spectrum of $Mo(NAr)_2(PMe_3)(\eta^2\text{-}PhC{\equiv}CPh)$ (C_6D_6).*

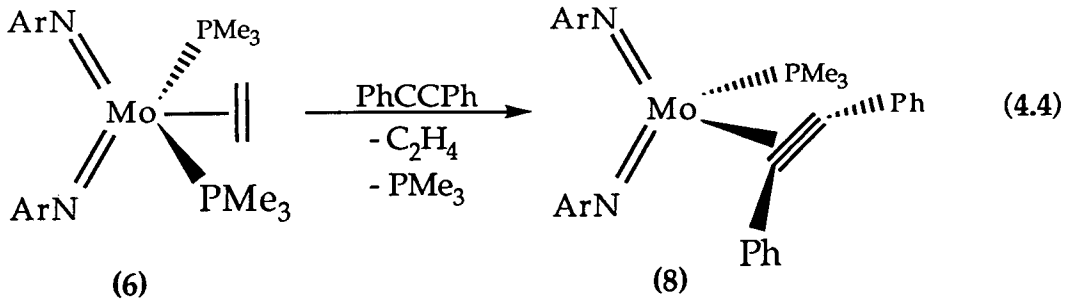

(6) (8) (4.4)

The room temperature 400 MHz ^{1}H NMR spectrum of (8), Figure 4.2, exhibited only one isopropyl septet associated with the imido, although the corresponding methyl resonance appeared as two overlapping doublets. Distortion of the isopropyl groups through steric interactions is believed to be the cause of this inequivalence, the methyl groups experiencing a greater effect than the methine proton.

A broad doublet resonance at δ 7.88 ppm has been attributed to the ortho protons of the acetylene phenyl ring which is effectively *cis* to the phosphine. This was assigned by analogy with the spectra obtained for the related tert-butyl imido complex (see Figure 4.3). Absolute assignment of the remainder of the phenylacetylene resonances proved difficult despite the use of ^{1}H-^{1}H COSY and NOE experiments (Figures 4.3 and 4.4), and was further complicated by the broadening observed on many of the aromatic proton resonances (elevated temperature spectra (60°C) exhibited similar broadening). This observation has been attributed to slow (hindered) rotation of the acetylene moiety. Irradiation of the trimethylphosphine resonance during NOE experiments gave responses from all the acetylenic and the imido protons. This suggests that the acetylene must be rotating "end-over-end" at a rate comparable with the timescale of the NOE experiment (ca. 10s).

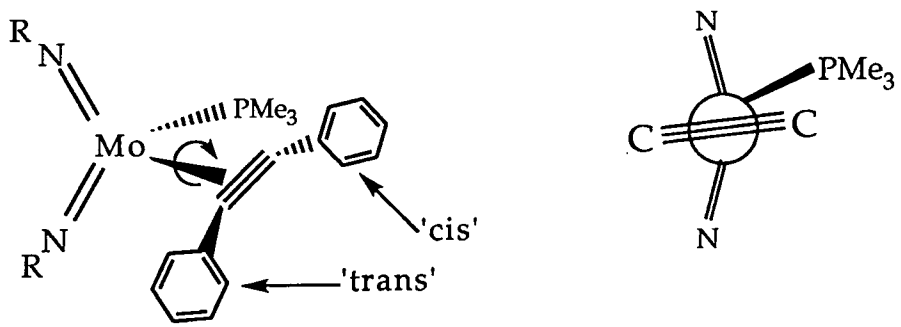

Figure 4.3 *Geometry of* $Mo(NR)_2(PMe_3)(\eta^2\text{-}Ph_2C_2)$ *(R=* ^{t}*Bu, Ar).*

The aromatic region of the 100 MHz ^{13}C NMR was complicated by the proximity of the resonances from both the imido substituents and the coordinated acetylene. The doublet resonance observed in both the proton coupled and decoupled spectra at δ 154.33 ppm has been attributed to the acetylenic carbon that is *cis* to the phosphine ligand and displays a phosphine coupling of 16.0 Hz. A similar value was obtained for the *cis* acetylenic carbon of the tert-butyl analogue of this complex (see Sections 3.4.6 and 4.1.2).

Assignment of the other aromatic carbon atoms was made by comparison with the spectra obtained for Mo(NAr)(N^{t}Bu)(PMe3)(η^2-PhC≡CPh)[30] and through the use of both HETCOR and COSY NMR experiments.

4.1.2 Reaction of Mo(N^{t}Bu)$_2$(PMe$_3$)(η^2-C$_2$H$_4$) (6) with PhC≡CPh

The four coordinate olefin complex Mo(N^{t}Bu)$_2$(PMe$_3$)(η^2-C$_2$H$_4$) (**10**) was treated with one equivalent of diphenylacetylene in heptane at 60°C for ten days. Slow cooling to room temperature allowed Mo(N^{t}Bu)$_2$(PMe$_3$)(η^2-PhC≡CPh) (**15**) to be isolated as yellow needles in virtually quantitative yield (Equation 4.5); the complex appears only slightly sensitive to both air and moisture, decomposing slowly over a period of 24 hours. However, the complex is not stable in chlorocarbon solvent, decomposing within several minutes to afford free diphenylacetylene and tert-butyl amine amine.

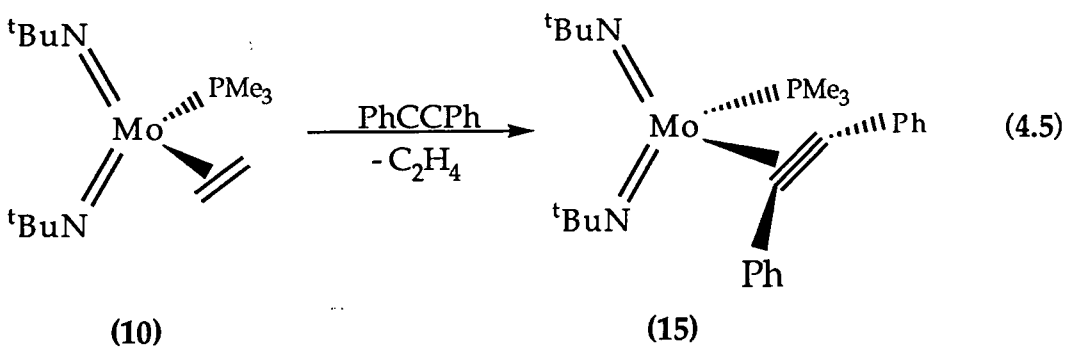

(10) (15) (4.5)

400 MHz ^1H NMR (Figure 4.4) confirmed the predicted metallocene-like geometry with the acetylene coordinated in a plane perpendicular to the N-Mo-N wedge (Figure 4.3). ^1H NOE experiments were used to assign

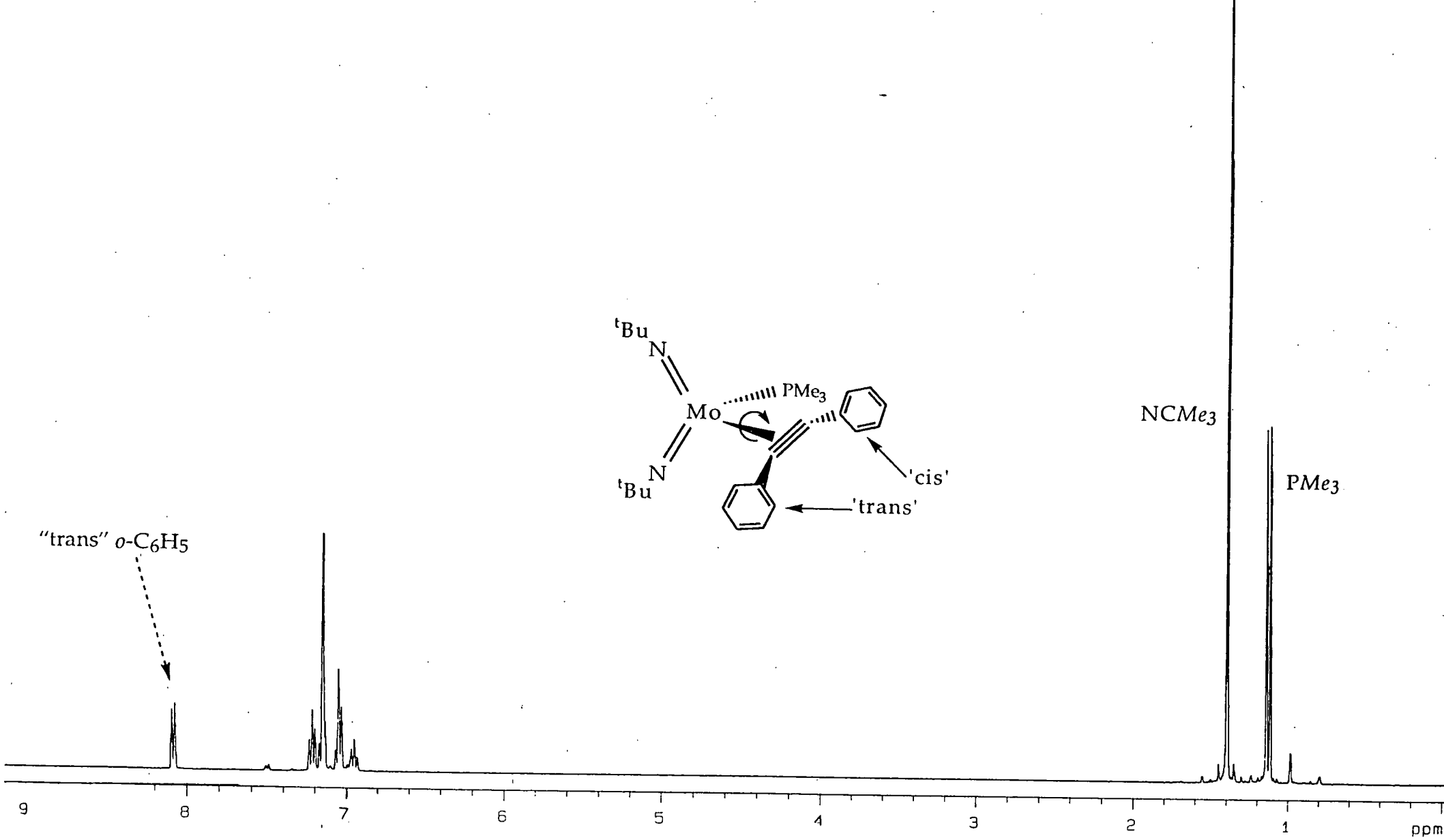

Figure 4.4 *400 MHz ^1H NMR spectrum of $Mo(N^tBu)_2(PMe_3)(\eta^2\text{-}PhC{\equiv}CPh)$ (C_6D_6).*

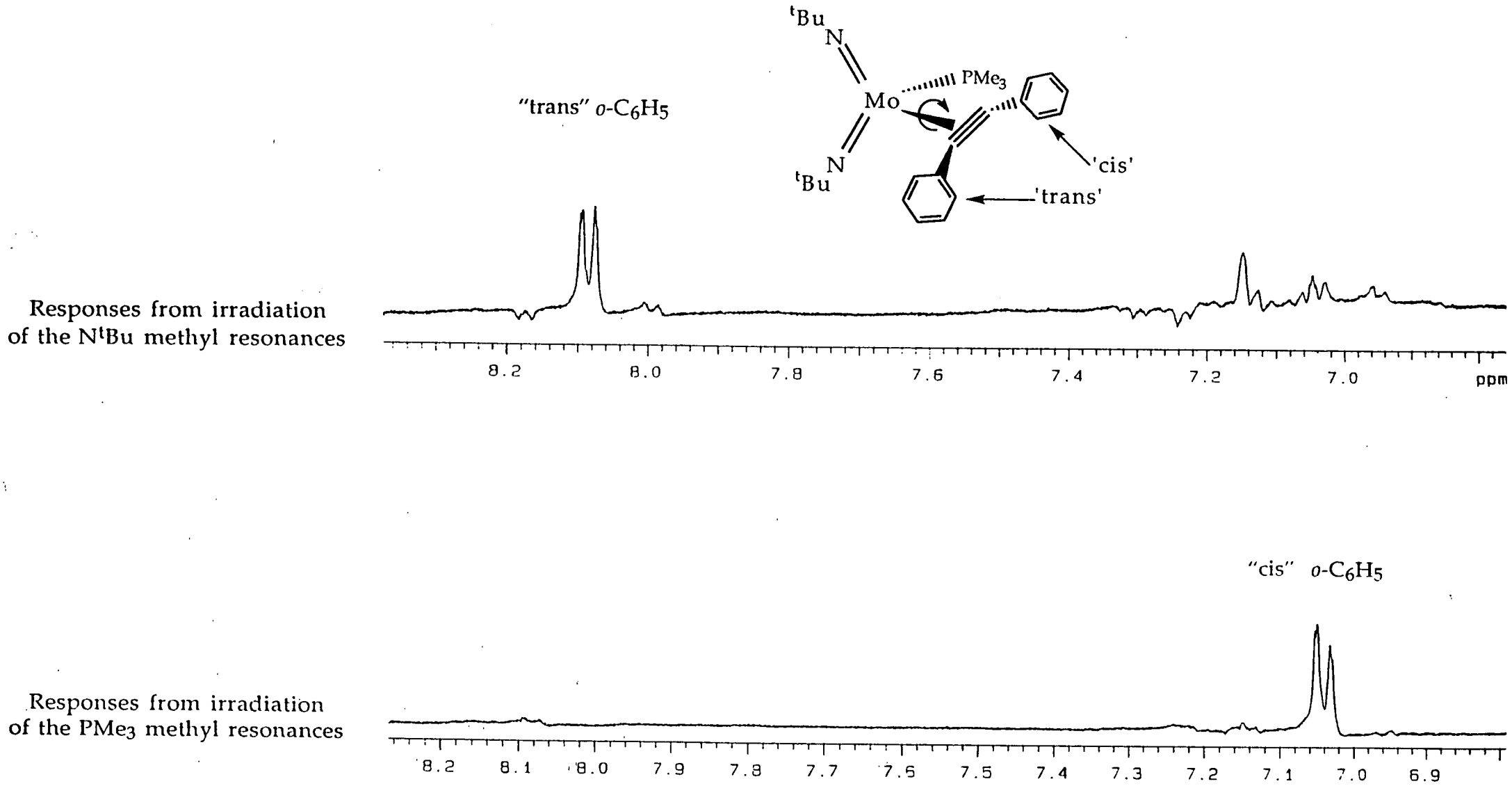

Figure 4.5 *NOE experiment for $Mo(N^tBu)_2(PMe_3)(\eta^2\text{-}PhC{\equiv}CPh)$ (C_6D_6).*

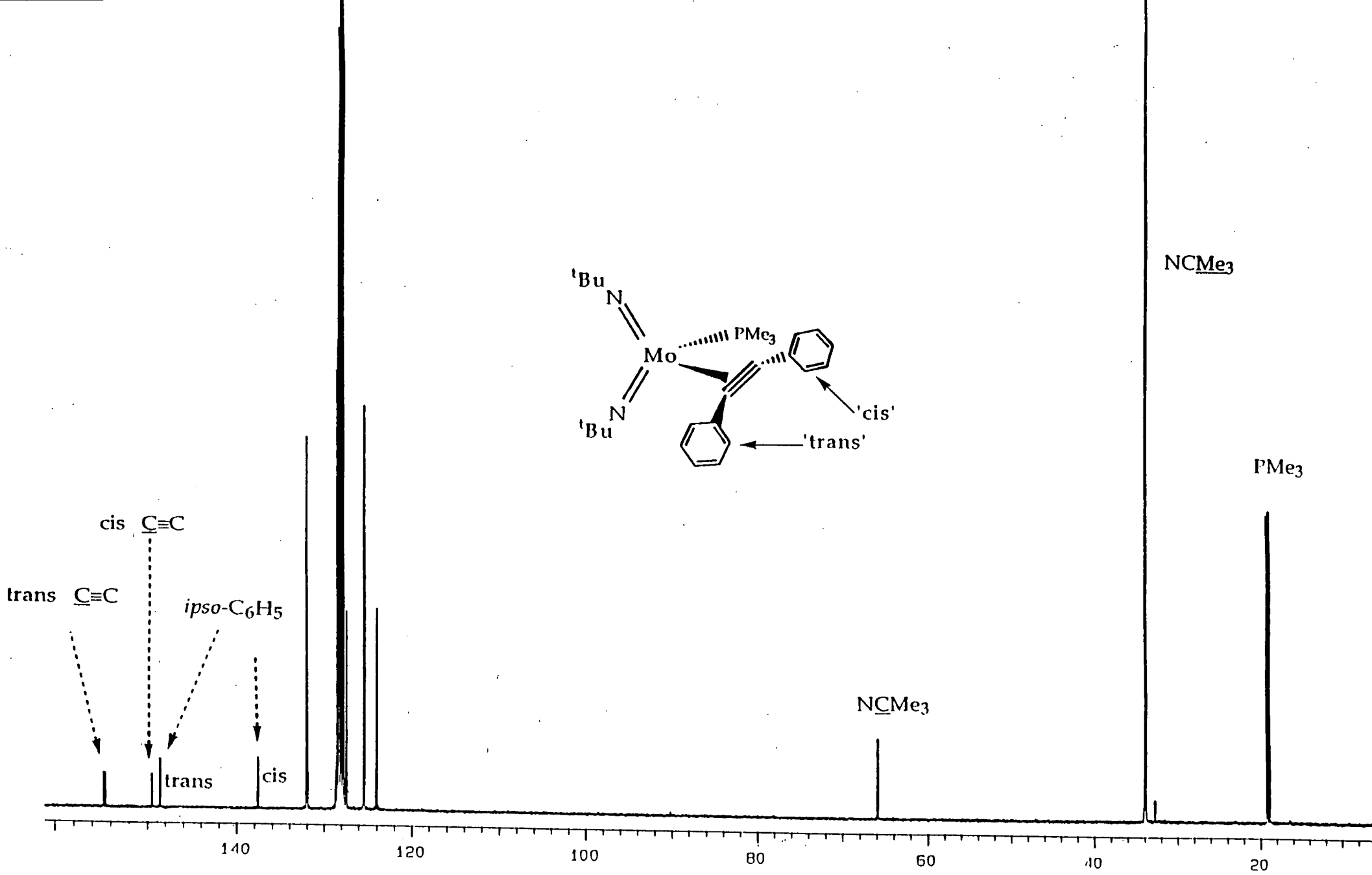

Figure 4.6 *100 MHz ^{13}C NMR spectrum of $Mo(N^tBu)_2(PMe_3)(\eta^2\text{-}PhC{\equiv}CPh)$ (C_6D_6).*

the orientation of the diphenylacetylene ligand (Figure 4.5). Support for this geometry was also obtained from the 100 MHz ^{13}C NMR data (Figure 4.6). Assignments were made on the basis of correlations obtained from ^{1}H / ^{13}C HETCOR experiments. Phosphorus-carbon couplings were confirmed by acquiring ^{13}C $\{^{31}P\}$ NMR spectra. The acetylene does not readily rotate about the metal-ligand(centroid) axis on the NMR timescale.

As discussed in Section 4.0, Templeton has correlated the number of electrons donated to the metal with the chemical shift of the two acetylenic carbons. The chemical shifts observed for (**15**), δ 149.41 and 154.62 ppm, lie approximately between values typically observed for two electron (110-120 ppm) and four electron (190-210 ppm) donor acetylenes. This intermediacy has been attributed to partial donation from the filled orthogonal π-system of the alkyne which would then be in competition with the $p\pi$-$d\pi$ metal-ligand interactions of the two imido groups.

4.1.3 Molecular Structure of $Mo(N^tBu)_2(PMe_3)(\eta^2\text{-}PhC{\equiv}CPh)$ (15)

A small (1.0 x 0.2 x 0.2 mm) yellow needle of (**15**) was mounted in a Lindemann capillary under an inert atmosphere and a molecular structure determination performed. The data were collected and the structure solved by Prof. J.A.K. Howard and Miss C. Wilson at the University of Durham. Selected bond distances and angles are presented in Tables 4.3 and 4.4.

Table 4.3 *Bond lengths (Angstroms) with estimated standard deviations in parentheses for* $Mo(N^tBu)_2(PMe_3)(\eta^2\text{-}PhC{\equiv}CPh)$.

Mo-C(1)	2.082(9)	Mo-C(2)	2.155(10)
Mo-N(1)	1.762(8)	Mo-N(2)	1.758(7)
Mo-P	2.466(3)	C(1)-C(2)	1.308(13)
C(1)-C(101)	1.447(13)	C(2)-C(201)	1.475(12)
C(101)-C(102)	1.410(12)	C(101)-C(106)	1.428(12)
C(102)-C(103)	1.366(14)	C(103)-C(104)	1.371(14)
C(104)-C(105)	1.384(14)	C(105)-C(106)	1.368(13)
C(201)-C(202)	1.409(13)	C(201)-C(206)	1.422(12)
C(202)-C(203)	1.394(13)	C(203)-C(204)	1.393(13)
C(204)-C(205)	1.393(14)	C(205)-C(206)	1.385(13)
N(1)-C(3)	1.443(12)	C(3)-C(4)	1.504(15)
C(3)-C(5)	1.533(14)	C(3)-C(6)	1.511(16)
N(2)-C(7)	1.452(12)	C(7)-C(8)	1.517(19)
C(7)-C(9)	1.507(15)	C(7)-C(10)	1.519(20)
P-C(11)	1.797(11)	P-C(12)	1.827(10)
P-C(13)	1.791(10)		

Table 4.4 *Bond angles (Degrees) with estimated standard deviations in parentheses for* $Mo(N^tBu)_2(PMe_3)(\eta^2\text{-}PhC{\equiv}CPh)$.

C(1)-Mo-C(2)	35.9(4)	C(1)-Mo-N(1)	107.5(3)
C(2)-Mo-N(1)	120.3(3)	C(1)-Mo-N(2)	109.2(4)
C(2)-Mo-N(2)	119.3(4)	N(1)-Mo-N(2)	117.5(3)
C(1)-Mo-P	121.9(3)	C(2)-Mo-P	86.0(3)
N(1)-Mo-P	100.6(3)	N(2)-Mo-P	100.7(3)
Mo-C(1)-C(2)	75.1(6)	Mo-C(1)-C(101)	142.9(6)
C(2)-C(1)-C(101)	142.0(9)	Mo-C(2)-C(1)	69.0(5)
Mo-C(2)-C(201)	152.6(7)	C(1)-C(2)-C(201)	138.4(9)
C(1)-C(101)-C(102)	121.7(8)	C(1)-C(101)-C(106)	122.2(7)
C(102)-C(101)-C(106)	116.1(8)	C(101)-C(102)-C(103)	121.6(8)
C(102)-C(103)-C(104)	120.5(9)	C(103)-C(104)-C(105)	120.7(9)
C(104)-C(105)-C(106)	119.5(9)	C(101)-C(106)-C(105)	121.7(8)
C(2)-C(201)-C(202)	121.4(8)	C(2)-C(201)-C(206)	120.5(8)
C(202)-C(201)-C(206)	118.0(8)	C(201)-C(202)-C(203)	120.5(9)

C(202)-C(203)-C(204)	121.1(9)	C(203)-C(204)-C(205)	118.4(8)
C(204)-C(205)-C(206)	121.8(8)	C(201)-C(206)-C(205)	120.0(9)
Mo-N(1)-C(3)	162.6(6)	N(1)-C(3)-C(4)	108.9(9)
N(1)-C(3)-C(5)	110.2(8)	C(4)-C(3)-C(5)	109.2(9)
N(1)-C(3)-C(6)	109.0(9)	C(4)-C(3)-C(6)	109.7(10)
C(5)-C(3)-C(6)	110.0(9)	Mo-N(2)-C(7)	171.6(7)
N(2)-C(7)-C(8)	107.3(9)	N(2)-C(7)-C(9)	109.8(9)
C(8)-C(7)-C(9)	110.2(9)	N(2)-C(7)-C(10)	108.9(9)
C(8)-C(7)-C(10)	111.3(11)	C(9)-C(7)-C(10)	109.3(10)
Mo-P-C(11)	112.9(4)	Mo-P-C(12)	115.3(3)
C(11)-P-C(12)	103.1(5)	Mo-P-C(13)	117.0(4)
C(11)-P-C(13)	102.9(5)	C(12)-P-C(13)	104.0(5)

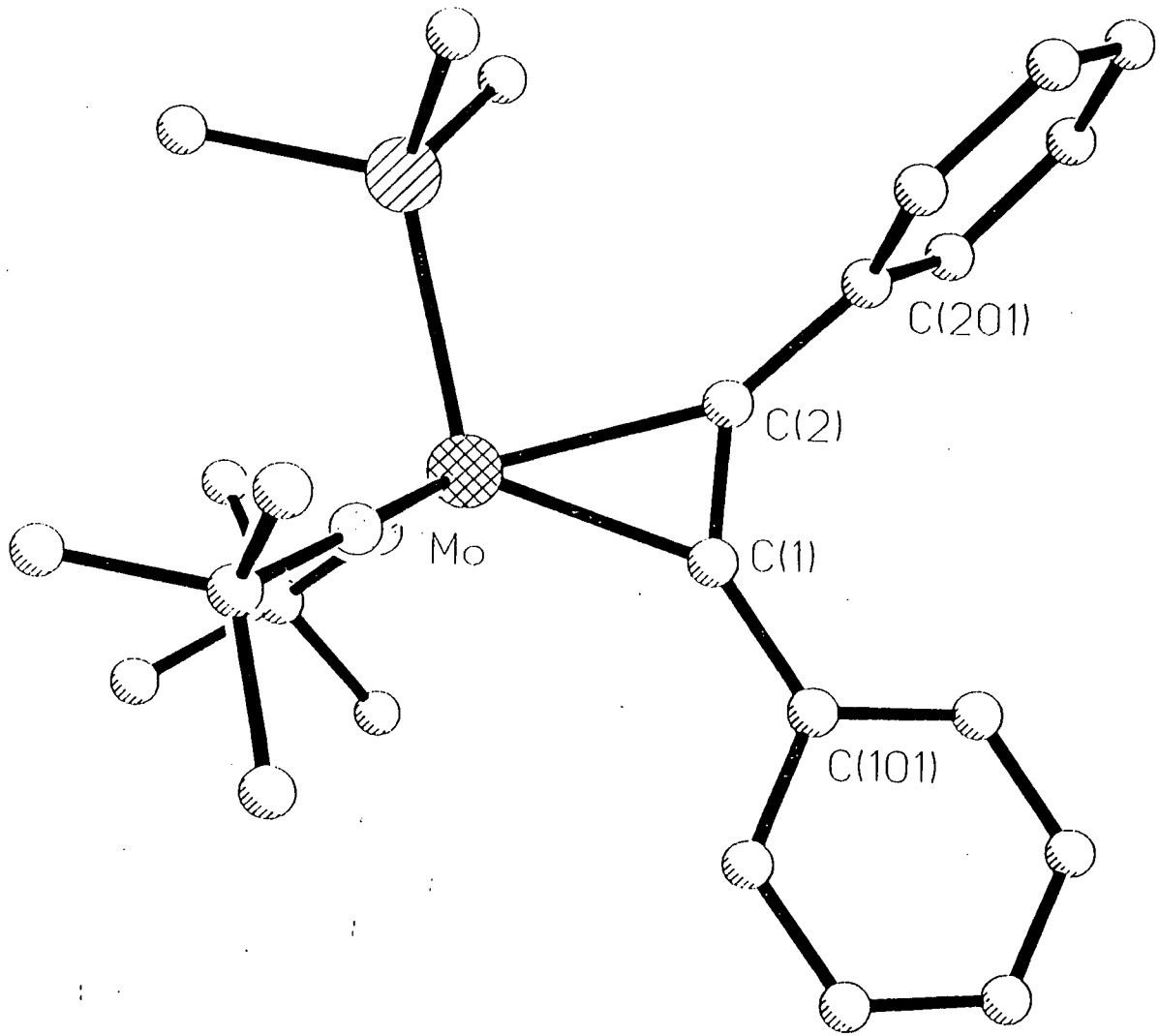

Figure 4.7 *Molecular structure of* $Mo(N^tBu)_2(PMe_3)(\eta^2\text{-}PhC{\equiv}CPh)$.

As predicted, the molecular structure was entirely consistent with (**15**), having adopted a metallocene-like pseudo-tetrahedral geometry (Figure 4.7a). The coordinated diphenylacetylene carbons lie in a plane with the Mo and P atoms, which deviates only 0.0164Å from planarity. The *ipso*-carbon atoms of the phenyl substituents also lie in this plane, the rms deviation from the plane defined by atoms C(1), C(2) and C(201) being 0.0015Å and 0.0099Å if the molybdenum atom is included in the definition of the plane. The phenyl rings themselves are, however, tilted out of this plane; the ring defined by atoms C(101)-C(106) is twisted by 22.8° and the C(201)-C(206) containing ring by 103.0° (Figures 4.7b). This uneven distortion and the unsymmetrical coordination of the acetylene [Mo-C(1) 2.082(9)Å, Mo-C(2) 2.155(10)Å] are both likely consequences of constraints imposed by the bulky phosphine.

There is considerable bending at the acetylenic carbon atoms as shown by the bond angles C(1)-C(2)-C(201) and C(2)-C(1)-C(101) which are 138.4(9) and 142.0(9)° respectively. This, together with the considerable lengthening of the C(1)-C(2) bond, 1.308(13)Å relative to the un-coordinated acetylene (≈ 1.20Å) is indicative of considerable back-donation from the d^2-metal centre. Thus, the coordinated acetylene resembles a *cis* olefin, something that is typical of the distortion arising upon coordination of the unsaturated ligand.[31] The metal to C≡C bond midpoint distance of 2.36Å and C(1)-C(2) bond length are both consistent with the acetylene acting as a two electron donor ligand, by comparison with $Cp_2Mo(\eta^2\text{-PhC}{\equiv}\text{CPh})$.[32]

The isolobal complex $Cp_2Ti(CO)(\eta^2\text{-PhC}{\equiv}\text{CPh})$ (Figure 4.8) synthesised by Floriani and co-workers[33] coordinates the acetylene in a relatively symmetrical manner (Ti-C(1) 2.384(9)Å, Ti-C(2) 2.369(10)Å). The two phenyl substituents twist out of the plane defined above by only 23.9° and 47.4°. The acetylenic C-C bond distance also reflects the close approach of the ligand to the metal centre. More back-donation making the bond significantly longer (C(1)-C(2) 1.345(15)Å) (cf. 1.308(13)Å for (**15**)).

The Mo-N-C bond angles of 162.6(6) and 171.6(7)° are typical of linear imido ligands,[34] while the Mo-N bond distances of 1.762(8) and 1.758(7)Å (equivalent to within 1σ) agree well with those obtained for the related propene complex (**11**) described in Chapter 3. The N-Mo-N angle of 117.5(3)° deviates little from the idealised tetrahedral angle.

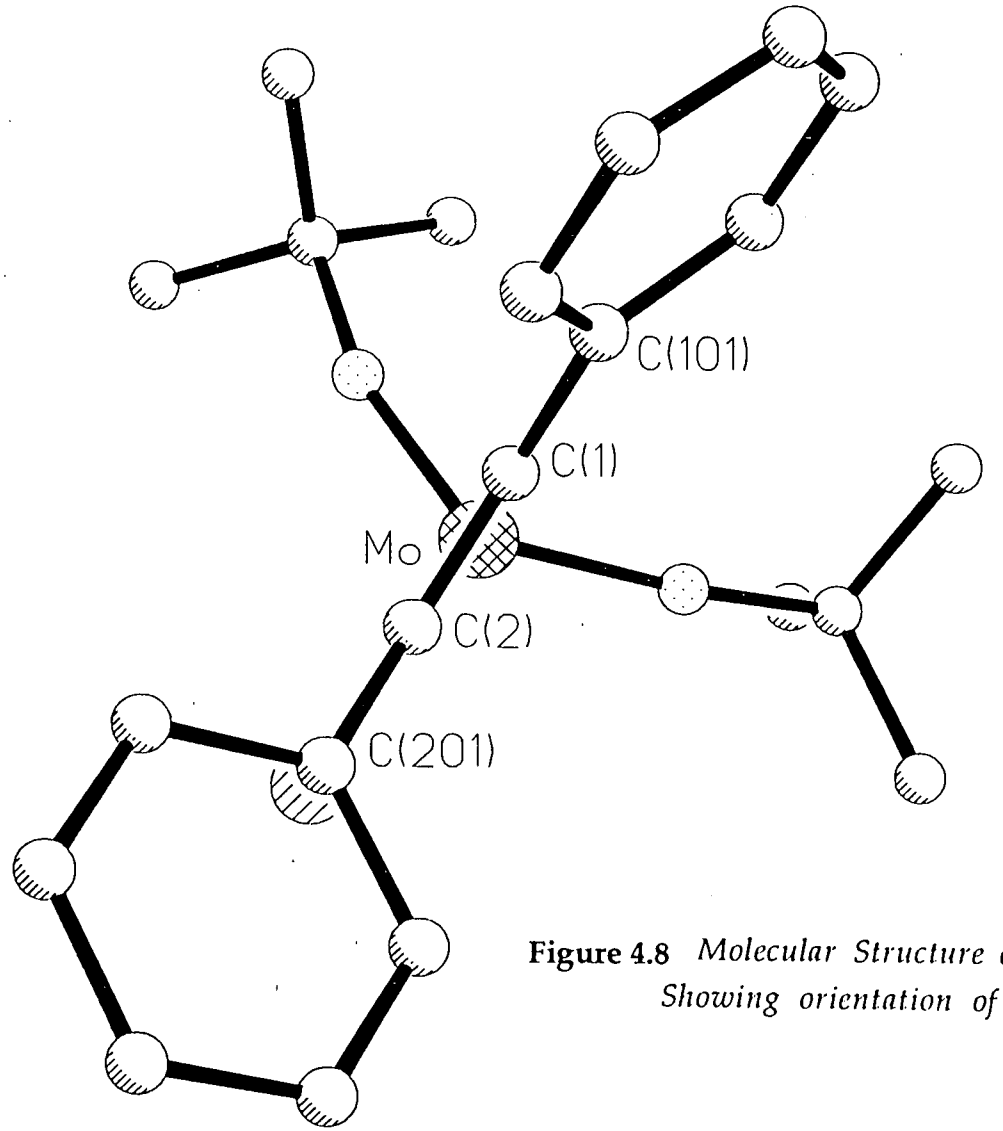

Figure 4.8 *Molecular Structure of* $Mo(N^tBu)_2(PMe_3)(\eta^2\text{-}PhC{\equiv}CPh)$ *Showing orientation of the phenyl rings.*

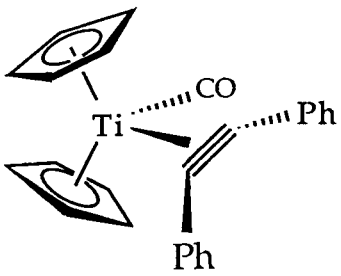

Figure 4.8
Floriani's $Cp_2Ti(CO)(\eta^2\text{-}PhC{\equiv}CPh)$ complex.

The basic geometry of the zirconium complex $Cp_2Zr(\eta^2\text{-}PhC{\equiv}CPh)(PMe_3)$[28] is very similar to that exhibited by **(15)**. The major structural parameters for the two species are compared in Table 4.5. This similarity reiterates the structural analogy that relates these two seemingly disparate complexes.

$Cp_2Zr(\eta^2\text{-}PhC{\equiv}CPh)(PMe_3)$		$Mo(N^tBu)_2(\eta^2\text{-}PhC{\equiv}CPh)(PMe_3)$	
$Cp_{(c)}$-Zr-$Cp_{(c)}$	127.38°	N-Mo-N	117.5(3)°
C≡C	1.36(6)Å	C≡C	1.308(13)Å
C(2)-C(1)-C(101)	134(4)°	C(2)-C(1)-C(101)	142.0(9)°
$(C{\equiv}C)_m$ — Zr	2.12Å	$(C{\equiv}C)_m$ — Mo	2.05Å
C(1)-C(2)-C(201)	133(4)Å	C(1)-C(2)-C(201)	138.4(9)°
Zr-C(1)	2.20(4)Å	Mo-C(1)	2.082(9)Å
Zr-C(2)	2.25(4)Å	Mo-C(2)	2.155(10)Å

Table 4.5 *Comparison of the main structural parameters of the pseudo-isolobal complexes $Cp_2Zr(\eta^2\text{-}PhC{\equiv}CPh)(PMe_3)$ and $Mo(N^tBu)_2(\eta^2\text{-}PhC{\equiv}CPh)(PMe_3)$. {$Cp_{(c)}$ = Cp ring centroid; $(C{\equiv}C)_m$ = acetylene bond midpoint}*

4.1.4 Reaction of $Mo(N^tBu)_2(PMe_3)(\eta^2\text{-}C_2H_4)$ (10) with PhC≡CH

Treatment of $Mo(N^tBu)_2(PMe_3)(\eta^2\text{-}C_2H_4)$ **(10)** with one equivalent of phenylacetylene followed by heating to 60°C for three days in an NMR tube smoothly afforded the corresponding phenylacetylene complex **(16)**, Equation 4.6.

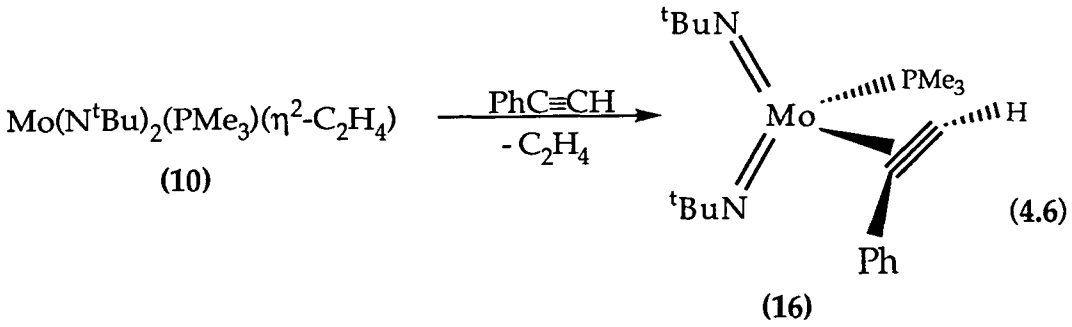

The acetylene aligns such that the substituent is located in an *outer* (*exo*) position This was established through NOE experiments; the only response observed when the methyl resonance of the PMe_3 was irradiated came from the acetylenic proton . The observed orientational preference of the unsaturated moiety minimises any interaction between the substituent and the phosphine.

The 400 MHz ^1H NMR spectrum (Figure 4.9) revealed a low field resonance (δ 8.58 ppm) which was assigned to the acetylenic proton. As for both of the diphenylacetylene complexes (**8**) and (**15**), the *ortho* protons of the phenyl ring were deshielded, appearing as a doublet at δ 8.17 ppm. The two tert-butyl imido substituents were equivalent, which indicated that the acetylene moiety was aligned in a plane containing the molybdenum and phosphorus atoms, and which bisected the N-Mo-N angle as observed in the solid state structure of (**15**). There was no evidence for rotation of the acetylene moiety on the NMR timescale.

In the ^{13}C NMR spectrum of (**16**) the acetylenic carbon at δ 138.25 exhibited coupling to phosphorus ($^2J_{PH}$ 23.6 Hz). Thus, the carbon atom that was effectively *cis* to the phosphine displayed the greater coupling. Templeton's analysis of ^{13}C NMR acetylenic carbon shifts indicates that the acetylene in this complex is acting as mid way between a 2 and a 4 electron ligand. This implies partial donation from the filled π system of the acetylene, although this will be in competition with the pπ-dπ metal ligand interactions.

The orientation of the phenylacetylene was determined from spectroscopic data and by comparison with the structurally characterised diphenylacetylene adduct. Support for this geometry was gained from two other diphenylacetylene adducts synthesised within this group, Mo(NAd)$_2$(PMe$_3$)(η^2-PhC≡CPh) (Ad= Adamantyl) and Mo(N^{t}Bu)(NAr)(PMe$_3$)(η^2-PhC≡CPh).[35] NMR data for the former was sufficient to unequivocally say that the complex had adopted a

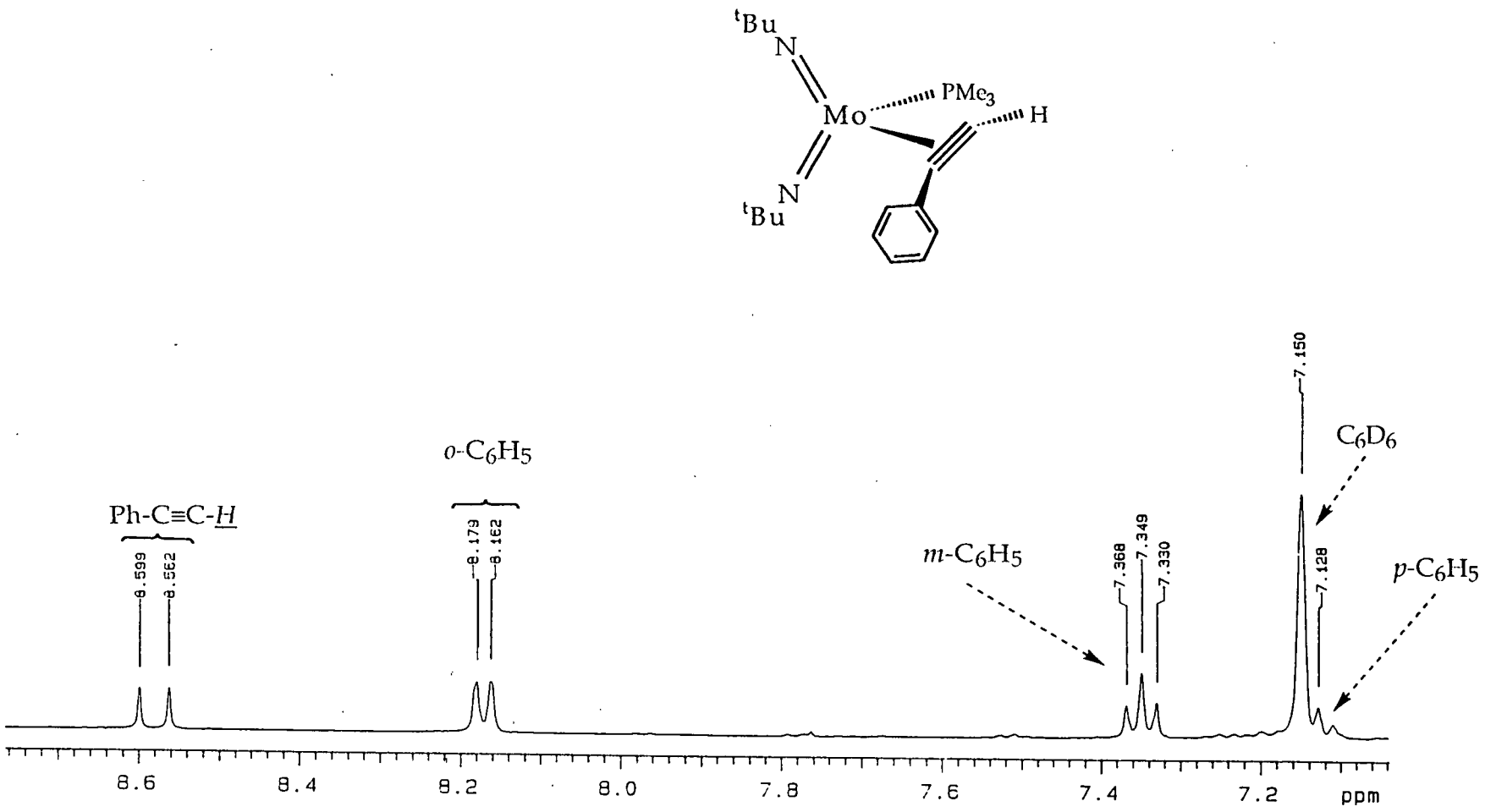

Figure 4.9 400 MHz ^{1}H NMR spectrum of $Mo(N^tBu)_2(PMe_3)(\eta^2\text{-}PhC{\equiv}CH)$ (C_6D_6) showing the aromatic region only.

metallocene-like geometry. Yet, NOE experiments on the mixed imido analogue indicated that the structure was not static and that on the NMR timescale the acetylene moiety was rotating with a rate somewhere between 0.1 and 40 Hz (based upon the time-window of the NOE experiment). A similar effect was also observed for Mo(N-2-$C_6H_4{}^tBu)_2(PMe_3)(\eta^2$-PhC≡CPh).

The NMR data for $Mo(NAr)_2(PMe_3)(\eta^2$-PhC≡CPh) (above) indicated that rotation of the acetylene was occurring. Such rotation is well established for acetylene ligands on transition metals.[36] A trend became apparent: complexes that possessed aromatic imido substituents exhibited slow rotation of the acetylene ligand, yet their alkyl-imido analogues appear static on the NMR timescale. This effect is likely to be due to the more electron donating alkyl groups (tert-butyl and adamantyl) raising the energy of the partially filled (d^2) metal d orbitals Thus, a better energy match with the π^* orbitals of the acetylene is achieved thereby forming a stronger π-back bond which will raise the energy barrier to rotation.[37]

4.1.5 Reaction of $Mo(NR)_2(PMe_3)(\eta^2$-PhC≡CPh) with PhC≡CPh

An attempt was made to generate a diacetylene complex, which might undergo oxidative coupling with the second equivalent of diphenylacetylene to generate a metallacycle, as demonstrated by Rausch for the related titanium complex $Cp_2Ti(PMe_3)(\eta^2$-HC≡CH).[38] The arylimido acetylene complex (**8**) was treated with a second equivalent of diphenylacetylene in an NMR tube (C_6D_6). Despite prolonged warming at 70°C no further reaction was apparent.

The reaction was repeated using the tert-butylimido analogue (**15**). Still no reaction was observed. Strong coordination of the phosphine in both cases is believed to be the cause of the inactivity.

4.1.6 Magnesium Reduction of $Mo(NR)_2Cl_2$.DME in the Presence of Ph_2C_2

The synthesis of a diacetylene complex was also attempted directly. An ampoule was charged with $Mo(NAr)_2Cl_2$.DME, diphenylacetylene and

an excess of activated magnesium turnings, according to equation 4.7. THF was added and the reaction stirred at room temperature for 18 hours.

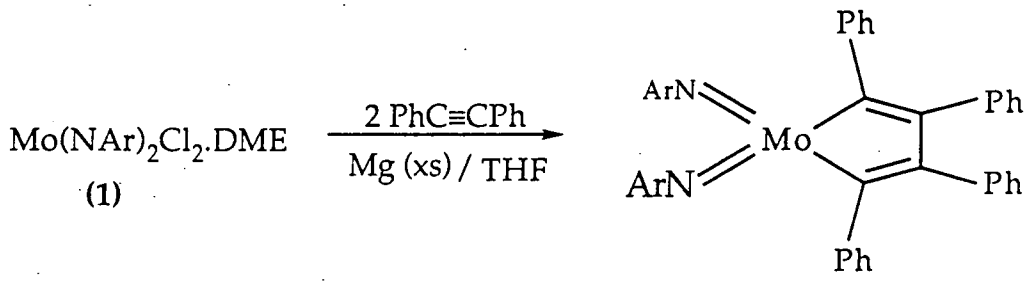

(4.7)

The solution slowly changed colour from red to dark brown with precipitation of $MgCl_2$ (as identified by IR). Subsequent removal of all volatiles *in vacuo* and extraction of the residue into diethylether, followed by recrystallisation at -78°C afforded a small amount of a pale yellow solid, whose nature remains unidentified, although unreacted diphenylacetylene could be detected in the crude product.

When a similar reaction was performed with $Mo(N^tBu)_2Cl_2.DME$ in the presence of PMe_3 the only product proved to be the imido-bridged diphosphine species, $Mo_2(N^tBu)_2(\mu\text{-}N^tBu)_2(PMe_3)_2$ (9), (Scheme 4.8). No further reaction is likely to occur with the diphosphine as it has proved particularly unreactive.

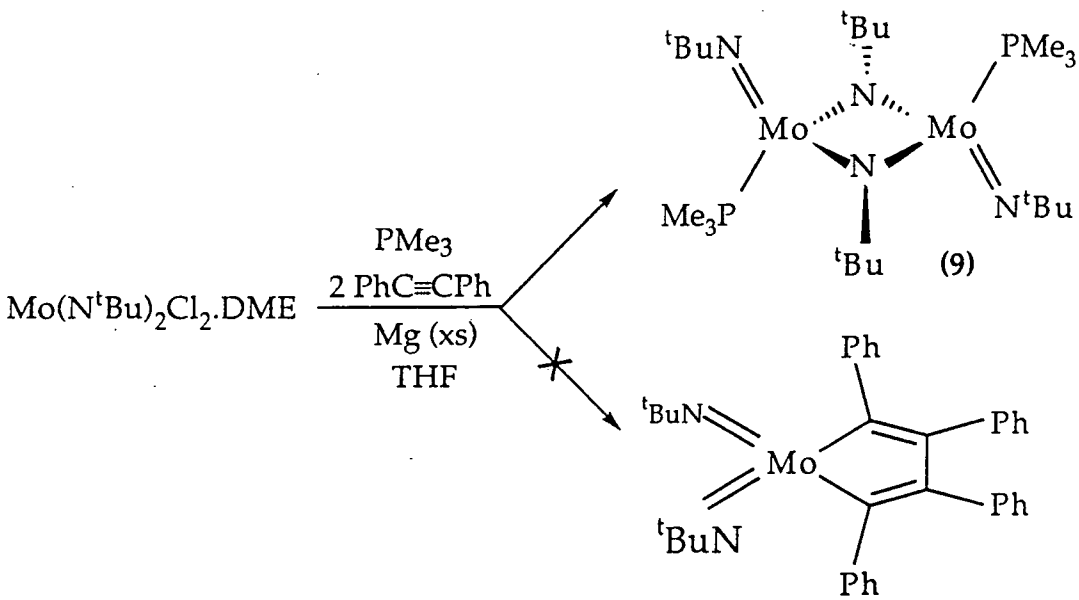

Scheme 4.8 *Magnesium reduction of $Mo(N^tBu)_2Cl_2.DME$ in the presence of two equivalents of diphenylacetylene.*

4.1.7 Reaction of $Mo(NR)_2(PMe_3)(\eta^2\text{-}PhC{\equiv}CPh)$ with H_2 and C_2H_4

C_6D_6 solutions of the diphenylacetylene adducts (8) (R= Ar) and (15) (R= ^{t}Bu) were both sealed under one atmosphere of hydrogen in NMR tubes. Despite prolonged warming at 100°C, no new species were formed, the ^{1}H NMR spectrum of the acetylene complex remaining unaltered in both cases. This lack of reactivity was somewhat surprising in light of a similar reaction performed with the related tert-butylimido ethylene complex (10) which underwent a slow reaction with hydrogen resulting in the formation of an as yet unidentified complex.

In an attempt to generate a bis (imido) metallacyclopentene a C_6D_6 solution of the tert-butyl imido olefin complex (15) was treated with excess ethylene. Despite prolonged heating to 60°C no reaction was forthcoming.

4.2 Displacement Reaction of $Mo(N^tBu)_2(PMe_3)(\eta^2\text{-}C_3H_6)$ (11) with PhN=NPh

The last section demonstrated the applicability of olefin displacement reactions involving $Mo(N^tBu)_2(PMe_3)(\eta^2\text{-}C_3H_6)$ (11) for the generation of bis (imido) complexes containing other unsaturated hydrocarbon ligands. To explore the limits of this strategy, reactions with other multiply bonded species were attempted.

A variety of transition metal complexes that contain the 1,2-diazene or azobenzene moiety have been isolated. They usually utilize one or both lone pairs on N as σ donors to give η^1 or bridged compounds (Figure 4.10).[39]

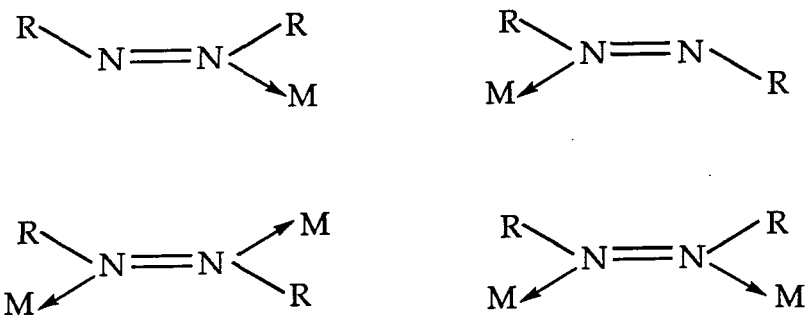

Figure 4.10 *η^1 bonding modes of azobenzenes.*

However, azobenzenes are also capable of bonding in an η^2 olefin-like manner (Figure 4.11), although π bonds may also be used (cf. RC≡CR'). For example the following two complexes have been structurally characterised: $Cp_2Ti(\eta^2\text{-PhN=NPh})$[40] and $(P\{tol\}_3)_3Ni(\eta^2\text{-PhN=NPh})$.

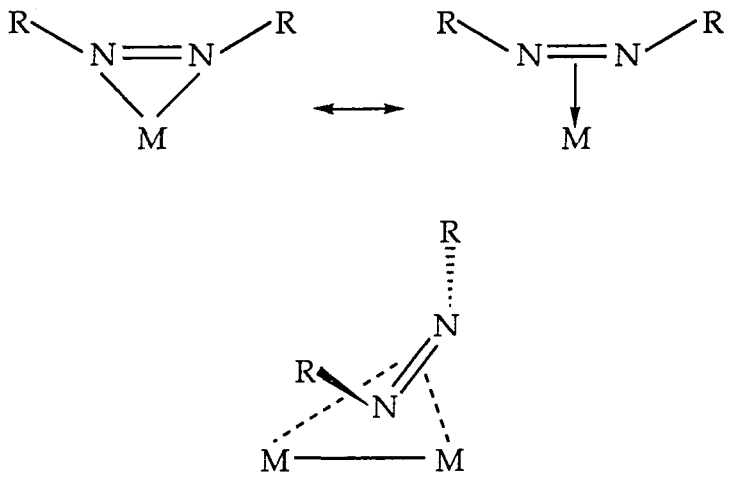

Figure 4.11 *η^2 and π-bridging bonding modes of azobenzenes.*

4.2.1 Reaction of $Mo(N^tBu)_2(PMe_3)(\eta^2\text{-}C_3H_6)$ (11) with PhN=NPh

A C_6D_6 solution of $Mo(N^tBu)_2(PMe_3)(\eta^2\text{-}C_3H_6)$ was treated with one equivalent of azobenzene (freshly sublimed) in an NMR tube. After heating the sample at 60°C for ten days, ^1H NMR clearly indicated that displacement of propene had taken place and that a single new species was formed. Thus, the reaction was repeated on a preparative scale.

After 10 days the reaction mixture (Equation 4.8) had changed colour from yellow to dark red. The heptane solution was filtered hot and allowed to cool slowly.

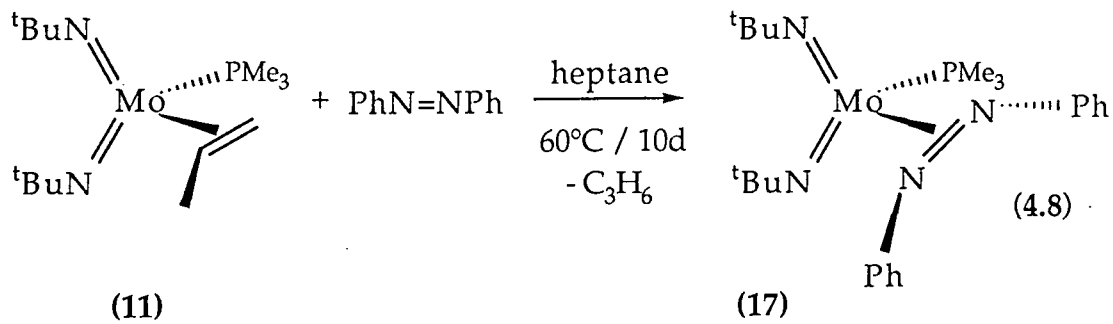

(4.8)

(11) **(17)**

A yellow solid (**17**) precipitated on reaching room temperature which was isolated in low yield. 200 MHz ^{1}H NMR analysis indicated the presence of both unreacted azobenzene and a new species. Despite repeated recrystallisation from a variety of solvents, and sublimation under reduced pressure, the complex was never isolated without azobenzene being present, a result of facile dissociation (possibly a consequence of both steric and electronic effects); this hampered IR and elemental analyses. The ^{1}H NMR spectra did, however, indicate that there were inequivalent imido groups and that the phosphine had remained coordinated to the metal centre.

Bergman and co-workers[41] have structurally characterised a base stabilised zirconocene complex [$Cp_2Zr(PhN{=}NPh)(py)$] which does indeed possess η^2 coordinated azobenzene. The nitrogen atoms of the azobenzene are clearly tetrahedral.[42] One phenyl ring lies above and the other phenyl ring below the plane defined by the atoms Zr, N(1), N(2), and N(py), Figure 4.12. If a similar geometry is adopted by (**17**) this would explain the inequivalence of the imido groups.

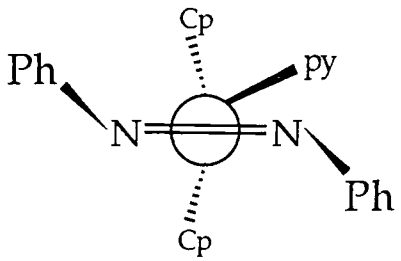

Figure 4.12
$Cp_2Zr(PMe_3)(\eta^2$-PhN=NPh): showing the tetrahedral geometry at each azobenzene nitrogen atom.

Interestingly (**17**) possesses two types of "NR" groups bound directly to the metal, Mo=N^{t}Bu and Mo(η^2-PhN=NPh). Thus, an attempt was made to exchange these ligands to form the mixed tert-butyl / phenyl bis (imido) and the unsymmetrical 1, 2-diazene, ^{t}BuN=NPh. However, despite prolonged heating to 120°C the ^{1}H NMR of the complex remained unaltered.

4.3 Attempts to Synthesise a Mo(NR)$_2$(PMe$_3$)(η^2-Benzyne) Complex

The recent synthesis of CpNb(NAr)$_2$(PMe$_3$)(η^2-C$_6$H$_4$)[43] led us to attempt the synthesis of the pseudo-isolobal molybdenum bis (imido) analogue.

4.3.1 Reaction of $Mo(NAr)_2Cl_2$.DME (1) with PhMgCl

Treatment of $Mo(NAr)_2Cl_2$.DME with two equivalents of phenylmagnesium chloride in the presence of PMe_3 using diethylether solvent cleanly affords the five coordinate diphenyl PMe_3 complex (18) as shown in Equation 4.9. The complex can be isolated in excellent yield after removal of all volatiles *in vacuo*, followed by recrystallisation from a saturated pentane solution at -30°C

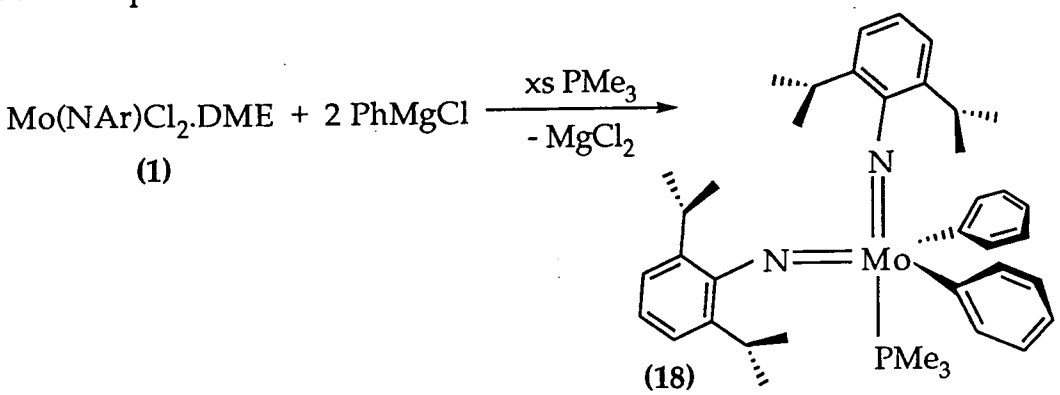

(4.9)

Both the 400 MHz ^1H and 100 MHz ^{13}C NMR spectra were unremarkable but consistent with the formation of the five coordinate base adduct (Figures 4.13 and 4.14).

Complex (18) has proved stable over a period of months in both the solid state and in hydrocarbon solution (under an inert atmosphere) at ambient temperature (≈20°C). Unlike the olefin or acetylene compounds described previously (18), is stable in chloroform at room temperature for several days.

4.3.2 The Molecular Structure of $Mo(NAr)_2(Ph)_2(PMe_3)$ (18)

Crystals suitable for an X-ray structure determination were obtained by prolonged cooling of a saturated pentane solution of (18). A crystal of suitable dimensions (0.25 x 0.20 x 0.30 mm) was sealed in a Lindemann capillary under an inert atmosphere. The data were collected and the structure solved by Prof. J.A.K. Howard and Miss S. Bahar at the University of Durham.[44] The molecular structure of (18) is illustrated in

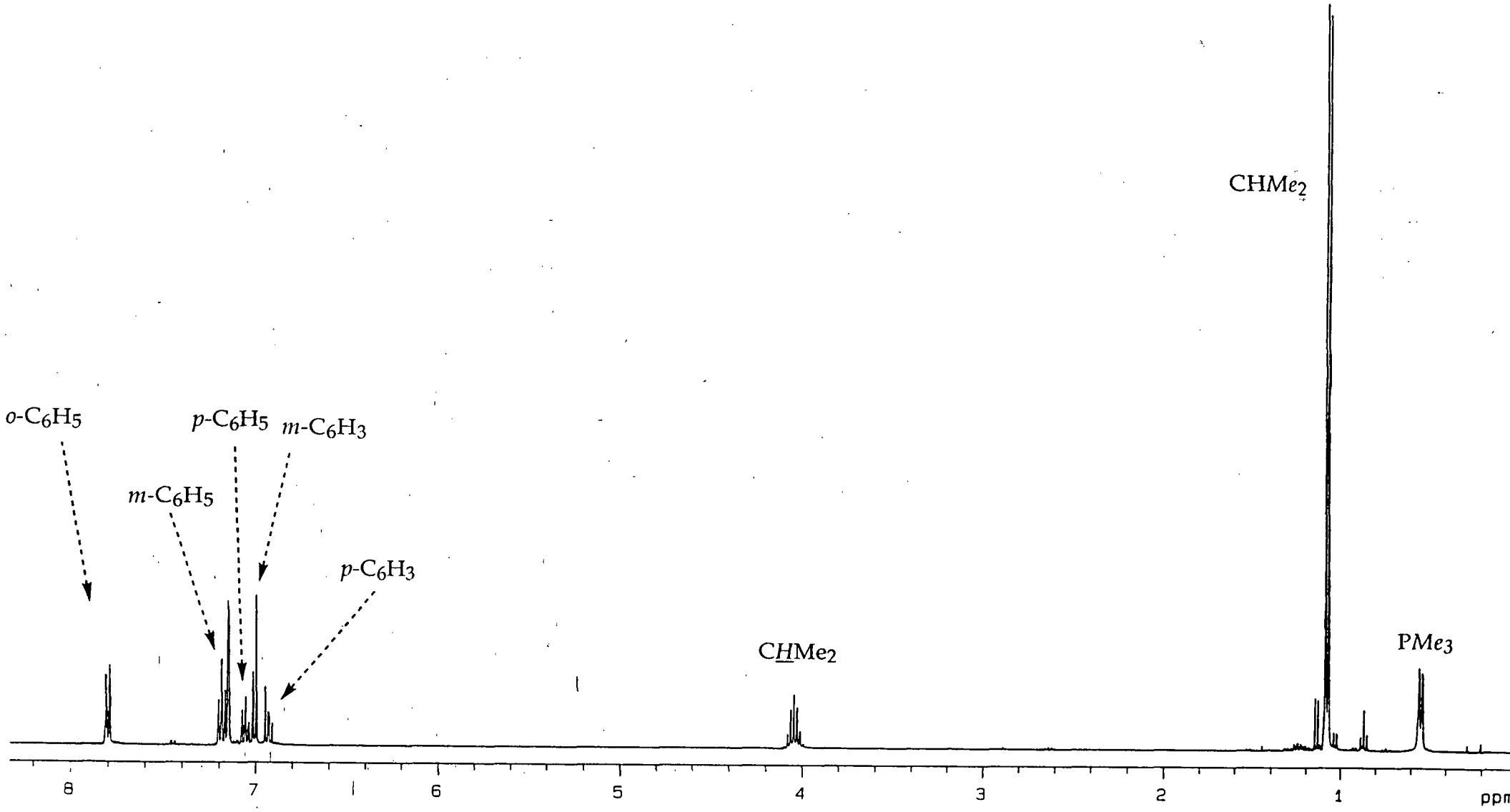

Figure 4.13 *400 MHz ^1H NMR spectrum of $Mo(NAr)_2(PMe_3)(Ph)_2$ (C_6D_6).*

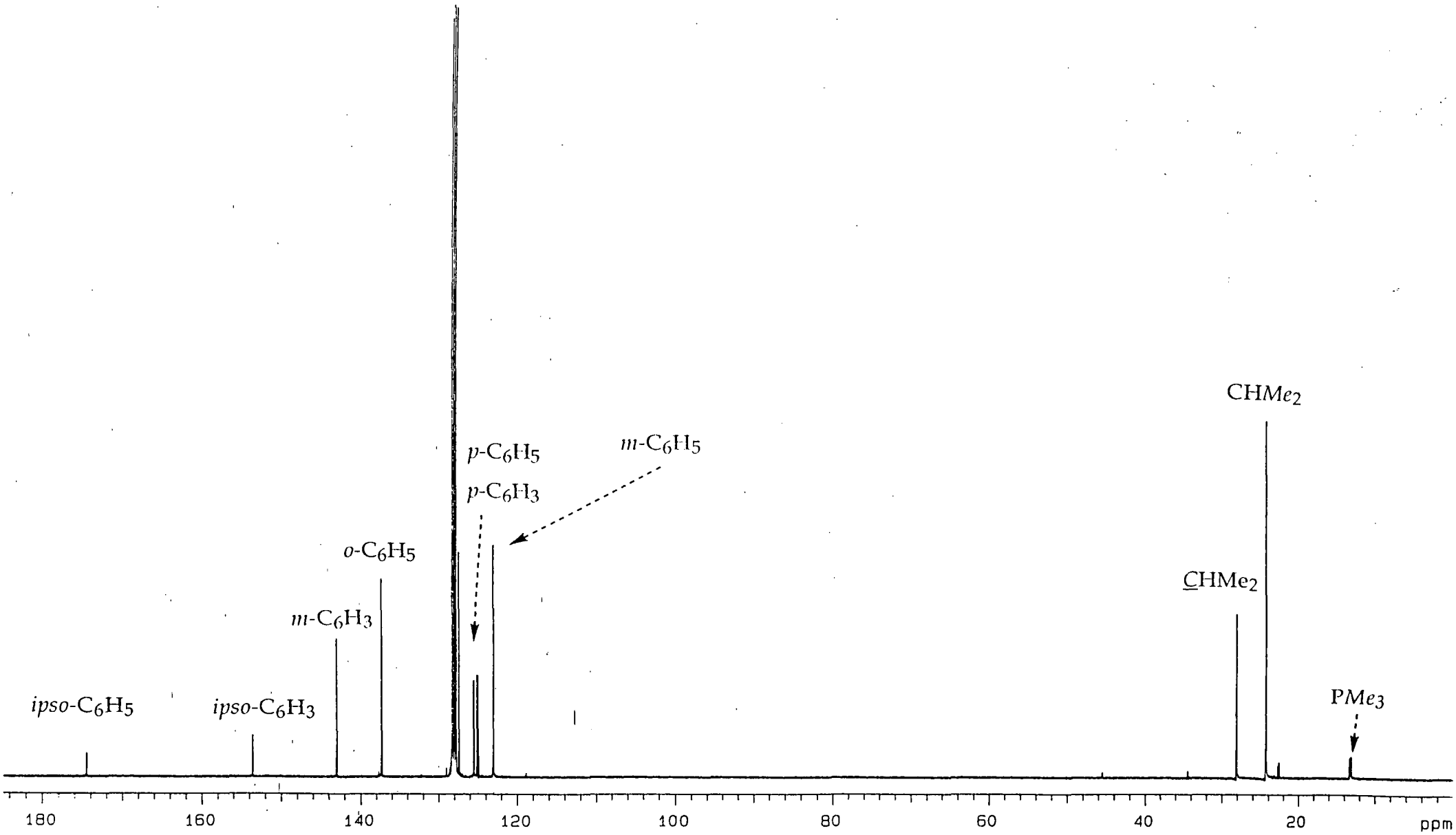

Figure 4.14 *100 MHz ^{13}C NMR spectrum of $Mo(NAr)_2(PMe_3)(Ph)_2$ (C_6D_6).*

Figure 4.15 with selected bond distances and angles collected in Tables 4.6 and 4.7.[45]

The structure determination revealed that there were two independent molecules in the unit cell. Both molecules exhibited a distorted trigonal bipyramidal geometry in which the phenyl ligands occupied equatorial sites with the PMe_3 in an axial position, and somewhat unexpectedly the imido groups occupied both axial and equatorial sites; this resulted in an average N-Mo-N angle of 108.65(2)°. However, this inequivalence does not extend to the solution state since the ^1H NMR spectra down to -60°C (C_7D_8) maintained equivalent imido environments.

The average Mo-N bond lengths of 1.778(3)Å (axial) and 1.764(3)Å (equatorial) are unexceptional and consistent with pseudo triple bonds.[46] The sightly elongated axial Mo-N bond may be a consequence of the *trans influence* of the PMe_3 ligand. The average angles at the imido nitrogens, 170.75(3)° for the longer axial and 152.3(3)° for the shorter equatorial groups reinforce the notion that the angle at the imido nitrogen is not a particularly sensitive indicator of M-N bond order.[47]

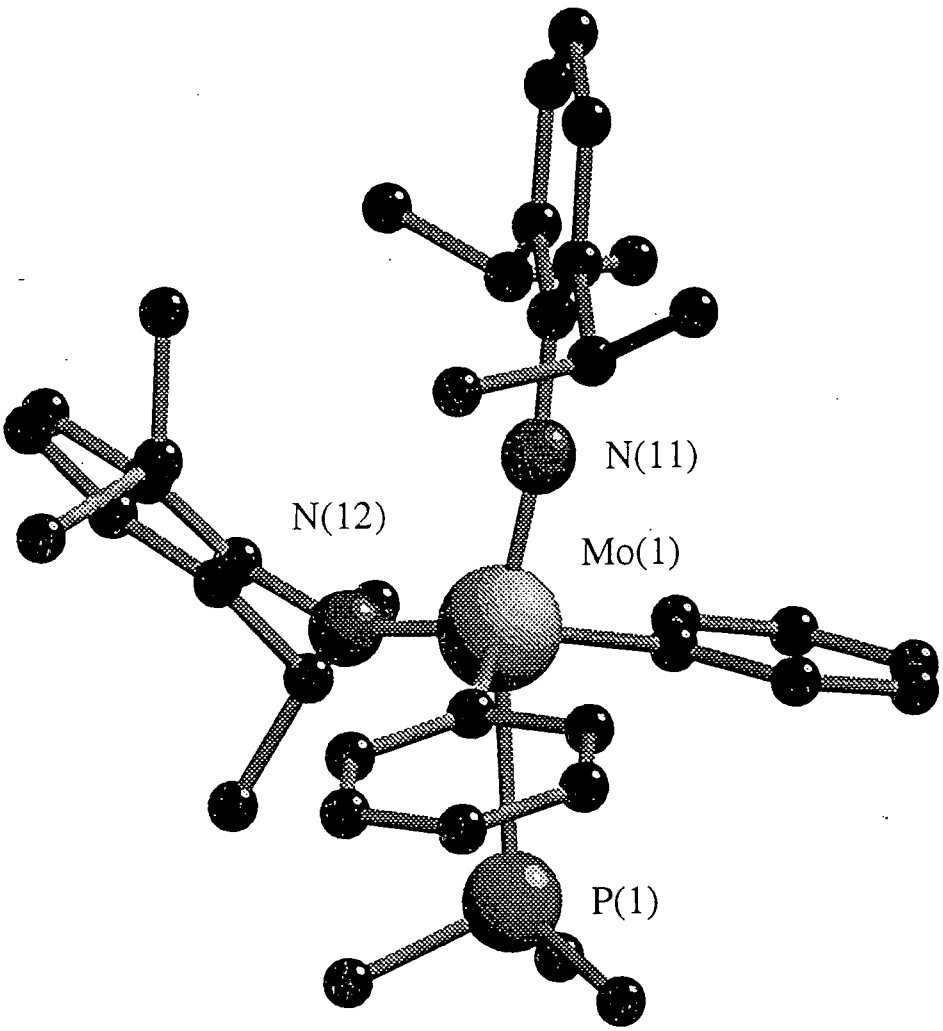

Figure 4.15 *Molecular structure of* $Mo(NAr)_2(PMe_3)(Ph)_2$.

Table 4.6 *Bond angles (Degrees) with estimated standard deviations in parentheses (one of the crystallographically independent molecules only) for $Mo(NAr)_2(Ph)_2(PMe_3)_2$ (**18**).*

N(11)-Mo(1)-P(1)	162.8(1)	C(10)-C(9)-C(8)	120.9(5)
N(12)-Mo(1)-P(1)	88.7(1)	C(11)-C(12)-C(7)	118.7(4)
N(12)-Mo(1)-N(11)	108.5(1)	C(108)-C(8)-C(7)	122.5(4)
C(61)-Mo(1)-P(1)	75.7(1)	C(108)-C(8)-C(9)	119.3(4)
C(61)-Mo(1)-N(11)	98.3(1)	C(112)-C(12)-C(7)	121.3(4)
C(61)-Mo(1)-N(12)	111.6(2)	C(112)-C(12)-C(11)	119.9(4)
C(67)-Mo(1)-P(1)	77.9(1)	C(202)-C(102)-C(2)	111.2(4)
C(67)-Mo(1)-N(11)	94.1(1)	C(203)-C(102)-C(2)	113.7(4)
C(67)-Mo(1)-N(12)	111.6(2)	C(203)-C(102)-C(202)	111.6(5)
C(67)-Mo(1)-C(61)	128.1(2)	C(206)-C(106)-C(6)	113.1(5)
C(1001)-P(1)-Mo(1)	116.0(2)	C(207)-C(106)-C(6)	110.3(5)
C(1002)-P(1)-Mo(1)	111.7(2)	C(207)-C(106)-C(206)	111.4(5)
C(1003)-P(1)-Mo(1)	119.7(2)	C(208)-C(108)-C(8)	113.3(5)
C(1002)-P(1)-C(1001)	100.9(3)	C(209)-C(108)-C(8)	109.6(5)
C(1003)-P(1)-C(1001)	102.2(3)	C(209)-C(108)-C(208)	111.2(5)
C(1003)-P(1)-C(1002)	104.1(3)	C(212)-C(112)-C(12)	112.3(5)
C(1)-N(11)-Mo(1)	169.4(3)	C(213)-C(112)-C(12)	111.7(5)
C(7)-N(12)-Mo(1)	153.1(3)	C(213)-C(112)-C(212)	110.2(5)
C(2)-C(1)-N(11)	118.8(4)	C(62)-C(61)-Mo(1)	115.9(3)
C(6)-C(1)-N(11)	119.8(4)	C(66)-C(61)-Mo(1)	126.4(3)
C(8)-C(7)-N(12)	120.3(4)	C(68)-C(67)-Mo(1)	117.9(3)
C(12)-C(7)-N(12)	119.5(4)	C(72)-C(67)-Mo(1)	125.2(3)
C(6)-C(1)-C(2)	121.4(4)	C(66)-C(61)-C(62)	117.7(4)
C(3)-C(2)-C(1)	117.1(4)	C(63)-C(62)-C(61)	120.8(4)
C(4)-C(3)-C(2)	121.7(4)	C(64)-C(63)-C(62)	120.2(5)
C(5)-C(4)-C(3)	120.6(4)	C(65)-C(64)-C(63)	119.7(4)
C(6)-C(5)-C(4)	121.2(4)	C(66)-C(65)-C(64)	120.4(5)
C(5)-C(6)-C(1)	118.0(4)	C(65)-C(66)-C(61)	121.2(4)
C(102)-C(2)-C(1)	121.1(4)	C(72)-C(67)-C(68)	116.8(4)
C(102)-C(2)-C(3)	121.9(4)	C(69)-C(68)-C(67)	122.4(5)
C(106)-C(6)-C(1)	122.4(4)	C(70)-C(69)-C(68)	120.6(5)
C(106)-C(6)-C(5)	119.6(4)	C(71)-C(70)-C(69)	119.4(5)
C(12)-C(7)-C(8)	120.2(4)	C(72)-C(71)-C(70)	120.6(5)
C(9)-C(8)-C(7)	118.2(4)	C(71)-C(72)-C(67)	120.1(5)

Table 4.7 *Bond lengths (Angstroms) with estimated standard deviations in parentheses (one of the crystallographically independent molecules only) for* $Mo(NAr)_2(Ph)_2(PMe_3)_2$.

Mo(1) - P(1)	2.682(1)	C(12) - C(112)	1.532(6)
P(1) - C(1001)	1.819(5)	C(102)- C(202)	1.516(8)
P(1) - C(1002)	1.808(7)	C(102)- C(203)	1.528(7)
P(1) - C(1003)	1.794(7)	C(106)- C(206)	1.521(8)
Mo(1) - N(11)	1.781(3)	C(106)- C(207)	1.537(8)
Mo(1) - N(12)	1.764(3)	C(108)- C(208)	1.520(8)
N(11) - C(1)	1.385(5)	C(108)- C(209)	1.514(9)
N(12) - C(7)	1.405(5)	C(112)- C(212)	1.542(8)
C(1) - C(2)	1.416(6)	C(112)- C(213)	1.510(8)
C(1) - C(6)	1.412(6)	Mo(1) - C(61)	2.174(4)
C(2) - C(3)	1.400(6)	Mo(1) - C(67)	2.176(4)
C(3) - C(4)	1.366(7)	C(61) - C(62)	1.407(6)
C(4) - C(5)	1.374(7)	C(61) - C(66)	1.376(6)
C(5) - C(6)	1.390(6)	C(62) - C(63)	1.387(6)
C(7) - C(8)	1.417(6)	C(63) - C(64)	1.375(7)
C(7) - C(12)	1.402(6)	C(64) - C(65)	1.372(7)
C(8) - C(9)	1.390(6)	C(65) - C(66)	1.391(7)
C(9) - C(10)	1.370(8)	C(67) - C(68)	1.388(6)
C(10) - C(11)	1.363(7)	C(67) - C(72)	1.393(6)
C(11) - C(12)	1.382(6)	C(68) - C(69)	1.380(7)
C(2) - C(102)	1.504(6)	C(69) - C(70)	1.355(8)
C(6) - C(106)	1.516(6)	C(70) - C(71)	1.372(8)
C(8) - C(108)	1.515(7)	C(71) - C(72)	1.416(7)

4.3.3 Thermolysis of $Mo(NAr)_2(Ph)_2(PMe_3)$ (18): Attempted Synthesis of $Mo(NAr)_2(PMe_3)(\eta^2$-Benzyne)

In an attempt to prepare a molybdenum benzyne complex, a C_6D_6 solution of the diphenyl species (**18**) was heated under an atmosphere of nitrogen at 60°C. After one week the ^1H NMR spectrum shown in Figure 4.16 was obtained. This remained unchanged despite prolonged heating. It appears that there are two clearly defined sets of resonances attributable to "Mo(NAr)" species, signified by the two isopropyl septets. The resonance at δ 3.97 ppm has been shown to be fluxional, two new septets being obtained at low temperature. Similarly, the broad singlet at δ 8.13 ppm splits into two doublets on cooling.

The ^1H NMR spectrum clearly indicates that, not only has benzene been liberated but also biphenyl.[48] The latter formed presumably through reductive elimination from the diphenyl precursor. The formation of biphenylene through benzyne coupling was ruled out by comparison with the NMR spectra of a known sample.[49] 2D NMR was used to correlate the resonances observed in the spectrum, although no correlation was observed for the signal at δ 8.13 ppm (Figure 4.17).

The 162 MHz $^{31}P\{H\}$ NMR spectrum (C_6D_6) (Figure 4.18) showed three resonances at δ 5.68 (t, J_{PP} 16.7 Hz), -5.76 (d, J_{PP} 16.7 Hz) and -21.79 (s, $\upsilon_{1/2}$ 41.8 Hz) ppm in a ratio of 1 : 2 : 12. As shown in Scheme 4.12, cyclometallation of the phospine could be possible. However, the phosphine chemical shifts are not characteristic of this type of species (typically -110ppm) supporting the notion of there being more than one reaction pathway. The small doublet at δ 0.54 ppm (J 6.8 Hz, 2H) in the ^1H NMR spectrum is thought to be associated with the smaller of the phosphine resonances.

Synthesis of the partially deuterated complex $Mo(NAr)_2(PMe_3)(d^5\text{-}Ph)_2$ (**19**) was undertaken. Subsequent thermolysis of (**19**) afforded a similar ^1H NMR spectrum to its *per-protio* analogue, although the resonances attributed to biphenyl and the broad resonance at δ 8.13 ppm were absent. This spectrum confirmed the origins of some of the aromatic species observed, and allowed the aromatic signals from the inequivalent imido ligands to be assigned.

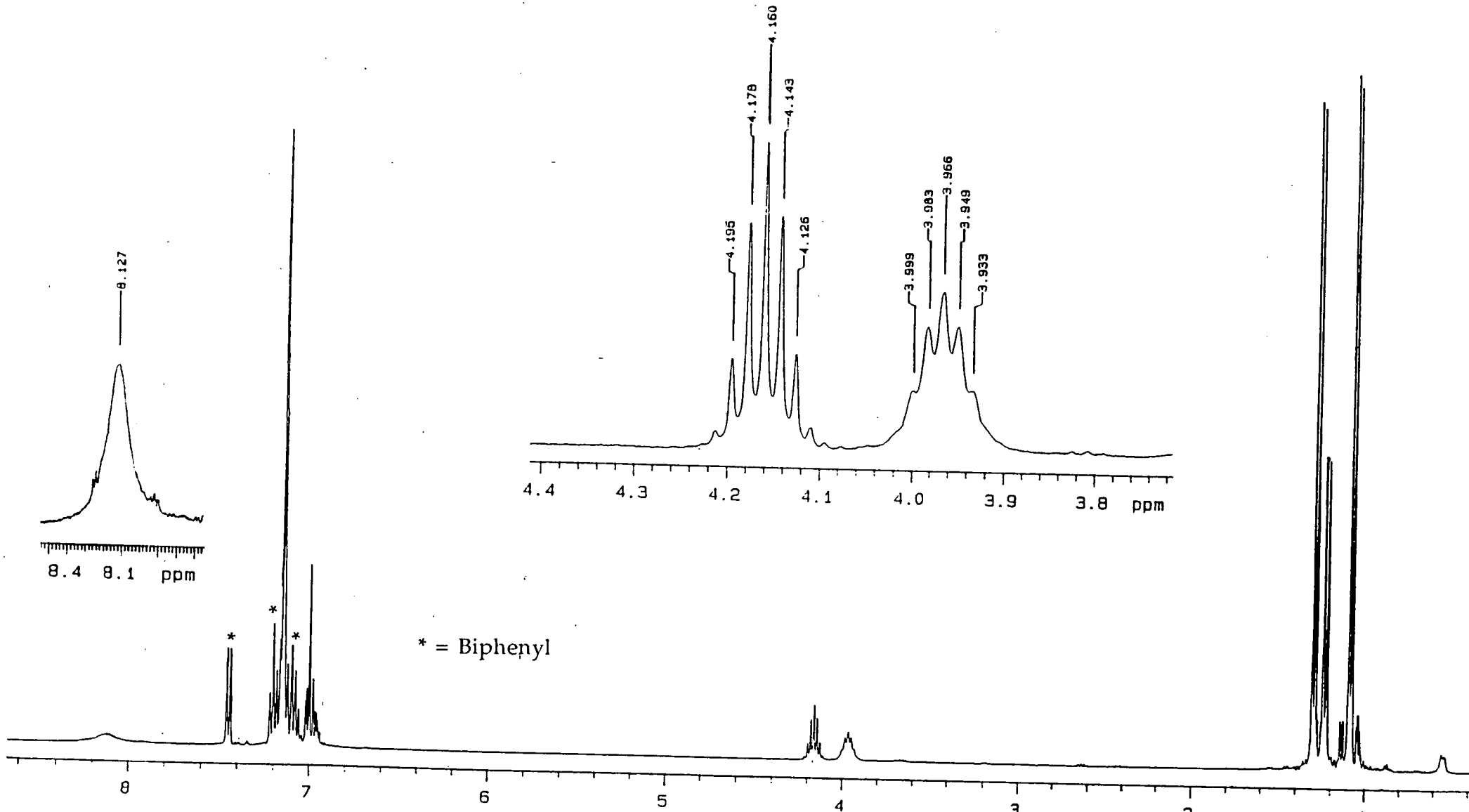

Figure 4.16 *400 MHz ^1H NMR of the thermolysis products of $Mo(NAr)_2(PMe_3)(Ph)_2$ (C_6D_6).*

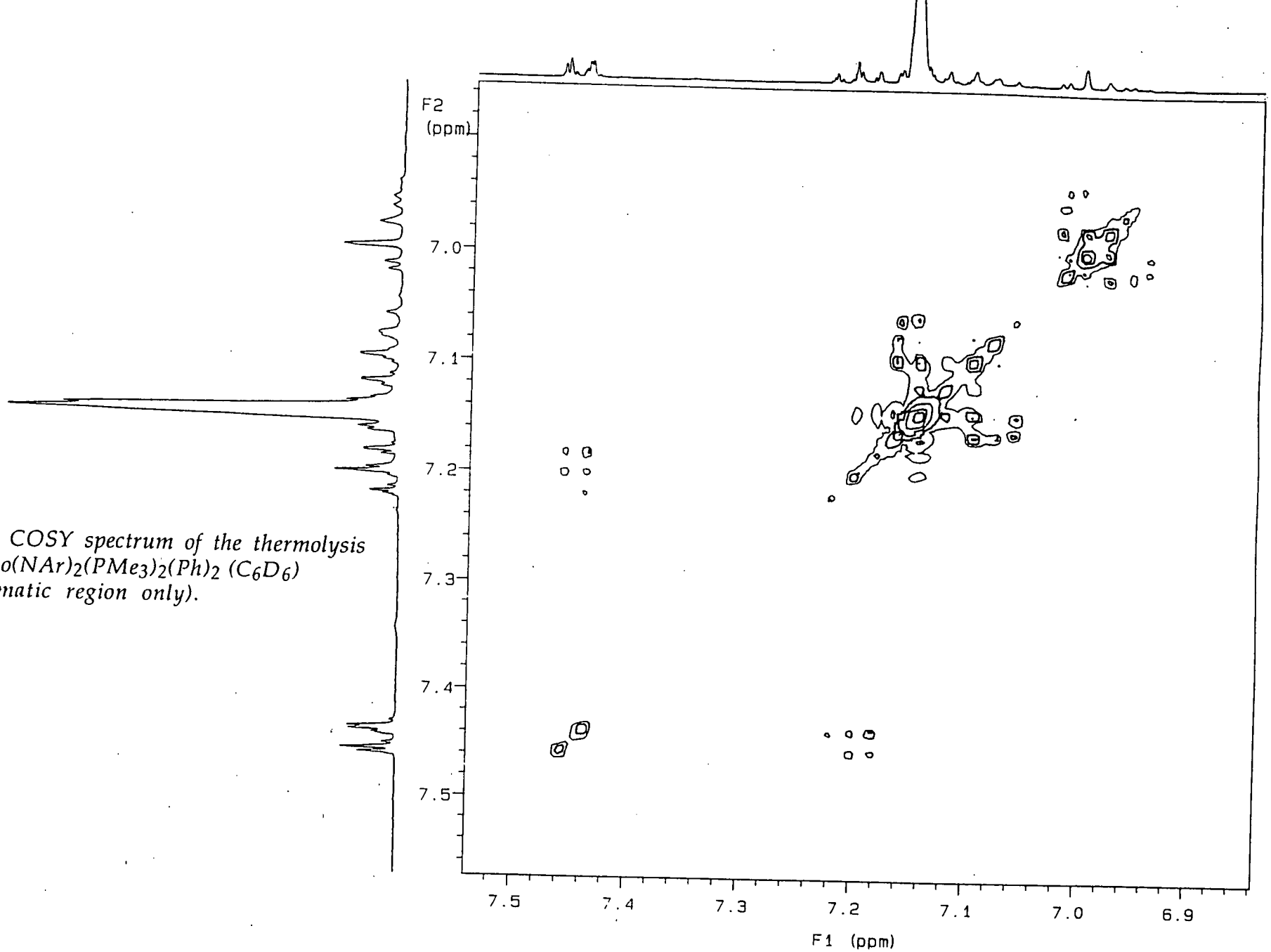

Figure 4.17 *^1H-^1H COSY spectrum of the thermolysis products of $Mo(NAr)_2(PMe_3)_2(Ph)_2$ (C_6D_6) (aromatic region only).*

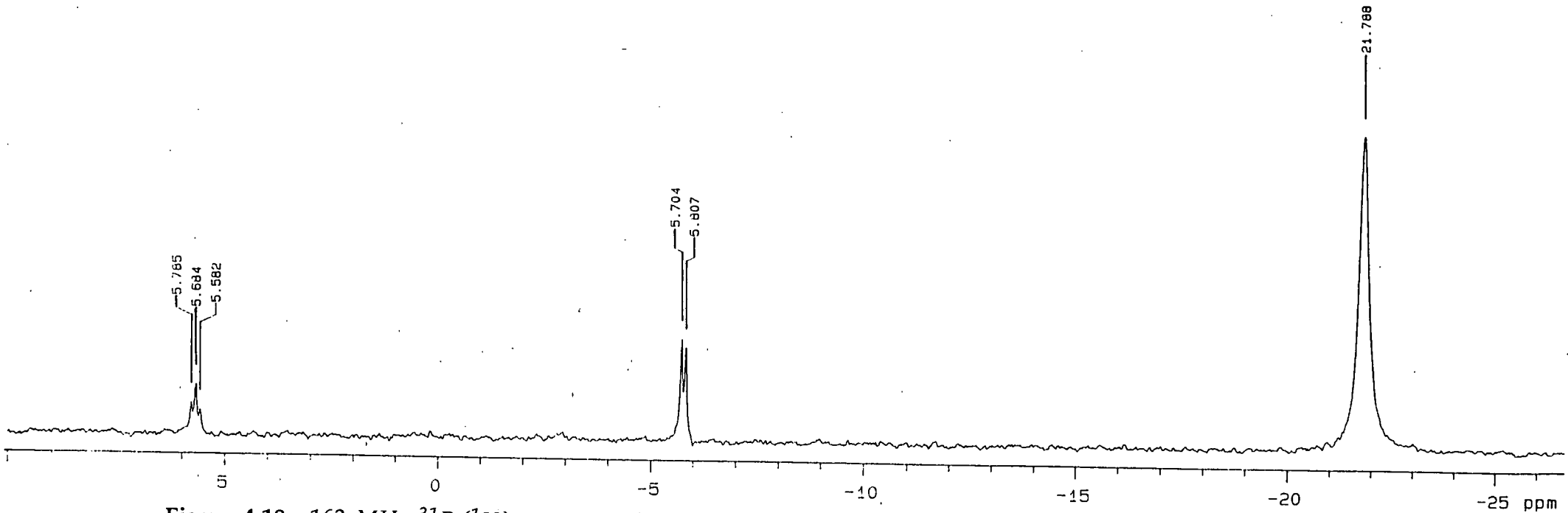

Figure 4.18 *162 MHz $^{31}P\{^{1}H\}$ spectrum of the thermolysis products of $Mo(NAr)_2(PMe_3)(Ph)_2$ (C_6D_6).*

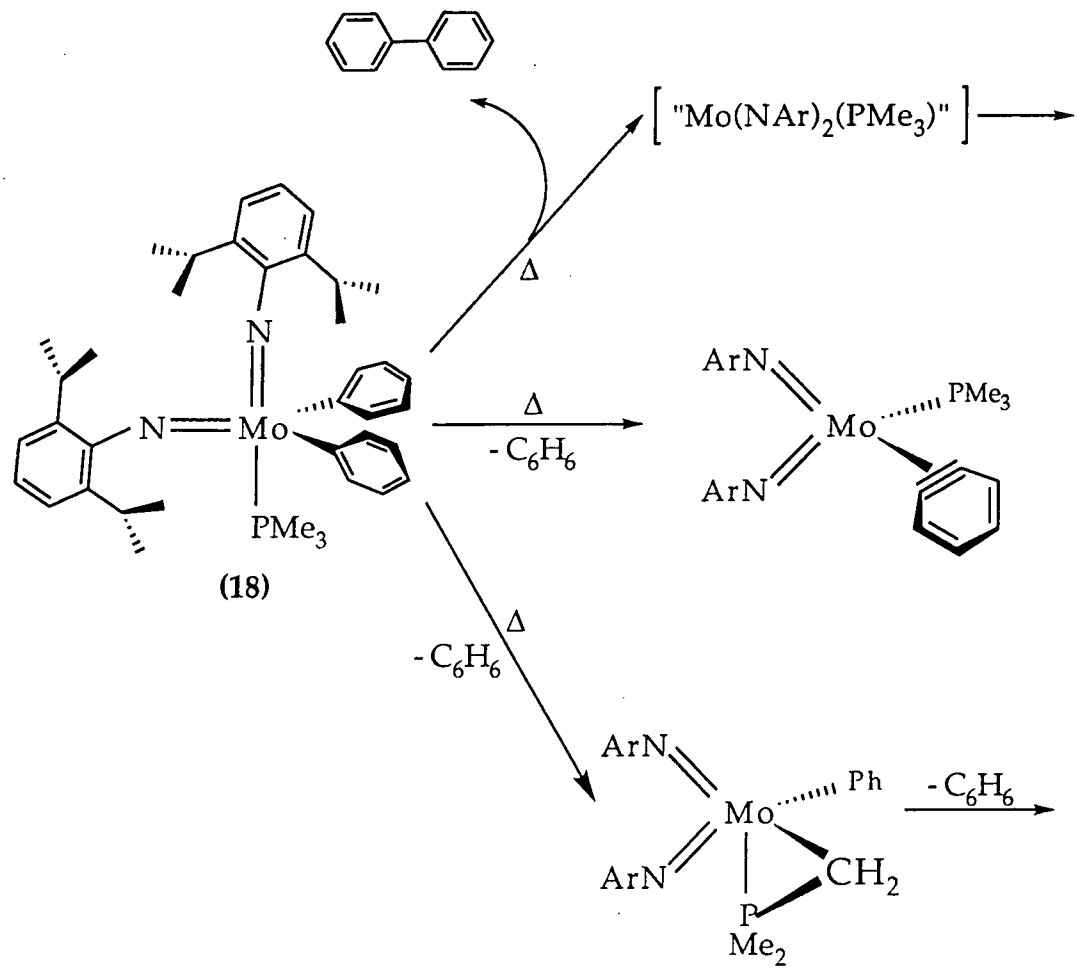

Scheme 4.12 *Possible products from the thermolysis of $Mo(NAr)_2(Ph)_2(PMe_3)$.*

Preparative scale reactions using the diphenyl complex (**18**) were attempted in a sealed vessel under an atmosphere of nitrogen. Decomposition proved facile if toluene was used as a solvent.[50] Yet, if the thermolysis was performed in benzene or heptane $Mo(NAr)_2(PMe_3)_2$ (**5**) could be isolated in low yield. GC-MS of volatiles produced indicated only the presence of PMe_3 and solvent.

To explore the thermolysis reaction further, a variety of other bis (imido) diphenyl complexes were synthesised. The complexes $Mo(NR)_2(Ph)_2(PMe_3)$ (R= ^{t}Bu (**20**) and Adamantyl (**21**)) and $Mo(NAr)_2(Ph)_2(PMe_2Ph)$ (**22**) were all synthesised from their parent dichlorides. Despite repeated attempts, no tractable product resulted from the reaction of $Mo(NPh)_2Cl_2$.DME with phenylmagnesium chloride. Attempts to synthesise the related complex $Mo(NAr)_2(PMe_3)_2(2\text{-}C_6H_4Me)_2$ resulted in the formation of an impure brown intractable product.

Thermolysis of the diphenyl species (**20**), (**21**), and (**22**) led only to the generation of biphenyl and a number of other products. The formation of more than one product reinforces the idea that multiple reactions can take place, as indicated in Scheme 4.12.

In attempts to "trap" the reactive benzyne fragment both selenium and ethene were added to the thermolysis products of (**18**). The reaction with selenium led to decomposition while the reaction with ethene caused the previously brown solution to rapidly turn dark red/purple. 200 MHz ^{1}H NMR of the latter reaction indicated the formation of new species which, despite comparison with the spectroscopic data obtained for Erker's[51] zirconocene metallaindane remain unidentified. However, resonances that resemble those from $Mo(NAr)_2(PMe_3)_2(\eta^2\text{-}C_2H_4)$ (**6**) were present. This, combined with the observation of small quantities of $Mo(NAr)_2(PMe_3)_2$ being isolated from various large-scale thermolysis reactions suggests that instead of generating the stable monophosphine benzyne complex, $Mo(NAr)_2(PMe_3)_2(\eta^2\text{-}C_6H_4)$ may be formed. By comparison with $Mo(NAr)_2(PMe_3)_2(\eta^2\text{-}C_3H_6)$, the bis (phosphine) benzyne is unlikely to be stable to isolation.

Thus, in summary, the generation of molybdenum bis (imido) benzyne complexes has proved problematical. Further studies are thus required to fully explain the thermolysis reaction of (**18**).

4.4 Attempted Preparation of Molybdenum bis (imido) Alkylidene Complexes

To extend the chemistry of molybdenum alkylidenes an attempt was made to generate bis (imido) complexes containing this functionality. These would be analogous to the unusual half-sandwich imido alkylidene complex (Figure 4.19a) synthesised recently by A.D. Poole in this group.[52] This latter species is isolobal with Schwartz's zirconocene alkylidene complex (Figure 4.19b).[53]

Section 3.2.8 described an attempt to synthesise a bis (imido) alkylidene *via* reaction of $Mo(NAr)_2(PMe_3)_2$ with $Ph_3P{=}C(H)(Ph)$, which proved unsuccessful, as did the reaction of $Mo(N^tBu)_2(PMe_3)(\eta^2\text{-}C_3H_6)$ with one equivalent of the same phosphorane (Section 4.2.1). Thus, a different approach was adopted.

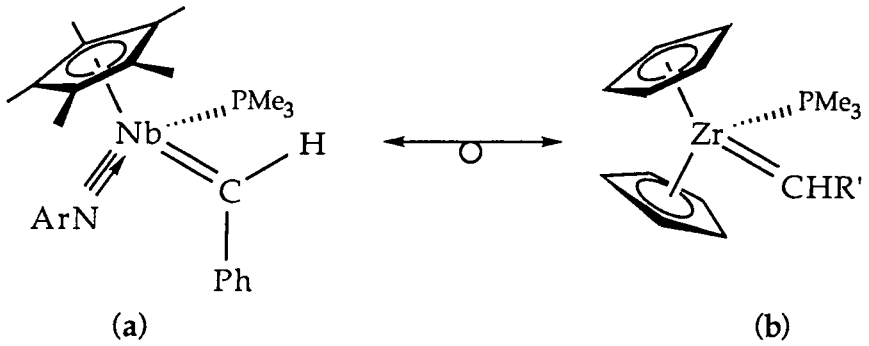

(a) (b)

Figure 4.19 *Isolobal Group 5 half-sandwich imido and Group 4 Zirconocene alkylidene complexes (R'= CH_2CMe_3).*

4.4.1 Reaction of $Mo(NAr)_2Cl_2$.DME (1) with $K(CH_2Ph)$ in the Presence of Excess PMe_3

The benzyl group was chosen over other alkyls such as neopentyl or neophyl as it was believed that the comparatively small size of the benzyl group would allow ready access of the donor PMe_3 ligand to the metal centre and thereby aid α H-abstraction.

Thus, the dichloride (1) was treated with two equivalents of potassium benzyl (KCH_2Ph) in the presence of excess trimethylphosphine using diethylether solvent. Stirring at room temperature for twelve hours gave a dark maroon solution which was accompanied by the precipitation of KCl (identified by IR). The solvent was then removed under reduced pressure and the product extracted and recrystallised from pentane (-30°C). This afforded an orange microcrystalline solid in good yield.

NMR and elemental analyses revealed that instead of forming the desired bis (benzyl) phosphine complex, preferential formation of the DME adduct $Mo(NAr)_2(CH_2Ph)_2$.DME (**23**) had occurred (Equation 4.10). It is thought that both sterics and the stability lent to the complex by the chelate effect of the coordinated DME favour the formation of this six coordinate base adduct over formation of the phosphine complex.

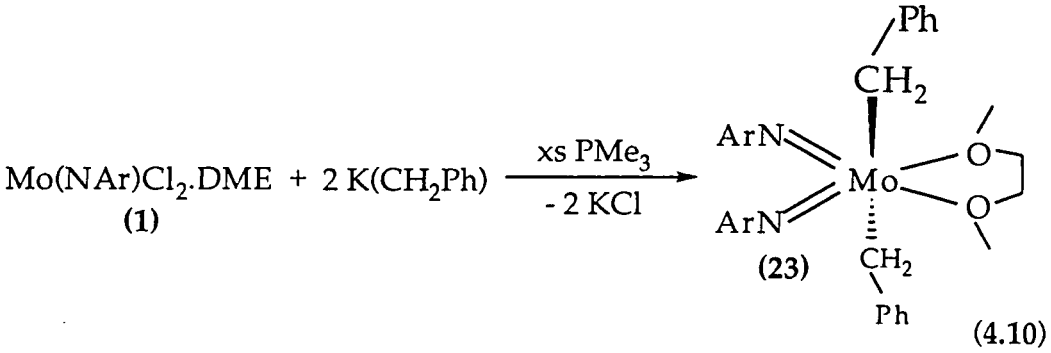

(4.10)

Thermolysis of C_6D_6 solutions of (**23**) (70°C) both in the absence and the presence of trimethylphosphine failed to yield any new products. The failure of the DME to dissociate prevents the two initially *trans* benzyl groups from adopting a mutually *cis* relationship suitable for an α-hydrogen abstraction process.

To overcome this problem attempts were made to isolate a DME free bis (benzyl) species by treating $Mo(NAr)_2Cl_2$.DME with benzylmagnesium chloride in the presence of excess phosphine (by analogy with the Grignard reaction used to synthesise the olefin complexes described in Chapter 2). It was envisaged that the nascent "magnesium" generated in the reaction might coordinate the DME and remove it from the metal coordination sphere. Yet, the reaction resulted only in the formation of an intractable brown oil.[54]

During the course of these studies Schrock reported the synthesis of $Mo(NAr)_2(CH_2Ph)_2$[55] *via* treatment of $Mo(NAr)_2Cl_2$.DME with KCH_2Ph in the presence of THF. A sample of this complex when heated in the presence of excess trimethylphosphine, remained unreacted.[56]

The failure to generate the five coordinate dialkyl phosphine complex analogous to $Mo(NAr)_2(Ph)_2(PMe_3)$ (**18**) indicates the subtle stereoelectronic effects that governs the stability of these molybdenum bis (imido) complexes.

4.4.2 Reaction of $Mo(N^tBu)_2Cl_2$ with $K(CH_2Ph)$ in the Presence of Excess PMe_3

Treatment of $Mo(N^tBu)_2Cl_2$.DME with two equivalents of potassium benzyl in the presence of excess PMe_3 afforded only a brown intractable oil.

Molybdenum bis (arylimido) dichloride can only be isolated as its DME base adduct. Yet, the analogous bis (tert-butyl) complex can be isolated as the base-free dichloride according to a reaction reported by Osborn, (Equation 4.11).[57] A slightly modified procedure was used to prepare the dichloride, which was subsequently recrystallised from hot heptane.[58]

$$MoO_2Cl_2 + 2\,{}^tBuNCO \xrightarrow[70°C]{CH_3CN} Mo(N^tBu)_2Cl_2 + 2\,CO_2 \qquad (4.11)$$

An ethereal solution of this base-free dichloride and one equivalent of potassium benzyl was treated with excess trimethylphosphine. On stirring at room temperature for 12 hours the yellow solution turned red/brown with associated precipitation of KCl. After removal of the diethylether *in vacuo* and subsequent extraction and recrystallisation from pentane at -78°C, $Mo(N^tBu)_2(CH_2Ph)(Cl)(PMe_3)$, (**24**), was obtained as a red crystalline solid in good yield.

The 200 MHz ^1H NMR (C_6D_6) data for compound (**24**) were consistent with the complex having an η^1 coordinated benzyl group.

The reaction of the mono-benzyl species with a further equivalent of potassium benzyl or treatment of the dichloride with two equivalents of potassium benzyl, both in the presence of excess phosphine, led to the formation of the same product, the base free complex $Mo(N^tBu)_2(CH_2Ph)_2$ (**25**) (Equation 4.12). This lack of phosphine coordination could be attributed to both steric and electronic effects. Yet, recently it has been shown that (**25**) does not coordinate the small rod-like acetonitrile molecule, indicating that either electronic effects or agostic interactions are the cause.

$$Mo(N^tBu)Cl_2 + 2\,K(CH_2Ph) \xrightarrow[-2\,KCl]{xs\ PMe_3} Mo(N^tBu)_2(CH_2Ph)_2 \quad (25) \qquad (4.12)$$

However, no α-agostic interactions[59] were apparent from either the 400 MHz ^1H and 100 MHz ^{13}C NMR (Figures 4.21 and 4.22) despite (**25**) being a formally 14 electron species.[60] There was also no evidence to suggest that the benzyl groups had coordinated in an η^2 or η^3 manner. The

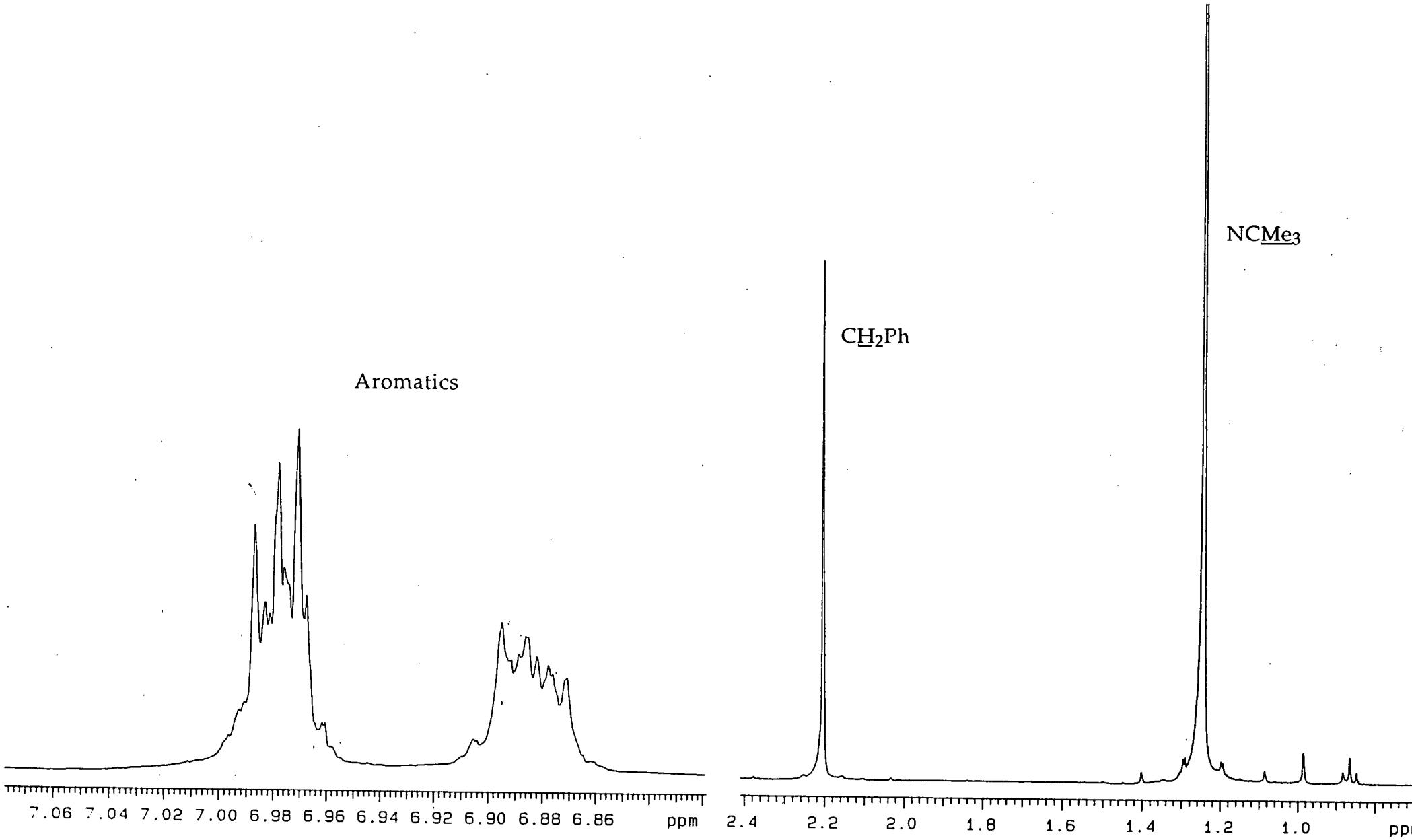

Figure 4.21 *400 MHz ^1H NMR spectrum of $Mo(N^tBu)_2(CH_2Ph)_2$.*

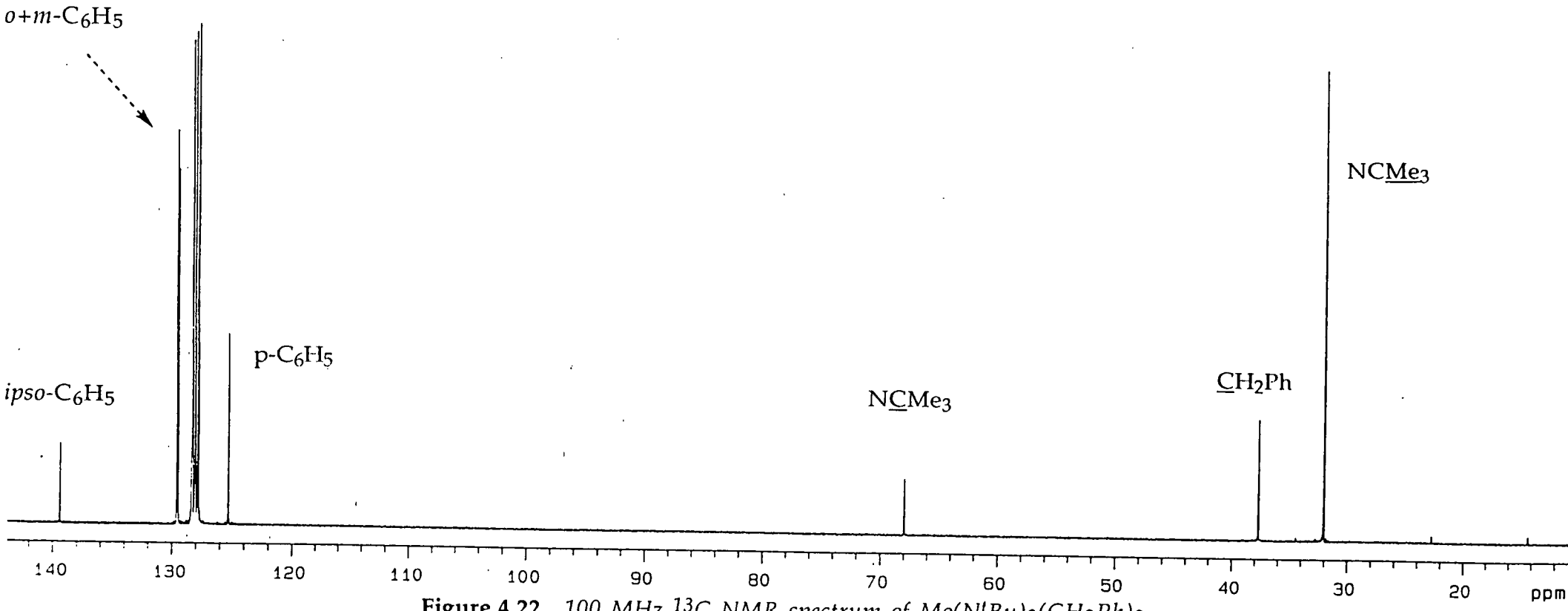

Figure 4.22 *100 MHz ^{13}C NMR spectrum of $Mo(N^tBu)_2(CH_2Ph)_2$.*

latter is usually indicated by the geminal coupling constant of the CH_2 unit, approaching that of an sp^2 rather than an sp^3 hybridised carbon, a highfield ^1H shift for the *ortho*-protons ($\approx\delta$ 6.5 ppm) and the *ipso*-carbon having an associated chemical shift of between 110 and 113 ppm.[61] Figure 4.20 illustrates the η^1, η^2, and η^3 benzyl coordination modes.

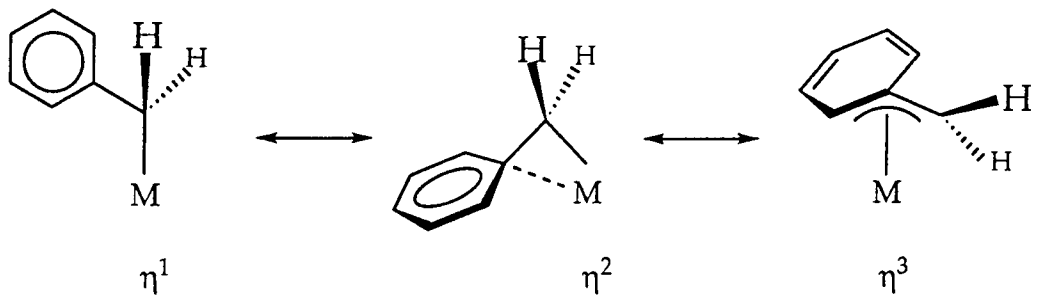

Figure 4.20 *Different bonding modes of the benzyl group.*

Despite prolonged heating of a C_6D_6 solution of $Mo(N^tBu)_2(CH_2Ph)_2$ (**25**) in the presence of excess PMe_3, no reaction occurred. This lack of reactivity may be caused by reversible formation of an η^3 benzyl (Scheme 4.10) blocking the vacant coordination site.

To establish if this was the case, a similar reaction was performed with $Mo(N^tBu)_2(CH_2C(Me)_2Ph)_2$ which can not rearrange and coordinate the alkyl group in anything but an η^1 manner. Yet, even after similar treatment no coordination of phosphine was observed, the bis (neophyl) complex remaining unaltered. Thus, formation of an η^2 or η^3 benzyl group does not cause the lack of reaction toward phosphine, it is more likely that steric effects play a much greater part. However, this result can not eliminate the possibility of α-agostic interactions.

In order to determine whether an agostic interaction is involved in the bonding of (**25**) both partial deuteration and molecular structure studies must be undertaken.

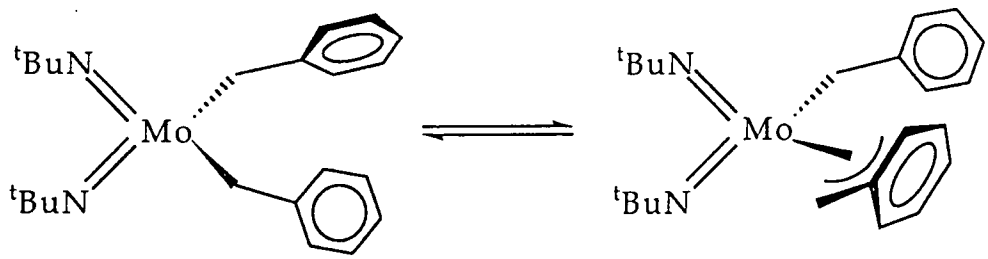

Scheme 4.10 *Reversible isomerisation of $Mo(N^tBu)_2(CH_2Ph)_2$.*

It is believed that a set of conditions need to be satisfied for successful α-abstraction to occur.[62] The α-hydrogen has to be "activated" towards abstraction, a process that is normally associated with the metal. A crowded coordination sphere may also be important. This latter point is likely to be the cause of the contrasting reactivity of $Cp^*Nb(NAr)(CH_2Ph)_2$. Thermolysis of this half-sandwich complex in the presence of PMe_3 slowly affords the desired benzylidene complex. The related cyclopentadienyl complex can not be isolated; decomposition of the latter is thought to proceed *via* an unstable benzylidene intermediate.[63] Thus, there is a fine balance between benzylidene formation and decomposition.

Interestingly, samples of both $Mo(NAr)_2(CH_2Ph)_2$ and its tert-butyl counterpart appear to be light sensitive. C_6D_6 solutions of each darken appreciably on standing in daylight, a process that is accelerated at higher temperatures. Yet, ^1H NMR indicates that the two species remain unchanged. This suggests that a likely strategy for the synthesis of the sought after bis (imido) alkylidene species may be through photolysis of these bis (benzyl) precursors, especially in the light of a report by Schrock which indicates that α-hydrogen abstraction reactions are enhanced by light.[64]

4.5 Attempted Synthesis of Molybdenum Tris (Imido) Complexes

Bergman[65] has recently reported the synthesis of the mononuclear complex $Cp_2Zr{=}N^tBu$ as its THF adduct (Scheme 4.15). It was isolated from the reaction of Cp_2ZrMe_2 with four equivalents of tert-butyl amine which generates initially the methyl amide. Subsequent loss of a further equivalent of methane yields the imido species. The complex is reported as having a near linear (174.4(3)°) and therefore four electron imido, making it formally a 20 electron complex. As a consequence the Zr-N distance is elongated, 1.826(4)Å.

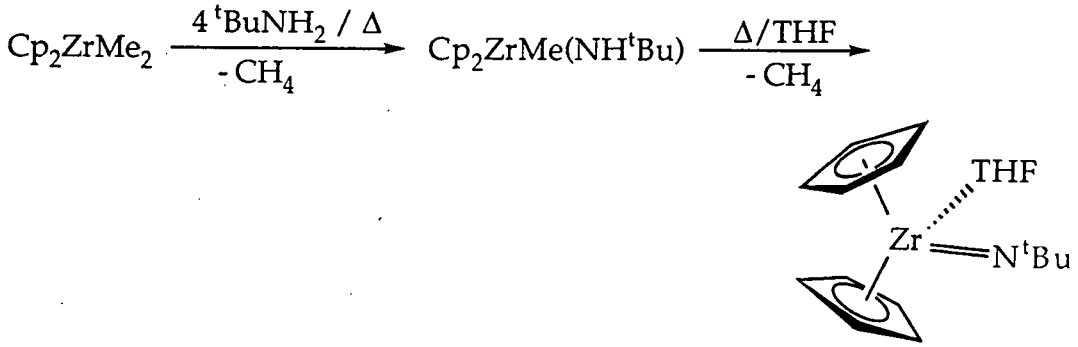

Scheme 4.15 *Synthesis of $Cp_2(THF)Zr{=}N^tBu$.*

Entry into this zirconocene imido system can also be achieved through the bis (amide) complex $Cp_2Zr(NH^tBu)_2$ which on thermolysis transiently generate the desired imido species.

The advent of a practical synthesis of the niobium and tantalum bis (imido) complexes $M(=NAr)_2Cl(py)_2$[66] readily allows the preparation of the Group 5 half-sandwich bis (imido) analogues of Bergman's zirconocene imido.

4.5.1 Preparation of $Mo(N^tBu)_2(NEt_2)(Cl)$

Bergman and Wigley's strategy involving generation of a bis (amide) species which is deprotonated to afford an imido complex, was attempted for the molybdenum bis (imido) system. The tert-butyl system was chosen due to the ready availability of the base free dichloride $Mo(N^tBu)_2Cl_2$. $Mo(N^tBu)_2(NEt_2)(Cl)$ (**26**) was then synthesised by treating an ethereal solution of $Mo(N^tBu)_2Cl_2$ with one equivalent of $LiNEt_2$ (Equation 4.13). After removal of volatiles under reduced pressure, an analytically pure yellow/brown oil was obtained. Despite repeated attempts, (**26**) could not be isolated as a solid.

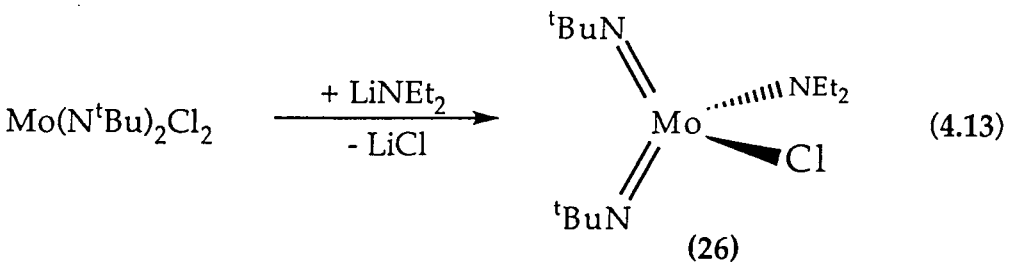

(4.13)

(26)

Two inequivalent imido ligands were observed in the 400 MHz ^1H NMR spectrum. One of the two amide methylene groups δ 2.64 ppm was severely broadened even at low temperatures (Figure 4.26). This is believed to be due to the proximity of a quadrupolar chlorine nucleus. The 100 MHz ^{13}C NMR spectrum was unremarkable.

4.5.2 Reaction of $Mo(N^tBu)_2Cl(NEt_2)$ (26) with LiNHAr

In an attempt to generate the bis (imido) complex a solution of (26) in ether was treated with one equivalent of LiNHAr in the presence of excess PMe_3 (Equation 4.11). The base was included in an attempt to force the two amides together and to stabilise the resulting imido complex.

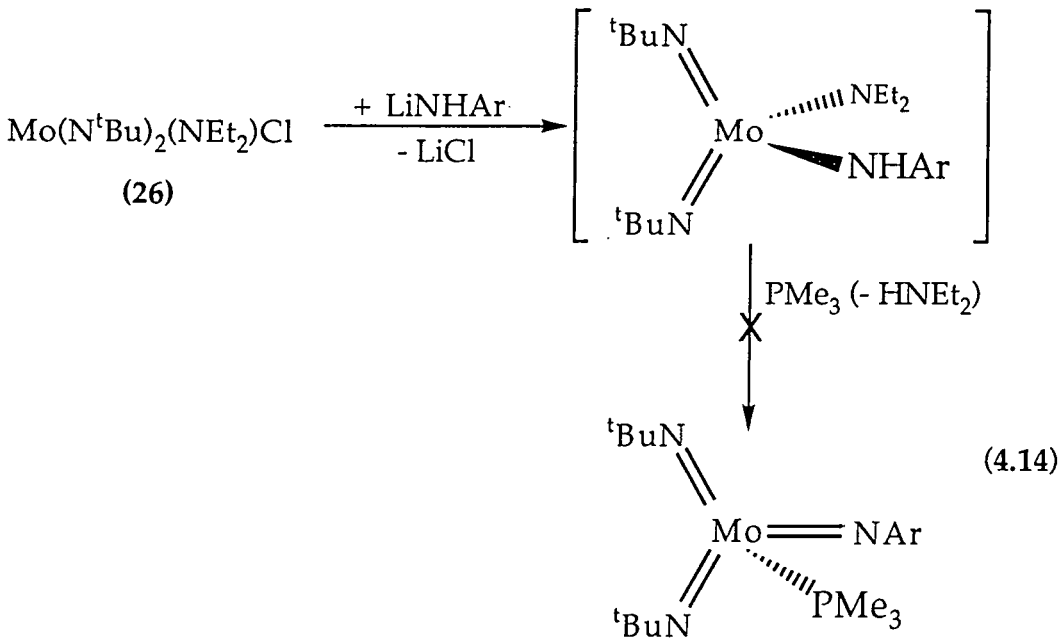

(4.14)

The light yellow solution was stirred at room temperature for 12 hours, the solution darkening to red with precipitation of LiCl (identified by IR). Removal of volatiles *in vacuo* afforded a dark red/brown oil. All attempts at recrystallisation/purification of the product were unsuccessful. A ^1H NMR spectrum of the crude product indicated that decomposition had occurred with a significant amount of $ArNH_2$ being generated.

Attempts to isolate the bis (amide), $Mo(N^tBu)_2(NEt_2)(NHAr)$ gave only similar intractable oily products. The instability of this bis (amide) is thought to result from the presence of the acidic amide proton.

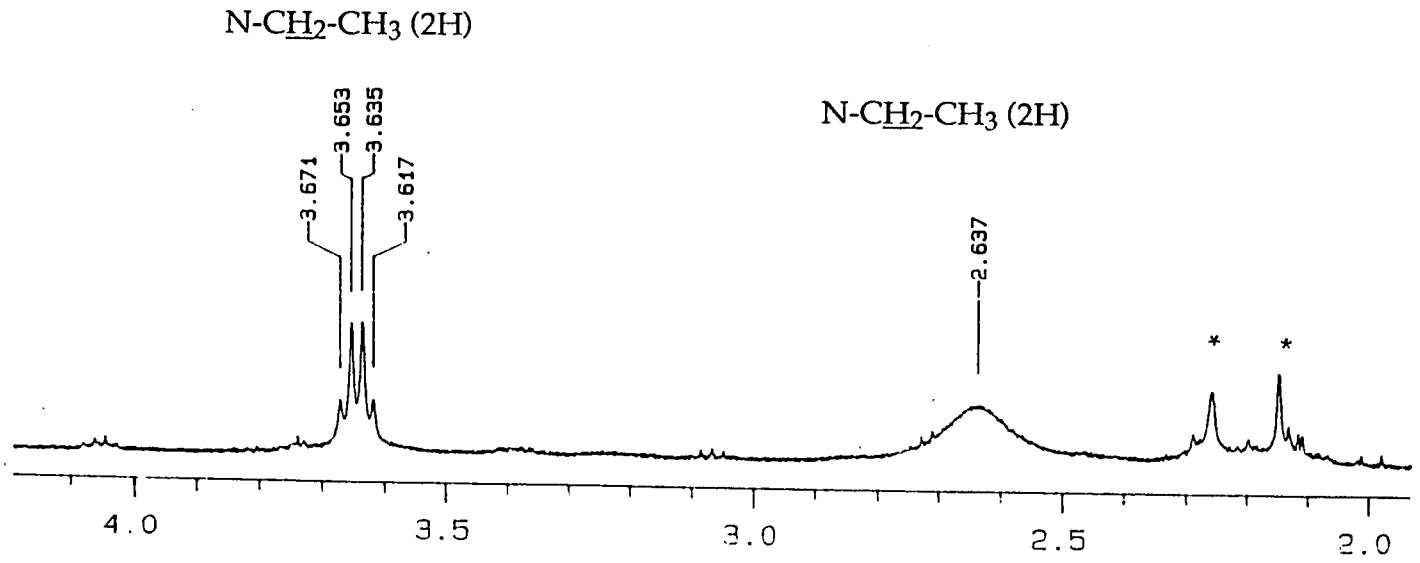

Figure 4.26 *400 MHz ^1H NMR spectrum of $Mo(N^tBu)_2(NEt_2)Cl$.*

** denotes impurity*

The broadening associated with one of the amide methylene groups is believed to arise through proximity to a quadrupolar chlorine nucleus.

4.6 Summary

This chapter has further probed the pseudo-isolobal relationship between Group 4 bent metallocenes and Group 6 bis (imido) complexes.

The synthesis of a variety of acetylene complexes was achieved *via* displacement from the appropriate olefin complex. It has been shown that complexes of the type $Mo(NR)_2(PMe_3)(\eta^2\text{-}R'C_1{\equiv}C_2R'')$ adopt a metallocene-like geometry in which the atoms Mo, P, C_1 and C_2 lie in a plane that bisects the N-Mo-N angle, Scheme 4.16.

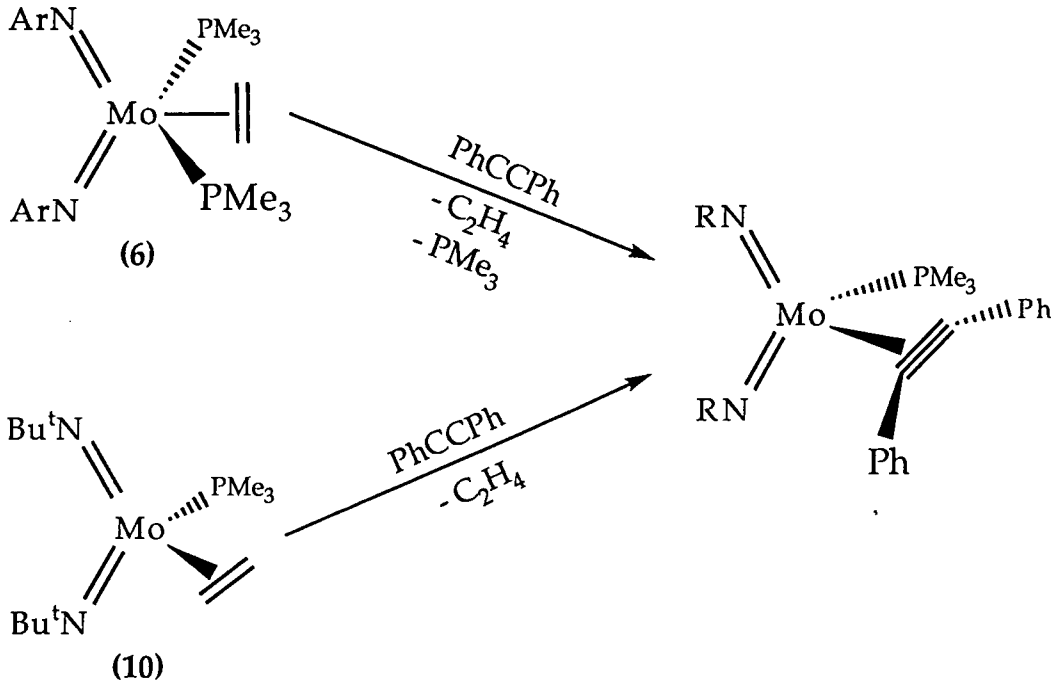

Scheme 4.16 *Synthesis of $Mo(NR)_2(PMe_3)(\eta^2\text{-}PhC{\equiv}CPh)$, [R= Ar, ^tBu].*

Solution NMR data indicated that when R is aromatic (e.g. Ar, 2-$^tBuC_6H_4$) the structure is not static on the NMR timescale, with the acetylene rotating about the metal—C≡C midpoint axis. However, when R is alkyl (e.g. Adamantyl, ^{t}Bu) the structure is rigid with the acetylene located in the plane defined above.

A number of diphenyl compounds, including the structurally characterised complex $Mo(NAr)_2(PMe_3)(Ph)_2$, have been synthesised as potential precursors to η^2-benzyne species *via* thermally induced α-elimination. Attempts to generate the unusual four coordinate bis (imido) phosphine complex, $Mo(NAr)_2(PMe_3)(\eta^2\text{-}C_6H_4)$, led to a variety of products.

Bis (imido) benzyl complexes have been synthesised *via* treatment of either $Mo(NAr)_2Cl_2$.DME or $Mo(N^tBu)_2Cl_2$ with potassium benzyl but don't afford benzylidene complexes when treated with excess PMe_3.

This chapter has further highlighted the applicability of the pseudo-isolobal relationship between bent metallocenes and Group 6 bis (imido) complexes for predicting both reactivity and geometry. However, during this study it became apparent there were differences in the reactivity of these two systems. This is likely to be a consequence of replacing the sterically demanding cyclopentadienyl group with the less bulky imido ligand. The cyclopentadienyl moiety interacts with a metal through five atoms, whereas an imido interacts through only one (M=NR). The reactivity of bis (imido) species is also intimately dependent upon the nature of the ligand substituent, ring substituent effects for cyclopentadienyl complexes are much less pronounced.

4.7 References

1 K. Tatsumi, R. Hoffmann, and J.L. Templeton, *Inorg. Chem.*, 1982, **21**, 466.

2 J.L. Templeton and B.C. Ward, *J. Am. Chem. Soc.*, 1980, **102**, 3288.

3 H.G. Alt, *J. Organomet. Chem.*, 1977, **127**, 349.

4 P.L. Watson and R.G. Bergman, *J. Am. Chem. Soc.*, 1979, **101**, 2055.

5 J.L. Thomas, *Inorg. Chem.*, 1978, **17**, 1507.

6 D.W. Hart and J. Schwartz, *J. Am. Chem. Soc.*, 1974, **96**, 8115.

7 D.W. Hart, T.F. Blackburn, and J. Schwartz, *J. Am. Chem. Soc.*, 1975, **97**, 679.

8 J.A. Labinger, D.W. Hart, W.E. Siebert, and J. Schwartz, *J. Am. Chem. Soc.*, 1975, **97**, 3851.

9 For a review of this chemistry see: S.L. Buchwald and R.B. Nielson, *Chem. Rev.*, 1988, **88**, 1047.

10 P.O. Whimp, *J. Organomet. Chem.*, 1971, **32**, C69; S.L. Buchwald, R.T. Lum, and J.C. Dewan, *J. Am. Chem. Soc.*, 1986, **108**, 7441.

11 K. Dehnicke, *Z. Anorg. Allg. Chem.*, 1986, **533**, 73.

12 S.J. McLain, R.R. Schrock, P.R. Sharp, M.R. Churchill, and W.J. Youngs, *J. Am. Chem. Soc.*, 1979, **101**, 263; M.R. Churchill and W.J. Youngs, *Inorg. Chem.*, 1979, **18**, 1697.

13 M.A. Bennett, T.W. Hambley, N.K. Roberts, and G.B. Robertson, *Organometallics*, 1985, **4**, 1992.

14 R.A. Bartlett, P.P. Power, and S.C. Shoner, *J. Am. Chem. Soc.*, 1988, **110**, 1966.

15 J.F. Hartwig, R.A. Anderson, and R.G. Bergman, *J. Am. Chem. Soc.*, 1989, **111**, 2719.

16 S.L. Buchwald, B.T. Wilson, and J.C. Huffman, *J. Am. Chem. Soc.*, 1986, **108**, 7411.

17 J. Arnold, G. Wilkinson, B. Hussain, and M.B. Hursthouse, *Organometallics*, 1989, **8**, 415.

18 G. Erker, *J. Organomet. Chem.*, 1977, **134**, 189.

19 G. Erker, and K. Kropp, *J. Am. Chem. Soc.*, 1979, **101**, 3659

20 The cyclobutenes are obtained in good yield by treating the metallacycle in situ with excess iodine followed by the addition of n-BuLi at -78 °C: G. Fachinetti, C. Floriani, F. Marchetti, and F. Mellini, *J. Chem. Soc. Dalton Trans.*, 1978, 1398.

21 S.L. Buchwald, E.A. Lucas, and J.C. Dewan, *J. Am. Chem. Soc.*, 1987, **109**, 4396.

22 R.R. Schrock, *J. Am. Chem. Soc.*, 1974, **96**, 6796.

23 J.L. Hérisson and Y. Chauvin, *Makromol. Chem.*, 1970, **141**, 161.

24 F.N. Tebbe, G.W. Parshall, and G.S. Reddy, *J. Am. Chem. Soc.*, 1978, **100**, 3611; T.R. Howard, J.B. Lee, and R.H. Grubbs, *J. Am. Chem. Soc.*, 1980, **102**, 6876; D.A. Straus and R.H. Grubbs, *J. Mol. Catal.*, 1985, **28**, 9.

25 T. Takahashi, D.R. Swanson, E. Negishi, *Chem. Letts.*, 1987, 623; E. Negishi, S.J. Holmes, J.M. Tour, J.A. Miller, F.E. Cederbaum, D.R. Swanson, and T. Takahashi, *J. Am. Chem. Soc.*, 1989, **111**, 3336.

26 L.B. Kool, M.D. Rausch, H.G. Alt, M. Herberhold, U. Thewalt, and B. Wolf, *Angew. Chem., Int. Ed. Engl.*, 1985, **5**, 394.

27 D.S. Williams, M.H. Schofield, and R.R. Schrock, In Press.

28 A.D. Poole, V.C. Gibson, and W. Clegg, *J. Chem. Soc. Chem. Commun.*, 1992, 237.

29 S.L. Buchwald, K.A. Kreutzer, and R.A. Fischer, *J. Am. Chem. Soc.*, 1990, **112**, 4600.

30 B. Whittle, M.Sc. Thesis, University of Durham, 1993.

31 S.D. Ibers and J.A. Ibers, *Adv. Organomet. Chem.*, 1976, **14**, 33.

32 K. Tatsumi and R. Hoffmann, *Inorg. Chem.*, 1982, **21**, 466; A. De Cian, J. Colin, M. Schappacher, L. Ricard, and R. Weiss, *J. Am. Chem. Soc.*,1981, **103**, 1850.

33 G. Fachinetti, C. Floriani, F. Marchetti, and M. Mellini, *J. Chem. Soc. Dalton Trans.*, 1978, 1398.

34 W.A. Nugent and J.M. Mayer, *"Metal Ligand Multiple Bonds"*, John Wiley and Sons, New York, 1988.

35 B. Whittle, M.Sc. Thesis, University of Durham, 1993.

36 L.M. Jackman and F.A. Cotton, "Dynamic Nuclear Magnetic Resonance Spectroscopy"; Academic Press, New York, 1975; and references therein.

37 For a discussion of the analogous rotation of olefins in metal complexes see: C.E. Holloway, G. Hulley, B.F.G. Johnson, and J. Lewis, *J. Chem. Soc. (A)*, 1970, 1653.

38 H.G. Alt, H.E. Engelhardt, M.D. Rausch and L.B. Kool, *J. Am. Chem. Soc.*, 1985, **107**, 3717.

39 See for example: F.A. Cotton and G. Wilkinson. *"Advanced Inorganic Chemistry"*, Fifth edition, John Wiley and Sons, New York, 1988 and references therein.

40 G. Fochi, C. Floriani, J.C. Bart, and G. Giunchi, *J. Chem. Soc. Dalton Trans.*, 1983, 1515; S. Gambarrotta, C. Floriani, V. Chiesi, and C. Guastini, *J. Chem. Soc. Chem. Commun.*, 1982, 1015.

41 P.J. Walsh, F.J. Hollander, and R.G. Bergman, *J. Am. Chem. Soc.*, 1990, **112**, 894.

42 A similar geometry is adopted by $Ti(O\text{-}2,6\text{-}C_6H_3{}^iPr_2)_2(\eta^2\text{-}PhNNPh)(py)_2$: L.D. Durfee, J.E. Hill, P.E. Fanwick, and I.P. Rothwell, *Organometallics*, 1990, **9**, 75.

43 J.K. Cockcroft, V.C. Gibson, J.A.K. Howard, A.D. Poole, U. Siemeling, and C. Wilson, *J. Chem. Soc. Chem. Commun.*, 1992, 1668.

44 S. Bahar, P.W. Dyer, V.C. Gibson, J.A.K. Howard, and C. Wilson, In Press.

45 Two crystallographically distinct molecules exist in the unit cell. Data for both molecules has been deposited with the Cambridge Structural Data Base. Data for only one of these two molecules has been tabulated, as there are no *significant* differences between the two. See the proceeding reference.

46 W.A. Nugent and J.M. Mayer, *"Metal Ligand Multiple Bonds"*, John Wiley and Sons, New York, 1988.

47 For further discussion of this phenomenon see Chapter 3.

48 NMR data for a recrystallised sample of biphenyl was used for comparison: ^1H (400 MHz, C_6D_6, 298K): δ 7.45 (m, 4H, *o*-C_6H_5), 7.20 (m, 4H, *m*-C_6H_5), 7.12 (m, 2H, *p*-C_6H_5); ^{13}C (100 MHz, C_6D_6, 298K): δ 141.66 (s, *ipso*-C_6H_5), 129.00 (d, *m*-C_6H_5), 127.45 (d, *o*-C_6H_5), 127.41 (*p*-C_6H_5).

49 A sample of biphenylene was obtained from Dr. H. MacBride. Spectroscopic data for biphenylene which exhibits a characteristic AA'BB' spin system: (400 MHz, C_6D_6, 298K): δ 6.50 (m, 4H), 6.40 (m, 4H).

50 Decomposition was signified by the generation of free $ArNH_2$ and PMe_3. Other decomposition products remain unidentified.

51 G. Erker and K. Krupp, *J. Am. Chem. Soc.*, 1979, **101**, 3659.

52 J.K. Cockcroft, V.C. Gibson, J.A.K. Howard, A.D. Poole, U. Siemeling, and C. Wilson, *J. Chem. Soc. Chem. Commun.*, 1992, 1668.

53 F.W. Hartner, J. Schwartz, and S.M. Clift, *J. Am. Chem. Soc.*, 1983, **105**, 640; S.M. Clift and J. Schwartz, *J. Am. Chem. Soc.*, 1984, **106**, 8300.

54 Recently the synthesis of $Mo(N^tBu)_2(CH_2Ph)_2$ has been successfully achieved through reaction of $Mo(N^tBu)_2Cl_2$.DME with $PhCH_2MgCl$: E.L. Marshall and V.C. Gibson, Unpublished results.

55 Recently Schrock has reported the synthesis of $Mo(NAr)_2(CH_2Ph)_2$, by treating $Mo(NAr)_2Cl_2$.DME with two equivalents of KCH_2Ph in diethylether in the presence of a small amount of THF, used to displace the coordinated DME: H.H. Fox, J.K. Lee, L.Y. Park, and R.R. Schrock, *Organometallics*, 1993, **12**, 759.

56 M. Coles and V.C. Gibson, unpublished results.

57 G. Schoettel, J. Kress, and J.A. Osborn, *J. Chem. Soc. Chem. Commun.*, 1989, 1062.

58 Osborn (previous reference) reports that the base-free dichloride can be isolated in 95% yield by recrystallisation from CH_2Cl_2/pentane. Yet, in our hands only a low yield of an impure product could be isolated in this manner. A modified procedure was adopted: MoO_2Cl_2 was added as a solid to a stirred solution of acetonitrile containing 2 equivalents of ^{t}BuNCO. After removal of acetonitrile and extraction with hot heptane and subsequent slow cooling of the solution, pure $Mo(N^tBu)_2Cl_2$ was isolated in a considerable higher yield.

59 The value of $^1J_{CH}$ is typically 75-100 Hz if an α-agostic interaction is present in a *static* system. If however, the system is fluxional then averaging of the coupling constants can occur resulting in a value similar to that exhibited by a normal sp^3 hybridised CH (≈120 Hz). See: M. Brookhart and M.L.H. Green, *J. Organomet. Chem.*, 1983, **250**, 395; M. Brookhart, M.L.H. Green, and L.L. Wong, *Prog. Inorg. Chem.*, 1988, **36**, 1.

60 However, the aromatic region of the ^{1}H spectrum was complicated which was attributed to rotation and "cogwheeling" of the phenyl

rings. Despite the acquisition of high temperature spectra further resolution of this region was not forthcoming.

61 N.H. Dryden, P. Legzdins, J. Trotter, and V.C. Yee, *Organometallics*, 1991, **10**, 2857; D.J. Crowther, R.F. Jordan, N.C. Baenziger, and A. Verma, *Organometallics*, 1990, **9**, 2574; A.K. Hughes, A. Meetsma, and J.H. Teuben, *Organometallics*, 1993, **12**, 1936.

62 J.H. Wengrovius and R.R. Schrock, *J. Organomet. Chem.*, 1981, **205**, 319.

63 A.D. Poole, Ph.D. Thesis, University of Durham, 1992.

64 C.D. Wood, S.J. McLain, and R.R. Schrock, *J. Am. Chem. Soc.*, 1979, **101**, 3210; L.W. Messerle, P. Jennische, R.R. Schrock, and G. Stucky, *J. Am. Chem. Soc.*, 1980, **102**, 6744.

65 P.J. Walsh, F.J. Hollander, and R.G. Bergman, *J. Am. Chem. Soc.*, 1988, **110**, 8729.

66 Y.W. Chao, P.A. Wexler, and D.E. Wigley, *Inorg. Chem.*, 1990, **29**, 4594.

Chapter Five- The Phillips Catalyst: An XPS and Mass Spectroscopic Study

5.0 Introduction

This chapter is concerned with the Phillips polymerisation catalyst (CrO_3/SiO_2) and uses XPS to examine the changes that occur at the surface during high temperature activation. The thermolysis of bulk samples of Cr_2O_3 and CrO_3 was studied and the observations made related to the supported system. Further investigations involved an *in situ* mass spectroscopic study of the activation of the related $Cr_3(OH)_2(Ac)_7/SiO_2$ system. A model system was used to probe the decomposition of the chromium (III) acetate groups on the surface. Lastly, a cursory examination of both the pre-reduction and polymerisation processes was undertaken using mass spectroscopy.

Supported oxide catalysts have played an important rôle in catalysis. They have a number of advantages over homogeneous systems which include:

a) The potential for separation and recovery of the catalyst.
b) Durability - the catalysts are capable of use in a variety of environments such as fixed and fluidized beds.
c) Generally high activity.
d) Thermal stability.
e) Ease of handling.

However, sometimes there is a fine balance between the use of homogeneous and heterogeneous systems. Heterogeneous systems have the following disadvantages: There is often more than one active site, in general the nature of the support is ill-defined, and that the selectivity of supported systems is usually low.

A number of supports are in common use such as silica, titania and alumina, although more recently organic polymer supports have become more widespread.[1] The oxide supports tend to have the advantage that they are more robust at high temperatures and are not degraded by reactive species such as oxygen. Thus, the following discussion will be limited to oxide supports only. The nature of such supports can be controlled in a variety of ways.[2] Surface area and chemical nature of the support are both important considerations for many catalyst systems.[1] The use of mixed oxide supports such as titania/alumina or silica/titania allow

the surface acidity or basicity to be varied, often an important consideration.

Many silicas used for catalyst supports are synthetic and are produced in one of two main ways. The first involves the acidification of silicate solutions.[3] Changes in reaction conditions causes variations in the nature of the resultant silica. Two types of oxide can be produced this way, sol-gel[4] and precipitated silicas. They differ in agglomerate size, the former having a large, well defined-internal surface, whilst precipitated silicas have less internal surface and more of an external surface. Lastly, fumed silica (e.g. Aerosil®) is formed when a volatile silicon compound such as $SiCl_4$ is injected into an oxygen/hydrogen flame, where high temperature hydrolysis occurs. This again generates a high external surface area silica.[5]

A normal silica surface contains hydrophilic silanol (Si-OH) and hydrophobic siloxane bridges (Si-O-Si).[6] The silanol groups have been classified by IR as isolated, hydrogen bonded, or geminal according to their environments (Figure 5.1).[7]

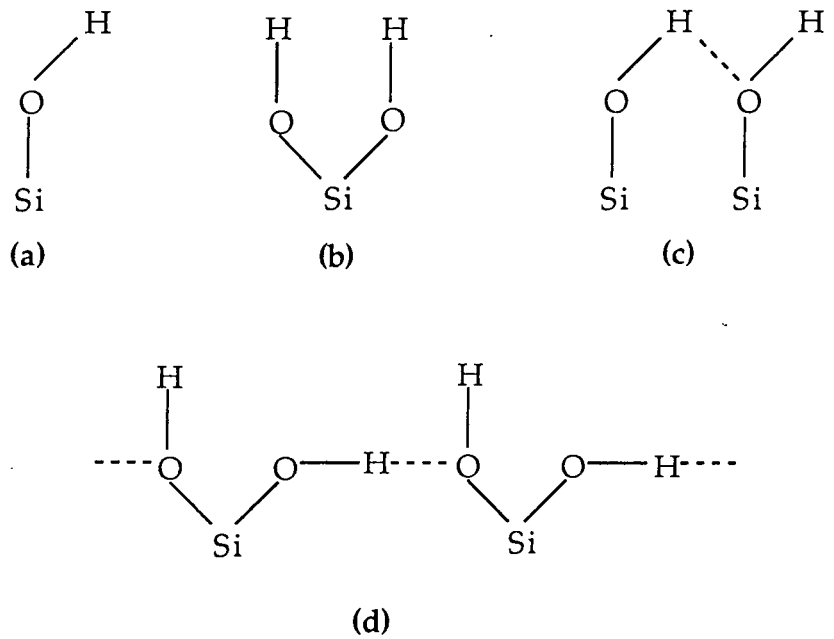

Figure 5.1 *Classification of silanol groups: (a) Isolated single group, (b) geminal groups, (c) hydrogen-bonded vicinal groups, and (d) hydrogen-bonded geminal groups.*

One of the most important properties of a silica support is the surface hydroxyl (silanol) density. This controls the number and dispersity of catalytically active species on the surface, as metals are typically attached

to the oxide through siloxide bonds, Si-O-M. The surface silanols have pKa's that lie in the range 4 to 7 and are thus weakly acidic or neutral. This value is dependent on the method of preparation of the silica.[1] The silanol density has been estimated using a number of chemical methods such as the thermal desorption of water and from surface reactions involving D_2, D_2O, Grignard reagents, halogen-containing molecules such as BCl_3, $AlCl_3$, $SiCl_4$ and chlorotrimethylsilanes, alkylaluminium compounds, B_2H_6 etc.[1] Experimental techniques such as IR and ^{29}Si (MAS) NMR have also been employed.

Siloxane bonds (Si-O-Si) are generally much less reactive and so don't play a large rôle in anchoring metals to the surface, although there is IR evidence to suggest that to some extent strained siloxane bridges in unannealed silica can be involved.[8]

Thermal treatment to 200°C is thought to remove all physically bound water, but hardly affects the surface silanols. The surface has a typical silanol density of 5 OH groups nm^{-2} (the precise number of silanols is dependent upon the nature of the silica). At elevated temperatures water is progressively eliminated as *neighbouring* silanol groups combine. At 800°C the number of silanols has decreased to approximately 1 OH nm^{-2}, which are believed to be isolated geminal functionalities. Despite prolonged heating to over 1000°C some silanol groups always remain at the surface.

Line narrowing studies of ^1H NMR spectra have demonstrated that the protons associated with the silica surface, migrate from oxygen to oxygen.[9] The proton "hopping" rate was observed to increase with temperature. The average "hopping" frequency was estimated to be approximately 10^{-4} s^{-1} at 500°C.

Heterogeneous silica-supported transition metal compounds play an increasingly important rôle as catalysts in the petrochemical industry. Since its discovery in the early 1950's[10] the Phillips catalyst has been the subject of much research. Even today the debate continues over the nature of the active chromium species and over the polymerisation mechanism. The catalyst is prepared by impregnating a chromium compound onto the surface of silica and then calcining under oxygen to activate the catalyst.

Hogan and Banks' original catalyst was prepared by impregnating silica with an aqueous solution of CrO_3, to a 1% chromium loading. Today many variants on this theme are employed.[11] There is a gradual

conversion to the use of chromium (III) precursors replacing toxic chromium (VI) species. Many reports have been made of mixed oxide supported catalysts (e.g. silica-titania). Promoted systems containing species like aluminium are becoming more prevalent. The work in this thesis has been restricted to two systems CrO_3/SiO_2 and $Cr_3(OH)_2(Ac)_7/SiO_2$.

The first question posed is the nature of the chromium species that results on activation (O_2 / 800°C), prior to contacting ethene. Changes in hydroxyl population have been measured in attempts to differentiate between chromate- and dichromate-like functionalities. A chromate species should react with two hydroxyls per chromium while dichromate with only one. These studies proved inconclusive, different results being obtained at different temperatures.[12] This inconsistency arises because more hydroxyls are lost at 200°C than at 800°C, thus the $\Delta OH/Cr$ replacement ratio will not be a constant 2 or 1, but will tend towards 2 at lower temperatures and 1 at higher temperatures. Thus, the number of displaced hydroxyls will depend upon the number and distribution of hydroxyls at the surface before impregnation.

A study which impregnated silica with chromyl chloride (CrO_2Cl_2) vapour was undertaken.[13] Chromate-like attachment would leave no chlorines at the surface, whereas a dichromate-like structure would leave one, Figure 5.2. Calcination up to 400°C led to no remaining chlorines. The polymerisation kinetics and polymer properties using the resultant catalyst were indistinguishable from those observed for the normal CrO_3/SiO_2 system. However, the mono-chloro catalyst proved inactive for polymerisation. This study indicates that pairing of chromium atoms (e.g. a dichromate-like structure) is not a requirement for polymerisation.

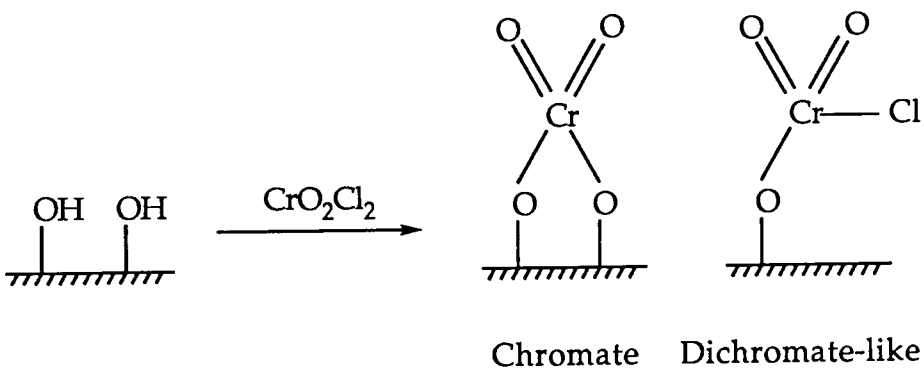

Figure 5.2 *CrO_2Cl_2 used as a model for CrO_3.*

Now, many researchers postulate that for chromium loadings of up to ≈1% polymeric CrO_3 oxide is broken up and becomes anchored to the silica surface *via* Cr-O-Si bonds, the most direct evidence came from using Raman spectroscopy.[14] The reaction proceeds with the elimination of water leaving a mononuclear, tetrahedral chromate species (Figure 5.3) on the oxide surface. Yet, if activation temperature was increased, a tendency for the formation of dichromate species became apparent. Most recently, Overton *et al* have identified chromate species to be the predominant product of calcination, although aggregates of CrO_3 were also detected using TPR, UV-VIS, and EPR.[15]

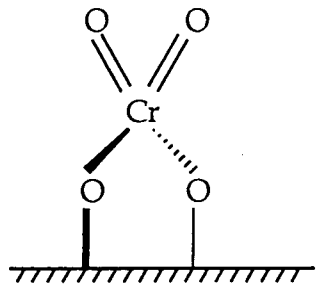

Figure 5.3 *Mononuclear chromium species believed to result from oxygen activation of CrO_3/SiO_2.*

This process is remarkable, as bulk CrO_3 decomposes to Cr_2O_3 and O_2 at approximately 190°C. Yet, in the presence of silica CrO_3 is stabilised up to about 900°C. For this stabilisation to occur, the chromium loading is critical. Activation of a system containing approximately 3% chromium leads to the formation of not only chromate species but also bulk α-Cr_2O_3.

Perhaps the biggest area of debate concerning the Phillips catalyst is the nature of the metal polymerisation centre, and the resultant polymerisation mechanism. Reports have been published that have postulated that the active chromium site could have an oxidation state from (II) to (V).

Much of the early work used ESR to try and elucidate the valence state of the chromium and favoured chromium (V).[16] These studies were usually complicated by the presence of more than one oxidation state, and was only indirect evidence at best.[17] This highlights one of the main problems in trying to pin down the precise valence state, i.e. the inability of many experimental techniques to *only* probe the active chromium sites. These studies are further hampered because of the 1% chromium

impregnated onto the support, it is believed that only a few percent (typically 3-10%) of this is responsible for ethene polymerisation.

By far the most likely oxidation state for chromium is (II). The first evidence for this came from Krauss[18] who quantitatively reduced the activated catalyst with CO at 350°C to chromium (II). This new species was found to readily support polymerisation. Since then a whole series of reports have been made that indicate that Cr (II) is in fact the valence state after initial reduction of the surface dichromate species.[19] Polymer produced by both a CO pre-reduced catalyst and the normal catalyst were found to be identical. This is indicative of the involvement of Cr(II) as many researchers have observed that small changes in catalyst pretreatment can dramatically change the properties of the resulting polymer. Further support for this value was obtained from an XPS study performed by Merryfield *et al.*[20] His study revealed that there was no apparent difference between the XPS spectra of the catalyst reduced by ethene and spectra from a CO reduced sample.

Despite the direct evidence in support of a Cr(II) site several research groups have proposed Cr(III). The most recent direct evidence came from Lunsford, who impregnated $CrCl_3$ onto silica.[21] Subsequent calcination *in vacuo* gave a catalyst that readily polymerised ethene.

To this day, the *true* valence of the active site still remains a mystery. Detection of the small amounts of catalytically active chromium still remains a major problem. However, with the advent of organochromium catalysts such as the Unipol System, Cp_2Cr/SiO_2,[22] it becomes increasingly evident that it is not just the valence state of chromium that is important, but also the nature of the ligands directly bound to chromium.

Many reports have been made which indicate that after oxygen activation the catalyst is not immediately capable of supporting polymerisation and that there is an induction time before polymerisation occurs.[23] However, once initiation has taken place, the rate of polymerisation then increases throughout the reaction. This dormant period is believed to result from simple reduction of the surface chromate by ethene affording formaldehyde, Figure 5.4.[24] Chromium (VI) is a powerful and well known oxidising agent which reacts with many organic compounds.

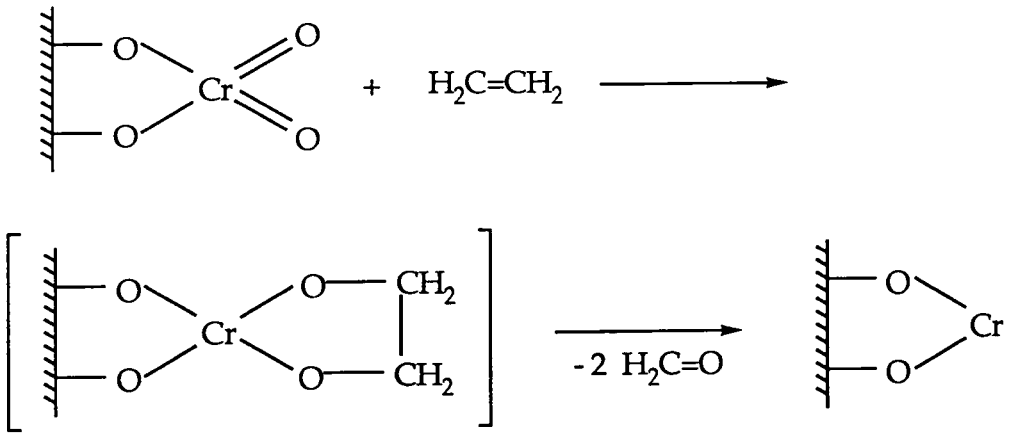

Figure 5.4 *Reduction of surface chromate species by ethene.*

Although most people now agree over the likely oxidation state of the active chromium species, the problems of initiation and subsequent polymerisation still have not been answered. However, distinction between these two processes is difficult as the latter is intimately dependent on the former.

McDaniel stated that the incorporation of the first ethene is probably slower than incorporation of succeeding monomer units.[25] Krauss proposed that the chromium (II) species initially coordinates two ethene molecules, which undergo oxidative addition forming a metallacyclobutane species with subsequent rearrangement to an allyl species and a chromium hydride.[26] Yet, this mechanism does not account for the formation of terminal groups (methyl or vinyl) that have been detected in the resulting polymer. Many other similar mechanisms were also postulated.[27] Some mechanisms were speculated to involve two adjacent chromium centres. A low temperature mechanism involving a Cr-CH_2-R-CH_2-Cr intermediate was intimated by Rebenstorf *et al.*[28] Dalla Lana and co-workers using IR proposed that ethene adsorbs molecularly and dissociatively forming a reactive pair of alkylidene structures linked to two chromium sites, Figure 5.5). Polymerisation is then believed to occur *via* normal insertion mechanisms.

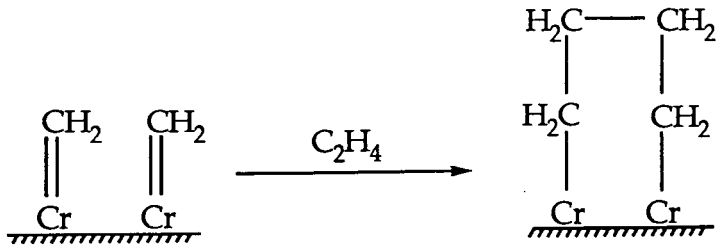

Figure 5.5 *Initiation mechanism involving a pair of chromium alkylidene intermediates.*

Alkylidene moieties have been postulated as being involved in the polymerisation process.[29] The mechanism they postulated is shown in Figure 5.6. However, this mechanism does not account for initiation and the source of the first H atom. Although a study by Weiss and Hoffmann demonstrated that the reduced Phillips catalyst when treated with a carbene source and olefins produced cyclopropanes in good yield.[30] They suggested that such species could play a part in the chemistry associated with the Phillips system.

Other researchers have discussed the possible effect of surface silanols in the initiation step. Water molecules evolved during the reduction/activation of the CrO_3/SiO_2 system can adsorb to form silanol groups adjacent to the chromium centres. Interaction between these two species may result in a decrease in the coordination unsaturation of the chromium sites, but could also oxidise the chromium (Equation 5.1).[31]

$$Cr^{2+} + 2H_2O \longrightarrow Cr^{3+} + 2H_2 + O_2 \qquad (5.1)$$

Groenveld *et al* [32] suggested direct involvement of silanols during the adsorption of the initial ethene molecule as shown in Equation 5.2. Furthermore Eley and co-workers[33] demonstrated that silanol groups interacted physically with the growing polymer chain. Overall the evidence suggests that silanol groups do play a intimate part in the initiation and polymerisation process.

$$H^+(\text{silanol}) + Cr^{2+} \rightleftharpoons H{-}Cr^{3+} \xrightarrow[C_2H_4]{} CH_3CH_2{-}Cr^{3+} \qquad (5.2)$$

An IR study of the OH region of the spectrum by Dalla Lana *et al* suggested that proton migration from silanols to chromium is caused by ethene adsorption and is not an equilibrium process as proposed by

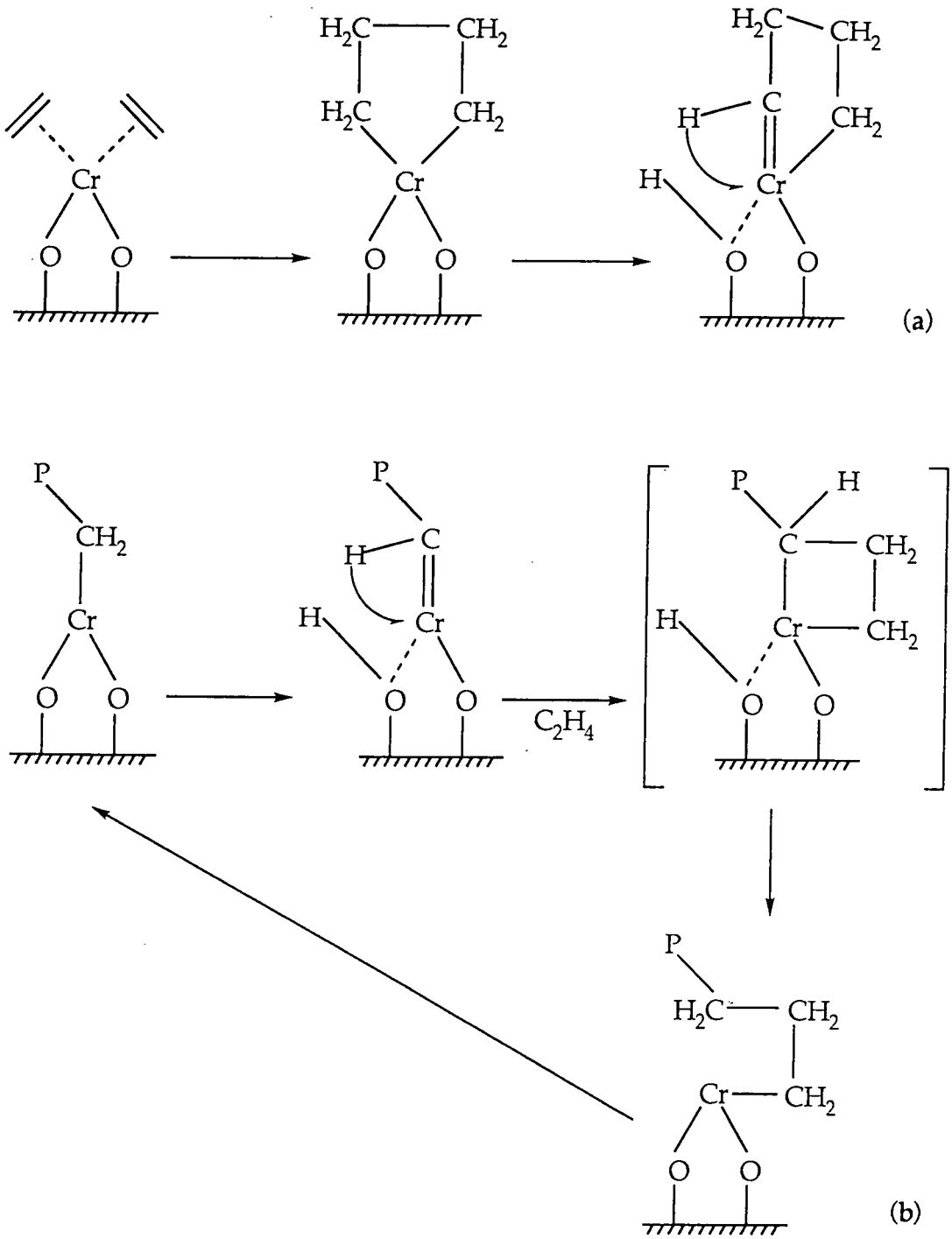

Figure 5.6 *Polymerisation mechanism postulated by Ghiotti et al. (a) chain initiation, (b) propagation.*

Groenveld (above). Another recent IR investigation using FTIR has intimated that methylene groups become bound to silanol groups adjacent to the active chromium centres.[34]

^{13}C NMR spectroscopy on the polymer isolated from a series of labelled monomer polymerisations indicated that there was no hydrogen scrambling during initiation which would be expected from some of the alkylidene mechanisms put forward,[35] although they can not be discounted. IR and NMR analysis of homopolymers produced using the Phillips system nearly always indicate the presence of one terminal vinyl and one methyl per chain, although structures with internal unsaturation occur very infrequently. This supports the idea that β-elimination is likely to cause chain termination, a view that fits in with the known chemistry of metal alkyls. It is well documented that transfer of hydrogen from the growing polymer chain to the chromium centre (and back again) occurs.[34]

The rate of chain termination relative to propagation determines the molecular weight of the polymer.[36] The molecular weight of the resulting polymer can be controlled once polymerisation has started by altering reaction conditions. For example, raising the temperature has been found to enhance the rate of chain termination. However, decreasing the ethene concentration has the reverse effect. Activity has been shown to be related to the propagation by near first order kinetics. Increasing the olefin concentration increases propagation without affecting termination, resulting in higher molecular weight polymer. In Ziegler-Natta chemistry hydrogen is known to act as a very efficient chain transfer reagent, and is used to control the molecular weight of the polymer. The hydrogen is believed to cause chain termination through σ-bond metathesis with the growing polymer chain. However, dihydrogen has no effect on Phillips systems. σ-bond metathesis will only occur for metals with a d^0 electron count, and thus is not likely to occur with Phillips catalysts (Figure 5.7).[37]

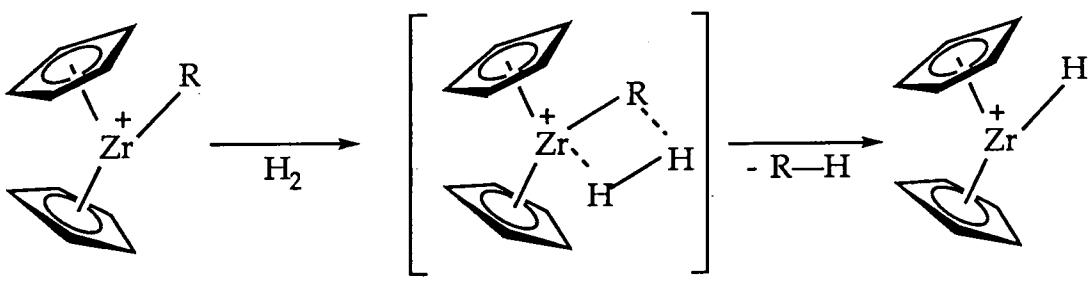

Figure 5.7 *Schematic representation of σ-bond metathesis.*

Polymerisation reactions are generally performed either in the gas phase (60-100°C) using a fluidized bed system, in hydrocarbon solvent at elevated ethene pressures and temperatures (<50 atm, 125-170°C), or in a slurry (poor solvent at 60-100°C).[38] The physical nature of the support itself can have a profound influence on the nature and molecular weight of the final polymer. Surface area and pore size distribution have been shown to be important catalyst parameters, bringing about differences in catalyst activity, molecular weight, and molecular weight distribution of the polymers produced.[35] Silicas with large pore volumes can accommodate chromium centres within the silica particle. Thus, when polymerisation has been initiated the growing polymer chain grows through the oxide particle.[39] At a critical polymer mass the silica will be forced to fragment exposing new active polymerisation centres. This means that as pore size is increased so the molecular weight of the polymer decreases.

5.1 Dehydroxylation of Silica

In order to examine the Phillips catalyst system in detail, no study would be complete without an examination of the oxide support itself. To this end, dehydroxylation of high surface area silica[40] has been examined using both XPS and quadrupole mass spectrometry.[41]

5.1.1 XPS Studies of the Dehydroxylation of Silica

Samples of Crosfield silica were dehydroxylated to varying extents by heating under a dry nitrogen flow for five hours over a range of temperatures. The high temperature limit was taken as 780°C, to avoid any possible sintering of the silica, a process that is known to occur at approximately 900°C.[42] The treated samples were then transferred under anhydrous conditions to the spectrometer *via* a nitrogen atmosphere dry box. XPS spectra were obtained for both the Si (2p) and O (1s) regions.

All the treatments gave, perhaps surprisingly, two overlapping Si (2p) XPS signals, which appeared at almost identical binding energies of ≈99.8eV and ≈101.8eV. The relative peak areas of these two signals did not

change significantly upon heating (Table 5.1). The more intense higher binding energy peak has been attributed to surface silicon functionalities, whilst the smaller peak is thought to arise from contributions from the bulk of the oxide.

The O (1s) region proved more interesting. Again two signals were detected, yet this time their relative peak areas changed significantly upon dehydroxylation (Table 5.1 and Figure 5.8).

Dehydroxylation Temperature (°C)	Si (2p) BE (± 0.2eV)		O (1s) BE (± 0.2eV)	
None	99.7 (8.6%)	101.8 (91.1%)	530.6 (1.9%)	533.4 (98.1%)
200	99.8 (8.6%)	101.5 (91.4%)	530.5 (3.0%)	533.6 (97.0%)
300	99.8 (9.0%)	101.8 (91.2%)	530.4 (3.1%)	533.6 (96.9%)
450	99.8 (8.9%)	101.8 (91.1%)	530.5 (3.8%)	533.7 (96.2%)
600	99.8 (8.6%)	101.6 (91.1%)	530.5 (4.3%)	533.5 (95.7%)
800	99.9 (8.9%)	101.8 (91.1%)	530.7 (4.9%)	533.4 (95.1%)

Table 5.1 *Si (2p) and O (1s) XPS signals obtained from the dehydroxylation of silica under nitrogen.*

Comparison of the graphs shown in Figure 5.8 with that presented by Hogan for the thermogravimetric analysis of silica (Figure 5.9),[43] reveals a similar discontinuity at approximately 100-150°C. Hogan attributed this sharp discontinuity to the end of loss of free water, and to the beginning of the more gradual loss of water by combination of silanol groups. These features are not nearly so well marked in the XPS experiments, presumably a consequence of the XPS study being preformed under UHV conditions which would remove some of the physisorbed water.

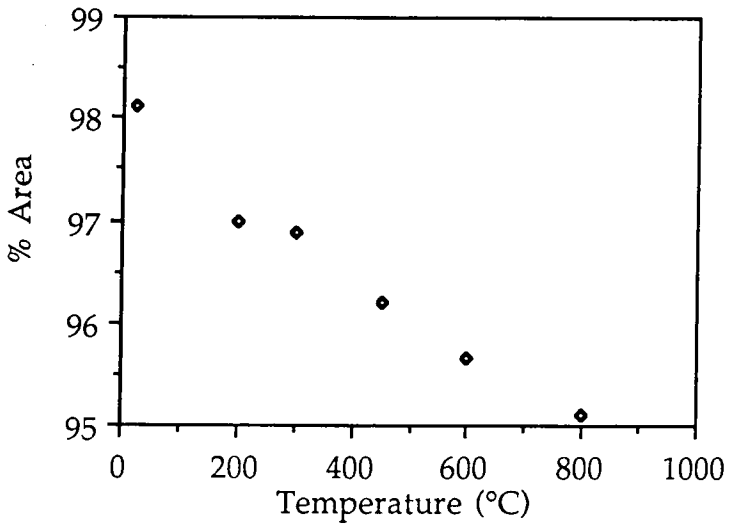

Figure 5.8a) *Changes in peak area of the higher energy (≈533.5eV) O (1s) XPS signal associated with thermal dehydroxylation of silica under nitrogen.*

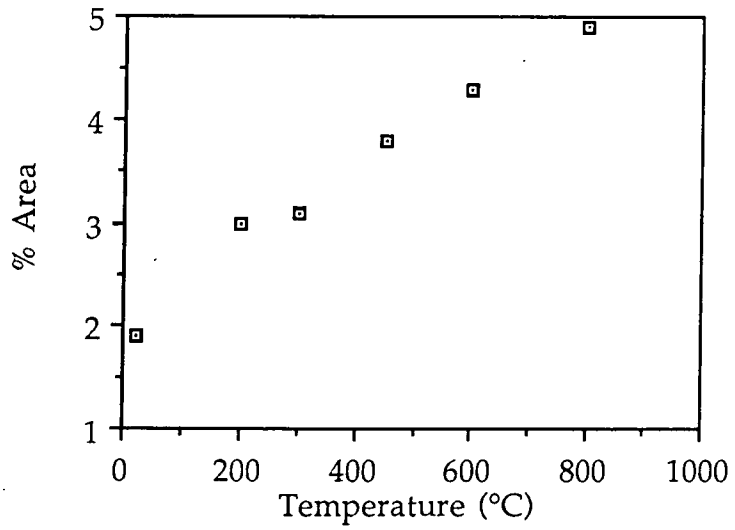

Figure 5.8b) *Changes in peak area of the lower energy (≈530.5eV) O (1s) XPS signal associated with thermal dehydroxylation of silica under nitrogen.*

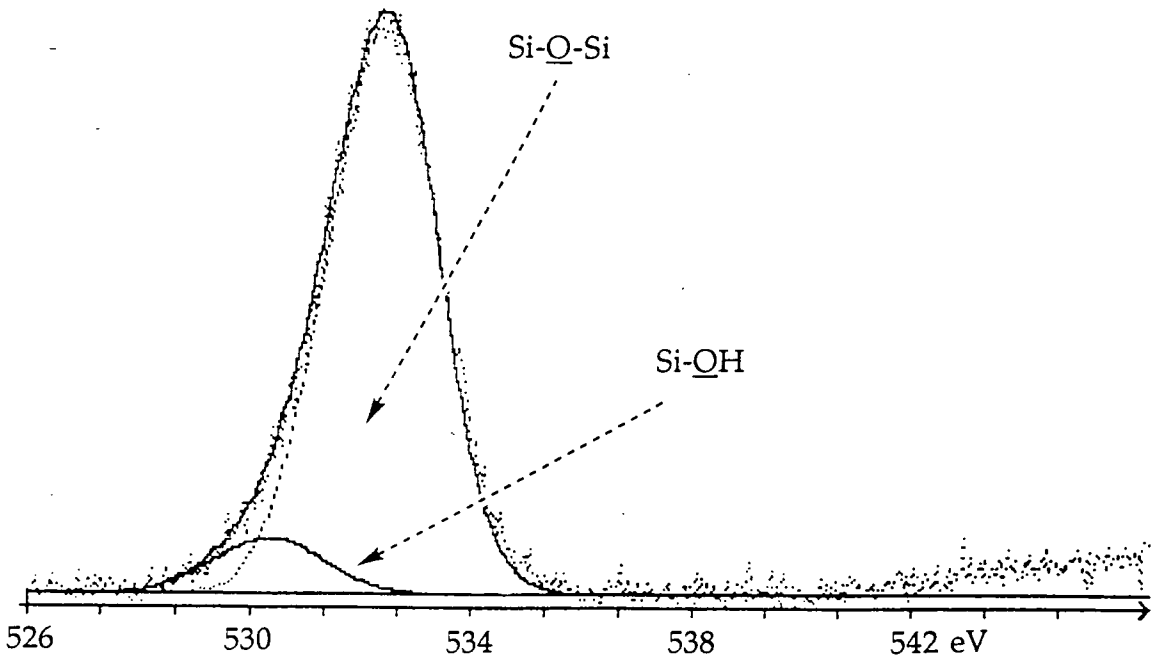

Figure 5.8c *Example of the results obtained from the O(1s) region of SiO_2 dehydroxylated under N_2 at 200°C.*

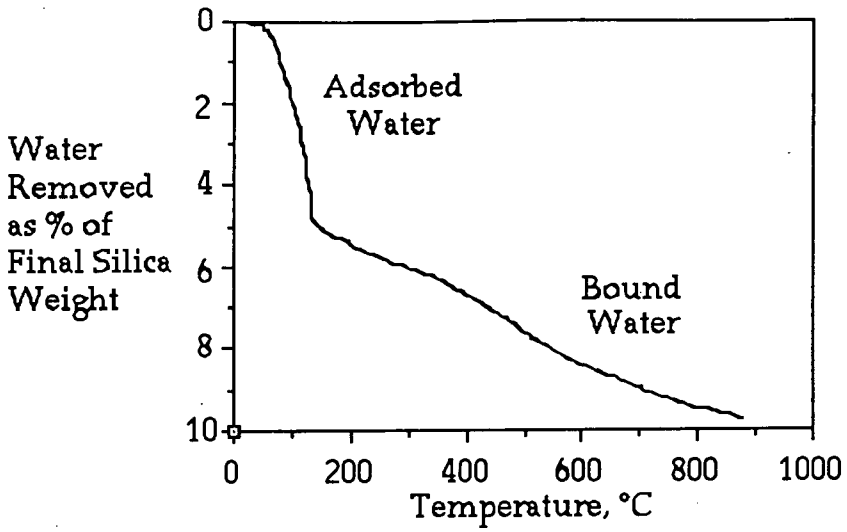

Figure 5.9 *Thermogravimetric analysis of silica.*

This agrees well with the assignments that can be made from the relative binding energies of the two O (1s) signals.
A simple treatment involving electronegativity arguments would predict that a terminal silanol (Si-OH) or chemisorbed water molecule would have oxygen atoms that are more electron deficient than those associated with bridging Si-O-Si units.[44] Thus, the higher binding energy peak (≈533.5eV) is believed to be attributable to oxygen atoms in both of the former environments. Hence, the lower binding energy peak can be assigned to oxygens in bridging positions, Si-O-Si.

This argument is consistent with the relative changes in intensity of the two O (1s) peaks. As the dehydroxylation temperature is increased then the relative intensity of the high binding energy peak decreases. This is consistent with loss of chemisorbed water and combination of adjacent silanol groups. Conversely, at higher temperatures, the percentage of oxygen atoms from Si-O-Si linkages increases. This latter peak can never become the major contributor to the O (1s) spectrum as it is impossible to completely dehydroxylate the silica surface, even on prolonged heating.[1] Only near surface species have been considered in this argument as XPS has a sampling depth of approximately 10-30Å.[45]

Similar dehydroxylation experiments were performed under a dry oxygen flow, as this is the gas that is used to "activate" the Phillips catalyst itself. The results obtained were almost identical to those obtained when nitrogen was employed.

5.1.2 *In Situ* Mass Spectroscopic Studies of the Dehydroxylation of Silica

Further exploration of the dehydroxylation process was made using an *in situ* quadrupole mass spectrometer and Temperature Programmed Desorption (TPD) techniques.

A small (1g) sample of Crosfield silica was loaded into a quartz microreactor tube.[46] The temperature was then raised at 1°C/minute (as for the previous study), and subsequently maintained at 780°C for 5 hours. Throughout this process the carrier gas (Ar or O_2) was monitored by a quadrupole mass spectrometer.

Carrier Gas	1st Peak Intensity (Temp °C)	2nd Peak Intensity (Temp °C)
Argon	4.5 (150°C)	3.3 (480°C)
Oxygen	3.5 (90°C)	0.5 (460°C)

Table 5.2 *Dehydroxylation of Silica. Water (mass 18) TPD profile, with corresponding peak heights.*

As expected only one mass, mass 18, corresponding to the loss of water was observed under both argon and oxygen. Water was evolved in two discrete temperature bands, Figure 5.10, which have been assigned as follows:

1st Peak	Loss of physisorbed water
2nd Peak	Loss of water through combination of adjacent silanol groups[47]

As Figure 5.10 indicates, there are differences apparent between the profiles obtained when oxygen and argon are employed. The peaks obtained under an oxygen atmosphere are attenuated and shifted to a slightly lower temperature than when argon is used. This observation has not been fully rationalised, although oxygen is likely to interact with the surface Si-OH groups and physisorbed water. This interaction must facilitate the loss of water, as dehydroxylation is occurring at a lower

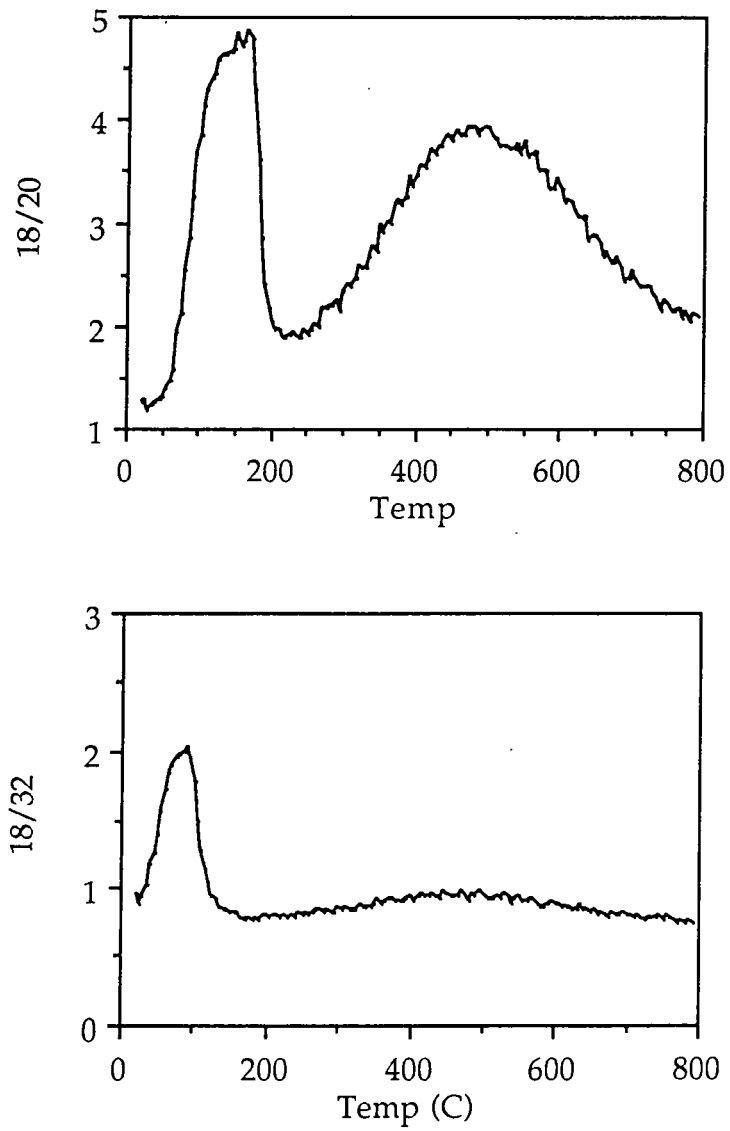

Figure 5.10 *Comparison of the water loss profiles for silica. (Top: Under Ar, Bottom: Under O_2).*

temperature. Curiously, the surface components seem identical for both samples when examined by XPS.[48]

Atomic oxygen is known to stabilise surface species and can markedly change reaction pathways.[49] Single crystal studies on the reaction of H_2O with Ag(110) suggested that surface water molecules equilibrated rapidly with oxygen atoms at the surface *via* proton exchange. The water exhibited a very strong interaction with the surface oxygen species.

5.2 XPS Studies of the Thermolysis of Bulk CrO_3 and Cr_2O_3

In breaking the Phillips catalyst system (CrO_3/SiO_2) up into its individual components, the next logical step is to consider the effects of various treatments upon bulk chromium oxides. To this end, chromium (III) and (VI) oxides have been examined in a similar manner to that employed for silica. As before, the bulk oxides were heated under a flow of the appropriate gas in a quartz microreactor. Subsequently, the residues were taken into a nitrogen atmosphere dry box where they were transferred to the spectrometer.

In the following study, changes observed in the chromium ($2p_{3/2}$) region of the XPS spectrum will be described in detail. The effects that were observed were mirrored in the chromium ($2p_{1/2}$) region (arising through spin orbit coupling[50]), although due to the lower intensity of this peak, curve fitting proved more difficult. Thus, discussion is limited only to the Cr ($2p_{3/2}$) region of the spectrum

5.2.1 Thermolysis and XPS Analysis of Bulk Cr_2O_3

Untreated chromium (III) oxide (I), gave three overlapping Cr ($2p_{3/2}$) XPS peaks as shown in Table 5.3 and Figure 5.11. The most intense peak appeared at lowest binding energy. A sample of (I) was heated under an oxygen flow to afford sample (II), with no apparent colour change. For comparison, a sample of (I) was subjected to the same thermal treatment as before, this time under nitrogen, affording sample (III).

Similarly, a sample of the untreated oxide (I) was subjected to outgassing at 10^{-3} torr for twenty four hours to give (IV), which was also

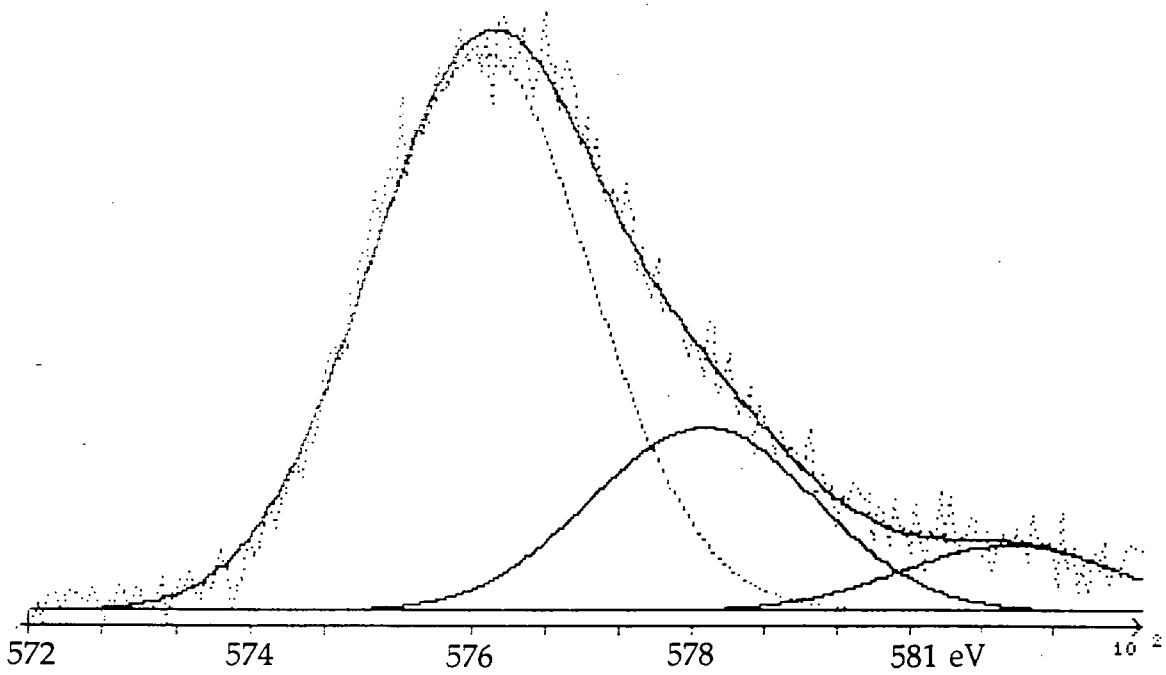

Figure 5.11 *Cr ($2p_{3/2}$) region of untreated Cr_2O_3.*

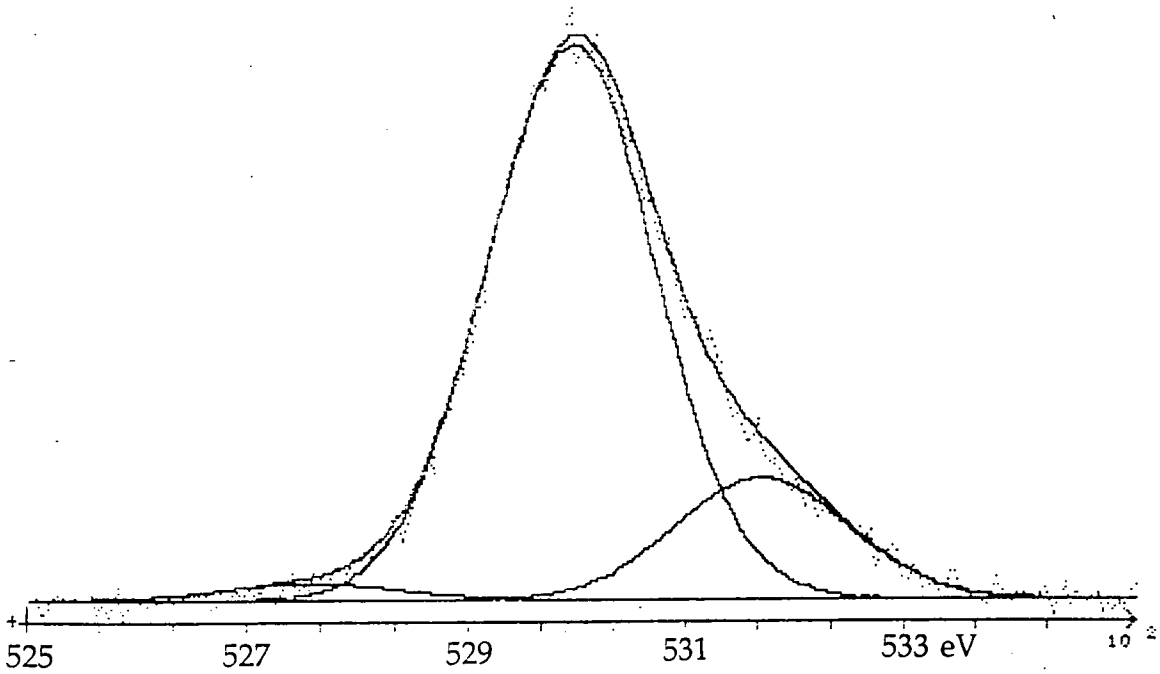

Figure 5.12 *O (1s) region of untreated Cr_2O_3.*

examined by XPS. The Cr ($2p_{3/2}$) XPS region again revealed three peaks which had similar intensities and binding energies to those observed for the untreated sample. This indicated that effects due to physisorbed water were minimal. Further comparisons will however, be made using sample (**IV**) as the reference for untreated Cr_2O_3. These results are summarised in Table 5.3.

SAMPLE		BINDING ENERGY eV (± 0.2 eV)			FWHM (eV)
Cr_2O_3	(I)	576.2 (73.2%)	578.2 (21.5%)	581.4 (5.4%)	2.8
$Cr_2O_3/\Delta/O_2$	(II)	576.3 (62.9%)	578 2 (27.9%)	580.3 (9.2%)	2.8
$Cr_2O_3/\Delta/N_2$	(III)	576.1 (66.0%)	578.2 (26.3%)	581.2 (7.7%)	2.8
Cr_2O_3 Vac.	(IV)	576.3 (69.3%)	578.5 (23.2%)	581.2 (7.5%)	2.8

Table 5.3 *Summary of Cr ($2p_{3/2}$) XPS data for Cr_2O_3. Relative peak areas shown in parentheses.*

Analysis of the O (1s) XPS spectra, Table 5.4 and Figure 5.12, for the same four samples revealed three peaks. However, the sample heated under oxygen, (**II**), also gave a new signal at 532.7 eV and showed the most dramatic shifts in binding energy. The sample that was outgassed at room temperature, (**IV**), gave three overlapping O (1s) signals, similar to (I). The peak at 530.1 eV exhibited a relative increase in intensity, indicating that the other two signals both had a contribution from physisorbed surface contaminants.

SAMPLE		BINDING ENERGY eV (± 0.2 eV)			
Cr_2O_3	(I)	528.2 (5.1%)	530.0 (74.5%)	531.7 (20.4%)	—
$Cr_2O_3/\Delta/O_2$	(II)	528.8 (5.4%)	530.2 (71.4%)	531.6 (17.6%)	532.7 (5.6%)
$Cr_2O_3/\Delta/N_2$	(III)	527.8 (4.1%)	529.6 (71.0%)	531.4 (24.9%)	—
Cr_2O_3 Vac.	(IV)	527.7 (2.3%)	530.1 (79.9%)	531.9 (17.8%)	—

Table 5.4 *Summary of O (1s) XPS data for Cr_2O_3. Relative peak areas shown in parentheses, and FWHM = 2.2 eV in all cases.*

In a previous study, Allen[51] stated that the O (1s) peak for untreated Cr_2O_3 was broadened to the high-binding energy side by water absorbtion. He found that in general a peak at *ca.* 2 eV greater than in the anhydrous sample was visible. This trend is not obviously apparent in our study,

although complete removal of all absorbed species was unlikely to have been realised under such a mild treatment.

5.2.2 Thermolysis and XPS Analysis of Bulk CrO_3

Untreated CrO_3 (**V**) was examined as above and gave two overlapping peaks in the Cr ($2p_{3/2}$) XPS spectrum at 577.3 and 579.8 eV, which had intensities of 15.9 and 84.1% respectively. Samples of CrO_3 were only heated to 150°C to avoid sublimation and decomposition. On heating under a flow of oxygen to afford sample (**VI**), an additional peak appeared at the expense of the 579.8 eV peak. Sample (**VII**) was obtained through the thermal treatment of CrO_3 (**V**) under nitrogen. These results are summarised in Table 5.5 and Figure 5.13.

SAMPLE		BINDING ENERGY eV (± 0.2 eV)			FWHM (eV)
CrO_3	**(V)**	577.3 (15.9%)	579.8 (84.1%)	—	2.6
$CrO_3/\Delta/O_2$	**(VI)**	577.4 (14.8%)	579 (75.8%)	582.8 (9.4%)	2.6
$CrO_3/\Delta/N_2$	**(VII)**	577.6 (15.9%)	579.8 (75.6%)	582.9 (8.5%)	2.6

Table 5.5 *Summary of Cr ($2p_{3/2}$) XPS data for CrO_3 samples. Relative peak areas shown in parentheses.*

Two overlapping O (1s) peaks were found for all three samples of CrO_3. Each sample displayed peaks of approximately similar binding energies. The important difference between the three samples was in the relative intensities of the peaks. The untreated sample (**V**) had peak intensities of 75.0 and 25.0%, whereas for the oxygen activated sample (**VI**) the intensities were 80.4 and 19.6%, with the nitrogen activated sample (**VII**) exhibiting similar intensities of 82.5 and 17%, Table 5.6 and Figure 5.14.

SAMPLE		BINDING ENERGY eV (± 0.2 eV)		FWHM (eV)
CrO_3	**(V)**	530.7 (75.0%)	532.4 (25.0%)	2.5
$CrO_3/\Delta/O_2$	**(VI)**	530.7 (80.4%)	532.4 (19.6%)	2.5
$CrO_3/\Delta/N_2$	**(VII)**	530.8 (82.5%)	532.8 (17.5%)	2.5

Table 5.6 *Summary of O (1s) XPS data for CrO_3 samples. Relative peak ares are shown in parentheses.*

By way of comparison, samples of some readily available chromates and dichromates were examined by XPS. These samples both gave one signal in the Cr ($2p_{3/2}$) region, and a doublet for the O (1s). The Cr ($2p_{3/2}$) and O (1s) XPS results from these samples are summarised in Table 5.7.

SAMPLE	Cr ($2p_{3/2}$) BINDING ENERGY (eV)	O (1s) BINDING ENERGY (eV)		FWHM (eV) Cr / O
$K_2Cr_2O_7$ **(VIII)**	580.0	530.7 (85.1%)	532.7 (14.9%)	2.2 / 2.3
K_2CrO_4 **(IX)**	579.6	530.1 (77.0%)	532.0 (23.0%)	2.0 / 2.2

Table 5.7 *Chromate and Dichromate Cr ($2p_{3/2}$) and O (1s) XPS data. Relative peak areas shown in parentheses, binding energies have an associated error of ±0.2 eV.*

5.2.3 Discussion of the Thermolysis of Bulk Samples of Cr_2O_3 and CrO_3

By way of comparison potassium dichromate and chromate were included in the study. Both samples gave two signals in the O (1s) XPS region, the peak at lower binding energy having the greater intensity. These peaks have been assigned to bridging and terminal oxo groups as illustrated in the following discussion. It is noted however, that previous studies have been unable to detect discrete doublets in the O (1s) region, although a slight broadening of this peak was noted.[51,52]

The dichromate anion is constructed from two tetrahedral CrO_4, units linked by sharing one oxygen atom, as shown in Figure 5.15.

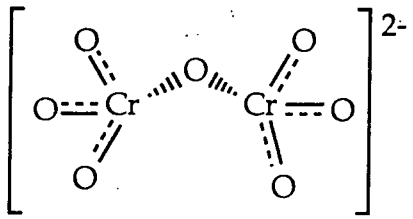

Figure 5.15 *Schematic representation of the dichromate anion.*

X-ray crystallographic studies have shown that all six terminal oxo groups are equivalent.[53] The anion 2- charge is believed to be delocalised over these groups. Thus, two types of oxygen are present in the ion, terminal and bridging. From a consideration of relative electronegativities, it is not unreasonable to assign a higher electron binding energy to an oxygen atom that occupies a bridging site relative to that for a terminal oxygen atom.

A comparison between the structure of the dichromate anion and the structure of the organic polymer poly (ether ether ketone), or PEEK, can be drawn, Figure 5.16. PEEK contains oxygen atoms in both ketone and ether environments. As expected two signals are observed in the O (1s) region in a 1:2 ratio, at binding energies of 531.25 and 533.33 eV (FWHM = 2.1 eV), respectively. From their relative intensities the peak at lower binding energy has been attributed to the ketonic oxygen, the other being assigned to oxygen atoms of the ether linkage.[54] Thus, assignment of the two O (1s) peaks for the dichromate anion can be made in terms of terminal *versus* bridging oxygen atoms. This was based on the relative intensities of the two signals, 1:5.6. Furthermore, the six electron rich terminal oxo groups (O^{2-}) would be expected to display a lower binding energy relative to the bridging oxygen (O^{-}).

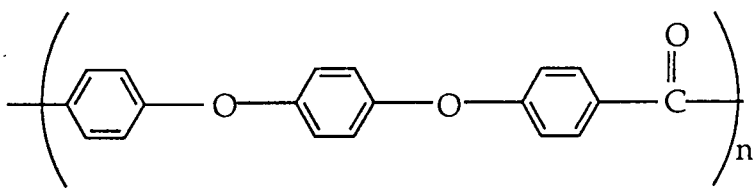

Figure 5.16 *The structure of Poly (ether ether ketone), PEEK.*

For comparison the chromate anion was examined, K_2CrO_4 (IX). This consists of isolated $[CrO_4]^{-}$ tetrahedra[55] in which all the oxygen atoms are equivalent, and should therefore give rise to only one O (1s) peak. Surprisingly, two peaks were observed at binding energies of 530.12 and 532.03 eV with intensities of 77.0 and 23.0% respectively, Table 5.7. This

second higher binding energy O (1s) signal has been attributed to the formation of surface Cr-OH functionalities, a phenomenon that has been observed previously.[51] Alternatively this peak could be attributed to the asymmetry that must be present at the surface of the bulk chromate. It is not unreasonable to view the chromate as in Figure 5.17, where two or more oxygen environments result from oxygen atoms that are either present at the surface or involved in the bulk structure. The oxygen atoms that occupy sites in the bulk are expected to have lower binding energies than for those associated with the "free" surface oxygens, especially if interactions with the associated potassium cations are invoked. XPS being a surface sensitive technique (typical sampling depths of ≈30Å) would preferentially detect the surface environment over the bulk structure, leading to the observed discrepancies in the O (1s) spectra.

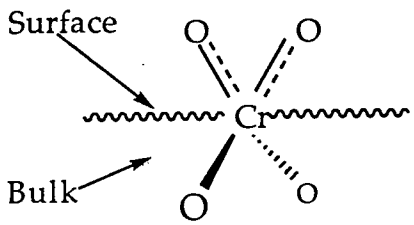

Figure 5.17 *Schematic representation of the surface of a bulk chromate.*

This rationale allows the spectrum of bulk CrO_3 (**V**) to be assigned in terms of terminal *versus* bridging oxygen atoms. The oxide consists of infinite chains of CrO_4 tetrahedra linked by the sharing of two vertices, as shown in Figure 5.18.

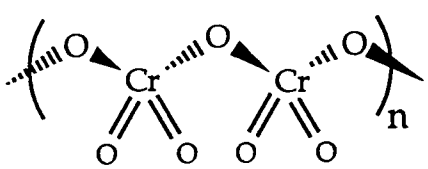

Figure 5.18 *Schematic representation of the structure of CrO_3.*

Two O (1s) peaks were observed, one at 530.7 eV (75.0%) and the other at 532.4 eV (25.0%). Some delocalisation of charge on adjacent terminal oxo groups is likely to cause their binding energy to be lower than expected. The bridging oxo groups should, from the assignments made for the dichromate sample (**VIII**), have O (1s) binding energies of approximately 532 eV, which fits well with the experimentally determined

value of 532.4 eV for this sample. The two peaks would be expected to show relative intensities of 1:2 (Cr-O-Cr : Cr=O), yet a ratio of 1:3 was observed. This anomaly has been attributed to the hygroscopic nature of **(V)**. Adsorbed water forming Cr-OH bonds, causing an increase in the intensity of the peak at 532 eV (cf. the value of the high binding energy peak observed for **(VIII)**). These surface Cr-OH species are likely to exhibit similar O (1s) electron binding energies to those exhibited by a bridging oxygen atom, e.g. Cr-O-Cr.

Two peaks were observed for both samples **(VI)** and **(VII)**, at positions now thought to be indicative of terminal oxo and bridging oxo groups. The major difference between the untreated sample, **(V)**, and activated samples, **(VI)** and **(VII)**, is the change in their ratios, Table 5.3. The peak at 530 eV increases in size from 75.0% in sample **(V)**, to 80.4% and 82.5% in samples **(VI)** and **(VII)** respectively. This effect has been attributed to the thermally induced loss of surface-bound hydroxyl groups, and is consistent with assignment of the higher binding energy peak observed for **(IX)**.

One surprising feature of this study was the observation of a weak N (1s) XPS signal from the oxygen treated sample of Cr_2O_3. The peak had an associated binding energy of ≈404 eV which is characteristic of chemisorbed nitrogen.[56] The only possible source of the nitrogen was from the nitrogen atmosphere used for the handling of the treated samples. This implies that some very active surface species must form during the thermolysis of this sample under oxygen. Yet, N_2 is isoelectronic with CO. Activated chromium species of the type likely to be at the oxide surface are known to react readily with CO, and thus, it is not unlikely that they could also react with N_2.

5.2.4 Summary of the XPS Analysis of the Thermolysis Products of CrO_3 and Cr_2O_3

The formation of a new high binding energy O (1s) signals for the oxygen treated Cr_2O_3 sample, **(VI)**, is consistent with the formation of what appear to be surface dichromate species (cf. the spectrum of $K_2Cr_2O_7$). This latter signal is unlikely to be due to Cr-OH contaminents as the sample was prepared under conditions where water was rigorously excluded. Similar conclusions have been reached by Zecchina using IR

spectroscopy, who also observed species that were consistent with the formation of surface dichromate functionalities.[57] The thermolysis product of Cr_2O_3 heated under nitrogen, sample (III), exhibited only redistribution of the intensities of the three O (1s) XPS signals compared to the untreated sample (I).

Complementary evidence for the oxygen induced surface transformation of Cr_2O_3 was obtained from the Cr ($2p_{3/2}$) XPS region. On heating (I) under oxygen a new signal became apparent at 580.3 eV. This correlates well with the spectrum of $K_2Cr_2O_7$. Little variation was observed for the remaining Cr ($2p_{3/2}$) signals. After similar treatment of (I) under nitrogen no new high binding energy peak was detectable.

When a similar study was performed with CrO_3, again no new O (1s) signal was observed. The mild conditions employed to avoid decomposing the oxide were not sufficient to bring about any surface rearrangement. However, a loss of intensity of the higher binding energy peak, of similar magnitude for each sample did result. This is consistent with Allen's[51] view that this signal is attributable to surface adsorbtion of water, forming Cr-OH functionalities. In contrast, a new high binding energy Cr ($2p_{3/2}$) peak (582.8 eV) was observed after heating under both N_2 and O_2. This is believed to be associated with partial dehydroxylation of the surface (cf. the value of 585.8 eV observed for water adsorbed on CrO_3 referenced against the Au $4f_{7/2}$ line[51]).

From this study it seems that the activation process used to obtain an active Phillips ethene polymerisation catalyst, namely the thermolysis of chromium (VI) oxide impregnated silica under oxygen at 780°C, is likely to produce chromate or dichromate like surface species. This is in accord with the view presented by a number of researchers.[58]

5.3 XPS Studies on the Phillips Catalyst System

Having examined both the silica support and bulk chromium oxides by XPS, the next step was to examine the Phillips catalyst itself. Two systems were examined. The traditional system, CrO_3/SiO_2 and $Cr_3(OH_2)(Ac)_7/SiO_2$.

5.3.1 XPS of SiO_2 / 1% Cr(VI)

Samples of the catalyst were activated under an oxygen atmosphere. The temperature was increased at a rate of 1°C/minute to 780°C, where it was maintained for five hours under a slow oxygen flow (1 l/hour). The catalyst was then allowed to cool under oxygen to room temperature at the same rate. The orange catalyst sample was then transferred (without exposure to the atmosphere) to a nitrogen atmosphere dry box from where it could be introduced into the spectrometer. XPS data were collected in the regions for chromium, oxygen and silicon. The results obtained from both the silicon and oxygen regions were uninformative, both resembling the spectra that were obtained for blank silica. This is believed to be due to the low chromium oxide content at the surface (typically 1%). The $Cr(2p_{3/2})$ spectra were more informative, Figure 5.19.

$$\text{Cr } (2p_{3/2})\text{: } 579.7 \text{ eV} \xrightarrow{O_2 \,/\, \Delta} 578.6 \text{ eV} \quad \Delta E = -1.1 \text{ eV}$$

$$\text{Cr : Si } 0.31 \xrightarrow{O_2 \,/\, \Delta} 0.26$$

Figure 5.19 *Comparison of the $Cr(2p_{3/2})$ XPS data obtained from unactivated and activated CrO_3/SiO_2.*

Activation is commonly believed to anchor the previously bulk chromium oxide to the silica surface through two siloxide bonds: Cr-Si-O.[59] This results in the formation of chromate-like species at the silica surface. The binding energy of 578.5 eV for the activated catalyst is in excellent agreement with the value obtained when bulk Cr_2O_3 was heated to similar temperatures (578.2 eV, Section 5.2.1). The latter was ascribed to the formation of chromate- or dichromate-like species at the oxide surface. The XPS data are thus consistent with the idea that there are indeed, chromate type species present at the surface of activated Phillips catalysts. Differentiation between the two proposed structures (**a**) and (**b**) in Figure 5.20 is not possible using XPS, as the electronic environment of chromium in both structures is similar.

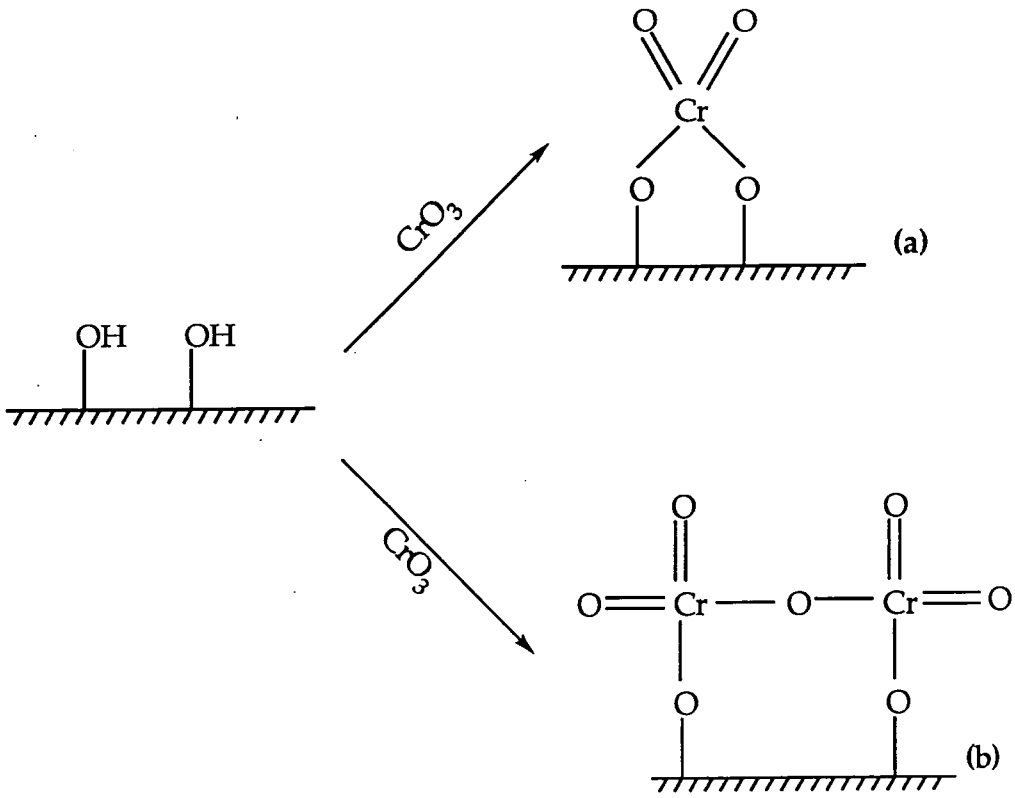

Figure 5.20 *Oxygen activation process to afford either chromate (a) or dichromate (b) species at the surface.*

McDaniels has studied this problem using IR.[13] His study indicated that for impregnations of up to 3% Cr, subsequent oxygen activation formed solely chromate (a) type structures on the silica surface.

The change in the chromium to silicon ratio that was observed 0.31 (unactivated) and 0.26 (activated) is consistent with "Cr" species becoming mobile in this temperature range and "spreading" over the silica surface. Similar mobility of chromium species across the support surface has been observed in an ^{29}Si (MAS) NMR study.[60]

One surprising feature of this XPS study was that an N (1s) signal was observed at 401.2 eV. This is characteristic of molecular physisorbed N_2. Again, as for the bulk oxides, this has been attributed to the extreme reactivity of the chromium species that are generated at the surface during the activation process. Once again, the isoelectronic relationship of N_2 and CO is cited to explain this phenomenon. CO is known to react readily with the activated Phillips catalyst. To the best of our knowledge there has been only one other report of nitrogen interacting with silica supported chromium species, in which N_2 was observed to chemisorb weakly by IR.[58]

5.3.2 XPS Studies on SiO_2 / 1% Cr (III) acetate

A similar study was performed on silica impregnated with chromium (III) acetate (to 1% Cr). The results from this analysis are presented in Figure 5.21.

$$Cr\ (2p_{3/2})\text{: } 578.2\ eV \xrightarrow{O_2\ /\ \Delta} 578.5\ eV \quad \Delta E = +0.3\ eV$$

$$Cr : Si\ 0.46 \xrightarrow{O_2\ /\ \Delta} 0.29$$

Figure 5.21 *Cr ($2p_{3/2}$) XPS results from activated and unactivated $Cr_3(OH)_2(Ac)_7/SiO_2$.*

The Binding Energy of the new chromium species (578.5 eV) is identical, within experimental error, to the value obtained for the CrO_3/SiO_2 system. This implies that the two systems possess similar chromium species after activation. This is consistent with the data obtained for the polymerisation process and for the properties of the polymer obtained from each system.[61]

Similarly, the degree of "spreading" of chromium across the surface, as measured by the Cr : Si ratio is virtually the same as for the CrO_3/SiO_2 system (Figure 5.19).

5.4 Mass Spectroscopic Studies of SiO_2 / Acetic Acid and SiO_2 / Cr(III) Acetate

The polymerisation mechanism of the Phillips catalyst has remained the focus of study since its discovery in the early 1950's.[62] Recently, industrially based chromium catalysts have moved away from the original chromium (VI) systems, and now use silica impregnated with soluble chromium (III) precursors. Activation of these chromium (III) systems affords catalysts that are identical in their activity and in the resultant polymer properties to the older chromium (VI) systems.

This current study has focused on the activation of a chromium (III) acetate / silica catalyst. To study the activation of the final catalyst a model catalyst system was built up from the individual components, or their closest analogues. The information obtained from each stage was then applied to the actual catalyst system. Break-up of the individual components has revealed interactions that can not be observed from a study of the actual catalyst system itself.

Control samples comprised of bulk chromium acetate, high surface area silica (Section 5.1.1), and silica washed with acetic acid (to 1 wt % acetate), followed by rinsing with distilled water.[63] The catalyst precursor was prepared by impregnating silica with an aqueous solution of basic chromium acetate $Cr_3(OH)_2(CH_3CO_2)_7$ (Crosfield Chemicals) and then dried.

Small (1g) samples of the various materials were loaded into a quartz microreactor. The reactor was then purged with the appropriate carrier gas (argon or oxygen). Subsequently, TPD studies were performed. These involved the slow heating of each sample (1°C/min) to 780°C. During this process the carrier gas was monitored using an *in situ* quadrupole mass spectrometer. This was multiplexed with a PC, which allowed up to 50 mass fragments to be analysed simultaneously.

TPD peak heights were normalized with respect to mass 20 under argon, and mass 16 under oxygen, and then multiplied by a factor of 100. A strong mass 14 signal was taken as being indicative of ketene;[64] whereas intense peaks at mass 15 and mass 16 were characteristic of methane. The assignment of carbon monoxide, oxygen and carbon dioxide was confirmed by the absence of adjacent hydrocarbon masses.

Molecule	Masses
$CH_2=C=O$	14
CH_4	16, 15
H_2O	18
CO	28
O_2	32
CO_2	44

Table 5.8 *Assignment of masses evolved during TPD experiments.*

5.4.1 TPD of Acetic Acid / Silica

Silica impregnated with aqueous glacial acetic acid exhibits physisorbed water desorption temperatures of around 110°C, Figure 5.22. The amount of physisorbed water desorbing is reduced relative to blank silica for both oxygen and argon treatments, Tables 5.2, and 5.9.

Mass	110°C	320°C	380°C	500°C
14	1.6	0.2 (b)	—	—
18	3.0	—	—	0.5
16	0.2	—	—	—
44	0.6	—	0.4	—
	H_2O + CH_2=C=O + CH_4 + CO_2	CH_2=C=O	CO_2	H_2O (b)

Table 5.9 *Summary of TPD feature peak heights for acetic acid / silica under argon (uncorrected for mass spectrometer sensitivity).*

Under argon, water evolution occurs at the same low temperature that mainly ketene and carbon dioxide are evolved, Schemes 5.1 and 5.2. The formation of ketene through decomposition of surface acetate groups formed by the dissociation of acetic acid on metal surfaces is well documented.[65,66,67] However, this decomposition is known to be somewhat more complicated on oxide surfaces.[68]

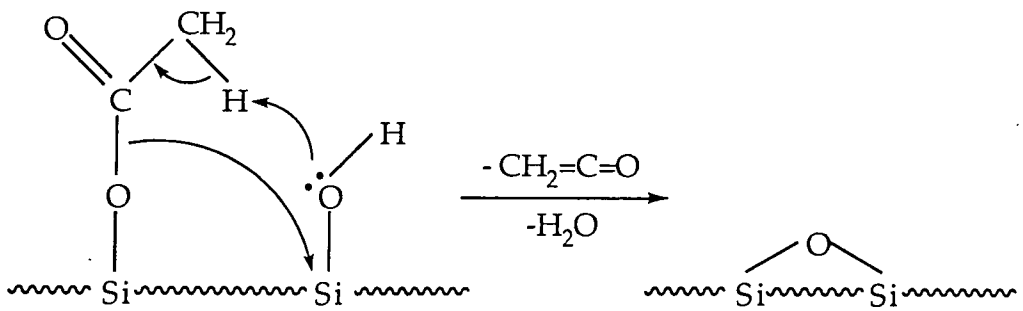

Scheme 5.1 *Mechanism of ketene formation from silica impregnated with acetic acid*

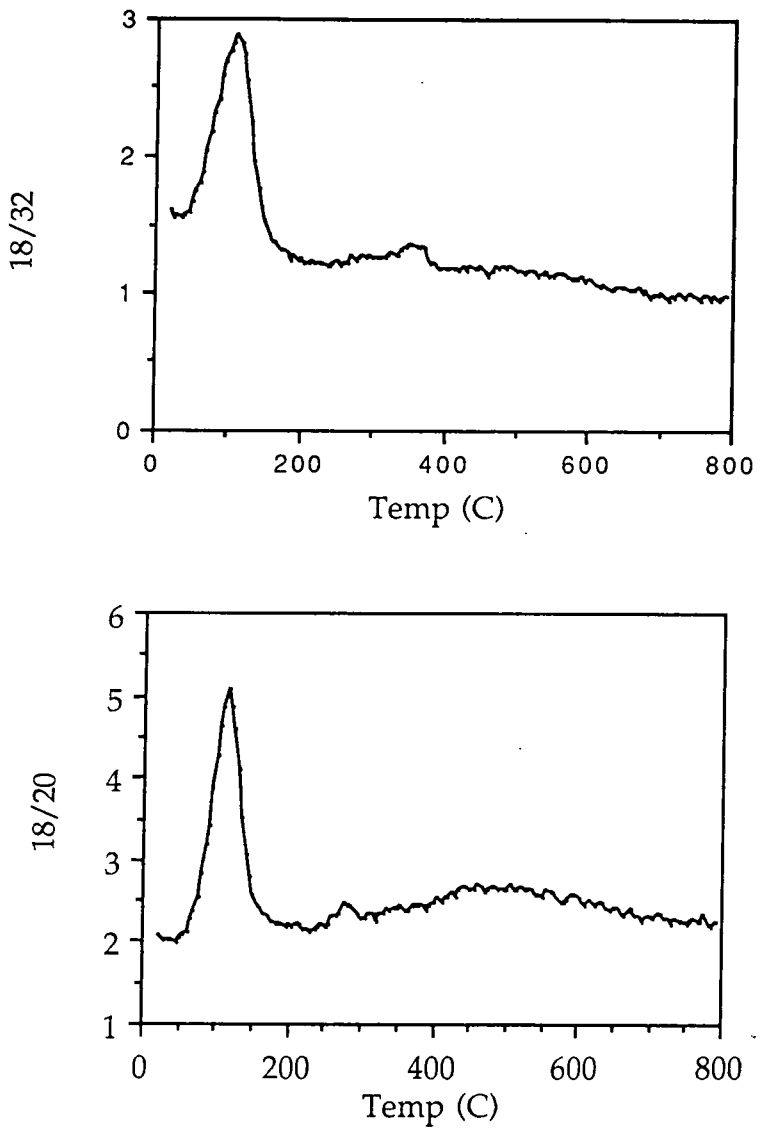

Figure 5.22 *Comparison of the water loss profile from SiO_2/Acetic acid under oxygen (top) and under argon (bottom).*

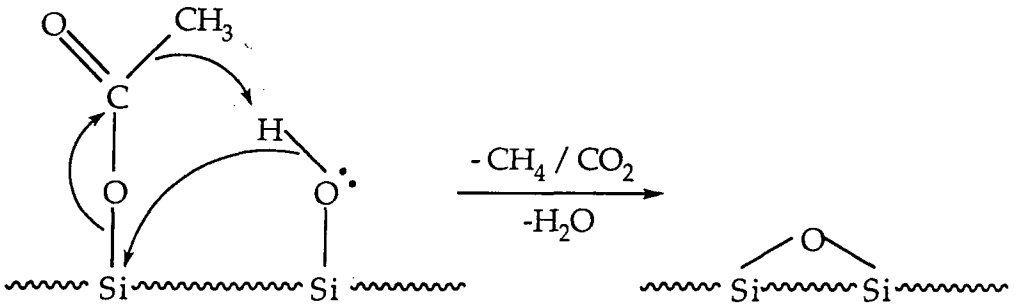

Scheme 5.2 *Mechanism of methane and carbon dioxide formation from silica impregnated with acetic acid*

The high temperature water peak, centred at approximately 500°C, is strongly attenuated with respect to the blank silica sample. This suggests that either surface hydroxyls are consumed at lower temperatures for this system forming ketene and carbon dioxide , or that surface hydroxyls were replaced by acetate groups during the wet impregnation step (Equation 5.3). Some carbon dioxide is also evolved at higher temperatures (380°C), and most probably originates from the decomposition of chemisorbed acetate groups. Similar decomposition products were obtained in a study by Madix.[69] Acetic acid adsorbed on an Ag(110) single crystal gave CO_2, CH_4, ketene and CH_3COOH as decomposition products at 640K.

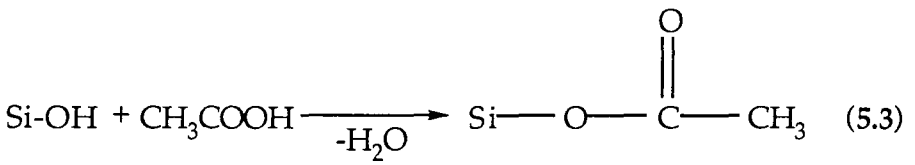

(5.3)

In the case of oxygen carrier gas (Table 5.10), the broad high temperature water feature remains attenuated compared to the oxygen treated silica sample. The selectivity of reactions occurring at low temperatures shifts in favour of combustion products (i.e. carbon monoxide and carbon dioxide) rather than ketene.

Mass	110°C	360°C
14	1.0	—
18	2.5	0.5
28	0.6	0.3
44	1.9	0.5
	H_2O $CH_2=C=O$ $CO + CO_2$	$CO_2 + CO$

Table 5.10 *Summary of TPD feature peak heights for acetic acid / silica under oxygen carrier gas (uncorrected for mass spectrometer sensitivity).*

5.4.3 TPD of Bulk $Cr_3(OH)_2(Ac)_7$

As for the silica and silica /acetic acid samples the bulk acetate was also subjected to a TPD analysis. On completion of the experiment under argon, the residue in the microreactor was still dark green in appearance, consistent with the sample having been converted to chromium (III) oxide.[70]

Mass	380°C	400°C	450°C
12	—	0.5	—
14	1.0	—	0.8
15	—	4.0	3.8
16	—	5.5	5.2
32	3.2	—	4.0
28	0.2	—	4.0
44	3.5	7.9	5.0
H_2O (b) 50-380°C	$CO+ O_2$ $+ CH_2=C=O$	$CO_2+ CH_4$	$CO_2+ CH_4$ $+ CO+ O_2$ $+ CH_2=C=O$

Table 5.11 *Summary of TPD feature peak heights for bulk $Cr_3(OH)_2(Ac)_7$ under argon (uncorrected for mass spectrometer sensitivity). (b) indicates that the peak was broad.*

The evolution of carbon dioxide and methane at 400°C occurs at the temperature at which water desorption drops, indicating that surface species which lead to water formation are consumed during carbon dioxide and methane production. This higher temperature profile results from simple combustion of ketene, CO and oxygen. Both types of decomposition mechanism operate at 450°C. Scheme 5.3.

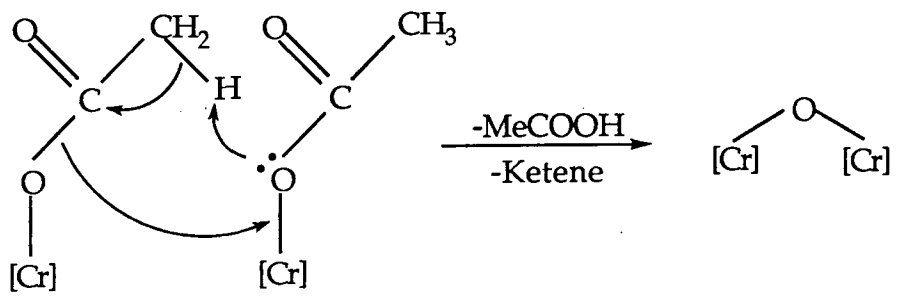

Scheme 5.3 *Reaction occurring at 380°C for decomposition of $Cr_3(OH)_2(Ac)_7$ under argon.*

On completion of the experiment under oxygen, the residue was again green in appearance.[22] The use of oxygen as carrier gas led to the simple combustion of the chromium acetate at 280°C.

Mass	280°C
28	21.0
44	6.8
H_2O (b) 50-490°C Dip at 230°C	$CO + CO_2$

Table 5.12 *Summary of TPD feature peak heights for bulk $Cr_3(OH_2)(Ac)_7$ under oxygen (uncorrected for mass spectrometer sensitivity).*

5.4.4 Silica impregnated with 1% Cr (III) acetate

On completion of the experiment under argon, the residue in the microreactor was green in appearance, this can be taken as being indicative of Cr (III). There is a window in the H_2O profile (Figure 5.23) which corresponds to the onset of precursor decomposition during which methane and carbon dioxide are evolved. Scheme 5.4. At this temperature there was a slight dip in the mass 18 (H_2O) TPD profile. This

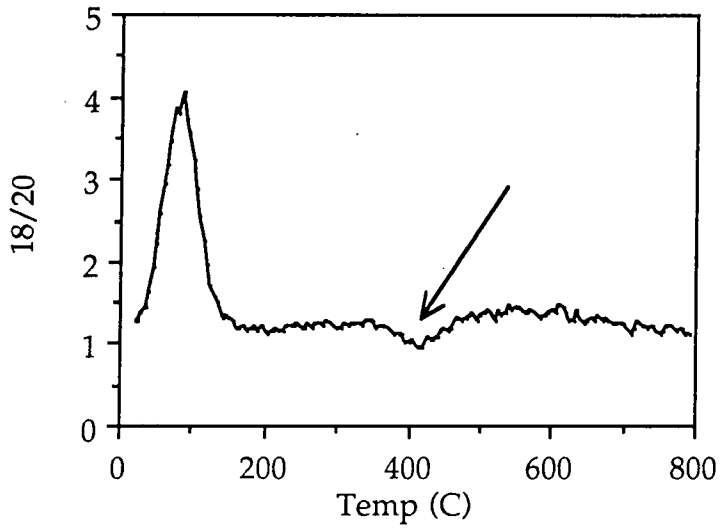

Figure 5.23 *Water loss profile for $Cr_3(OH)_2(Ac)_7/SiO_2$ under argon. The arrow indicates the "dip" in the profile.*

is believed to result from consumption of H_2O forming species during the combustion reaction. Combination of the latter with the observation that methane is evolved implies that mobile surface protons are used to form methane, this being the only likely source.

$$Cr(CH_3CO_2) + Si—OH \xrightarrow{Ar} Si—O—Cr + CO_2 + CH_4$$

Scheme 5.4 *Reaction of surface protons with bound acetate groups with subsequent formation of methane.*

Mass	90°C	400°C	600°C
15	—	0.9	—
16	—	1.1	—
18	2.8	0.3 dip	2.0 (b)
28	0.2	0.3	—
44	—	1.1	—
	$H_2O + CO_2$	$CO_2 + CH_4$	H_2O

Table 5.13 *Summary of TPD feature peak heights for silica impregnated with Cr(III) acetate under argon (uncorrected for mass spectrometer sensitivity). (b) indicates that the profile is very broad.*

This reaction occurs at precisely the same temperature (400°C) to that observed for bulk chromium acetate under the same conditions. However, the adjacent TPD features previously noted for bulk chromium acetate are absent when supported on silica.

Mass	110°C	90°C
14	0.1	—
18	1.3	0.2
28	0.5	0.2
44	1.5	0.5
	$CO_2 + CO + H_2O$	$CO_2 + CO + H_2O$

Table 5.14 *Summary of TPD feature peak heights for silica impregnated with Cr(III) acetate under oxygen (uncorrected for mass spectrometer sensitivity).*

On completion of the experiment under oxygen, the residue in the microreactor had turned bright orange, which was taken as being

indicative of Cr (VI). Carbon dioxide and water are the major desorption species during thermolysis. Carbon monoxide is most likely to arise from incomplete combustion of the methyl groups contained in the acetate groups. This partial combustion is thought to occur through slow "delivery" of oxygen to the surface in an equilibrium set up by the adsorption and desorption of surface species.

It is interesting to note that chromium acetate supported on silica decomposes much more readily than in its bulk state (i.e. at lower temperatures). The availability of surface species opens up new decomposition pathways that are not present in the bulk.

5.4.5 Mass Spectroscopic Studies of SiO_2 / CrO_3

An identical *in situ* mass spectroscopic study of the activation of the CrO_3/SiO_2 system has been carried out. Again, the catalyst (1g) was loaded into the microreactor and the system purged with the appropriate carrier gas (argon or oxygen) before commencing the experiment.

When oxygen carrier gas was used the only product that was observed was water. This was evolved in one broad peak at 110°C with a relative intensity comparable to that associated with the chromium (III) acetate system (≈1.0). A broad, high temperature water loss feature was observed, centred at ≈480°C. This is believed to correspond to the transformation of bulk oxide into the surface anchored chromate species. After thermolysis the catalyst is a characteristic bright orange.

When the same experiment was repeated using argon as carrier gas the catalyst turned green. Water and a small quantity of oxygen was evolved in a broad feature starting at approximately 180°C. This was taken as being indicative of decomposition of CrO_3 giving Cr_2O_3.

5.4.6 Conclusions

The mechanism for dehydroxylation of untreated silica under argon and oxygen appear to differ markedly in the amount of water that is actually removed from the oxide surface. The dehydroxylation process occurs between neighbouring hydroxyl groups, which combine to eliminate water.[9] Under oxygen it appears that this process is inhibited, possibly due to the physisorption or weak chemisorption of either O_2 or

O^{2-}; this is likely to inhibit proton migration across the oxide surface meaning that only physically adjacent hydroxyl groups can interact to eliminate water.

TPD analysis performed under both argon and oxygen of bulk $Cr_3(OH)_2(Ac)_7$ and $Cr_3(OH)_2(Ac)_7$ impregnated onto silica, revealed that the reaction mechanism is intimately dependent upon the carrier gas used. Generally, samples treated under dry argon exhibited the desorption of ketene indicated by the presence of mass fragment 14.[69] Surprisingly, the decomposition pathway altered slightly for the supported sample under argon, which showed both a lower decomposition temperature and the *direct* involvement of a surface proton species. This reacted with acetate groups liberating methane. Both supported and unsupported samples of the acetate exhibited partial combustion when treated under an oxygen atmosphere as expected.

The observation that the surface hydroxyl groups can play an active part in the chemistry that occurs at the oxide surface has important implications for the polymerisation mechanism of the Phillips catalyst. Often, the hydroxyls are assumed to have no rôle in this reaction.[35,71]

5.5 Mass Spectroscopic Investigation of the Ethene Polymerisation Process

In an attempt to probe the first insertion process of an active Phillips type catalyst with ethene, the same *in situ* mass spectroscopic system was utilised. Throughout this study the $Cr_3(OH)_2(Ac)_7/SiO_2$ catalyst was employed. Activation was achieved by calcination under an oxygen flow (1 l/hour). The temperature was increased at 1°C/min to 780°C where the temperature was maintained for 5 hours. The system was allowed to cool under an oxygen flow. During the activation process mass spectra were recorded. These were compared with the results obtained in Section 5.4.4. If either the mass spectra differed or if after activation the catalyst was not orange it was discarded and presumed inactive.

5.5.1 A Mass Spectroscopic Study of the CO Pre-reduction Catalysts

It is well documented that if, after calcination under oxygen, the active orange catalyst is pre-reduced under a flow of carbon monoxide at elevated temperatures then the induction time before ethene polymerisation occurs is eliminated.[72] The reaction is generally assumed to generate chromium carbonyl species which then react with ethene. To study this process further a sample of the catalyst was calcined under oxygen as normal. The system was then cooled to 350°C under oxygen affording a bright orange catalyst. Neat CO was then passed over the catalyst at this elevated temperature for 15 minutes while mass spectra were being collected.

On contacting CO the catalyst instantaneously turned a very intense bright red. This colour faded over a period of one minute to give a dark blue/green coloured catalyst, known to be characteristic of the pre-reduced system.[73] No further changes were apparent.

Carbon dioxide was evolved simultaneously with the formation of the intense red colour (Figure 5.24). No other species were observed over the mass range 1-50. The two terminal oxo groups present are removed from the chromium centre as CO_2 leaving a chromium carbonyl species at the surface (Scheme 5.5). IR studies have proved inconclusive as to the nature of the resultant carbonyl,[74] although chemisorption experiments indicated that the dicarbonyl was the preferred product from reduction at approximately 300°C.

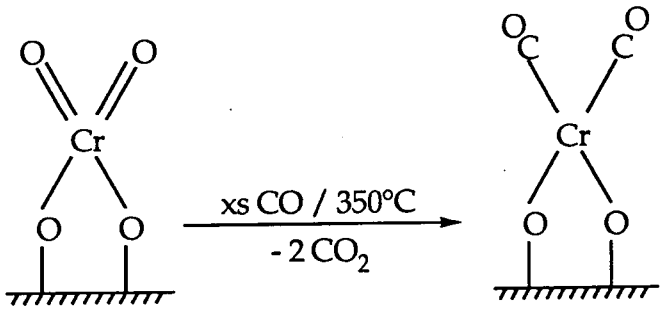

Scheme 5.5 *Pre-reduction using CO.*

After CO pre-reduction the system was switched over to a dry argon gas flow (1 l/hour) and purged while the temperature was allowed to reach 110°C. At this temperature ethene was admitted as a 50/50 argon mix at a similar flow rate. Mass spectroscopic studies were performed throughout the ethene reaction time (typically three hours).

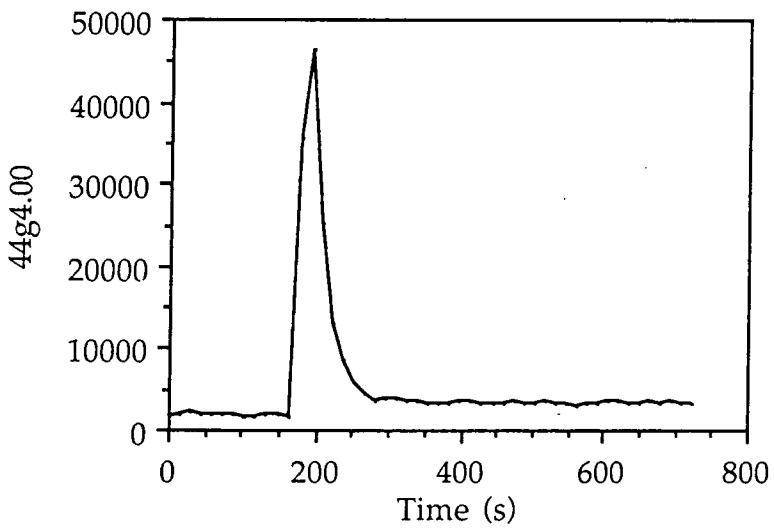

Figure 5.24 *Treatment of activated $Cr_3(OH)_2(Ac)_7/SiO_2$ with CO leads to the evolution CO_2 at 350°C.*

The IR studies of Ghiotti and co-workers demonstrated that at low pressures (≤ 15 torr) reversible ligand displacement reactions occur. Our mass spectroscopic study was unable to detect the dissociation of CO when ethene was admitted to the system. The large ethene concentration swamped the mass 28 fragment, and thus the small amount of CO likely to be liberated could not be detected. To overcome this problem a smaller amount of ethene (≈20cm^3) was passed over a freshly pre-reduced catalyst sample. Disappointingly, the concentration of ethene was still too large to allow for an accurate comparison of the known fragmentation pattern of ethene with the fragmentation obtained in this experiment. Further studies are required to overcome the problems associated with the large volumes of ethene present. The use of isotopically enriched ethene is envisaged to be the most convenient solution.

5.5.2 A Mass Spectroscopic Study of the Interaction of Ethene with an Activated Sample of $Cr_3(OH)_2(Ac)_7/SiO_2$

In attempts to probe the ethene induced catalyst reduction and subsequent polymerisation initiation process a sample of the $Cr_3(OH)_2(Ac)_7/SiO_2$ catalyst was activated under an oxygen flow as above. After five hours at 780°C the catalyst was allowed to cool under oxygen to 150°C where the temperature was maintained. Argon was used to purge oxygen from the reactor system until no trace of oxygen could be detected mass spectroscopically (≈2-3 hours). Ethene was then admitted to the reactor as a 50/50 argon mixture at a flow rate of approximately 1 l/hour for three hours.

Mass spectra were obtained for all masses between 0 and 50. The analysis of the fragmentation patterns was again complicated by the large excess of ethene present. Unfortunately the experimentally determined fragmentation[75] of the predicted product methanal[24] coincides with that determined for ethene. However, a pulse of water (characterised by masses 17 and 18) was observed as the sample contacted ethene. CO_2 was also evolved over the same time span, decaying away only slowly (Figure 5.25). The source of the water remains a mystery although comparable amounts were obtained from other experiments with the same system. One possible origin may be that during oxygen activation the gas flow was insufficient to remove all the water from the surface. A number of

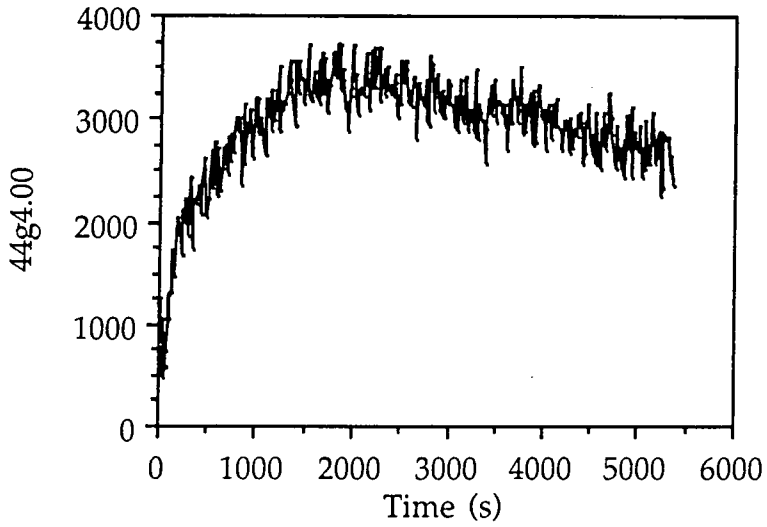

Figure 5.25 *On contacting ethene an activated sample of $Cr_3(OH)_2(Ac)_7/SiO_2$ liberates CO_2. The quantity of CO_2 being liberated slowly decreases with time.*

researchers[76] have speculated that an inadequate gas flow during oxygen activation can lead to the formation of silanol groups adjacent to the chromium centres leading to an inactive catalyst. To this end samples of the catalyst that had been treated with ethene were subjected to a thermal desorption study. If oxygen was used as carrier gas trace quantities of CO_2 and water were observed; trace amounts of carbon monoxide and water were observed if the experiment was repeated using argon carrier gas. These results were inconclusive, as similar products could be envisaged from combustion of adsorbed ethene. Hence, a sample of the ethene treated catalyst has been submitted for analysis by electron microscopy in an attempt to see either silica fragmentation or small quantities of polymer.

In an attempt to identify the products from the initiation step activated catalyst was treated with a flow of dry propene. A significant amount of mass 44 (propanal) was detected. However, in light of the observation of CO_2 evolution from the analogous reaction with ethene no weight can be lent to this result.

Further mass spectroscopic studies are required to fully investigate the chemistry associated with the ethene reaction. To be able to accurately compare fragmentation patterns and relative intensities an internal inert reference is required. Thus, a mixture of ethene/helium of known concentration could be used. Some details of the reaction may be more readily understood if GC-MS was employed to examine the gaseous products evolved.

It would be interesting to probe the initial olefin induced reduction with a number of other olefins such as cyclohexene, but-2-ene, and styrene. In all cases carbon-carbon double bond cleavage would be expected with subsequent aldehyde generation.

5.6 A Possible Mechanism of Initiation and Polymerisation for the Phillips Catalyst

The involvement of surface protons has important implications for the Phillips catalyst. As mentioned in the text, a number of research groups using IR techniques have speculated over the involvement of silanol groups in the polymerisation process. Our study of silica/acetate systems lends direct evidence for their involvement. Consideration of the

chemistry of both molecular systems and the related Unipol system (Cp_2Cr/SiO_2) has allowed us to tentatively propose a mechanism for the initiation of polymerisation for the Phillips catalyst which involves protonation by surface hydroxyl groups (Scheme 5.6).

Initial impregnation and removal of solvent leaves bulk chromium (VI) oxide deposited on the silica surface. High temperature oxygen activation is presumed to afford a chromate-like species (**A**) on the oxide surface. A reactive chromium centre results from reduction of the surface chromate species. This reduction can be achieved by either pre-reduction with CO to afford a chromium dicarbonyl species (**B**) or by ethene itself. The latter reaction has been shown to proceed *via* oxidation of the olefin forming two equivalents of methanal. The pre-reduced catalyst is known to react immediately with ethene with subsequent formation of polymer.

The polymer obtained from both normal and pre-reduced catalysts is identical. IR studies have shown that displacement of CO by ethene is relatively facile. Thus, it is likely that the chromium centre after ethene induced dissociation of CO is similar to that achieved through simple reduction with ethene (**C**). This leaves a di-olefin complex analogous to that proposed by Ghiotti (Section 5.0). The induction time observed with normal Phillips systems has long been attributed to the slow reduction of the di-oxo complex by ethene.

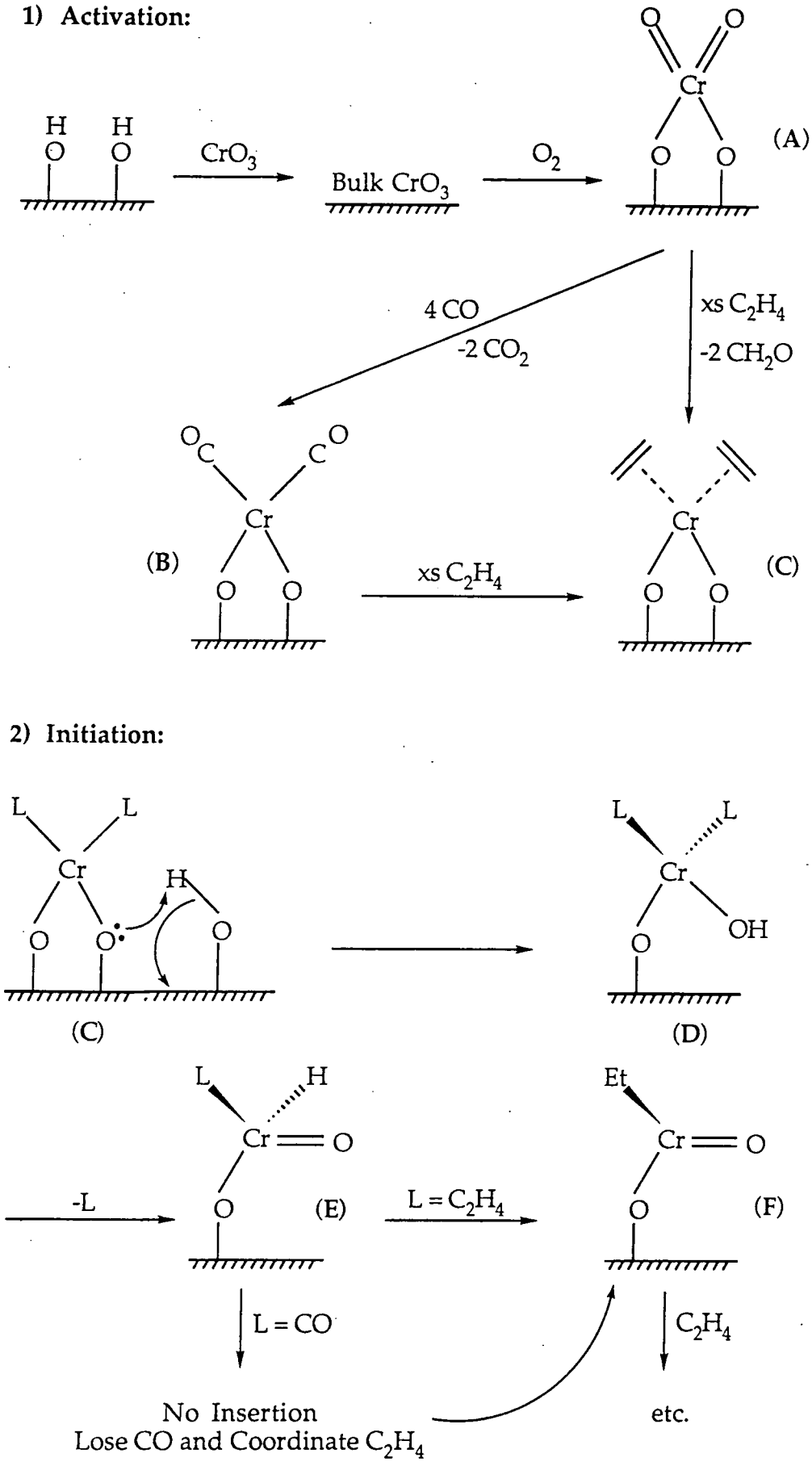

Figure 5.6 *Mechanism of activation and initiation proposed for the Phillips Catalyst.*

Once olefin coordination to the reduced metal centre has been achieved polymerisation initiation appears facile. Surface protons have been shown to interact readily with acetic acid and chromium (III) acetate impregnated onto silica. Thus, similar interactions are likely for species (**C**) (Scheme 5.6, Step 2). It is not unreasonable to invoke an interaction between one of the two siloxide oxygens with a neighbouring silanol group. This could transiently form a species like that represented by (**D**). A rearrangement is likely which would result in the formation of a chromium-oxo hydride (**E**) with concomitant loss of ethene (L). Insertion of ethene into the metal hydride resulting in the formation of an oxo alkyl (**F**) should prove facile. Subsequent polymerisation *via* a normal insertion mechanism is likely for chain propagation.

Comparisons with molecular chemistry indicate that both metal-oxo hydrides and alkyls can be synthesised and have proved quite stable. Bercaw *et al* reported the isolation of the first well defined oxo hydride complex, $Cp^*_2Ta(H)(=O)$. This was obtained through hydrolysis of the methylidene complex $Cp^*_2Ta(H)(=CH_2)$ and was believed to proceed *via* a tantalum hydroxide species, presumably through intramolecular O-H α-H elimination (Equation 5.4).[77]

$$Cp^*_2Ta(H)(=X) \xrightarrow[-H_2X]{H_2O} [Cp^*_2Ta\text{-}OH] \longrightarrow Cp^*_2Ta(H)(=O) \qquad (X = CH_2, C{=}CH_2) \qquad (5.4)$$

Similarly, Mayer and co-workers have described the synthesis and characterisation of both rhenium-oxo hydride and alkyl complexes (Equations 5.5 and 5.6).[78]

$$Re(O)I(MeC{\equiv}CMe)_2 + Zn^iPr_2 \longrightarrow$$

$$Re(O)^iPr(MeC{\equiv}CMe)_2 + [Re(O)(MeC{\equiv}CMe)_2]_2 \qquad (5.5)$$

$$Re(O)I(MeC{\equiv}CMe)_2 + {}^nBu_3SnH \longrightarrow$$

$$Re(O)H(MeC{\equiv}CMe)_2 + {}^nBuSnI \qquad (5.6)$$

More recently, and perhaps more interestingly Theopold *et al* have described the synthesis of high-valent chromium-oxo alkyl complexes (Scheme 5.7).[79] This indicates that the species proposed in Scheme 5.6 are tenable, although it was shown that neither $Cp^*Cr(O)_2(Me)$ nor $Cp^*Cr(O)(Me)_2$ reacted with ethene. This report does however underline the fact that strongly π-donating oxo ligands can stabilise unusually high oxidation state complexes.

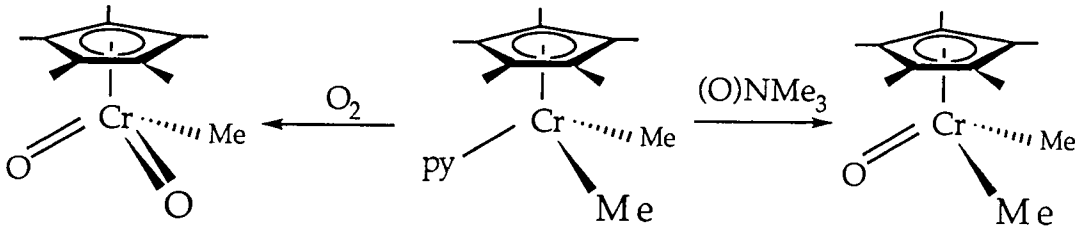

Scheme 5.7 *Synthesis of Chromium-oxo alkyl complexes.*

Further indirect support for the mechanism proposed in Scheme 5.6 can be gained from consideration of the related Unipol system (Cp_2Cr/SiO_2). Applying the same mechanism as in Scheme 5.6 results in the formation of the silica bound species "CpCr(H)" (Scheme 5.8 (**b**)) through reaction of the chromium centre with an adjacent silanol. Yet, if the mechanism is reversed with attack of the siloxide oxygen on a silanol proton the chromium complex would be lost from the surface. It is well known that in the Unipol process the "CpCr" moiety remains bound to the oxide support, and that the Cp ligand does not become incorporated into the growing polymer chain on reaction with ethene.[80]

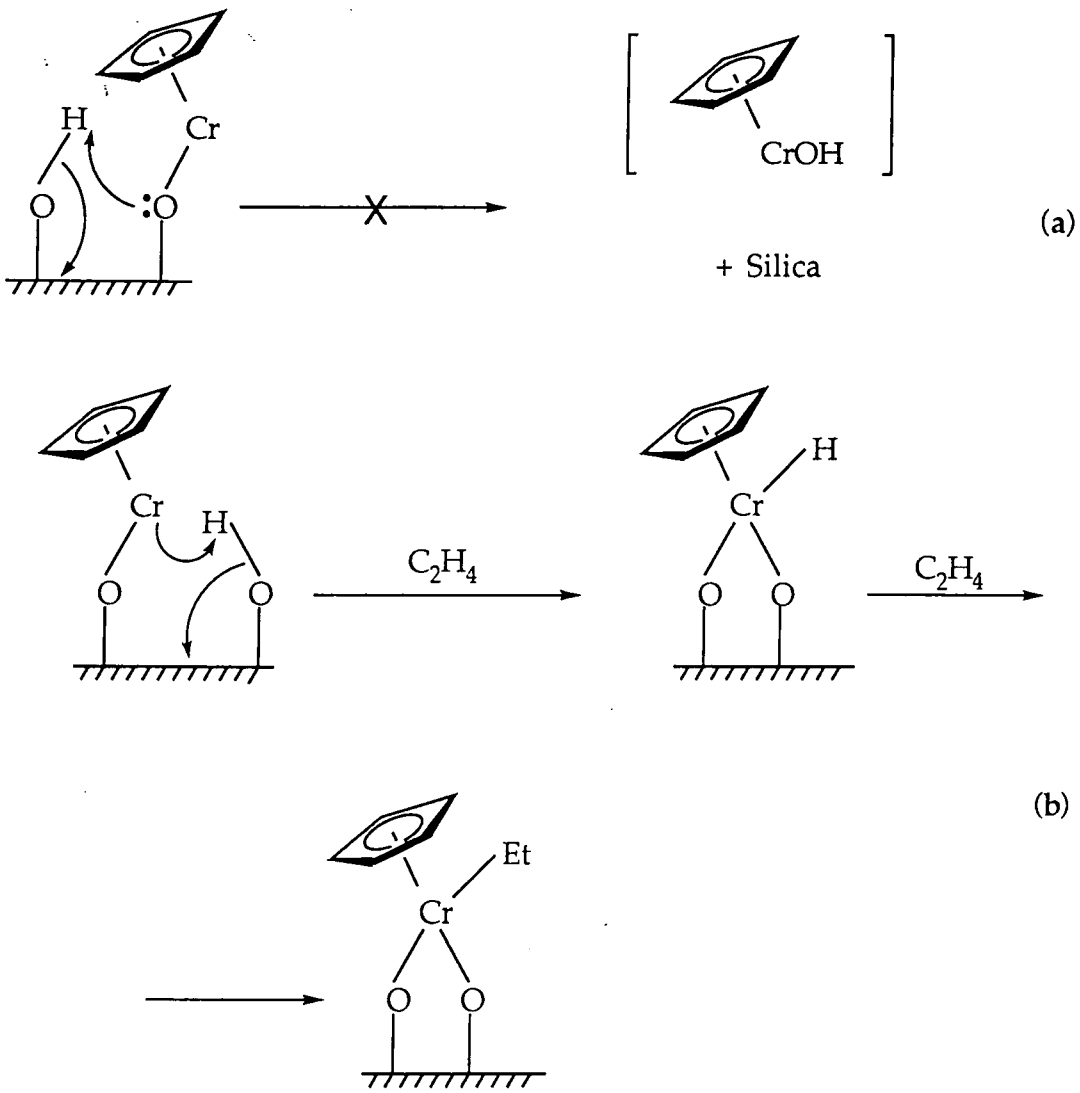

Scheme 5.8 *Possible mechanism for polymerisation initiation of the Unipol catalyst.*

Poliakoff and co-workers[81] have studied intermolecular hydrogen-bonding to uncharged metal centres. A spectroscopic investigation in hydrocarbon and supercritical xenon and krypton between fluoro alcohols and $(\eta^5\text{-}C_5R_5)ML_2$ (R= H, Me; M= Co, Rh, Ir; L= CO, C_2H_4, N_2 and PMe_3) was undertaken. Their experiments showed that H-bonding was relatively widespread. In addition the experiments in supercritical xenon indicated that this H-bonding can lead to protonation of the metal centre. This observation indicates that the interaction of the chromium centre in Scheme 5.8 (**b**) with an adjacent silanol is reasonable. This first step could be viewed as in Figure 5.27.

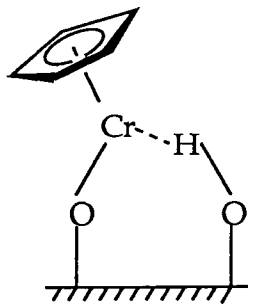

Scheme 5.27
Possible Hydrogen Bonding Interaction between a surface chromium species and an adjacent silanol group.

In summary, the mechanism proposed in Scheme 5.6 seems likely from results obtained for homogeneous systems. Furthermore, it agrees with other studies by Groenveld and Dalla Lana who both intimated that silanol groups play a major role in catalysis by supported chromium oxide species.

5.7 Summary

Examination of the thermolysis of Cr_2O_3 by XPS indicated that a new high binding energy O (1s) signal became apparent under an oxygen atmosphere. Comparison with samples of K_2CrO_4 led us to conclude that chromate-like functionalities were formed at the oxide surface.

Further XPS studies on the oxygen activation of CrO_3/SiO_2 and $Cr_3(OH)_2(Ac)_7/SiO_2$ indicated that similar chromium species were formed. Comparison of the Cr:Si ratios of both systems indicated that during the thermolysis "spreading-out" of the chromium over the oxide surface occurred. Surprisingly, examination of the N (1s) XPS region for samples of activated Cr_2O_3 and CrO_3/SiO_2 revealed that dinitrogen was adsorbing at the surface, an indication of the extreme reactivity of the chromium sites generated.

An *in situ* mass spectroscopic study of the thermolysis of silica, silica/acetic acid and silica/$Cr_3(OH)_2(Ac)_7$ indicated that the oxide is not innocent as often assumed. The silica can readily act as a proton source and can thus determine the course of the chemistry associated with the surface. This in combination with results from a number of molecular systems allowed us to propose a mechanism for the initiation and polymerisation by the Phillips catalyst.

Cursory examination of the initial reaction of ethene with activated samples of the Phillips catalyst indicate that activation conditions can

dramatically alter the nature of the resultant catalyst. Further studies using isotopically enriched olefins and internal intensity references are required to fully examine this process.

5.8 References

1 Y. Iwasawa (ed.), *"Tailored Metal Catalysts"*, Reidel, Dordrecht, 1986, and references therein.

2 Y. Iwasawa, *Adv. Catal.*, 1987, **35**, 187.

3 Degussa AG., Technical Bulletin No. 72: Pigments.

4 M. Schraml-Marth, K.L. Walther, A. Wokaun, B.E. Handy, and A. Baiker, *Journal of Non-Crystalline Solids*, 1992, **143**, 93.

5 "Aerosil Fumed Silica," Technical Bulletin, Degussa AG.

6 A.J. McFarlan and B.A. Morrow, *J. Phys. Chem.*, 1991, **95**, 5388; A.J. McFarlan and B.A. Morrow, *J. Phys. Chem.*, 1992, **96**, 1395; J. Jagiella, G. Ligner, E. Papirer, *J. Col. and Int. Sci.*, 1990, **137**, 1990; A. Burneau, O. Barrés, J.P. Gallas, J.C. Lavalley, *Langmuir*, 1990, **6**, 1364; B. Himmel. T,H. Gerber, and A.G. Neumann, *Physica Status Solidi A*, 1985, K127; G. Ligner, A. Vidal, H. Balard, E. Papirer, *J. Col. and Int. Sci.*, 1989, **133**, 200; G. Ligner, A. Vidal, H. Balard, E. Papirer, *J. Col. and Int. Sci.*, 1990, **134**, 486; A. Burneau, O. Barrés, A. Vidal, H. Balard, E. Papirer, *Langmuir*, 1990, **6**, 1389; I. Tsuchiya, *J. Phys. Chem.*, 1982, **86**, 4107.

7 A.J. Van Rosmalen and J.C. Mol, *J. Phys. Chem.*, 1978, **82**, 2748.

8 B.A. Morrow and I.A. Cody, *J. Phys. Chem.*, 1976, **80**, 1995.

9 W.K. Hall, *Acc. Chem. Res.*, 1975, **8**, 257.

10 J.P. Hogan and R.L. Banks, U.S. Pat. 2,825,721 (filed Aug. 1954, issued Mar 1956).

11 E.A. Benham, P.D. Smith, E.T. Hsieh, and M.P. McDaniel, *J. Macromol. Sci. -Chem.*, 1988, **A25**, 259.

12 A. Zecchina, E. Garrone, G. Ghiotti, C. Morterra, and E. Borello, *J. Phys. Chem.*, 1965, **79**, 966; J. Hogan, *J. Polym. Sci., Part A*, 1970, **8**, 2637.

13 M.P. McDaniel, *J. Catal.*, 1981, **67**, 71.

14 D.S. Kim, J.M. Tatibout, and I.E. Wachs, *J. Catal.*, 1992, **136**, 209.

15 A. Ellison, T.L. Overton, and L. Bencze, *J. Chem. Soc. Faraday Trans.*, 1993, 843.

16 V.B. Kazansky and Y.I. Pecherskaya, *Kinet. Catal. (Engl. Transl.)*, 1961, **2**, 417; P. Cossee and L.L. VanReijen, *Proc. Int. Congr. Catal., 2nd*, 1960, 1679.

17 A. Clark, *Catal. Rev.*, 1969, **3**, 145.

18 H.L. Krauss and H. Stach, *Inorg. Nucl. Letts.*, 1968, **4**, 393; H.L. Krauss and H. Stach, *Z. Anorg. Allg. Chem.*, 1969, **366**, 280.

19 A. Zecchina, E. Garrone, G. Ghiotti, C. Morterra, and E. Borello, *J. Phys. Chem.*, 1975, **79**, 966; A. Zecchina, E. Garrone, G. Ghiotti, and S. Coluccia, *J. Phys. Chem.*, 1975, **79**, 972; B. Fubini, G. Ghiotti, L. Stradella, E. Garrone, and C. Morterra, *J. Catal.*, 1980, **66**, 200; E. Garrone, G. Ghiotti, C. Morterra, and A. Zecchina, *Z. Naturforsch., B*, 1987, **42**, 728; B. Rebenstorf, *Acta Chem. Scand.*, 1989, **43**, 413.

20 R. Merryfield, M.P. McDaniel, and G. Parks, *J. Catal.*, 1982, **77**, 348.

21 D.D. Beck and J.H. Lunsford, *J. Catal.*, 1981, **82**, 98; D.L. Myers and J.H. Lunsford, *J. Catal.*, 1985, **92**, 260.

22 F.J. Karol, G.L. Karapinka, C. Wu, A.W. Dow, R.N. Johnson, and, W.L. Carrick, *J. Polym. Sci., Part A*, 1972, **10**, 2609.

23 M.P. McDaniel, *Adv. Catalysis*, 1985, **33**, 47; T.J. Pullukat, R.E. Hoff, and M. Shida, *J. Pol. Sci. Polym. Chem. Ed.*, 1980, **18**, 2857; A. Follestad, S. Helleborg, and V. Almquist, *Stud. Surf. and Catal.*, T. Keii and K. Soga, Eds., Elsevier, Holland, **56**, 63.

24 L.M. Baker and W.L. Carrick, *J. Org. Chem.*, 1968, **33**, 616.

25 M.P. McDaniel, *Adv. Catal.*, 1985, **33**, 47.

26 H.L. Krauss and E. Hums, *Z. Naturforsch., B, Anorg. Chem., Org. Chem.*, 1979, **34b**, 1628.

27 M.P. McDaniel, and D.M. Cantor, *J. Catal.*, 1983, **82**, 98; G. Ghiotti, E. Garrone, and A. Zecchina, *J. Mol. Catal.*, 1988, **46**, 61.

28 B. Rebenstorf and R. Larsson, *J. Mol. Catal.*, 1981, **11**, 247; B. Rebenstorf, *Acta. Chem. Scand.*, 1989, **43**, 413; B. Rebenstorf, *J. Catal.*, 1989, **117**, 71.

29 G. Ghiotti, E. Garrone, S. Coluccia, C. Morterra, and A. Zecchina, *J. Chem. Soc. Chem. Commun.*, 1979, 1032.

30 K. Weiss and K. Hoffmann, *J. Mol. Catal.*, 1985, **28**, 99.

31 H.J. Lugo and J.H. Lunsford, *J. Catal.* 1985, **91**, 155; L.L. Van Reijen and W.H.M. Sachtler, P. Cossee and D.M. Brouwer, *"Proceedings, 3rd International Congress on Catalysis, Amsterdam,"* 1964, p829, Wiley, New York, 1965.

32 C. Groenveld, P.P.M.M. Wittgen, H.P.M. Swinnen, A. Wernson, and G.C.A. Schuit, *J. Catal.*, 1983, **83**, 346.

33 D.D. Eley, C.H. Rochester, and M.S. Scurrell, *Proc. R. Soc. Lond. A*, 1972, **329**, 375.

34 M. Nishimura and J.M. Thomas, *Catal. Letts.*, 1993, **19**, 33.

35 M.P. McDaniel and D.M. Cantor, *J. Polym. Sci., Polym. Chem. Ed.*, 1983, **21**, 1217.

36 M.P. McDaniel, *Adv. Catal.* 1985, **33**, 47.

37 M.E. Thompson, S.M. Baxter, A.R. Bulls, B.J. Burger, M.C. Nolan, B.D. Santarsiero, W.P. Schaefer, and J.E. Bercaw, *J. Am. Chem. Soc.*, 1987, **109**, 203.

38 J.P. Hogan, D.D. Norwood, and C.A. Ayres, *J. Appl. Poly. Sci.: Applied Polymer Symposium*, 1981, **36**, 40.

39 M.P. McDaniel, Adv. Catal., 1985, 33, 47.

40 The silica that was employed throughout this study was supplied by Crosfield Chemicals and has a surface area = 323 m^2g^{-1} and a pore volume = 1.81 cm^3g^{-1}.

41 For experimental details for both experiments see Chapter 7 of this thesis.

42 W.J. Jozwiak, I.G. Dalla Lana, and R. Fiedorow, *J. Catal.*, 1990, **121**, 183.

43 J.P. Hogan and D.R. Witt, *Award Symposium on Olefin Polymerisation and Disproportionation (Metathesis)*, Joint Meeting of the American Chemical Society and the Chemical Society of Japan, Honolulu, April, 1979.

44 The relative Pauling electronegativities of Si, O, and H are 1.90, 3.44, and 2.20 respectively, taken from *"Inorganic Chemistry"*, J.E.Huheey, Third Edition, Harper International, Cambridge, 1983.

45 D. Briggs and M.P. Seah, *"Practical Surface Analysis"*, Vol. 1, Edts., Wiley and Sons, New York, 1990.

46 For full experimental details see Chapter 6, Section 6.5 of this thesis.

47 V. Bollis, F. Fubini, L. Marchese, G. Marta, and D. Costa, *J. Chem. Soc. Faraday Trans.*, 1991, **87**, 497; J.P. Gallas, J.C. Lavalley, A. Burneau, and O. Barrés, *Langmuir*, 1991, **7**, 1235; Y. Iwasawa, "Tailored Metal Catalysts", ed., Reidel, Dordrecht, 1986.

48 See Chapter 5, Section 5.1.1.

49 The decomposition of acetic acid on Rh(110) surfaces is drastically effected by the presence of atomic oxygen, nitrogen and carbon: Y. Li and M. Bowker, *J. Catal.*, 1993, **142**, 630.

50 A detailed description of spin orbit coupling is given by: D. Briggs and M.P. Seah, *"Practical Surface Analysis"*, Vol. 1, Edts., Wiley and Sons, New York, 1990.

51 G.C. Allen, M.T. Curtis, A.J. Hooper, and P.M. Tucker, *J. Chem. Soc. (Dalton)*, 1973, 1675.

52 C.R. Brundle and M.B. Robin, *"Determination of Organic Structures by Physical Methods,"* eds. F. Nachod and G. Zuckerman, Academic Press, New York, 1971, Vol. 3, p. 1.

53 B. Krebs and K. Hasse, *Acta Cryst*, B32, 1976, 1334.

54 G. Bearson and D. Briggs *"High Resolution XPS of Organic Polymers: The Scienta ESCA300 Database"*, J. Wiley and Sons, New York, 1992.

55 J.A. McGinnety, *Acta Cryst*, B28, 1972, 2845.

56 G.R. Rao and C.N. Rao, *J. Chem. Soc. Chem. Commun.*, 1990, 357; A. Nilsson, H. Tillborg, and N. Mårtensson, *Physical Review Letters*, 1991, **67**, 1015.

57 A. Zecchina, S. Coluccia, E. Guglielminotti, and G. Ghiotti, *J. Phys. Chem.*,1971, **75**, 2774; A.A. Davydov, *J. Chem. Soc. Faraday Trans.*, 1991, **87**, 913.

58 P. McDaniel, *J. Catal.*, 1981, **67**, 71; G. Hierl and H.L. Krauss, Z. *Anorg. Allg. Chem.*, 1975, **415**, 57; A. Zecchina, E. Garrone, G. Ghiotti, C. Morterra, and E. Borello, *J. Phys. Chem.*, 1975, **79**, 966; A. Ellison, T.L. Overton, and L. Bencze, *J. Chem. Soc. Faraday Trans.*, 1993, **89**, 843.

59 J.P. Hogan, *J. Polym. Sci. A-1*, 1970, **8**, 2637; H.L. Krauss, in *"Proceedings, 5th International Conference on Catalysis, Palm Beach, 1972"* (J.W. Hightower, Ed.), Vol. 1, p207, North Holland, Amsterdam, 1973; A. Zecchina, E. Garrone, G. Ghiotti, C. Morterra, and E. Borello, *J. Phys. Chem.*, 1975, **79**, 966.

60 J.A. Chudek, G. Hunter, C.H. Rochester, and T.F.S. Smith, *J. Catal.*, 1992, **136**, 246.

61 Private communication from Crosfield Chemicals.

62 M.P. McDaniel, *Ind. Eng. Chem. Res.*, 1988, **27**, 1559.

63 Acetate groups impregnated onto silica surfaces have been identified by a variety of chemical means: D. Jewett and J. Lawless, *Naturwissen*, 1981, **68**, 570.

64 K.S. Kim and M.A. Barteau, *Langmuir*, 1988, **4**, 945.

65 Acetate decomposition on Cu and Ag surfaces is known to afford ketene by dehydrogenation accompanied by C-O bond cleavage: M. Bowker and R. Madix, *J. Appl. Surf. Sci.*, 1981, **8**, 299; M.A. Barteau, M. Bowker, and R. Madix, *J. Catal.*, 1981, **67**, 118.

66 Ketonization of acetic acid is dependant upon the metal. Acetic acid decomposes on Ni generating CO_2 and CO: R.J. Madix, J.L. Falconer, A.M. Suszko, *Surf. Sci.*, 1976, **54**, 6; G.R. Schoofs and J.B. Benziger, *Surf. Sci.*, 1984, **143**, 359.

67 The decomposition of acetic acid on MgO afforded ketene and water as the sole products. L. Parrot, J.W. Rogers, and J.M. White, *Applications of Surface Science*, 1978, **1**, 443.

68 K.S. Kim and M.A. Barteau, *Langmuir*, 1988, **4**, 945.

69 M.A. Barteau, M. Bowker, and R.J. Madix, *J. Catal.*, 1981, **67**, 118.

70 M. Grotowska, R. Wojciechowska, and W. Wojciechowski, *Journal of Thermal Analysis*, 1990, **36**, 2365.

71 C. Groenveld, P.P.M.M. Wittgen, J.P.M. Swinnen, A. Wernsen, and G.C.A. Schuit, *J. Catal.*, 1983, **35**, 335.

72 H.L. Krauss and H. Stach, *Inorg. Nucl. Chem. Lett.*, 1968, **4**, 393.

73 M.P. McDaniel and S.J. Martin, *J. Phys. Chem.*, 1991, **95**, 3289.

74 G. Ghiotti, E. Garrone, and A. Zecchina, *J. Mol. Catal.*, 1988, **46**, 61.

75 Experimentally determined fragmentation of methanal: 12(3.3), 13 (4.3), 16 (1.7), 28 (30.9), 29 (100), 30 (38.5), 31 (1.9).

76 This topic has been reviwed by: W.J. Jozwiak, I.G. Dalla Lana, and R. Fiedorow, *J. Catal.*, 1990, **121**, 183 and references therein.

77 A. van Asselt, B.J. Burger, V.C. Gibson, and J.E. Bercaw, *J. Am. Chem. Soc.*, 1986, **108**, 5347.

78 E. Spaltenstein, T.K.G. Erikson, S.C. Critchlow, and J.M. Mayer, *J. Am. Chem. Soc.*, 1989, **111**, 617.

79 S.K. Noh, R.A. Heintz, B.S. Haggerty, A.L. Rheingold, and K.H. Theopold, *J. Am. Chem. Soc.*, 1992, **114**, 1892.

80 B.J. Thomas and K.H. Theopold, *J. Am. Chem. Soc.*, 1988, **110**, 5902; *J. Polym. Sci., Polym. Chem. Ed.*, 1974, **12**, 1549.

81 S.G. Kazarian, P.A. Hamley, and M. Poliakoff, *J. Am. Chem. Soc.*, 1993, **115**, 9069.

Chapter Six- Experimental Details

6.1 GENERAL

6.1.1 Experimental Techniques, Solvents and Reagents for Chapters 2-4

All manipulations of air and / or moisture sensitive compounds were performed on a conventional vacuum / inert atmosphere (nitrogen) line using standard Schlenk and cannula techniques, or in an inert (nitrogen) atmosphere filled dry box.

The following solvents were dried by prolonged reflux over a suitable drying agent, being freshly distiled and deoxygenated prior to use (drying agent in parentheses): toluene (sodium metal), pentane (sodium metal), heptane (sodium metal), petroleum ether (40-60°C, lithium aluminium hydride), tetrahydrofuran (sodium benzophenone ketyl), diethylether (lithium aluminium hydride), dichloromethane (calcium hydride), 1,2-dimethoxyethane (potassium metal), and acetonitrile (calcium hydride).

NMR solvents were dried by vacuum distillation from a suitable drying agent (in parentheses) and stored under nitrogen or vacuum prior to use: d_6-benzene (phosphorus (V) oxide), d_8-toluene (phosphorus (V) oxide), chloroform (phosphorus (V) oxide), and d_2-dichloromethane (phosphorus (V) oxide).

Elemental Analyses were performed by the microanalytical services of this department.

Infrared Spectra were recorded on Perkin-Elmer 577 and 457 grating spectrophotometers using CsI windows. Absorbtions abbreviated as: s (strong), m (medium), w (weak), br (broad), s (sharp), sh (shoulder).

Mass Spectra were recorded on a VG 7070E Organic Mass Spectrometer.

NMR Spectra were recorded on the following machines, at the frequencies listed, unless otherwise stated: Bruker AMX500, ^1H (500.14 MHz), 31P (202.46 MHz); Varian VXR400, ^1H (399.95 MHz), ^{13}C (100.58 MHz), ^{31}P (161.90 MHz); Bruker AC250, ^1H (250.13 MHz), ^{13}C (62.90 MHz),

^{31}P(101.26 MHz); Varian Gemini 200, ^{1}H (199.98 MHz), ^{13}C (50.29 MHz); Varian XL 200, ^{1}H (200.06 MHz). The following abbreviations have been used for band multiplicities: s (singlet), d (doublet), t (triplet), q (quartet), sept (septet), m (multiplet), vct (virtually coupled triplet). Chemical shifts are quoted as δ in ppm with respect to the following unless otherwise stated: ^{31}P (dilute aq. H_3PO_4, 0 ppm); ^{13}C (C_6D_6, 128.0 ppm; $CDCl_3$, 77.0 ppm; C_7D_8, 125.2 ppm); ^{1}H (C_6D_6, 7.15 ppm; $CDCl_3$, 7.26 ppm; C_7D_8, 6.98 ppm; CD_2Cl_2, 5.25ppm).

The following chemicals were prepared by previously published procedures: Me_3SiNHR[1], and Me_3CCH_2MgCl[2]. Modified preparative procedures for the following are described below: PMe_3[3], and KCH_2Ph.[4] All other chemicals were obtained commercially and used as received unless stated otherwise.

Preparation of PMe_3

A 5l round bottom flask, fitted with a pressure equalising dropping funnel, efficient mechanical stirrer bar and dry-ice condenser, was charged with magnesium turnings (180g, 7.5 mol.) and di-n-butyl ether (2 litres, sodium dried). The apparatus was then purged with nitrogen. A nitrogen atmosphere was maintained throughout the experiment. Methyl iodide (1000g, 7.05 mol.) was added dropwise to the stirred suspension over a period of *ca.* 2 h., at such a rate as to maintain a reaction temperature of ca. 30°C. Upon completion of the addition, the mixture was allowed to cool to room temperature whilst stirring for another 2h. Subsequently the mixture was cooled to 0°C and a degassed solution of triphenylphosphite (660g, 2.13 mol.) in di-n-butyl ether (*ca* 500 cm^3) was added dropwise with stirring, over a period of 3h. After approximately half the phosphite / ether solution has been added the reaction became viscous due to the precipitation of magnesium salts. Consequently a further 500 cm^3 of di-n-butylether was added. After the addition, the mixture was allowed to cool to room temperature and was stirred for a further 2 h. The dropping funnel was then replaced with a distillation take-off device connected *via* a condenser to a 500cm^3 round bottomed flask cooled in dry-ice / acetone. The reaction mixture was then heated to *ca.* 140°C and the fraction boiling between 35°-80°C was collected (*ca.* 400cm^3). Further distillation through a

15cm, glass helix-packed column, collecting the fraction boiling between 39°-41°C, provided pure PMe_3. Yield, 104g (64%).

Preparation of Potassium Benzyl (KCH_2Ph)

Sublimed potassium butoxide (3.59g, 32mmol.) was placed in a Schlenk with toluene (40cm^3). N-butyl-lithium (20cm^3, 32mmol.) was added dropwise *via* a syringe to the stirring solution, forming a thick orange precipitate. The reaction was allowed to stir for *ca.* 1/2 h. at room temperature, then the solution was removed by filtration, to leave the precipitate, which was subsequently washed with toluene (3 x 40cm^3) and dried *in vacuo.* Yield 2.5g (60%).

6.2 Experimental Details to Chapter Two

6.2.1 Reaction of Na_2MoO_4 with $ArNH_2$: *Preparation of $Mo(NAr)_2Cl_2.DME$ (1)*

Solutions of triethylamine (27.1cm^3, 194.4 mmol.), chlorotrimethylsilane (68cm^3, 534.6 mmol.), and 2,6-diisopropylaniline (18cm^3, 97.2 mmol.) in 1, 2-dimethoxyethane were added sequentially to a stirred suspension of anhydrous sodium molybdate, Na_2MoO_4, (10g, 48.6 mmol.) in 1, 2-dimethoxyethane (100cm^3) at room temperature. The reaction mixture was then heated at 70°C for 12 h. to leave a dark red solution and a large quantity of white precipitate. The solution was filtered from the solid, which was washed with ether (3 x 50cm^3), and the washings combined. The solvent was then removed *in-vacuo* to afford red, analytically pure $Mo(NAr)_2Cl_2.DME$. Yield 28.9g (98%).

Elemental Analysis for $C_{28}H_{44}N_2O_2Cl_2Mo$ Found (Required): %C 55.0 (55.3) %H 7.2 (7.3) %N 4.5 (4.6).

^{1}H NMR data (400MHz, C_6D_6, 298K): δ 7.01 (d, 4H, *m*-C_6H_3), 6.82 (t, 2H, *p*-C_6H_3), 4.29 (sept., 4H, $CHMe_2$), 3.44 (s, 6H, $MeOCH_2CH_2OMe$), 3.18 (s, 4H, $MeOCH_2CH_2OMe$), 1.25 (d, 24H, $CHMe_2$).

^{13}C NMR data (100.6 MHz, C_6D_6): δ 154.2 (*ipso*-C_6H_3), 145.5 (*p*-C_6H_3), 128.0 (*m*-C_6H_3), 123.9 (o-C_6H_3), 71.3 (*Me*OCH_2CH_2OMe), 62.8 ($MeOCH_2CH_2OMe$), 28.2 ($CHMe_2$), 25.2 ($CHMe_2$).

6.2.2 Reaction of Na_2MoO_4 with $^tBuNH_2$: *Preparation of* $Mo(N^tBu)_2Cl_2.DME$

The method outlined in Section 5.2.1 was used for the reaction of Na_2MoO_4, (10g, 48.6 mmol.) with DME solutions of triethylamine (27.1cm^3, 194.4 mmol.), chlorotrimethylsilane (68cm^3, 534.6 mmol.), and tert-butylamine (18cm^3, 97.2 mmol.). The reaction mixture was then heated at 70°C for 12 h. to leave a pale yellow solution and a large quantity of white precipitate. The solution was filtered from the solid, which was washed with ether (3 x 50cm^3), and the washings combined. The solvent was then removed *in-vacuo* to afford yellow, analytically pure $Mo(N^tBu)_2Cl_2.DME$. Yield 15.4g (98%).

Elemental Analysis for $C_{12}H_{28}N_2O_2Cl_2Mo$ Found (Required): %C 36.0 (36.1) %H 7.2 (7.1) %N 6.9 (7.0).

Infrared Data (Nujol, CsI, cm^{-1}): 1360 (m), 1250 (m), 1210 (m), 1115 (m), 1090 (m), 1050 (s), 1025 (m), 860 (s), 830 (m), 800 (s), 600 (m), 570 (m, br), 465 (m, br), 375 (w), 330 (s).

^{1}H NMR data (400MHz, C_6D_6, 298K): δ 3.48 (s, 6H, *Me*OCH_2CH_2OMe), 3.23 (s, 4H, $MeOCH_2CH_2OMe$), 1.40 (s, 18H, CMe_3).

^{13}C NMR data (100.6 MHz, C_6D_6): δ 71.72 (s, CMe_3), 70.61 (t, $^1J_{CH}$ 146.8, $MeOCH_2CH_2OMe$), 62.64 (q, $^1J_{CH}$ 144.6, *Me*OCH_2CH_2OMe), 30.15 (q, $^1J_{CH}$ 127.5, CMe_3).

6.2.3 Reaction of Na_2MoO_4 with 2,6-$C_6H_3Cl_2NH_2$: *Preparation of* $Mo(N\text{-}2,6\text{-}C_6H_3Cl_2)_2Cl_2.DME$

The method outlined in sections 5.2.1 was employed for the reaction of Na_2MoO_4, (10g, 48.6 mmol.) with triethylamine (27.1cm^3, 194.4

mmol.), chlorotrimethylsilane (68cm^3, 534.6 mmol.), and 2,6-dichloroaniline (15.7cm^3, 97.2 mmol.) in 1, 2-dimethoxyethane.

The reaction mixture was then heated at 70°C for 12 h. On reaching 50°C there was a dramatic colour change, further heating caused the solution to gradually turn dark red with evolution of a large quantity of solid. The solution was filtered from the pale pink solid, which was washed with ether (3 x 50cm3), and the washings combined. The solvent was then removed *in-vacuo* to afford a dark red solid which contained both unreacted amine and the desired bis (imido) product. The amine was removed by sublimation under dynamic vacuum. 10g. Yield 10.0g (50%).

The ^{1}H NMR gave very broad peaks which were not resolved on cooling a $CDCl_3$ solution of the compound. This broadness has been attributed to facile dissociation of DME in solution. (See main text).

Elemental Analysis : Elemental analyses were inconsistent.

^{1}H NMR data (200MHz, C_6D_6, 298K): δ 6.84 (m, 2H), 6.68 (m, 2H), 6.08 (m, 2H), 3.52 (s, br, 6H, *Me*OCH$_2$CH$_2$O*Me*), 3.07 (s, br, 4H, MeOC*H*$_2$C*H*$_2$OMe).

6.2.4 Reaction of Na_2MoO_4 with $PhNH_2$: *Preparation of $Mo(NPh)_2Cl_2$.DME*

The procedure outlined in Section 5.2.1 was used for the reaction of Na_2MoO_4 (5g, 25 mmol.) with solutions of triethylamine (14cm^3, 100 mmol.), chlorotrimethylsilane (34.9cm^3, 275 mmol.), and aniline (4.7g, 50 mmol.) in DME. On addition of aniline the previously clear solution immediately turned dark yellow. The solution was heated to 70°C for 12h. after which time the solution had turned dark red. On work-up solvent was removed under reduced pressure from the dark red solution to afford analytically pure $Mo(NPh)_2Cl_2$.DME. Yield, 10.20g, (98%).

Elemental Analysis were inconsistent.

^{1}H NMR data (200MHz, C_6D_6, 298K): δ 7.3 (d, 4H, *o*-C_6H_5), 6.89 (t, $^3J_{HH}$ 8.0 Hz, 4H, *m*-C_6H_5), 6.69 (t, $^3J_{HH}$ 7.3 Hz, 2H, *p*-C_6H_5), 3.43 (br, 4H, MeOC*H*$_2$C*H*$_2$OMe), 3.24 (br, 6H, *Me*OCH$_2$CH$_2$O*Me*).

6.2.5 Reaction of Na_2MoO_4 with $^tBuNH_2$ and $ArNH_2$: *Preparation of Mo(NAr)(N^{t}Bu)Cl$_2$.DME (2)*

The method outlined above was used for the reaction of Na_2MoO_4, (9g, 43.7 mmol.) with solutions of triethylamine (25cm^3, 175 mmol.), chlorotrimethylsilane (61cm^3, 481 mmol.), 2,6-diisopropylaniline (8.3cm^3, 43.7 mmol.), and tert-butyl amine (4.6cm^3, 43.7 mmols) in 1, 2-dimethoxyethane. The reaction mixture was then heated at 70°C for 12 h. to leave a dark red solution and a large quantity of white precipitate. The solution is filtered from the solid, which is washed with ether (3 x 50cm^3), and the washings combined. The solvent is then removed *in-vacuo* to afford red, a mixture of $Mo(NAr)_2Cl_2$.DME, $Mo(N^tBu)_2Cl_2$.DME, and $Mo(NAr)(N^tBu)Cl_2$.DME. Subsequent recrystallisation from Et_2O (-30°C) gave the mixed imido (**2**) preferentially. Yield after 3 recrystallisations 11.0g (50%).

Elemental Analysis for $C_{20}H_{26}N_2O_2Cl_2Mo$ Found (Required): %C 47.7 (47.7) %H 7.4 (7.2) %N 5.4 (5.6).

Infrared Data (Nujol, CsI, cm^{-1}): 3040 (s), 1360 (s), 1330 (s), 1290 (s), 1220 (br,s), 1100 (m), 1060 (s), 1020 (m), 860 (s), 600 (s), 515 (m), 400 (m), 350 (s), 330 (s).

^{1}H NMR data (400MHz, C_6D_6, 298K): δ 7.13(d, $^3J_{HH}$ 7.6 Hz, 2H, *m*-C_6H_3), 6.95 (t, $^3J_{HH}$ 8.0 Hz, 1H, *p*-C_6H_3), 4.32 (sept., $^3J_{HH}$ 6.8 Hz, 2H, C*H*Me$_2$), 3.41 (s, 6H, *Me*OCH$_2$CH$_2$O*Me*), 3.18 (s, 4H, MeOC*H*$_2$C*H*$_2$OMe). 1.42 (d, $^3J_{HH}$, 6.8 Hz, 12H, CH*Me*$_2$), 1.3 (s, 9H, C*Me*$_3$).

^{13}C NMR data (100.6 MHz, C_6D_6): δ 154.42 (s, *ipso*-C_6H_3), 143.1 (s, *o*-C_6H_3), 125.89 (d, $^1J_{CH}$ 160.3 Hz, *p*-C_6H_3), 123.27 (d, $^1J_{CH}$ 123.8 Hz, *m*-C_6H_3), 75.42 (s, CMe$_3$), 70.63 (t, $^1J_{CH}$ 146.1 Hz, MeOCH$_2$CH$_2$OMe), 62.38 (q, $^1J_{CH}$ 145.0 Hz, *Me*OCH$_2$CH$_2$O*Me*), 29.41 (q, $^1J_{CH}$ 127.4 Hz, C*Me*$_3$), 28.10 (d, $^1J_{CH}$ 134.7 CHMe$_2$), 24.82 (br, q, $^1J_{CH}$ 126.0 CH*Me*$_2$).

6.2.6 Reaction of Na_2MoO_4 with 1,8-Diaminonaphthalene

Solutions of triethylamine ($8.5cm^3$, 60 mmol.), chlorotrimethylsilane ($21cm^3$, 165 mmol.), and 1,8-diaminonaphthalene (2.37g, 15 mmols) in 1, 2-dimethoxyethane were added sequentially to a stirred suspension of anhydrous sodium molybdate, Na_2MoO_4, (3g, 15 mmol.) in 1, 2-dimethoxyethane ($100cm^3$) at room temperature. On addition of the diamine the solution rapidly turned black. The reaction mixture was then heated at 70°C for 12 h. to leave a dark solution and a large quantity of precipitate. The orange/brown solution was filtered from the black solid, which was washed with ether (3 x $50cm^3$), and the washings combined. The solvent was then removed *in-vacuo* to afford brown solid, which was subsequently recrystallised from CH_2Cl_2. Prolonged cooling at -30°C afforded a red/brown microcrystalline solid (1.8g).

Elemental Analysis Found : %C 40.91. %H 4.74, %N 7.94, %Mo 11.63, %Cl 19.24.

Infrared Data (Nujol, CsI, cm^{-1}): 3300 (w), 3040 (m, sh), 2700 (w, br), 1560 (m, br), 1340 (m), 1320 (m), 1265 (m), 1240 (m), 1165 (m), 1080 (m), 1065 (w), 855 (s), 790 (m), 755 (s), 730 (s), 700 (w). 675 (w), 625 (w, br), 560 (w), 420 (m, br), 355 (m), 330 (m), 300 (s).

^{1}H NMR data (400MHz, $CDCl_3$, 298K): Initial Spectrum δ 8.09 (br), 7.93 (dd, $^3J_{HH}$ 5.6 Hz, 1.6 Hz), 7.50 (m), 7.40 (dd, $^3J_{HH}$ 5.6Hz, 1.6 Hz), 7.26 (s), 6.78 (s, br), 6.62 (d, $^3J_{HH}$ 7.6 Hz), 6.60 (d, 3JHH 7.6 Hz), 5.30 (s), 3.17 (m).

^{13}C NMR data (100.6 MHz, $CDCl_3$): Initial Spectrum δ 146.99 (d, J_{CH} 8.4 Hz), 143.48 (d, J_{CH} 8.8 Hz), 134.90 (s), 128.04 (d, $^1J_{CH}$ 140.3 Hz), 127.35 (s), 127.06 (d, $^1J_{CH}$ 160.1 Hz), 125.17 (d,$^1J_{CH}$ 163.1 Hz), 124.52 (s), 119.23 (d, $^1J_{CH}$ 154.1 Hz), 110.73 (d, $^1J_{CH}$ 165.2 Hz), 53.42 (s), 46.88 (t, $^1J_{CH}$ 141.1 Hz).

6.2.7 Reaction of $(NH_4)_2Cr_2O_7$ with RNH_2 (R= Ar, ^tBu): *Preparation of $[Cr_2Cl_9]$ $[NHEt_3]_3$ (4)*

Ammonium dichromate, $(NH_4)_2Cr_2O_7$ (1.0g, 3.97 mmol.) was treated under nitrogen with triethylamine (4.5cm^3, 32.3 mmol.), chlorotrimethylsilane (8.8cm^3, 70 mmol.) and 2, 6-diisopropylphenyl amine [$ArNH_2$] (3.0cm^3, 15.9 mmol.) at room temperature followed by heating to 70°C for 12 h in DME solvent. On filtration an intense red/purple solution was obtained, which was combined with the DME washings of the pale brown precipitate. Subsequent removal of solvent under reduced pressure afforded an extremely air and moisture sensitive dark red paramagnetic solid (**4**). Yield 2.1g (72%).

Crystals suitable for a molecular structure determination were obtained by layering a CH_2Cl_2 solution of (**4**) with toluene. A product that analysed as the same as (**4**) was also obtained if the reaction was performed using tert-butyl amine to replace the arylamine.

Elemental Analysis for $C_{18}H_{48}N_3Cl_9Cr$ Found (Required): %C 30.2(29.6). %H 6.3 (6.6), %N 5.5 (5.8), %Cr 11.22 (14.25), %Cl 40.1 (43.7).

Infrared Data (Nujol, CsI, cm^{-1}): 3070 (w,sh), 1285 (w), 1265 (w), 1160 (w), 1080 (m), 1040 (s), 810 (w,br), 350 (s,br).

6.3. Experimental Details to Chapter Three

6.3.1 Reaction of $Mo(NAr)_2Cl_2$.DME with Mg in the Presence of PMe_3: *Preparation of $Mo(NAr)_2(PMe_3)_2$ (5)*

Trimethylphosphine (0.51cm^3, 4.92 mmol), was condensed onto a solution of $Mo(NAr)_2Cl_2$.DME, (0.5g, 0.82 mmol), and activated magnesium turnings (0.02g, 0.90 mmol.), in THF (50cm^3) cooled at -196°C. Upon warming to RT a dark brown colouration became apparent, slowly changing to an intense dark green after 3 hours at RT. Volatiles were subsequently removed *in-vacuo* and a dark green solution was extracted with pentane, by filtration, leaving white magnesium chloride. Recrystallisation from a saturated pentane solution at -78°C afforded a dark green solid. Yield, 0.49g, 60%.

Elemental Analysis for $C_{30}H_{52}N_2P_2Mo$ Found (Required): %C 59.98 (60.18); %H 8.69 (8.77); %N 4.4 (4.68).

Infrared Data (Nujol, CsI, cm^{-1}): 1580 (w), 1340 (w), 1300 (m), 1270 (m), 1100 (m), 1060 (m), 1020 (m), 955 (m), 940 (m), 841(m), 840 (m), 800 (m), 760 (m), 665 (m), 465 (s).

Mass Spectral Data (EI, m/z) 600$[M]^+$, 520 [M-PMe_3].

^{1}H NMR data (400MHz, C_6D_6, 298K): δ 7.19 (d, $^3J_{CH}$ 9.2 Hz, 4H, *m*-C_6H_3), 6.91 (t, $^3J_{CH}$ 7.6 Hz, 2H, *p*-C_6H_3), 3.73 (sept., $^3J_{CH}$ 6.8 Hz, 4H, C*H*Me_2), 1.32 (d, $^3J_{CH}$ 7.2 Hz, 24H, CH*Me*$_2$), 1.03 (br, $\upsilon_{1/2}$ 36 Hz, 18H, P*Me*$_3$).

^{13}C NMR data (100.6 MHz, ^{1}H coupled, C_6D_6): δ 155.45 (s, *ipso*-C_6H_3), 135.74 (s, *o*-C_6H_3), 122.78 (d, $^1J_{CH}$ 150.7 Hz, *m*-C_6H_3), 117.75 (d, $^1J_{CH}$ 157.1 Hz, *p*-C_6H_3), 26.43 (d, $^1J_{CH}$ 126.7 Hz, CHMe_2), 25.17 (CH*Me*$_2$), 22.31 (br, P*Me*$_3$).

6.3.2 Reaction of $Mo(NAr)_2(PMe_3)_2$ (5) with CO

One atmosphere of carbon monoxide was introduced into a thick walled ampoule containing a solution of $Mo(NAr)_2(PMe_3)_2$ (0.5g, 0.84 mmol.) in pentane at -78°C. On warming to room temperature, an immediate reaction took place resulting in the formation of an orange brown solution and the formation of a yellow precipitate after 30 minutes. After three hours the solution was filtered and then subsequently concentrated and placed at -30°C. On prolonged cooling a small quantity (0.05g) of a brown solid was isolated. ^{1}H NMR of this solid revealed the presence of a number of products signified by more than one arylimido septet. Further analysis was precluded by complex nature of the products.

IR analysis of the insoluble yellow precipitate indicated a variety of carbonyl environments. Again further analysis was not sought due to the complexity of the mixture.

syringe. The reaction vessel was evacuated and allowed to warm to RT, with stirring, where one atmosphere of nitrogen was re-admitted to the ampoule. After stirring for 3 hours solvent was removed under reduced pressure and a dark purple pentane solution extracted off the $MgCl_2$ residues by filtration. Dark red crystals were obtained from a saturated cooled (-30°C) pentane solution. Yield 0.93g, 60%.

Elemental Analysis for $C_{32}H_{56}N_2P_2Mo$ Found (Required): %C 61.1 (61.3) %N 4.3 (4.5) %H 9.4 (9.0).

Infrared Data (Nujol, CsI, cm^{-1}): 2580 (w,br), 1575 (w,br) [C_2H_4], 1415 (w), 1335 (m), 1270 (m), 1180 (w), 1095 (w,br), 945 (s, br), 800 (w, br), 745 (s), 725 (m, br).

^{1}H NMR data (C_6D_6, 400 MHz, 298 K): δ 7.04 (d, $^3J_{HH}$ 7.6 Hz, 4H, *m*-C_6H_3), 6.87 (t, $^3J_{HH}$ 7.2 Hz, 2H, *p*-C_6H_3), 3.42 (br, $\upsilon_{1/2}$ 57.2 Hz, 4H, C*H*Me_2), 1.70 (s, 4H, C_2H_4),.1.30 (d, $^3J_{HH}$ 6.8 Hz, 24H, CH*Me*$_2$), 1.07 (s, 18H, P*Me*$_3$).

^{13}C NMR data (C_6D_6, 100.6 MHz, 298 K): δ 154.11 (s, *ipso*-C_6H_3), 137.59 (s, *o*-C_6H_3), 122.83 (d, $^1J_{CH}$ 152.5 Hz, *p*-C_6H_3),.119.77 (d, $^1J_{CH}$ 157.9 Hz, *m*-C_6H_3), 32.77 (t, $^1J_{CH}$ 156.1 Hz, C_2H_4), 27.30 (d, $^1J_{CH}$ 129.4 Hz, $CHMe_2$), 24.75 (q, $^1J_{CH}$ 128.2 Hz, CH*Me*$_2$), 15.13 (q, $^1J_{CH}$ 126.0 Hz, P*Me*$_3$),

^{31}P NMR data (C_6D_6, 101.3 MHz, 298 K, external ref. aq. H_3PO_4): δ -14.81 (s, PMe_3).

6.3.10 Reaction of $Mo(NAr)_2Cl_2$.DME with n-PrMgCl in the Presence of PMe_3

A similar procedure was adopted to that used for the synthesis of $Mo(NAr)_2(PMe_3)_2(\eta^2\text{-}C_2H_4)$. $Mo(NAr)_2Cl_2$.DME (1.5g, 2.5 mmol.) was treated with n-PrMgCl (2.5 cm^3, 2M, 5.0 mmol) and excess trimethylphosphine (0.7 cm^3, 6.2 mmol.). The reaction mixture turned dark red/purple after 3 hours at room temperature. However, on removal of solvent under reduced pressure, the solution began to change colour to green. On work-up $Mo(NAr)_2(PMe_3)_2$ was isolated.

6.3.11 Reaction of $Mo(NAr)_2Cl_2$.DME with EtMgCl in the Presence of xs C_2H_4

One atmosphere of ethene was introduced into an ampoule containing a solution of $Mo(NAr)_2Cl_2$.DME (1.0g, 1.7 mmol.) and EtMgCl ($1.6cm^3$, 2M, 3.4 mmol.) in Et_2O at -78°C. On warming to room temperature the solution slowly darkened, and after 24 hours at RT was a dark brown colour. On filtration and removal of volatiles under reduced pressure a brown intractable oil was isolated. No consistent analysis could be obtained.

6.3.12 Reactions of $Mo(NAr)_2(PMe_3)_2(\eta^2\text{-}C_2H_4)$ with PhC≡CPh

An NMR tube was charged with $Mo(NAr)_2(PMe_3)_2(C_2H_4)$ (30mg, 0.048 mmol.) and PhC≡CPh (8.9mg, 0.05 mmol.) and C_6D_6 ($0.8cm^3$). The solution gradually turned from red/purple to orange overnight, complete conversion to the acetylene adduct was achieved after 10 days at 60°C. The ^1H NMR spectrum was consistent with the formation of $Mo(NAr)_2(PMe_3)(\eta^2\text{-}PhC{\equiv}CPh)$, see Section 6.4.1.

6.3.13 Reaction of $Mo(N^tBu)_2Cl_2$.DME with EtMgCl in the Presence of PMe_3:

Preparation of $Mo(N^tBu)_2(PMe_3)(C_2H_4)$ (6)

Onto a frozen (-196°C) solution of $Mo(N^tBu)_2Cl_2$.DME (1.0g, 5 mmol) in diethylether (40 cm^3) was condensed trimethylphosphine (0.5 cm^3, 10 mmol). One atmosphere of nitrogen was then introduced and a 2M solution of C_2H_5MgCl (5.0 cm^3, 10.0 mmol) was introduced *via* a syringe. The reaction vessel was evacuated and allowed to warm to RT, with stirring, where one atmosphere of nitrogen was re-admitted to the ampoule. After stirring for 3 hours solvent was removed under reduced pressure and a dark purple pentane solution extracted off the $MgCl_2$ residues by filtration. Yellow crystals were obtained from a saturated cooled (-30°C) pentane solution. Yield 1.1g, 65%.

Elemental Analysis for $C_{13}H_{31}N_2PMo$ Found (Required): %C 45.6 (45.6) %N 8.1 (8.2) %H 9.1 (9.1).

Infrared Data (Nujol, CsI, cm^{-1}): 1355 (s), 1285 (w), 1255 (s), 1215 (s), 1135 (s), 1105 (s, br), 1020 (m, br), 950 (s, br), 890 (w), 845 (w), 800 (s), 670 (w).

^{1}H NMR data (C_6D_6, 400 MHz, 298 K): δ 2.26 (td, $^3J_{HH}$ 11.6 Hz, 2H, C_2H_4), 1.37 (s, 18H, $NCMe_3$), 1.16 (td, 2H, $^3J_{HH}$ 11.3 Hz, C_2H_4), 1.13 (d, 9H, $^2J_{PH}$ 8.8 Hz, PMe_3).

^{13}C NMR data (C_6D_6, 100.6 MHz, 298 K): δ 64.78 (s, $NCMe_3$), 33.70 (q, $^1J_{CH}$ 125.8 Hz, $NCMe_3$), 31.76 (td, $^1J_{CH}$ 152.4 Hz, $^2J_{PC}$ 9.9 Hz, C_2H_4), 20.96 (t, 1JCH 156.1 Hz, C_2H_4), 19.10 (qd, $^1J_{CH}$ 132.7, $^1J_{PC}$ 24.7Hz, PMe_3).

^{31}P NMR data (C_6D_6, 101.26 MHz, 298 K, external ref. aq. H_3PO_4): δ 22.55 (s, PMe_3).

6.3.14 Reaction of $Mo(N^tBu)_2Cl_2$.DME with n-PrMgCl in the Presence of PMe_3: *Preparation of $Mo(N^tBu)_2(PMe_3)(C_3H_6)$ (7)*

A similar procedure to that used in the previous section was used to react $Mo(N^tBu)_2Cl_2$.DME (1.0g, 5 mmol.) with n-PrMgCl (5.0 cm^3, 10.0 mmol) in the presence of trimethylphosphine (0.5 cm^3, 10 mmol). On work-up yellow crystals were obtained from a cooled (-30°C) pentane solution. Yield 1.2g (70%).

Elemental Analysis for $C_{14}H_{33}N_2PMo$ Found (Required): %C 47.0 (47.1) %N 7.7 (7.9) %H 9.2 (9.4).

Infrared Data (Nujol, CsI, cm^{-1}): 1355 (m), 1305 (w), 1285 (m), 1260 (s), 1220 (s), 1185 (w), 1150 (w), 1110 (m), 1045 (w), 1020 (w), 950 (s), 900 (w), 845 (w), 800 (s), 670 (w), 575 (w, br).

^{1}H NMR data (C_6D_6, 400 MHz, 298 K): δ 3.23 (tqd, 1H, $^3J_{HH}$ 10.8 Hz, $^2J_{HH}$ 6.3 Hz, $^3J_{PH}$ 1.4 Hz, CH_2=C*H*Me), 2.24 (d, 3H, $^3J_{HH}$ 6.3 Hz, CH_2=CH*Me*), 1.36 (s, 9H, NCMe3), 1.34 (s, 9H, $NCMe_3$), 1.22 (ddd, 1H, $^3J_{HH}$ 10.8 Hz, $^2J_{HH}$ 5.4 Hz, $^3J_{PH}$ 5.2 Hz, C*H*$_2$=CHMe), 1.12 (d, 9H, $^2J_{PH}$ 8.7 Hz, PMe_3), 1.02 (dd, 1H, $^3J_{HH}$ 10.8 Hz, $^2J_{HH}$ 5.4 Hz, $^3J_{PH}$ 5.2 Hz, C*H*$_2$=CHMe).

^{13}C NMR data (C_6D_6, 100.6 MHz, 298 K): δ 65.32 (s, $NCMe_3$), 65.03 (s, $NCMe_3$), 39.93 (d, $^1J_{CH}$ 147.7 Hz, CH_2=CHMe), 37.42 (td, $^1J_{CH}$ 147.9 Hz, $^1J_{PC}$ 9.5 Hz) CH_2=CHMe), 34.06 (q, $^1J_{CH}$ 125.1 Hz, $NCMe_3$), 33.86 (q, $^1J_{CH}$ 125.1 Hz, $NCMe_3$), 27.46 (q, $^1J_{CH}$ 124.4 Hz, CH_2=$CHMe$), 19.51 (qd, $^1J_{CH}$ 127.6 Hz, $^1J_{PC}$ 28.2 Hz, PMe_3).

^{31}P NMR data (C_6D_6, 101.26 MHz, 298 K, external ref. aq. H_3PO_4): δ 22.00 (s, PMe_3).

6.3.15 Reaction of $Mo(N^tBu)_2(PMe_3)(C_3H_6)$ (11) with C_2H_4

Ethene (0.08 mmol.) was condensed on to a frozen C_6D_6 solution of $Mo(N^tBu)_2(PMe_3)(C_3H_6)$ (30mg, 0.08 mmol.) in an NMR tube at -196°C. The sample was smoothly converted to the corresponding ethene complex on heating at 60°C for 12 hours.

6.3.16 Reaction of $Mo(N^tBu)_2(PMe_3)(C_3H_6)$ (11) with CO

One atmosphere of carbon monoxide was introduced into a thick walled glass ampoule containing a solution of $Mo(N^tBu)_2(PMe_3)(C_3H_6)$ (1.0g, 2.6 mmol.) in Et_2O at -78°C. On warming to room temperature the solution slowly darkened with evolution of an orange precipitate. After three hours ar RT the solution was filtered and the orange solid isolated. The infrared spectrum indicated the formation of a mixture of products.

Infrared Data (Nujol, CsI, cm^{-1}): 2070 (w),1970 (sh), 1935 (sh), 1890 (s,br), 1790 (s), 1335 (m), 1230 (s,br), 1205 (sh), 1190 (w, br), 1015 w,br), 945 (s), 840 (w), 800 (w), 715 (w), 665 (w), 600 (w, br), 465 (m, br).
Elemental Analysis %C 32.7, %N 0.73, % H 4.11.

6.3.17 Reaction of $Mo(N^tBu)_2(PMe_3)(C_3H_6)$ (11) with Se

Onto a frozen heptane ($50cm^3$) solution of $Mo(N^tBu)_2(PMe_3)(C_3H_6)$ (0.25g, 0.73 mmol.) and selenium (0.058g, 0.73 mmol.) was condensed PMe_3 ($0.1cm^3$, 0.73 mmol.) in a thick walled glass ampoule. On warming to

room temperature the selenium powder was gradually consumed. The reaction was then heated under one atmosphere of nitrogen for 6 days to afford a dark claret solution. The solution was filtered and concentrated. On prolonged cooling at -30°C dark red purple crystals were isolated. Yield 100mg.

Elemental Analysis Found: %C 34.4 %N 8.1 %H 7.0, %Se 21.0, %Mo 20.6, %P 4.1.

Infrared Data (Nujol, CsI, cm^{-1}): 1355 (m), 1300 (w), 1280 (w), 1225 (m), 1205 (s, br), 1165 (sh), 1125 (m), 1085 (m), 1020 (w), 995 (w), 945 (s, br), 840 (w), 800 (m), 715 (m, br), 660 (w), 615 (m), 530 (w, vbr), 465 (w, vbr), 400 (w, vbr).

Mass Spectral Data (EI, m/z) 224, 156, 141, 125, 113, 97, 91, 84, 76, 69, 55.
^{1}H NMR data (C_6D_6, 400 MHz, 298 K): δ 1.92 (s, 9H, NC*Me*$_3$), 1.81 (s, 9H, NC*Me*$_3$), 1.75 (d, $^{2}J_{PH}$ 8.4 Hz, 9H, PMe_3), 1.54 (s, 9H, NC*Me*$_3$), 1.50 (s, 9H, NC*Me*$_3$), 1.15 (s, 9H, NC*Me*$_3$), 1.11 (s, 9H, NC*Me*$_3$).

^{13}C NMR data (C_6D_6, 100.6 MHz, 298 K): δ 70.03 (s, $NCMe_3$), 69.40 (s, $NCMe_3$), 69.04 (s, $NCMe_3$), 68.15 (s, $NCMe_3$), 66.78 (s, $NCMe_3$), 66.30 (s, $NCMe_3$), 37.02 (q, $^{1}J_{CH}$ 125.6 Hz, NC*Me*$_3$), 36.39 (q, $^{1}J_{CH}$ 126.3 Hz, NC*Me*$_3$), 33.21 (q, $^{1}J_{CH}$ 131.0 Hz, NC*Me*$_3$), 32.49 (q, $^{1}J_{CH}$ 118.3 Hz, NC*Me*$_3$), 32.22 (q, $^{1}J_{CH}$ 126.7 Hz, NC*Me*$_3$), 30.78 (q, 126.7 Hz, NC*Me*$_3$), 20.55 (qd, $^{1}J_{PC}$ 25.6 Hz, $^{1}J_{CH}$ 129.4 Hz, P*Me*$_3$).

^{31}P NMR data (C_6D_6, 161.9 MHz, 298 K, external ref. aq. H_3PO_4): δ 0.40 (pseudo-triplet, J_{SeP} 49.9 Hz,*P*Me_3).

6.3.18 Reaction of MoO_2Cl_2 with EtMgCl in the Presence of PMe_3: *Preparation of $Mo(O)Cl_2(PMe_3)_3$ (13)*

MoO_2Cl_2 (0.25g, 1.3 mmol.) was added *via* a transfer tube to DME (20cm^3). Trimethylphosphine (0.52 cm^3, 5 mmol.) was condensed onto the frozen solution at -196°C. One atmosphere of nitrogen was then introduced and a 2M solution of C_2H_5MgCl (0.63 cm^3, 2.6 mmol) was introduced *via* a syringe. The reaction vessel was evacuated and allowed to warm to RT, with stirring, where one atmosphere of nitrogen was re-

admitted to the ampoule. After stirring for 3 hours solvent was removed under reduced pressure and a dark green/blue toluene solution extracted off the $MgCl_2$ residues by filtration. On removal of solvent under reduced pressure a green/ blue solid was isolated. Yield 0.10g (20%).

Elemental Analysis for $C_9H_{27}Cl_2P_3OMo$ Found (Required): %C 26.2 (26.3) %H 6.6 (6.6).

Infrared Data (Nujol, CsI, cm^{-1}): 1305(w,sh), 1285 (w), 1265 (m), 1090 (m, br), 1020 (m, br), 950 (s, br) [Mo=O stretch], 800 (s), 670 (w), 465 (w), 390 (w).

^{1}H NMR data (C_6D_6, 400 MHz, 298 K): δ 1.38 (vct, $^3J_{PH}$ 4.0 Hz), 1.27 (d, $^1J_{PH}$ 8.0 Hz), -16.25 (*), -32.90 (*).

* Paramagnetic contribution from $MoCl_3(PMe_3)_3$.

^{13}C NMR data (C_6D_6, 100 MHz, {^{1}H}, 298 K): δ 20.54 (d, $^1J_{PC}$ 23.9 Hz), 15.981 (vct, $^1J_{PC}$ 12.Hz).

6.3.19 Reaction of $Cr(N^tBu)_2Cl_2$ with EtMgCl in the Presence of PPh_3

Onto a frozen (-196°C) solution of $Cr(N^tBu)_2Cl_2$ (0.25g, 1.0 mmol.) in diethylether (20 cm^3) was condensed trimethylphosphine (0.4 cm^3, 4.0 mmol.). One atmosphere of nitrogen was then introduced and a 2M solution of C_2H_5MgCl (1.0 cm^3, 2.0 mmol) was introduced *via* a syringe. The reaction vessel was evacuated and allowed to warm to RT, with stirring, where one atmosphere of nitrogen was re-admitted to the ampoule. After stirring for 3 hours solvent was removed under reduced pressure and a dark black pentane solution extracted off the $MgCl_2$ residues by filtration. A small quantity of a red/purple solid was obtained after removal of pentane *in vacuo*.

Elemental Analysis %Cr 11.0, %C 69.3, %N 7.1, %H 6.4.

Analogous procedures were used for the reactions involving both PMe_3 and PMe_2Ph, although the analyses of the corresponding products proved variable.

6.3.20 Reaction of $Cr(N^tBu)_2Cl_2$ with PPh_3: *Preparation of $Cr(N^tBu)_2Cl_2(PPh_3)$ (14a)*

A toluene solution (50cm^3) of $Cr(N^tBu)_2Cl_2$ (0.3g, 1.1 mmol.) and PPh_3 (0.29g, 1.1 mmol.) was stirred at room temperature for 3 hours. After three hours an solid had precipitated from a brown solution. The solution was removed by filtration and the orange solid isolated and dried *in vacuo*. The product was subsequently recrystallised through cooling of a warm (50°C) THF solution. Yield 0.33g (55%).

Elemental Analysis for $C_{26}H_{33}N_2Cl_2PCr$ Found (Required): %C 58.9 (59.2), %N 5.2 (5.3), % H 6.0 (6.3).

^{1}H NMR data ($CDCl_3$, 400 MHz, 298 K): δ 7.75 (m, 5H, PPh_3), 7.44 (d, 10H, PPh_3), 1.34 (s, 18H, $NCMe_3$).

^{13}C NMR data ($CDCl_3$, 100.6 MHz, 298 K): δ 134.91 (br, d, $^1J_{CH}$ 157.5 Hz,), 131.31 (d, $^1J_{CH}$ 162.5 Hz, C_6H_5), 128.6 (d, $^1J_{CH}$ 162.4 Hz, C_6H_5), 81.98 (s, $NCMe_3$), 30.09 (q, $^1J_{CH}$ 128.94, $NCMe_3$).

6.3.21 Reaction of $Cr(N^tBu)_2Cl_2(PPh_3)$ (14a) with EtMgCl

EtMgCl (0.52 cm^3, 1.0 mmol.) was syringed under nitrogen onto a frozen Et_2O solution (-78°C) of $Cr(N^tBu)_2Cl_2(PPh_3)$ (0.27g, 0.5 mmol.). The ampule was then allowed to warm to room temperature. After stirring for 3 hours the solvent was removed under reduced pressure and a dark black pentane solution extracted off the $MgCl_2$ residues by filtration. A small quantity of a red/purple solid was obtained after removal of pentane *in vacuo*.

Elemental Analysis %Cr 10.2, %C 69.1, %N 3.4%, %H 6.54.

Infrared Data (Nujol, CsI, cm^{-1}): 1590 (w), 1265 (s), 1090 (s, br), 1020 (s, br), 800 (s, br), 695 (s), 500 (m, br), 395 (m, br).

6.4. Experimental Details to Chapter Four

6.4.1 Reaction of $Mo(NAr)_2(PMe_3)_2(C_2H_4)$ (6) with PhC≡CPh: *Preparation of $Mo(NAr)_2(PMe_3)(PhC{\equiv}CPh)$*

An thick walled glass ampoule was charged with $Mo(NAr)_2(PMe_3)_2(C_2H_4)$ (0.81g, 1.3 mmol.), PhC≡CPh (0.23g, 1.30 mmol.), and heptane (30 cm^3). The ampoule was heated to 60°C for 10 days, after which time the solution had turned red. The ampoule was allowed to cool slowly to RT with the formation of orange florets. Yield 0.61g (66%).

A sample of the acetylene adduct was subsequently recrystallised from a concentrated THF solution at -10°C.

Elemental Analysis for $C_{41}H_{53}N_2PMo$ Found (Required): %C 70.3 (68.9), %N 3.4 (4.0), % H 8.0 (7.6).

Infrared Data (Nujol, CsI, cm^{-1}): 2600 (w, br), 1750 (br, m), 1590 (m), 1345 (m, sh), 1325 (m), 1265 (s), 1245 (m), 1165 (w), 1110 (w), 1100(w), 1065 (m), 900 (s), 850 (m), 765 (s), 695 (s), 580 (m), 450 (m).

Mass Spectral Data (EI, m/z) 702 $[M]^+$, 522 [M-PhC≡CPh], 444 [M-PhC≡CPh-PMe_3].

^{1}H NMR data (C_6D_6, 400 MHz, 298 K): δ 7.88 (d, br, $^3J_{PH}$ 4.8 Hz, *o*-Ph, 2H), 7.24 (s, br, 4H), 7.08 (2d's, 4H, *m*-NAr), 7.01 (dd, 2H, *p*-NAr), 7.05 (m, br, Ph_2C_2), 6.90 (m, br, Ph_2C_2), 4.06 (sept., 4H, $^3J_{CH}$ 6.8 Hz, $CHMe_3$), 3.56 (m, 7H, THF), 1.41 (m, 7H, THF), 1.20 (2d's, 24H, $CHMe_3$), 1.10 (d, $^3J_{PH}$ 9.6 Hz, PMe_3).

^{13}C NMR data (C_6D_6, 100.6 MHz, 298 K): δ 155.90 (s, *ipso*-C_6H_5-t), 154.50 (d, Ph_2C_2-c, $^3J_{PC}$ 16 Hz), 153.94 (s, *ipso*-NAr), 146.44 (s, Ph_2C_2-t), 142.60 (s, *Co* NAr), 135.17 (s, *ipso*-C_6H_5-c), 131.82 (d, $^1J_{CH}$ 159.5 Hz), 129.00 (m,*m*-C_6H_5), 128.5 (m,*m*-C_6H_5), 126.04 (d, $^1J_{CH}$ 162.2 Hz, C*p*-C_6H_5), 125.38 (d, $^1J_{CH}$ 156.8 Hz, *p*-C_6H_5), 124.16 (d, $^1J_{CH}$ 159.2 Hz, *p*-NAr), 122.56 (d, $^1J_{CH}$ 152.3 Hz), 67.79 (t, $^1J_{CH}$ 147.9 Hz, THF), 28.19 (q, $^1J_{CH}$ 128.6 Hz, $CHMe_2$), 26.43 (d, $^1J_{CH}$ 132.8 Hz, THF), 23.95 (q, $^1J_{CH}$ 124.0 Hz, $CHMe_3$), 23.71 (q, $^1J_{CH}$ 124.0 Hz, $CHMe_3$), 16.93 (qd, $^1J_{CH}$ 130.6, $^1J_{PC}$ 29.1 Hz, PMe_3).

^{31}P NMR data (C_6D_6, 161.9 MHz, 298K): δ 15.22 (s, PMe_3).

{t and c denote trans and cis.}

6.4.2 Reaction of $Mo(N^tBu)_2(PMe_3)(C_2H_4)$ (10) with PhC≡CPh: *Preparation of $Mo(N^tBu)_2(PMe_3)(PhC{\equiv}CPh)$ (15)*

An analogous procedure (6.4.1) was used for the reaction of $Mo(N^tBu)_2(PMe_3)(C_2H_4)$ (0.5g, 1.5 mmol.) with PhC≡CPh (0.27g, 1.5 mmol.) in heptane (50 cm^3). Stirring at 60°C for 10 days afforded an orange/brown solution. Slow cooling to RT afforded fine yellow needles in near quantitative yield. Further yellow crystals were obtained from a saturated cooled (-30°C) heptane solution, to give an near quantitative overall yield, 0.47g, 95%.

Elemental Analysis for $C_{25}H_{37}N_2P_1Mo$ Found (Required): C% 61.03 (60.97), H% 7.64 (7.59), N% 5.41 (5.69).

Infrared Data (Nujol, CsI, cm^{-1}): 2605 (w), 1730 (m), 1590 (m), 1565 (w, sh), 1350 (s), 1305 (w), 1285 (m), 1255 (s, br), 1215 (s, br), 1170 (w), 1100 (m, br), 1065 (m), 1020 (m, br), 950 (s, br), 850 (w), 800 (s), 765 (m), 750 (s), 690 (s), 585 (m), 545 (m), 500 (m), 460 (w, br), 440 (w), 380 (w), 350 (w).

^{1}H NMR data (C_6D_6, 400 MHz, 298 K): δ 8.09 (d, 2H, *o*-Ph_2C_2), 7.22 (t, 3H, *m*-Ph_2C_2), 7.15 (t, 2H, *m*-Ph_2C_2), 7.05 (m, 3.5H, *p*-Ph_2C_2), 6.95 (m, 1.5H, *p*-Ph_2C_2), 1.40 (s, 18H, $NCMe_3$), 1.13 (d, PMe_3, $^2J_{PH}$ 9.2 Hz).

^{13}C NMR data {^{31}P} (C_6D_6, 100.6 MHz, 298 K): δ 154.62 ($^1J_{PC}$ 18.7 Hz, Ph_2C_2-t), 149.41 ($^2J_{PC}$ 2.3 Hz, Ph_2C_2-c), 148.53 ($^3J_{PC}$ 5.0 Hz, *ipso*-C_6H_5-t), 137.58 ($^3J_{PH}$ 3.0 Hz, *ipso*-C_6H_5-c), 132.02 (d, $^1J_{CH}$ 159.0 Hz, *o*-C_6H_5-t), 128.49 (*m*-C_6H_5-c), 128.34 (*m*-C_6H_5-t), 127.39 (*p*-C_6H_5-t), 125.40 (d, $^1J_{CH}$ 158.7 Hz, *o*-C_6H_5-c), 124.00 (d, $^1J_{CH}$ 160.7 Hz, *p*-C_6H_5-c), 65.88 (s, $NCMe_3$), 33.94 (q, $^1J_{CH}$ 126.0 Hz, $NCMe_3$), 19.05 (q, $^1J_{CH}$ 130.4 Hz, $^1J_{PC}$ 28.2 Hz, PMe_3).

{t and c denote trans and cis.}

^{31}P NMR data (C_6D_6, 101.3 MHz, 298 K, external ref. aq. H_3PO_4): δ 16.18 (s, PMe_3).

Assignment	^{1}H δ (ppm)	J (Hz)
o-*Ph*C≡CPh (trans)	8.09(d)	$^3J_{HH}$ 7.6
m-*Ph*C≡CPh (trans)	7.22(t)	$^3J_{HH}$ 7.2
m-*Ph*C≡CPh (cis)	7.15(m)	—
p-*Ph*C≡CPh (trans)	7.05(m)	—
o-*Ph*C≡CPh (cis)	7.04(m)	—
p-*Ph*C≡CPh (cis)	6.95(t)	$^3J_{HH}$ 7.6
NC(*Me*)$_3$	1.40(s)	—
PMe$_3$	1.13(d)	$^2J_{PH}$ 9.2

Table 6.1 *Summary of the 400 MHz ^{1}H NMR data for Mo(N^{t}Bu)$_2$(PMe$_3$)(η^2-PhC≡CPh) (15).*

6.4.3 Reaction of Mo(N^{t}Bu)$_2$(PMe$_3$)(C$_2$H$_4$) (10) with PhC≡CH: *Preparation of Mo(N^{t}Bu)$_2$(PMe$_3$)(PhC≡CH) (16)*

Mo(N^{t}Bu)$_2$(PMe$_3$)(C$_2$H$_4$) (30mg, 0.09 mmol.) was treated with PhC≡CH (9mg, 0.09 mmol.) in C$_6$D$_6$ (0.8 cm^3)in an NMR tube. On heating to 60°C for 10 days the solution turned orange/brown with the formation of the corresponding acetylene adduct.

^{1}H NMR data (C$_6$D$_6$, 400 MHz, 298 K): δ 8.58 (d. $^3J_{PH}$ 14.8 Hz, 1H, PhCC*H*), 8.17 (d, $^3J_{HH}$ 6.8 Hz, 2H, *o*-C$_6$H$_5$), 7.35 (t, $^3J_{HH}$ 7.6 Hz, 2H, *m*-C$_6$H$_5$), 7.13 (t, $^3J_{HH}$ 7.6 Hz, 2H, *p*-C$_6$H$_5$), 1.36 (s, 18H, NC*Me*$_3$), 1.20 (d, $^2J_{PH}$ 9.6 Hz, 9H, PMe$_3$).

^{13}C NMR data (C$_6$D$_6$, 100 MHz, 298 K): δ 153.03 (s, br, C≡C*t*), 138.25 (dd, $^2J_{PC}$ 23.6 Hz, $^1J_{CH}$ 187.7 Hz), 137.73 (d, $^3J_{PC}$ 3 Hz, *ipso*-C$_6$H$_5$), 132.59 (d, $^1J_{CH}$ 158.3 Hz, *o*-C$_6$H$_5$), 128.41 (*m*-C$_6$H$_5$,coincident with solvent), 127.58 (*p*-C$_6$H$_5$, coincident with solvent), 65.47 (s, NCMe$_3$), 34.00 (q,$^1J_{CH}$ 126.0 Hz, NC*Me*$_3$), 19.10 (q, $^1J_{PC}$ 29.4 Hz, $^1J_{CH}$ 129.8 Hz, P*Me*$_3$).

^{31}P NMR data (C$_6$D$_6$, 161.9 MHz, 298 K, external ref. aq. H$_3$PO$_4$): δ 20.29 (s, *P*Me$_3$).

6.4.4 Reaction of $Mo(NAr)_2Cl_2$.DME (1) with PhC≡CPh in the Presence of Mg

An ampoule was charged with $Mo(NAr)_2Cl_2$.DME (0.5g, 0.82 mmol.), PhC≡CPh (0.29g, 1.7 mmol.), and magnesium turnings (22mg, 0.91 mmol.). THF (50 cm3) was condensed into the vessel at -196°C. On warming to RT the solution gradually turned brown. After 10 days at RT the solvent was removed under reduced pressure. All attempts to isolate a tractable product led to decomposition.

6.4.5 Reaction of $Mo(N^tBu)_2Cl_2$.DME with PhC≡CPh in the Presence of Magnesium and PMe_3

A similar procedure was adopted for the reaction of $Mo(N^tBu)_2Cl_2$.DME (0.5g, 1.25 mmol.) with PhC≡CPh (0.2g, 1.25 mmols.), Mg (0.03g, 1.5 mmol.) and PMe_3 (0.2 cm^3, 1.9 mmol.) in THF (50 cm^3). On warming to RT the solution gradually turned dark blue/green. Removal of solvent afforded the bis (phosphine) complex $[Mo(N^tBu)(\mu\text{-}N^tBu)(PMe_3)]_2$.

6.4.6 Reaction of $Mo(N^tBu)_2(PMe_3)(C_3H_6)$ with Azobenzene: *Preparation of $Mo(N^tBu)_2(PMe_3)(\eta^2\text{-}Ph\text{-}N{=}N\text{-}Ph)$ (17)*

A heptane (40 cm^3)solution of $Mo(N^tBu)_2(PMe_3)(C_3H_6)$ (0.1g, 0.28 mmol.) and freshly sublimed azobenzene (0.05g, 0.28 mmol.) was heated to 60°C for 10 days, during which time the solution became dark red. On cooling to RT a yellow solid was precipitated. More solid was isolated from cooling of the saturated heptane solution at -78C. The overall yield was inaccurate as it proved impossible to free the product from unreacted azobenzene.

^{1}H NMR data (C_6D_6, 200 MHz, 298 K): δ 7.76 (d, 2H, *o*-C_6H_5), 7.61 (d, *o*-C_6H_5), 7.28 (m), 7.24 (m), 1.28 (s, 9H, NC*Me*$_3$), 1.00 (s, 9H, NC*Me*$_3$), 0.87 (d, $^2J_{PH}$ 10 Hz, P*Me*$_3$).

6.4.7 Reaction of $Mo(NAr)_2Cl_2$.DME (1) with PhMgCl in the Presence of PMe_3: *Preparation of $Mo(NAr)_2(Ph)_2(PMe_3)$ (18)*

Trimethylphosphine (0.85 cm^3, 8.2mmol.) was condensed onto a solution of $Mo(NAr)_2Cl_2$.DME, (2g, 3.3mmol), and PhMgCl (0.9g, 6.6mmol.), in diethylether solvent (30 cm^3) cooled to -196°C. Upon warming to RT a brown solution became apparent. After stirring at RT for a further 12 h, and removal of solvent under reduced pressure a red pentane solution was extracted off the $MgCl_2$ residues by filtration. Recrystallisation from a saturated cooled (-30°C) pentane solution afforded red cubic crystals. Yield 1.45g, 65%.

Elemental Analysis for $C_{39}H_{53}N_2PMo$ Found (Required) %C 67.7 (69.2), %N 3.9 (4.1), %H 7.9 (7.9).

Infrared Data (Nujol, CsI, cm^{-1}): 3125 (w, sh), 2360 (w, br), 1330 (w, br), 1265 (s), 1095 (s, br), 1020 (s, br), 950 (w), 800 (s), 750 (m), 700 (w), 470 (w, br), 380 (w, br).

^{1}H NMR data (C_6D_6, 400 MHz, 298 K): δ 7.80 (m, 4H, *o*-C_6H_5), 7.19 (t, $^3J_{HH}$ 7.2 Hz, 4H, *m*-C_6H_5), 7.06 (t, $^3J_{HH}$ 7.2 Hz, 2H, *p*-C_6H_5), 7.01 (d, $^3J_{HH}$ 7.2 Hz, 4H, *m*-C_6H_3), 6.93 (t, $^3J_{HH}$ 6.8 Hz, 2H, *p*-C_6H_3), 4.04 (Sept., $^3J_{HH}$ 6.4 Hz, 4H, C*H*Me_2), 1.08 (d, $^3J_{HH}$ 6.8Hz, 24H, CH*Me*$_2$), 0.54 (d, $^2J_{PH}$ 7.6 Hz, 9H, P*Me*$_3$).

^{13}C NMR data (C_6D_6, 100.6 MHz, 298 K): δ 174.47 (s, *ipso*-C_6H_5), 153.55 (s, *ipso*-C_6H_3), 143.03 (s, *m*-C_6H_3), 137.29 (d, $^1J_{CH}$ 156.7 Hz, *o*-C_6H_5), 127.37 (d, *m*-C_6H_5), 125.47 (d, $^1J_{CH}$ 166.4 Hz, *p*-C_6H_5), 125.08 (d, $^1J_{CH}$ 156.0 Hz, *p*-C_6H_3), 123.01 (d, $^1J_{CH}$ 160.6 Hz, *m*-C_6H_5), 28.13 (d, $^1J_{CH}$ 129.4 Hz, $CHMe_2$), 24.32 (q, $^1J_{CH}$ 125.4 Hz, CH*Me*$_2$), 13.20 (q, $^1J_{CH}$ 129.5 Hz, $^1J_{PC}$ 16.8 Hz, P*Me*$_3$).

^{31}P (C_6D_6, 101.3 MHz, 298 K, external ref. aq. H_3PO_4): δ -24.44 (s, *P*Me_3).

VT ^{1}H NMR (C_7D_8, 400 MHz): All resonces remain unchanged on cooling to -80°C

6.4.8 Reaction of $Mo(NAd)_2Cl_2$.DME with PhMgCl in the Presence of PMe_3: *Preparation of $Mo(NAd)_2(Ph)_2(PMe_3)$ (21)*

An analogous procedure was adopted to that used in the previous section for the reaction of $Mo(NAd)_2Cl_2$.DME (2g, 3.6 mmol.) with PhMgCl (3.6 cm^3, 7.2 mmol.) and PMe_3 (0.75 cm3, 7.2 mmol.) in Et_2O. Pale green crystals were obtained from a concentrated pentane solution at -78°C. Yield 1.1g (50%).

Elemental Analysis for $C_{35}H_{49}N_2PMo$ Found (Required): %C 66.9 (67.3), %N 4.2 (4.5), %H 7.8 (7.9).

^{1}H NMR data (C_6D_6, 400 MHz, 298 K): δ 7.81 (m, 4H, *o*-C_6H_5), 7.25 (t, $^1J_{CH}$ 7.6 Hz, 4H, m-C_6H_5) 7.10 (t, $^1J_{CH}$ 7.2 Hz, 2H, *p*-C_6H_5), 2.05 (d, br, $^1J_{CH}$ 2.8 Hz, 12H, NAd), 1.95 (s, 6H, NAd), 1.51 (q, $^1J_{CH}$ 12.4 Hz, 12H, NAd), 0.63 (d, $^2J_{PH}$ 17.5 Hz. P*Me*$_3$).

^{13}C NMR data (C_6D_6, 100.6 MHz, 298 K): δ 171.46 (*ipso*-C_6H_5), 139. 86 (d, $^1J_{CH}$ 155.5 Hz, *o*-C_6H_5), 126.7 (d, $^1J_{CH}$ 148.3 Hz, *m*-C_6H_5), 124.51 (d, $^1J_{CH}$ 158.2 Hz, *p*-C_6H_5), 68.79 (s, NAd), 45.58 (t, $^1J_{CH}$ 127.4 Hz, NAd), 36.61 (t, $^1J_{CH}$ 126.3 Hz, NAd), 30.10 (d, $^1J_{CH}$ 131.6, Hz, NAd), 13.94 (qd, t, $^1J_{CH}$ 129.0 Hz, $^1J_{PC}$ 17.4 Hz, P*Me*$_3$).

^{31}P NMR data (C_6D_6, 101.3 MHz, 298 K, external ref. H_3PO_4): δ -23.86 (*P*Me$_3$).

6.4.9 Reaction of $Mo(NAr)_2Cl_2$.DME with PhMgCl in the Presence of PMe_2Ph: *Preparation of $Mo(NAr)_2(Ph)_2(PMe_2Ph)$ (22)*

An analogous procedure was used for the reaction of $Mo(NAr)_2Cl_2$.DME (0.5 g, 0.82 mmol.) and PMe_2Ph (0.23 g, 1. 7 mmol.) with PhMgCl (0.8 cm3, 1.7 mmol.) in Et_2O. After stirring at room temperature for 4h, a clear red solution was obtained. Filtration and removal of solvent under reduced pressure afforded a red solid. Subsequent recrystallisation from pentane at -78°C afforded gave red crystals. Yield 0.25 g (41%).

Elemental Analysis for $C_{44}H_{51}N_2PMo$ Found (Required): %C 70.8 (71.5), %N 3.4 (3.8), %H 8.1 (7.5).

^{1}H NMR data (C_6D_6, 400 MHz, 298 K): δ 7.73 (d, 4H, $^3J_{HH}$ 6.8 Hz, *m*-C_6H_5), 7.12 (t, $^3J_{HH}$ 7.6 Hz), 7.03 (m), 6.98 (m), 6.91 (m), 4.07 (sept., $^3J_{HH}$ 7.2 Hz, 4H, C*H*Me$_2$), 1.06 (d, $^3J_{HH}$ 6.4 Hz, 24H, CH*Me*$_2$,), 0.99 (d, $^2J_{PH}$ 6 Hz, P*Me*$_2$Ph).

^{13}C NMR data (C_6D_6, {^{1}H}, 100.6 MHz, 298 K): δ 174.72 (*ipso*-C_6H_5), 153.86 (*ipso*-PMe$_2$-C_6H_5), 143.16, 137.04, 130.83 (d, J_{PC} 9.5 Hz, *m*-PMe$_2$-C_6H_5), 127.24, 125.44 (d, J_{PC} 20.9 Hz, *o*-PMe$_2$-C_6H_5), 123.08, 28.17 (CHMe$_2$), 24.43 (CH*Me*$_2$), 12.46 (d, $^1J_{PC}$ 12.9 Hz, P*Me*$_2$Ph).

^{31}P NMR data (C_6D_6, 101.3 MHz, 298 K, external ref. H_3PO_4): δ -18.98 (*P*Me$_3$).

6.4.10 Reaction of $Mo(N^tBu)_2Cl_2$.DME with PhMgCl in the Presence of PMe_3: *Preparation of $Mo(N^tBu)_2(Ph)_2(PMe_3)$ (20)*

An analogous procedure was used for the reaction of $Mo(N^tBu)_2Cl_2$.DME (0.5 g, 1.25 mmol.) and PMe_3 (0.52 cm^3, 5 mmol.) with PhMgCl (1.3 cm^3, 2.5 mmol.) in Et_2O. After stirring at room temperature for 4h, an olive green solution was obtained. Filtration and removal of solvent under reduced pressure afforded a green/brown solid. Subsequent recrystallisation from pentane at -78°C afforded gave green crystals. Yield 0.25 g (43%).

Elemental Analysis for $C_{23}H_{37}N_2PMo$ Found (Required): %C 58.0 (59.0), %N 5.7 (6.0), %H 7.9 (8.0).

Infrared Data (Nujol, CsI, cm^{-1}): 3025 (m), 1570 (m), 1300 (w), 1285 (w), 1260 (s), 1215 (s), 1110 (w,br), 1055 (w, br), 1020 (m), 955 (s), 800 (s), 625 (s), 500 (s).

^{1}H NMR data (C_6D_6, 400 MHz, 298 K): δ 7.72 (d, 4H, $^3J_{HH}$ 6.8 Hz, *m*-C_6H_5), 7.69 (d), 7.20 (m), 7.10 (m), 1.36 (s, 18H, NC*Me*$_3$), 0.56 (d, 9H, PMe$_3$).

^{13}C NMR data (C_6D_6, 100.6 MHz, 298 K): δ 171.38 (s, ipso-C_6H_5), 139.48 (d, $^1J_{CH}$ 156.4 Hz, *o*-C_6H_5), 126.76 (d, $^1J_{CH}$ 108.3, *m*-C_6H_5), 124.49 (d, $^1J_{CH}$ 158.7

Hz, *p*-C_6H_5), 67.90 (s, $NCMe_3$), 31.81 (q, $^1J_{CH}$ 126.6 Hz, $NCMe_3$), 13.84 (qd, $^1J_{PC}$ 17.6 Hz, $^1J_{CH}$ 123.21 Hz, PMe_3).

^{31}P NMR data (C_6D_6, 101.3 MHz, 298 K, external ref. H_3PO_4): δ -24.61 (PMe_3).

6.4.11 Reaction of $Mo(NAr)_2Cl_2$.DME (1) with KCH_2Ph in the Presence of PMe_3 *Preparation of $Mo(NAr)_2(CH_2Ph)_2$.DME (23)*

Diethylether (40 cm^3) was added to a mixture of $Mo(NAr)_2Cl_2$.DME (0.25 g, 0.41 mmol.) and KCH_2Ph (0.11 g, 0.82 mmol.) in an ampoule. The solution was frozen and PMe_3 (0.1 cm^3, 0.82 mmol.) condensed into the ampoule at -196°C. The mixture was allowed to warm to RT and stirred for three hours. Subsequent filtration of the maroon solution from the residues and removal of solvent under reduced pressure gave a red waxy solid. Recrystallisation from pentane afforded a red microcrystalline solid. Yield 0.19 g (65%).

Elemental Analysis for $C_{42}H_{50}N_2O_2Mo$ Found (Required): %C 69.7 (70.2), %N 3.7 (3.9), %H 6.8 (7.0).

^1H NMR data (C_6D_6, 200 MHz, 298 K): δ 7.53 (d, $^3J_{HH}$ 7.3 Hz, 4H, *o*-$CH_2C_6H_5$), 7.10 (m), 6.89 (m, 8H), 6.58 (t, $^3J_{HH}$ 8.0 Hz, 2H, *p*-C_6H_3), 3.90 (sept., $^3J_{HH}$ 7.2 Hz, 4H, $CHMe_2$), 2.78 (s, 4H, $MeOCH_2CH_2OMe$), 2.68 (s, 6H, $MeOCH_2CH_2OMe$), 1.27 (d, $^3J_{HH}$ 6.0 Hz, 4H, $CHMe_2$).

^{13}C NMR data (C_6D_6, {^1H}, 100.6 MHz, 298 K): δ 155.48 (s, *ipso*-$CH_2C_6H_5$), 153.64 (s, *ipso*-C_6H_3), 138.49 (s, *o*-C_6H_3), 130.0 (*o*-C_6H_5), 122.33 (*m*-C_6H_3, *m*-C_6H_5), 121.61 (*p*-C_6H_3), 120.88 (*p*-C_6H_5), 70.96 ($MeOCH_2CH_2OMe$), 58.13 ($MeOCH_2CH_2OMe$), 38.8 (CH_2Ph), 28.00 ($CHMe_2$), 23.90 ($CHMe_2$).

6.4.12 Reaction of $Mo(N^tBu)_2Cl_2$ with KCH_2Ph in the Presence of PMe_3 *Preparation of $Mo(N^tBu)_2(CH_2Ph)_2$ (25)*

An analogous procedure was adopted for the reaction of $Mo(N^tBu)_2Cl_2$ (0.25 g, 0.81 mmol.) with KCH_2Ph (0.211 g, 1.62 mmol.) in

three hours at RT the solvent was removed under reduced pressure and a brown pentane solution isolated by filtration. Subsequent cooling (-78°C) of a saturated pentane solution afforded yellow crystals. Yield 0.2g (59%).

Elemental Analysis for $C_{20}H_{28}N_2Mo$ Found (Required): %C 57.0 (57.1), %N 6.2 (6.7), 6.6 (6.7).

^{1}H NMR data (C_6D_6, 400 MHz, 298 K): δ 6.98 (m, 6H, C_6H_5), 6.88 (m, 4H, C_6H_5), 2.21 (s, 4H, CH_2Ph), 1.24 (s, 18H, $NCMe_3$).

^{13}C NMR data (C_6D_6, 100.6 MHz, 298 K): δ 139.37 (*ipso*-C_6H_5), 129.55 (m, *o*-C_6H_5), 129.46 (m, *m*-C_6H_5), 125.26 ($^1J_{CH}$ 160.7, $^2J_{CH}$ 7.64 Hz, *p*-C_6H_5), 67.94 ($^2J_{CH}$ 4.2 Hz, $NCMe_3$), 37.65 ($^1J_{CH}$ 137.7, $^3J_{CH}$ 4.2 Hz,CH_2Ph), 31.98 ($^1J_{CH}$ 126.8, $^3J_{CH}$ 4.1 Hz, $NCMe_3$).

6.4.13 Reaction of $Mo(N^tBu)_2Cl_2$ with KCH_2Ph in the Presence of PMe_3
Preparation of $Mo(N^tBu)_2(CH_2Ph)(Cl)(PMe_3)$ (24)

$Mo(N^tBu)_2(CH_2Ph)(Cl)(PMe_3)$ was obtained through the treatment of $Mo(N^tBu)_2Cl_2$.DME (0.25g, 0.81 mmol) with KCH_2Ph (0.1 g, 0.81 mmol.) in Et_2O. After stirring at RT for three hours the solvent was removed under reduced pressure and the product extracted with pentane. Prolonged cooling of this solution (-78°C) afforded a red microcrystalline solid. Yield 0.19g (66%).

Elemental Analysis for $C_{18}H_{34}N_2PClMo$ Found (Required): %C 48.7 (49.0), %N 6.2 (6.4), %H 7.6 (7.8).

^{1}H NMR data (C_6D_6, 200 MHz, 298 K): δ 7.62 (d, $^3J_{HH}$ 6.8 Hz, 2H,*o*-C_6H_5), 7.22 (t, $^3J_{HH}$ 8.9 Hz, 2H, *m*-C_6H_5), 6.92 (t, $^3J_{HH}$ 9.0 Hz, 1H, *p*-C_6H_5), 3.72 (s, 2H, CH_2Ph), 1.12 (s, 18H, $NCMe_3$), 1.05 (d, $^3J_{PH}$ 8.9 Hz, 9H, PMe_3).

6.4.14 Reaction of $Mo(N^tBu)_2Cl_2$ with $LiNEt_2$
Preparation of $Mo(N^tBu)_2(Cl)(NEt_2)$ (26)

Ether was added to a mixture of $Mo(N^tBu)_2Cl_2$ (0.25 g, 0.81 mmol.) and $LiNEt_2$ (0.06 g, 0.81 mmol.). The reaction was left stirring at RT for 12h

and afforded a lemon yellow solution. Filtration and removal of solvent under reduced pressure gave a brown oil, in near quantitative yield.

Elemental Analysis Variable.

Infrared Data (Nujol, CsI, cm^{-1}): 1360 (s), 1260 (s) 1250 (s), 1210 (s, br), 1100 (s, br), 1020 (s, br), 890 (w), 800 (s), 600 (w, br) 465 (w), 390 (w), 340 (m).

^{1}H and ^{13}C NMR data are collected in Table 6.2.

Assignment	^{1}H NMR δ (ppm)	^{13}C NMR δ (ppm)
$NCMe_3$	1.31 (s)	29.95 ($^{1}J_{CH}$ 127.5 Hz)
$NCMe_3$	1.40 (s)	32.15 ($^{1}J_{CH}$ 127.1 Hz)
$NCMe_3$	—	72.06
$NCMe_3$	—	69.75
CH_2Me	2.64 (br)*	—
CH_2Me	3.64 (q, $^{3}J_{HH}$ 7.2 Hz)‡	—
CH_2Me	1.08 (t, $^{3}J_{HH}$ 6.8 Hz)*	14.85 ($^{1}J_{CH}$ 126.4 Hz)*
CH_2Me	1.09 (t, $^{3}J_{HH}$ 7.2 Hz)‡	16.92 ($^{1}J_{CH}$ 126.4 Hz)‡
CH_2Me		45.49 ($^{1}J_{CH}$ 136.4 Hz)*
CH_2Me	—	58.39 ($^{1}J_{CH}$ 136.2 Hz)‡

Table 6.2 *400 MHz ^{1}H and 100 MHz ^{13}C NMR data for $Mo(N^tBu)_2(NEt_2)Cl$ (26) (* and ‡ denote associated species).*

6.5 Experimental Details to Chapter Five

6.5.1 XPS Acquisition and Peak Fitting

X-ray photoelectron spectroscopy (XPS) was carried out on an AEI ES200 spectrometer (base pressure 1 x 10^{-9} Torr). Mg K_α X-ray radiation (1253.6 eV) was used as the excitation source. Data was acquired in the fixed retarding ratio (FRR) analyser mode. Activated oxide samples were mounted onto a steel probe tip using double-sided sticky tape and then inserted into the spectrometer from the glovebox. Samples were rotated 30° from the horizontal towards the the X-Ray source. All XPS binding energy shifts are given relative to the binding energy of any adventitious carbon in the sample, which was taken as having a binding energy of 285

eV. All XPS spectra accumulated were fitted using a Gausian curve function with curves of equal FWHM, using a Marquart minimisation computer program.

6.5.2 XPS of Bulk Chromium Oxides

Chromium (III) oxide (99.0%, Hopkin and Williams Ltd.), chromium (VI) oxide (99.0%, BDH), potassium chromate (Analar, BDH), potassium dichromate (Analar, BDH), sodium chromate tetrahydrate (Analar, BDH), and ammonium dichromate (Analar, BDH) were all used without further purification. Nitrogen (oxygen free) and oxygen were obtained from BOC and were both dried by passing them through concentrated sulphuric acid and then over columns of dry phosphorous pentoxide powder (May and Baker) and activated 4A molecular sieves (Aldrich). A sample of PEEK, poly (ether ether ketone), was obtained from ICI.

Oxide samples were placed in a quartz microreactor, equipped with a detachable sample collection vessel which allowed transfer of activated material without exposure to air. Chromium (III) oxide was heated at 1 °C/min under a flow of dry oxygen to 800 °C while chromium (VI) oxide was activated under similar conditions to 150 °C (higher temperatures would have resulted in melting and decomposition). The samples were maintained at their maximum temperatures for five hours, before cooling at 1 °C/min to room temperature. The samples were then transferred into a sample collection vessel, whilst still under a flow of oxygen, and then taken into a nitrogen atmosphere glovebox (approx. 10 ppm water and approx. 1.5 ppm oxygen). From here the samples could be directly transfered into an electron spectrometer for XPS analysis.

6.5.3 Mass Spectroscopic Studies of Acetate Containing Systems

Control samples comprised of bulk chromium acetate (Aldrich, 98+%), high surface area silica (Crosfield Chemicals, surface area = 323 m^2g^{-1}, pore volume = 1.81 cm^3g^{-1}), and silica washed with acetic acid (to 1 wt % acetate), followed by rinsing with distilled water. The catalyst precursor was prepared by impregnating silica with an aqueous solution of

basic chromium acetate $Cr_3(OH)_2(CH_3CO_2)_7$ (Crosfield Chemicals) and then dried.

1g of material was loaded into a quartz reactor tube. Dry argon or oxygen carrier gas was passed over the substrate at 1 lh^{-1}, and the furnace ramped at 1°C min^{-1}. A VG SX200 quadrupole mass spectrometer was connected *via* a heated fine capillary tube to the microreactor. The mass spectrometer was multiplexed to a PC computer, allowing the simultaneous collection of up to 50 mass profiles. Firstly, the whole mass spectrum was recorded as a function of furnace temperature, which facilitated the identification of all the desorbing species. Subsequently this experiment was repeated with fresh samples, and TPD profiles were obtained by tuning into the most intense masses during heating.

6.5.4 Polymerisation Studies

A similar procedure and experimental set up was used to probe the polymerisation mechanism using *in situ* mass spectroscopy as for the acetate systems. Both ethene and propene (Aldrich) were dried by passing them through phosphorus pentoxide and 4A molecular sieve columns. The ethene was of an appropriate grade known to support polymerisation in slurry reactors. Carbon monoxide (Aldrich) was used as received.

6.6 Introduction to Photoelectron Spectroscopy and MS Techniques

6.6.1 Introduction

Photoelectron spectroscopy involves the ejection of electrons from atoms or molecules following bombardment by photons.5 The ejected electrons are called photoelectrons.

The effect was observed originally on surfaces of easily ionisable metals such as the alkali metals. Bombardment of the surface with photons of tunable frequency did not produce any photoelectrons until the threshold frequency was reached. At this frequency υ_t, the photon energy was just sufficient to overcome the work function Φ of the metal, so that:[5]

$$h\upsilon_t = \Phi$$

At higher frequencies the excess energy of the photons is converted into kinetic energy of the photoelectrons:[5]

$$h\upsilon_t = \Phi + \frac{1}{2} m_e v^2$$

where m_e and v are the mass and velocity of the photoelectrons respectively.

Photoelectron spectroscopy is a simple extension of the photoelectric effect involving the use of higher energy incident photons. The sample surface is irradiated by a source of low energy X-rays under ultra high vacuum (UHV) conditions. Photoionisation takes place in the sample surface, the resultant photoelectrons having kinetic energy (E_k) which is related to the incident X-ray energy ($h\upsilon$) binding energy of the electron (E_b) and the material work function (Φ) by the Einstein relation:[5,6,7]

$$E_k = h\upsilon - E_b - \Phi$$

The inner shell or core electrons are basically in atomic orbitals, and their binding energies are characteristic of the atoms. However, slight changes occur for the inner-shell binding energies that are dependant on the nature of the chemical environment. These changes in the core level binding energies, or chemical shifts, are due to alterations in the electron density of the valence shell: a more highly oxidised species gives rise to a higher binding energy, while a more reduced species shows the opposite effect.[9]

The essential constituents of a photoelectron spectrometer are an intense monochromatic light source, an energy analyzer for the ejected electrons, and a detector for the energy analyzed electrons. A brief description of each component is given in the following sections.

6.6.2 X-Ray Source

Choice of material for a soft X-ray source in XPS depends on two considerations:[8]

a) The line width must not limit the energy resolution required in the technique.

b) The characteristic X-ray energy must be high enough that a sufficient range of core electrons can be photo ejected.[4]

After consideration of the above, the most common anodes for soft X-ray production are magnesium and aluminium.[5,9] Monochromation of the X-rays is essential for both good resolution and sensitivity. A thin aluminium window (≈2μm) is used to remove stray electrons, reducing heating effects, and any contamination from the source..

6.6.3 Energy Analysers

In XPS, electron energy analysers are of the electrostatic type as electromagnets and permanent magnets are difficult to construct and handle in a UHV system. Most universally used analysers are the cylindrical mirror analyser (CMA) and the concentric hemispherical analyser (CHA).[5]

The CHA employs two coaxial cylinders (one at earth and one at a negative potential) and is simple to construct. Energy analysis is performed by scanning the potential on the outer cylinder. The advantage of the CMA is that there is a large angle of acceptance of electrons, leading to high transmission, and is thus favoured for Auger electron spectroscopy.

The CMA is most favoured for XPS. Two hemispheres are placed concentrically, with a potential on each, greatest on the outer hemisphere. Changing the potential difference allows electrons of different energies to be transmitted. The intensity of the resultant signal is proportional to the size of the entrance slit width.

6.7 Quadrupole Mass Spectrometer

The mass spectrometer used throughout this thesis was a Vacuum Generators SX200, which uses a four electric pole (a "quadrupole") mass analyzer and no magnetic field. This consists of the following components: Gaseous Molecule Input, Ion Source, Ion Optics, Quadrupole Analyser, Collector, Electron Multiplier, Amplifier and Computer Interface.

Gaseous species entering the mass spectrometer are bombarded with a beam of electrons which causes ionization and positive ion formation.[10]

These positive ions are separated on the basis of mass (strictly mass/charge, but the majority of ions are singly charged), and the result is quantitatively recorded as a spectrum of these positively charged ion fragments.

Ions entering from the top travel with a constant velocity in a direction parallel to the poles (z-direction), but acquire oscillations in the x and y directions (Figure 6.1). This results from the application of both a dc and a radio frequency voltage to the poles. There is a so-called "stable" oscillation that allows an ion to pass from one end of the quadrupole to the other without striking the poles; this oscillation is dependant on the mass-to-charge ratio of the ion. Thus, ions of only one value of m/e will travel the length of the analyzer, the remaining ions have unstable oscillations and will therefore collide with the poles. Mass selection is performed by varying each of the dc and radio frequencies while the ratio of the two remains constant.

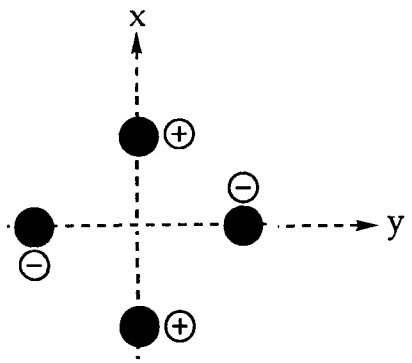

Figure 6.1
Quadrupole arrangement.

In the SX-200 QMS either a Faraday Cup detector or an electron multiplier is used as the ion detector. Which is used depends upon the pressure in the Vacuum chamber (Faraday 10^{-5} to 10^{-11} mbar; SEM 10^{-7} to 10^{-13} mbar), and the scan speed of the spectrum.

Quarupoles operate with low source voltages and the velocity of high mass ions is thus relatively slow. These ions undergo fewer oscillations under the influence of the quadrupole fields, and limit the ability of the quadrupole to perform mass analysis. Focussing these ions into and out of the quadrupoles is also more difficult, and therefore the apparent transmission of high mass ions through the quadrupole is reduced. Slower moving high mass ions are less efficiently detected in a standard electron multiplier.

reduced. Slower moving high mass ions are less efficiently detected in a standard electron multiplier.

6.8 References

1 R.R. Schrock, J.S. Murdzek, G. Bazan, M. DiMare, M. O'Regan, *J. Am. Chem. Soc.*, 1990, **112**, 3875.

2 R.R. Schrock, *J. Am. Chem. Soc.*, 1985, **107**, 5957.

3 W. Wolfsberger and H. Schmidbaur, *Synth. React. Inorg. Metal-Org. Chem.*, 1974, **4**, 149.

4 Schlosser, M and Hartmann, J., Angew. Chem. Int. Ed. Engl., 1973, ,12, 508.

5 J.M. Hollas, *"Modern Spectroscopy,"* Wiley and Sons, New York, 1987, p260.

6 A.D. Baker and D. Betteridge, *"Photoelectron Spectroscopy- Chemical and analytical Aspects,"* Pergamon, 1972.

7 A.B. Christie *"Methods of Surface Analysis- Techniques and Applications,"* Ed. J.M. Walls, Cambridge University Press, 1989.

8 J.C. Riviere *"Practical Surface Analysis,"* Eds. D. Briggs and M.P. Seah, Vol. 1, Second Edition, Wiley and Sons, 1990.

9 J.D. Carette and D. Roy, *"Topics in Current Physics- Electron Spectroscopy for Surface Analysis,"* Ed. H. Ibach, 1977.

10 R.M. Silverstein, G.C. Bassler, and T.C. Morrill, *"Spectrometric Identification of Organic Compounds,"* Wiley and Sons, Fourth Edtn., 1980; D. Briggs, A. Brown, J.C. Vickerman, *"Handbook of Static Secondary Ion Mass Spectrometry,"* Wiley and Sons, 1989; Micromass SX-200 Quadrupole Mass Spectrometer Instrument Manual, Vacuum Generators Limited; K.L. Busch *"Ion Spectroscopies for Surface Analysis,"* Eds. A.W. Czanderna and D.M. Hercules, Plenum Press, 1991; J.D. Morrison *"Gaseous Ion Chemistry and Mass Spectrometry,"* Wd. J. Futrell, Wiley and Sons, 1986.

Appendices-
Crystal Data, Colloquia, and Lectures

APPENDIX 1A: CRYSTAL DATA FOR $Mo(N^tBu)(NAr)Cl_2.DME$

$C_{20}H_{36}Cl_2N_2O_2Mo$:	503.35
Crystal System:	Triclinic
Space Group:	$P\bar{1}$ (#2)
Cell Dimensions:	a = 9.830(5)Å
	b = 9.993(5)Å
	c = 13.799(6)Å
	α = 70.92(4)°
	β = 85.54°
	γ = 71.62°
	U = 1215.3(1.1)Å^3
	Z = 2
	D_c = 1.376 g cm^{-3}.
Final R-value:	0.0257 (R_w = 0.0269%)

APPENDIX 1B: CRYSTAL DATA FOR $[Cr_2Cl_6(\mu\text{-}Cl)_3]\,[NHEt_3]_3$

$C_{18}H_{48}Cl_9Cr_2N_3$:	729.6
Crystal System:	Monoclinic
Space Group:	$P2_1/c$
Cell Dimensions:	a = 19.100(8)Å
	b = 10.270(4)Å
	c = 17.342(6)Å
	α = 90.0°
	β = 96.90°
	γ = 90.0°
	U = 3377(2)Å^3
	Z = 4
	D_c = 1.44 g cm^{-3}.
Final R-value:	0.043 (R_w = 0.043)

APPENDIX 1C: CRYSTAL DATA FOR $Mo(NAr)_2(PMe_3)_2$

$C_{20}H_{36}Cl_2N_2O_2Mo$:	598.6
Crystal System:	Monoclinic
Space Group:	C2/*c*
Cell Dimensions:	a = 25.848(6)Å
	b = 25.848(3)Å
	c = 21.340(3)Å
	$\alpha = 90.0°$
	$\beta = 107.72°$
	$\gamma = 90.0°$
	U = 13581(4)Å^3
	Z = 16
	$D_c = 1.171$ g cm^{-3}.
Final R-value:	0.0594 ($R_w = 0.0576$)

This molecule crystallised with one full molecule and two half molecules in the asymmetric unit. The two half molecules are situated on the 2-fold axes with the Mo atoms constrained to be on the special positions 0.5, *y*, 0.25, and 0, *y*, 0.25 with their anisotropic thermal factors constrained to be consistent with the 2-fold symmetry.

APPENDIX 1D: CRYSTAL DATA FOR $Mo(NAr)_2(PMe_3)_2(\eta^2\text{-}C_2H_4)$

$C_{32}H_{56}N_2P_2Mo_2$:	626.7
Crystal System:	Monoclinic
Space Group:	C2/*c*
Cell Dimensions:	a = 20.508(4)Å
	b = 9.867(2)Å
	c = 17.417(3)Å
	$\alpha = 90.0°$
	$\beta = 98.52°$
	$\gamma = 90.0°$
	U = 3485.5Å^3
	Z = 4
	$D_c = 1.194$ g cm^{-3}.
Final R-value:	0.036 ($R_w = 0.035$)

APPENDIX 1E: CRYSTAL DATA FOR $Mo(N^tBu)_2(PMe_3)(\eta^2\text{-}C_3H_6)$

$C_{14}H_{33}N_2PMo$:	356.3
Crystal System:	Triclinic
Space Group:	$P\bar{1}$
Cell Dimensions:	a = 9.312(2)Å
	b = 9.723(2)Å
	c = 11.203(2)Å
	α = 78.85(4)°
	β = 88.23°
	γ = 85.94°
	U = 992.5(4)Å^3
	Z = 2
	D_c = 1.192 g cm^{-3}.
Final R-value:	0.0405 (R_w = 0.0598)

APPENDIX 1F: CRYSTAL DATA FOR $Mo(N^tBu)_2(PMe_3)(\eta^2\text{-}PhC{\equiv}CPh)$

$C_{25}H_{37}N_2PMo$:	492.5
Crystal System:	Orthorhombic
Space Group:	*Pbca*
Cell Dimensions:	a = 13.980(3)Å
	b = 15.332(6)Å
	c = 24.988(9)Å
	α = 90.0°
	β = 90.0°
	γ = 90.0°
	U = 95356(3)Å^3
	Z = 8
	D_c = 1.221 g cm^{-3}.
Final R-value:	0.0594 (R_w = 0.0688)

APPENDIX 1G: CRYSTAL DATA FOR $Mo(NAr)_2(Ph)_2(PMe_3)$

$C_{39}H_{53}N_2PMo$:	676.74
Crystal System:	Monoclinic
Space Group:	P_{c1}/c
Cell Dimensions:	a = 26.202(2)Å
	b = 12.677(3)Å
	c = 23.512(3)Å
	$\alpha = 90.0°$
	$\beta = 99.889(7)°$
	$\gamma = 90.0°$
	U = 7693.87Å^3
	Z = 8
	$D_c = 1.168$ g cm^{-3}.
Final R-value:	0.0431% (R_w = 0.0477%)

Appendix 2

First Year Induction Courses: October 1990

The course consists of a series of one hour lectures on the services available in the department.

1. Departmental Safety
2. Safety Matters
3. Electrical Appliances and Infrared Spectroscopy
4. Chromatography and Microanalysis
5. Atomic Absorbtion and Inorganic Analysis
6. Library Facilities
7. Mass Spectroscopy
8. Nuclear Magnetic Resonance
9. Glass Blowing Techniques

Examined Lecture Courses: October 1990-April 1991

Three courses were attended consisting of 6 one hour lectures followed by a written examination in each.

"Solids and Surfaces," Dr. J.P.S. Badyal (6 lectures) and Dr N.D.S. Canning (6 lectures).
"Synthetic Polymers," Prof. W.J. Feast.

Research Colloquia, Seminars and Lectures Organised By the Department of Chemistry.

* - Indicates Colloquia attended by the author.

During the Period 1990-1991

4th October	* Dr. M. Bochmann, University of East Anglia, Synthesis, Reactions and Catalytic Activity of Cationic Titanium Alkyls.
11th October	Dr. W.A. MacDonald, ICI Wilton, "Materials for the Space Age."
26th October	* Prof. R. Soulen, South Western University, Texas, "Preparation and Reactions of Bicycloalkenes."
31st October	Dr. R. Jackson, Newcastle University, "New Synthetic Methods: a-Amino Acids and Small Rings.
1st November	Dr. N. Logan, Nottingham University, "Rocket Propellants."
6th November	* Dr. P. Kocovsky, Uppsala University, "Stereo-Controlled Reactions Mediated by Transition and Non-Transition Metals."
8th November	Dr. S.K. Scott, Leeds University, "Clocks, Oscillations and Chaos."
14th November	Prof. T. Bell, SUNY, Stoney Brook, U.S.A., Functional Molecular Architecture and Molecular Recognition.
21st November	* Prof. J. Prichard, Queen Mary & Westfield College, London University, "Copper Surfaces and Catalysts."

28th November	Dr. B.J. Whitaker, Leeds University, "Two-Dimensional Velocity Imaging of State-Selected Reaction Products."
29th November	Prof. D. Crout, Warick University, "Enzymes in Organic Synthesis."
5th December	* Dr. P.G. Pringle, Bristol University, "Metal Complexes with Functionalised Phosphines."
13th December	* Prof. A.H. Cowley, University of Texas, "New Organometallic Routes to Electronic Materials."
15th January	Dr. B.J. Alder, Lawerence Livermore Labs., California "Hydrogen in all its Glory."
17th January	Dr. P. Sadler, Nottingham University, "Comet Chemistry."
30th January	Prof. E. Sinn, Hull University, "Coupling of Little Electrons in Big Molecules. Implications for the Active Sites of (Metalloproteins and other) Macromolecules."
31st January	Dr. D. Lacey, Hull University, "Liquid Crystals."
6th February	Dr. R. Bushby, Leeds University, "Biradicals and Organic Magnets."
14th February	Dr. M.C. Petty, Durham University, "Molecular Electronics."
20th February	* Prof. B.L. Shaw, Leeds University), "Synthesis with Coordinated, Unsaturated Phosphine Ligands."
28th February	* Dr. J. Brown, Oxford University, "Can Chemistry Provide Catalyts Superior to Enzymes?"

6th March	Dr. C.M. Dobson, Oxford University, "NMR Studies of Dynamics in Molecular Crystals."
6th March	Dr. D. Gerrard, British Petroleum, "Raman Spectroscopy for Industrial Analysis."
7th March	Dr. J. Markam, ICI Pharmaceuticals, "DNA Fingerprinting."
24th April	* Prof. R.R. Schrock, M.I.T, "Metal-Ligand Multiple Bonds and Metathesis Initiators."
25th April	Prof. T. Hudlicky, Virginia Polytechnic Institute, "Biocatalysis and Symmetry Based Approaches to the Efficient Synthesis of Complex Natural Products."
30th June	* Prof. M.S. Brookhart, University of N. Carolina, "Olefin Polymerisation, Oligomerisation and Dimerization Using Electrophilic Late Transition Metal Catalysts."
29th July	Dr. M.A. Brimble, Massey University, New Zealand, "Synthetic Studies Towards the Antibiotic Griseusin-A."

During the Period 1991-1992

17th September	* Prof. R.D. Fischer, University of Hamburg, "From Organo-f-Element Systems to Organo-Main-Group Polymers."
17th October	Dr. J.A. Salthouse, University of Manchester, "Son et Luminere - a Demonstration Lecture."
31st October	Dr. R. Keeley, Metropolitan Police Forensic Science, "Modern Forensic Science."

6th November	* Prof. B.F.G. Johnson, Edinburgh University, "Cluster-Surface Analogies."
7th November	Dr. A.R. Butler, St. Andrews University, "Traditional Chinese Herbal Drugs: a Different Way of Treating Disease."
13th November	Prof. D. Gani, St Andrews University, "The Chemistry of PLP Dependant Enzymes."
20th November	* Dr. R. More O'Ferrall, University College, Dublin, "Some Acid-Catalysed Rearrangements in Organic Chemistry."
28th November	Prof. I.M. Ward, IRC in Polymer Science, University of Leeds, *The SCI Lecture*, "The Science and Technology of Orientated Polymers."
5th December	Dr. W.D. Cooper, Shell Research, "Colliod Science, Theory and Practice."
4th December	* Prof. R. Grigg, Leeds University, "Palladium Catalysed Cyclisation and Ion Capture Processes."
5th December	Prof. A.L. Smith, ex Unilever, "Soap, Detergents and Black Puddings."
22nd January	Dr. K.D.M. Harris, St. Andrews University, "Understanding the Properties of Solid Inclusion Compounds."
29th January	Dr. A. Holmes, Cambridge University, "Cycloaddition Reactions in the Service of the Synthesis of Piperdine and Indolizidine Natural Products."
30th January	Dr. M. Anderson, Shell Research, "Recent Advances in the Safe and Selective Chemical Control of Insect Pests."

12th February	* Prof. D.E. Fenton, Sheffield University, "Polynuclear Complexes of Molecular Clefts as Models for Copper Biosites."
13th February	Dr. J. Saunders, Glaxo Group Research Ltd., "Molecular Modelling in Drug Discovery."
19th February	* Prof. E.J. Thomas, Manchester University, "Applications of Organostannanes to Organic Synthesis."
20th February	* Prof. E. Vogel, University of Cologne, *The Musgrave Lecture*, "Porphyrins, Molecules of Interdisciplinary Interest."
25th February	Prof. J.F. Nixon, University of Sussex, *The Tilden Lecture*, "Phosphaalkynes, New Building Blocks in Inorganic and Organometallic Chemistry."
26th February	Prof. M.L. Hitchman, Strathclyde University, "Chemical Vapour Deposition."
11th March	* Dr. S.E. Thomas, Imperial College, "Recent Advances in Organoiron Chemistry."
5th March	* Dr. N.C. Billingham, University of Sussex, "Degradable Plastic - Myth or Magic?"
12th March	Dr. R.A. Hann, ICI Imagedata, "Electronic Photography - An Image of the Future."
18th March	Dr. H. Maskill, Newcastle University, "Concerted or Stepwise Fragmentation in a Deamination-Type Reaction."

7th April	Prof. D.M. Knight, Philosophy Department, University of Durham, "Interpreting Experiments: the Beginning of Electrochemistry."
6th May	* Prof. T. Marder, University of Waterloo, "Metal Catalysed Alkene Hydroboration."
13th May	Dr. J.C. Gehret, Ciba Geigy, Basel, "Some Apects of Industrial Agrochemical Research."

During the Period 1992-1993

15th October	Dr. M. Glazer and Dr. S. Tarling, Oxford University and Birbeck College, London, "It pays to be British!- The Chemists Rôle as an Expert Witness in Patent Litigation."
20th October	* Dr. H.E. Bryndza, Du Pont Central Research, "Synthesis, Reactions and Thermochemistry of Metal (Alkyl) Cyanide Complexes and Their Impact on Olefin Hydrocyanation Catalysis."
22nd October	Prof. A. Davies, University College London, The *Ingold-Albert Lecture* "The Behaviour of Hydrogen as a Pseudometal."
28th October	* Dr. J.K. Cockcroft, University of Durham, "Recent Developments in Powder Diffraction."
29th October	* Dr. J. Emsley, Imperial College, London, "The Shocking History of Phosphorus."
4th November	* Dr. T.P. Kee, University of Leeds, "Synthesis and Co-ordination Chemistry of Silylated Phosphites."
5th November	Dr. C.J. Ludman, University of Durham, "Explosions, A Demonstration Lecture."

11th November	Prof. D. Robins, Glasgow University, "Pyrrolizidine Alkaloids: Biological Activity, Biosynthesis and Benefits."
12th November	Prof. M.R. Truter, University College, London, "Luck and Logic in Host-Guest Chemistry."
18th November	* Dr. R. Nix, Queen Mary College, London, "Characterisation of Heterogeneous Catalysts."
25th November	Prof. Y. Vallee, University of Caen, "Reactive Thiocarbonyl Compounds."
25th November	Prof. L.D. Quin, University of Massachusetts, Amerherst, "Fragmentation of Phosphorus Heterocycles as a Route to Phosphoryl Species with Uncommon Bonding."
26th November	Dr. D. Humber, Glaxo, Greenford, "AIDS- The Development of a Novel Series of Inhibitors of HIV."
2nd December	* Prof. A.F. Hegarty, University College, Dublin, "Highly Reactive Enols Stabilised by Steric Protection."
2nd December	Dr. R.A. Aitken, University of St. Andrews, "The Versatile Cycloaddition Chemistry of $Bu_3P.CS_2$."
3rd December	Prof. P. Edwards, Birmingham University, *The SCI Lecture*, "What is Metal?"
9th December	Dr. A.N. Burgess, ICI Runcorn, "The Structure of Perfluorinated Ionomer Membranes."
20th January	Dr. D.C. Clary, University of Cambridge, "Energy Flow in Chemical Reactions."

21st January	Prof. L. Hall, Cambridge, "NMR- Window to the Body."
27th January	* Dr. W. Kerr, University of Strathclyde, "Development of the Pauson-Khand Annulation Reaction: Organocobalt Mediated Synthesis of Natural and Unnatural Products."
28th January	Prof. J. Mann, University of Reading, "Murder, Magic and Medicine."
3rd February	Prof. S.M. Roberts, University of Exeter, "Enzymes in Organic Synthesis."
10th February	Dr. D. Gillies, University of Surrey, "NMR and Molecular Motion in Solution."
11th February	Prof. S. Knox, Bristol University, *The Tilden Lecture*, "Organic Chemistry at Polynuclear Metal Centres."
17th February	Dr. R.W. Kemmitt, University of Leicester, "Oxatrimethylenemethane Metal Complexes."
18th February	Dr. I. Fraser, ICI Wilton, "Reactive Processing of Composite Materials."
22nd February	Prof. D.M. Grant, University of Utah, "Single Crystals, Molecular Structure, and Chemical Shift Anisotropy."
24th February	Prof. C.J.M. Stirling, University of Sheffield, "Chemistry of Flat-Reactivity of Ordered Systems."
10th March	* Dr. P.K. Baker, University College of North Wales, Bangor, "Chemistry of Highly Versatile 7-Coordinate Complexes."
11th March	Dr. R.A.Y. Jones, University of East Anglia, "The Chemistry of Wine Making."

17th March	Dr. R.J.K. Taylor, University of East Anglia, "Adventures in Natural Product Synthesis."
24th March	Prof I.O. Sutherland, University of Liverpool, "Chromogenic Reagents for Cations."
13th May	* Prof. J.A. Pople, Carnegie-Mellon University, Pittsburgh, USA, *The Boys-Rahman Lecture*, "Applications of Molecular Orbital Theory."
21st May	* Prof. L. Weber, University of Bielefeld, "Metallo-phospha Alkenes as Synthons in Organometallic Chemistry."
1st June	Prof. J.P. Konopelski, University of California, Santa Cruz, "Synthetic Adventures with Enantiomerically Pure Acetals."
2nd June	* Prof. P. Ciardelli, University of Pisa, "Chiral Discrimination in the Stereospecific Polymerisation of Alpha Olefins."
7th June	Prof. R.S. Stein, University of Massachusetts, "Scattering Studies of Crystalline and Liquid Crystalline Polymers."
16th June	Prof. A.K. Covington, University of Newcastle, "Use of Ion Selective Electrodes as Detectors in Ion Chromatography."
17th June	Prof. O.F. Nielson, H.C. Ørsted Institute, University of Copenhagen, "Low-Frequency IR and Raman Studies of Hydrogen Bonded Liquids."

Conferences and Symposia Attended.

(*denotes paper presentation)

1. *"Symposium in Honour of Professor Peter L. Pauson:- Organometallic Chemistry of the Transition Metals,"*
University of Strathclyde, Glasgow, 19th October 1990.

2.* *"Advanced Inorganic Materials,"*
Ambleside, 3rd July, 1991.

3. *"Waddington Graduate Symposium on Inorganic Chemistry,*
University of Durham, 17th December 1990.

4. *"Autumn Meeting of the Royal Society of Chemistry",*
University of York, 29th September 1991.

5. *"North East Graduate Symposium,"*
University of Durham, 3rd April 1992.

6.* *"3rd International Conference on the Chemistry of the Early Transition Metals,"*
University of Sussex, 26th July 1992.

7.* *"ICI Poster Competition,"*
University of Durham, 11th December 1992.

Publications

1) "Four Coordinate Bis (Imido) Alkene Complexes of Molybdenum (IV); Relatives of the Zirconocene Family,"
P.W. Dyer, V.C. Gibson, J.A.K. Howard, B. Whittle, and C. Wilson, *J. Chem. Soc. Chem. Commun.*, 1992, 1666.

2) "Synthesis, Structural Characterisation and Reactivity of the d^2 Pseudo-metallocene Complex $Mo(N\text{-}2,6\text{-}^{i}PrC_6H_3)_2(PMe_3)_2$,"
P.W. Dyer, V.C.Gibson, J.A.K. Howard, and C. Wilson, *J. Organomet. Chem.*, 1993, **462**, C15.

3) "Fenske-Hall Calculations on the Model Compounds $Mo(NH_2)(PH_3)(C_2H_4)$ and $Mo(NH_2)(PH_3)_2(C_2H_4)$"
P.W. Dyer, V.C. Gibson, C.E. Housecroft, and L.C. Parlett, Submitted.

4) "A High Yield, One-Pot Synthesis of a Binuclear Cr (III)- Chloride Complex, $[Cr_2Cl_9]$ $[Et_3NH]_3$,"
P.W. Dyer, V.C. Gibson, and J.C. Jeffery, Submitted (Polyhedron).

5) "The Characterisation of Surface Oxygen Species Formed on Bulk Chromium Oxides,"
J.P.S. Badyal, P.W. Dyer, and V.C. Gibson, Submitted.

6) "A Mechanistic Study of the Activation of Chromium (III) Acetate Supported on Silica,"
P.W. Dyer, G. Bell, V.C. Gibson and J.P.S. Badyal, Submitted.